This item was submitted to Loughborough's Research Repository by the author.
Items in Figshare are protected by copyright, with all rights reserved, unless otherwise indicated.

The influence of the start up procedure of the emulsion copolymerization of styrene and butyl acrylate in a semi-batch reactor

PLEASE CITE THE PUBLISHED VERSION

PUBLISHER

© Mohammed Al-Tamimi

LICENCE

CC BY-NC-ND 4.0

REPOSITORY RECORD

Al-Tamimi, Mohammed A.. 2019. “The Influence of the Start up Procedure of the Emulsion Copolymerization of Styrene and Butyl Acrylate in a Semi-batch Reactor”. figshare. https://hdl.handle.net/2134/12582.

Loughborough University

This item was submitted to Loughborough University as an MPhil thesis by the author and is made available in the Institutional Repository (https://dspace.lboro.ac.uk/) under the following Creative Commons Licence conditions.

creative commons

COMMONS DEED

Attribution-NonCommercial-NoDerivs 2.5

You are free:

- to copy, distribute, display, and perform the work

Under the following conditions:

Attribution. You must attribute the work in the manner specified by the author or licensor.

Noncommercial. You may not use this work for commercial purposes.

No Derivative Works. You may not alter, transform, or build upon this work.

- For any reuse or distribution, you must make clear to others the license terms of this work.
- Any of these conditions can be waived if you get permission from the copyright holder.

Your fair use and other rights are in no way affected by the above.

This is a human-readable summary of the Legal Code (the full license).

Disclaimer

For the full text of this licence, please go to:
http://creativecommons.org/licenses/by-nc-nd/2.5/

THE INFLUENCE OF THE START UP PROCEDURE ON THE EMULSION COPOLYMERIZATION OF STYRENE AND BUTYL ACRYLATE IN A SEMI-BATCH REACTOR

By

Mohammed A. Al-Tamimi

An MPhil Thesis

Submitted in partial fulfilment of the requirements for the award of Master of Philosophy of Loughborough University

April 2008

© by Mohammed Al-Tamimi

To my parents

ACKNOWLEDGEMENTS

The first people I would like to acknowledge for their support and help in completing this project are my supervisors. I am grateful to professor Chris Rielly and professor Brian Brooks for encouraging my curiosity, challenging my ideas, and for providing the criticism that I needed in order to complete this thesis.

I would also like to thank the following members of staff for their continuous assistance during the experimental work: Mr. A. Milne, Mr. D. Smith, and Mr. S. Creedon.

My deepest debt, however, is to my family whose love and support have sustained and nourished me throughout these years of research and writing.

Finally, I would like to thank King Abdulaziz City for Science and Technology (KACST) and the government of Saudi Arabia for supporting my work through the doctoral scholarship, and the Saudi Arabian Cultural Bureau in London for their assistance.

ABSTRACT

The emulsion copolymerization of Styrene (Sty)-Butyl acrylate (BuA) was carried out in a semibatch reactor with sodium lauryl sulphate (SLS) as surfactant and potassium persulphate (KPS) as initiator. The effects related to the distribution of the monomer, the surfactant, and the initiator on the copolymer composition and the overall behaviour of the reactor were thoroughly studied.

It was found that BuA rich initial charge increased the polymerization rate, reduced the particle sizes, and minimized the composition drift. The experimental data showed that the free unadsorbed surfactant in the reactor increased with increasing the fraction of the BuA monomer initially charged in the reactor. This led to an increase in the number of polymer particles and in return increased the polymerization rate. In addition, cross-linked copolymer was obtained when the BuA content was high indicating the possibility of gel effect which as well led to the apparent increase in the polymerization rate. The water-solubilities of the monomers did not affect the reaction kinetics or the copolymer composition. This was demonstrated experimentally and by means of mathematical modeling.

Reducing the surfactant and the initiator concentrations showed the general behaviour of lower polymerization rates and larger particle sizes. The copolymer composition was not affected by the changes in the surfactant and the initiator concentrations in the reactor. Feeding part of the initiator or the surfactant during the semibatch stage while maintaining constant concentrations showed major effects on the sizes and the numbers of the polymer particles, and the polymerization rate. This is believed to be related to the change in the agitation intensity as a result of varying the volume of the initial charge. No effects were observed on the copolymer composition and the monomers mass fraction in the particles.

Table of Contents

ABSTRACT I

LIST OF TABLES V

LIST OF FIGURES VI

INTRODUCTION 1

1. POLYMERIZATION REACTIONS 3

1.1. FREE-RADICAL POLYMERIZATION 5
1.1.1. FREE-RADICAL POLYMERIZATION MECHANISMS 5
1.2. CHAIN COPOLYMERIZATION 8
1.2.1. KINETICS OF COPOLYMERIZATION (THE TERMINAL MODEL) 10
1.2.2. MONOMER REACTIVITY RATIOS 12
1.2.3. COPOLYMER COMPOSITION DRIFT 14
1.2.4. AZEOTROPIC COPOLYMERIZATION 16

2. EMULSION POLYMERIZATION 18

2.1. TYPICAL INGREDIENTS AND THEIR ROLE 18
2.1.1. DISPERSING MEDIUM 18
2.1.2. EMULSIFIER 19
2.1.3. MONOMERS 21
2.1.4. INITIATORS 22
2.1.5. OTHER COMPONENTS 23
2.2. PARTICLE NUCLEATION 24
2.2.1. HETEROGENEOUS (MICELLAR) NUCLEATION 24
2.2.2. HOMOGENEOUS NUCLEATION 27
2.3. POLYMERIZATION RATE BEHAVIOR 27
2.4. POLYMERIZATION RATE (SMITH-EWART KINETICS) 31
2.4.1. HOMOPOLYMERIZATION 31
2.4.2. COPOLYMERIZATION 33
2.5. NUMBER OF POLYMER PARTICLES 38
2.6. MONOMER PARTITIONING 40
2.6.1. MODELS FOR ESTIMATION OF MONOMER CONCENTRATIONS IN DIFFERENT PHASES 40
2.6.2. CONSTANT PARTITION COEFFICIENTS MODEL 44

3. STYRENE (STY)-BUTYL ACRYLATE (BUA) EMULSION COPOLYMERIZATION 48

3.1. POLYMERIZATION RATE 48
3.1.1. AGITATION EFFECTS 48
3.1.2. BUA COMPOSITION EFFECTS 51
3.1.3. EFFECTS OF REACTION TEMPERATURE 52
3.1.4. SURFACTANT AND INITIATOR EFFECTS 53
3.1.5. SOLUBILITY EFFECTS 54

3.2. MOLECULAR WEIGHT 54
3.3. PARTICLE FORMATION 57
3.4. COPOLYMER COMPOSITION 59
3.5. CONCLUSION 61

4. EXPERIMENTAL PROCEDURE 62

4.1. APPARATUS, PROCEDURE, AND REAGENTS 63
4.1.1. APPARATUS 63
4.1.2. PROCEDURE 64
4.1.3. REAGENTS 65
4.2. ANALYSIS 65
4.2.1. CONVERSION 65
4.2.2. PARTICLE SIZE 66
4.2.3. COMPOSITION 66
4.2.4. NUMBER OF POLYMER PARTICLES (N_p) 67
4.2.5. SURFACE TENSION MEASUREMENT 67

5. PRELIMINARY EXPERIMENTS 69

5.1. EXPERIMENTAL SETUP TESTING 69
5.2. AGITATION EFFECTS 71
5.3. CONCLUSION 74

6. COPOLYMER COMPOSITION ANALYSIS 75

6.1. INTRODUCTION 75
6.2. CONSTRUCTING THE IR CALIBRATION CURVE 85
6.2.1. PREPARATION OF HOMOPOLYMERS 85
6.2.2. OBTAINING THE IR SPECTRA 86
6.3. VALIDATING THE CALIBRATION CURVE 91
6.4. CONCLUSION 97

7. EFFECTS OF MONOMER FEEDING POLICY 99

7.1. INTRODUCTION 99
7.2. MONOMERS DISTRIBUTION EFFECTS 99
7.2.1. INSTANTANEOUS AND OVERALL CONVERSION EVOLUTIONS 101
7.2.2. COPOLYMER COMPOSITION EVOLUTION 117
7.2.3. COPOLYMER PARTICLES EVOLUTION 124
7.3. CONCLUSION 135

8. EFFECTS OF SURFACTANT AND INITIATOR ON THE COPOLYMER 137

8.1. INTRODUCTION 137
8.2. SURFACTANT DISTRIBUTION EFFECTS 137
8.2.1. EFFECTS OF SURFACTANT CONCENTRATION IN THE INITIAL CHARGE 137

8.2.2. DISTRIBUTION OF THE SURFACTANT BETWEEN THE INITIAL CHARGE AND THE SUBSEQUENT FEED 147
8.3. INITIATOR DISTRIBUTION EFFECTS 154
8.3.1. EFFECTS OF INITIATOR CONCENTRATION IN THE INITIAL CHARGE 155
8.3.2. DISTRIBUTION OF THE INITIATOR BETWEEN THE INITIAL CHARGE AND THE SUBSEQUENT FEED 164
8.4. SURFACE TENSION EVOLUTION 169
8.5. CONCLUSION 171

9. GENERAL CONCLUSIONS 174

9.1. CONCLUSIONS 174
9.1.1. MONOMER EFFECTS ON THE STY-BUA COPOLYMER 174
9.1.2. SURFACTANT EFFECTS ON THE STY-BUA COPOLYMER 176
9.1.3. INITIATOR EFFECTS ON THE STY-BUA COPOLYMER 178
9.2. FUTURE WORK 179

APPENDICES 180

APPENDIX A: PHYSICAL AND CHEMICAL PROPERTIES OF THE REACTION COMPONENTS 181
APPENDIX B: EXPERIMENTAL PROCEDURES FROM THE LITERATURE 183
APPENDIX C: MATLAB® IMPLEMENTATION OF THE CONSTANT PARTITION COEFFICIENTS MODEL 190
APPENDIX D: REPRODUCIBILITY AND ERROR PROPAGATION 197

REFERENCES 210

List of Tables

Table 1.1	Typical free radical chain copolymerization reactivity ratios
Table 2.1	Typical values associated with emulsion polymerization
Table 2.2	Water-solubilities of some common monomers
Table 2.3	Various copolymer systems tested for terminal model
Table 3.1	MW characteristics of different Sty/BuA copolymer latexes
Table 4.1	Recipe used in the copolymerization of Sty/BuA
Table 4.2	Agitation speeds and their corresponding Reynolds numbers and power inputs
Table 5.1	Test experiments recipe and feeding strategy
Table 5.2	Recipe and feeding strategy for the 150 and 300 rpm runs
Table 6.1	Copolymer composition as obtained by three independent analytical techniques
Table 6.2	Polybutyl acrylate solution polymerization recipe
Table 6.3	Different PS-PBuA homopolymers blends based on the monomers molecular weights
Table 6.4	FT-IR absorbance ratios of different homopolymer blends
Table 6.5	Recipe of azeotropic copolymerization of Sty-BuA in solution
Table 6.6	Recipe of azeotropic copolymerization of Sty-BuA in emulsion
Table 7.1	The recipes of the experiments related to the study of the monomers effects on the copolymer
Table 7.2	Concentration of SLS in the reactor
Table 7.3	Effective molecular area of SLS molecule on polymer particle at 60/40 Sty/BuA
Table 8.1	The recipes of the experiments related to the study of the surfactant effects on the copolymer
Table 8.2	The recipes of the experiments related to the study of the initiator effects on the copolymer

List of Figures

Figure 1.1	Schematic diagram of the initiation and propagation steps for polystyrene
Figure 1.2	Instantaneous composition of copolymer (F_1) as a function of monomer composition (f_1) for different reactivity ratios (r_1/r_2)
Figure 2.1	Simplified representation of an emulsion polymerization system
Figure 2.2	Simplified illustration of the emulsion polymerization homogeneous and heterogeneous nucleation
Figure 2.3	Polymerization rate stages in emulsion polymerization
Figure 2.4	Conversion stages in a batch emulsion polymerization
Figure 2.5	Copolymer composition (F_1) vs. feed composition (f_1) for the copolymer styrene (M1)-diethyl fumarate (M2)
Figure 2.6	Propagation rate constant vs. feed composition (f_1) for the copolymer styrene (M1)-diethyl fumarate (M2)
Figure 2.7	Dependence of the final number of polymer particles on the surfactant concentration (Smith-Ewart case 2)
Figure 2.8	Conversions (A) and copolymer compositions (B) data calculated by the three different partitioning models of BuA/Sty with 30 wt% solids content and seed/monomer ratio of 0.1
Figure 2.9	Effects of solids content on the three partitioning models for Sty/BuA copolymerization
Figure 2.10	Effects of seed/monomer ratio on the three partitioning models for Sty/BuA copolymerization
Figure 4.1	Schematic diagram illustrates the apparatus
Figure 4.2	Surface tension evolutions with surfactant concentration of water saturated with BuA and Sty monomers at 70 °C
Figure 5.1	Instantaneous conversion evolution with time compared with the data from Zubitur and Asua (2001)
Figure 5.2	Schematic of the reactor used by Zubitur and Asua (2001)
Figure 5.3	Front view schematic of 4-blades flat blade agitator
Figure 5.4	Time evolution of the instantaneous conversion (A) and the particle size and number of polymer particle (B) for the 150 and 300 rpm runs
Figure 6.1	UV calibration curve
Figure 6.2	IR KBr transmission spectra of STY/2-EHA in the region 2000-1500 cm^{-1}
Figure 6.3	IR calibration curve based on the PS peak at 1602 cm^{-1} (A), IR calibration curve based on the 2-EHA peak at 1158 cm^{-1} (B), ratio of the absorbances of the bands 1602 and 1158 cm^{-1} as a function of the ratio of the monomer mole fraction in the copolymer (C), and comparison between the estimated values of copolymer composition based on the three independent techniques (D)
Figure 6.4	IR spectra of a mixture of DXL and DHL homopolymers and for a copolymer
Figure 6.5	IR calibration curves between the molar fraction of DH units (f_{DH}) and selected IR peaks
Figure 6.6	Variation of Tg with DH mole fraction in the copolymer
Figure 6.7	Aldrich™ IR spectra of PS (A) and PBA (C) homopolymers compared to the IR spectra of Fisher™ PS (B) homopolymer and PBA (D) homopolymer which is prepared by solution polymerization
Figure 6.8	FT-IR spectra of different PS-PBA blends
Figure 6.9	An illustration of IR baseline correction
Figure 6.10	FT-IR calibration curves

Figure 6.11	Instantaneous conversion and butyl acrylate content (A) and the z-average and number of polymer particles (B) evolution with time for the azeotropic batch emulsion copolymerization
Figure 6.12	The composition drift of the azeotropic batch emulsion copolymerization
Figure 7.1	The time evolution of the instantaneous (A) and the overall (B) conversions for the experiments R1-R4
Figure 7.2	The time evolution of the instantaneous (A) and the overall (B) conversions for the experiments R5-R8
Figure 7.3	The total moles (A) and overall mole fraction (B) of injected monomers for the experiments R1-R4
Figure 7.4	The total moles (A) and overall mole fraction (B) of injected monomers for the experiments R5-R8
Figure 7.5	The time evolution of the monomers mass fraction in the polymer particles for 180 minutes feeding time experiments
Figure 7.6	The time evolution of the monomers mass fraction in the polymer particles for 90 minutes feeding time experiments
Figure 7.7	Feeding time effect on the instantaneous (A) and overall (B) conversions for Sty rich initial charge experiments
Figure 7.8	Feeding time effect on the instantaneous (A) and overall (B) conversions for BuA rich initial charge experiments
Figure 7.9	The time evolution of the instantaneous (A) and the overall (B) conversions for the experiments R9-R12
Figure 7.10	The time evolution of the total moles of monomer injected to the reactor for the experiments R9-R12
Figure 7.11	The time evolution of the monomers mass fraction in the polymer particles for the experiments R9-R12
Figure 7.12	The time evolution of the copolymer composition for the experiments R1-R8
Figure 7.13	The time evolution of the composition drift during the semibatch stage for the experiments R1-R8
Figure 7.14	The time evolution of the copolymer composition for the experiments R9-R12
Figure 7.15	The time evolution of the composition drift during the semibatch stage for the experiments R9-R12
Figure 7.16	The time evolution of the particle sizes for the experiments R1-R8
Figure 7.17	The time evolution of the number of polymer particles for the experiments R1-R8
Figure 7.18	The evolution of molecular area of SLS at saturation on the polymer particle with MMA content in the copolymer
Figure 7.19	The time evolution of the theoretical particle coverage with SLS molecules at saturation (A) and the unadsorbed SLS molecules in the reactor (B) for the experiments R1-R4
Figure 7.20	The time evolution of the theoretical particle coverage with SLS molecules at saturation (A) and the unadsorbed SLS molecules in the reactor (B) for the experiments R5-R8
Figure 7.21	The time evolution of the particle sizes (A) and the number of polymer particles (B) for the experiments R9-12
Figure 8.1	The time evolution of the instantaneous (A) and overall (B) conversions for the experiments R13-R16
Figure 8.2	The time evolution of the particle sizes (A) and number of polymer particles (B) for the experiments R13-R16
Figure 8.3	The time evolution of the theoretical particle coverage with SLS molecules at saturation (A) and the unadsorbed SLS molecules in the reactor (B) for the experiments R13-R16

Figure 8.4	The time evolution of the monomers mass fraction in the polymer particles for the experiments R13-R16
Figure 8.5	The time evolution of the copolymer composition (A) and composition drift (B) for the experiments R13-R16
Figure 8.6	The order of dependence of the number of polymer particles on the surfactant concentration for the runs R13-R16
Figure 8.7	The effects of the SLS feed on the instantaneous (A) and overall (B) conversions for the experiments R14, R17, and R18
Figure 8.8	The effects of the SLS feed on the particle sizes (A) and number of polymer particles (B) for the experiments R14, R17, and R18
Figure 8.9	The evolution of the number of polymer particles (A) and particle sizes (B) with overall SLS ratio
Figure 8.10	The time evolution of the monomers mass fraction in particles (A) and SLS overall ratio (B) for the experiments R17 and R18
Figure 8.11	The time evolution of the copolymer composition (A) composition drift (B) and the effects of the SLS overall ratio in the reactor on the evolution of the composition drift (C) for the experiments R14, R17, and R18
Figure 8.12	The time evolution of the instantaneous (A) and overall (B) conversions for the experiments R19-R22
Figure 8.13	The time evolution of the particle sizes (A) and number of polymer particles (B) for the experiments R19-R22
Figure 8.14	The time evolution of the copolymer composition (A) and composition drift (B) for the experiments R19-R22
Figure 8.15	The time evolution of the monomers mass fraction in the particles for the experiments R19-R22
Figure 8.16	The order of dependence of number of polymer particles on the initiator concentration for the runs R19-R22
Figure 8.17	The time evolution of the instantaneous (A) and overall (B) conversions for the experiments R19, R25, and R26
Figure 8.18	The time evolution of the particle sizes (A) and number of polymer particles (B) for the experiments R19, R25, and R26
Figure 8.19	The time evolution of the composition (A) and composition drift (B) for the experiments R19, R25, and R26
Figure 8.20	The effects of initiator feed on the instantaneous (A) and overall (B) conversions for the experiments R20, R23, and R24
Figure 8.21	The effects of initiator feed on the particle sizes (A) and number of polymer particles (B) for the experiments R20, R23, and R24
Figure 8.22	The effects of initiator feed on the monomers mass fraction in the particles for the experiments R20, R23, and R24
Figure 8.23	The effects of initiator feed on the copolymer composition (A) and composition drift (B) for the experiments R20, R23, and R24
Figure 8.24	The time evolution of the surface tension for 100% SLS and KPS in the initial charge and semibatch feed of monomers

Introduction

Emulsion polymerization is an important industrial process for producing polymers dispersed in an aqueous medium. Batch, semi-batch, and continuous reactors are widely used in the polymer industry. Operating these reactors according to an optimal recipe is important. The recipe includes the loading conditions, reactor temperature profile, feeding policy, and feeding rate profiles.

In the literature a lot of work was devoted to batch processes which might be adequate as a starting point to understand the process and could be suitable for a lab scale, however, semi-batch and continuous processes are dominating the industry and they are the main processes in the production of polymers. Semi-batch techniques usually offer more flexibility than batch or continuous techniques. In batch processes, all reactants are completely added to the reaction vessel at the start of the polymerization, whereas in semi-batch processes only part of the formulation is added at the beginning of the reaction, the remainder being added to the reaction vessel according to a predetermined schedule.

Adjusting the feed rates of monomers and other ingredients during the course of reaction overcomes the limitations of batch processes (e.g. heat transfer in the large-scale reactor), and polymer lattices with high added value can be obtained. However, this complicates the process further by introducing the problem of controlling the distribution of the components between the initial reactor charge and the subsequent feed.

Latex products (e.g. styrene/alkyl acrylate copolymers) are widely used in coatings, adhesives, thermoplastics, and rubber industries. This was a result of the possibility of obtaining a large number of polymer products through the variation of the copolymer composition and the polymerization process. Control of the latex properties is the key to guarantee the quality of latex products. For example, the adhesive properties are dependent on the composition of the copolymer. Changes in

the monomer ratio due to batch-to-batch discrepancies might cause manufacturing problems and products with undesirable properties. In order to control characteristics like copolymer composition, the development of such advanced polymer production systems requires an understanding in some depth of the interacting physical and chemical phenomena, which occur during polymerization. The Styrene (Sty)-Butyl acrylate (BuA) system is particularly interesting due to the nature of its components and the corresponding homopolymers. Styrene is a highly hydrophobic monomer and butyl acrylate is a more polar and water-soluble.

The objective of this work is to investigate the effects of various reaction parameters and the effects related to the distribution of the recipe between the initial reactor charge and the subsequent feed on the composition drift and the overall behavior of the emulsion copolymerization of Sty-BuA in a semibatch reactor. The main variables that will be investigated are the concentrations of the monomer, sodium lauryl sulfate (SLS), and initiator in the initial charge and the subsequent feed. The effects related to the agitation speed on the kinetics of the system will be investigated. An adequate level of understanding can be achieved through computer modeling. Therefore, some existing models will be investigated and compared to the experimental results; improvements might be recommended whenever possible.

Next, a literature review which covers the emulsion polymerization in general, and the emulsion copolymerization of Styrene-Butyl acrylate in particular will be presented in the first three chapters. Afterward, the experimental setup and some basic and advanced analysis techniques will be given in chapters four, five, and six. The effects of the different variables on the emulsion copolymerization of Sty-BuA copolymer will be given in chapters seven and eight.

Finally, it should be noted that the final application of the resulting latex system is not the objective of this study. The main aim is for a better understanding of the process and an improved control of the composition and the other properties of the copolymer.

1. Polymerization Reactions

Polymerization is the process of joining together repeated simple units of small molecules by covalent bonds to produce high-molecular-weight polymers. Both natural and synthetic polymers are built from these simple units known as monomers. Importantly, the range of properties that can be achieved depends on the strategy used to assemble these units as well as the nature of the monomer molecules. There are basically two approaches to polymer formation: step growth and chain growth polymerizations.

In *step growth (or condensation) polymerization*, reaction takes place between monomers containing functional groups that react in high yield to form one larger polyfunctional molecule. Examples of such functional groups are carboxylic acids, which react with alcohols to form esters and with amines to form amides. Usually step growth reactions yield a by-product (e.g. water); because of the loss of this compound during the polymerization process, reactions of this type are often called *condensation reactions*. The reaction continues until almost all of one of the reagents is used up. Nylon 66 is an example of a common polymeric clothing material, involving one each of two monomers, hexamethlene diamine and adipic acid, reacting to form a dimer of Nylon 66.

Chain growth (or addition) polymerization involves combining monomers starting from a single reactive site and growing the polymer chain from that site without the formation of by-products. The reactive site can be a cation, an anion, or a radical (a molecule that contains at least one unpaired electron). The type of chain growth polymerization selection depends on the monomer(s) to be used and the requirements of the target polymer. Polyethylene and polystyrene are examples of polymers made by chain growth polymerization where the monomers used are ethylene and styrene, respectively.

It is worth noticing that the polymerization processes might be classified as homogeneous or heterogeneous systems. In *homogeneous polymerizations*, all the reactants (i.e. monomers, initiator, and solvents) are soluble and compatible with the resulting polymer; whereas in *heterogeneous polymerizations* the reactants are insoluble.

Homogeneous polymerization comprise *bulk* and *solution polymerizations*. *Bulk polymerization* is carried out in the absence of any solvent or dispersant and is thus the simplest in terms of formulation. In bulk polymerization the reaction mixture consists of the monomers, a soluble initiator (in case of chain growth polymerization); and sometimes a modifier (e.g. rheology modifiers). This type of polymerization is highly exothermic and extremely viscous. It is mainly used for making pure polymeric products (e.g. optical grade polymethyl methacrylate). In *solution polymerizations*, the monomer, initiator, and resulting polymer are all soluble in the solvent. Due to the fact that it can be difficult to remove the solvent from the finished viscous polymer, solution polymerization is best for polymers that are commercially used in solution form, such as adhesives and surface coatings.

Heterogeneous systems consist of suspension polymerization and emulsion polymerization. In *suspension polymerization* the monomer is dispersed in a liquid (usually water) by high stirring rates and by the addition of stabilizers. A monomer-soluble initiator is added in order to initiate chain-growth polymerization. The polymer is obtained in the form of granules or beads and it is mainly used for making plastic resins. *Emulsion polymerization* is widely used for producing many polymers; it involves the formation of a stable emulsion (known as latex) of monomer in water using an emulsifying agent. The common ingredients are monomers, dispersing medium, initiator, emulsifying agent, and sometimes a transfer agent to control the chains length.

The copolymerization of styrene and butyl acrylate is accomplished by radical chain polymerization; therefore this type of polymerization will be explored in the next sections.

1.1. Free-Radical Polymerization

Free radical polymerization is the most widespread method of chain growth polymerization for a wide range of monomers. Free radical polymerizations are chain reactions in which every polymer chain grows by addition of a monomer to the free radical reactive site called the "active center". The addition of the monomer(s) to this site induces the transfer of the active center to the newly created chain end.

Free radical polymerization is characterized by many attractive features, such as applicability for a wide range of polymerizable groups - including styrenic, vinylic, acrylic and methacrylic derivatives - as well as tolerance to many solvents, small amounts of impurities and many functional groups present in the monomers. However, classical free radical polymerization has some limitations, inherent to its mechanism. In particular, it is difficult to control polymer molecular weights and polydispersities, as well as to introduce defined end-groups, or to prepare special macromolecular architectures such as block copolymers. Next, a discussion of homogeneous free-radical polymerization will be presented.

1.1.1. Free-Radical Polymerization Mechanisms

Radical chain polymerization consists of a sequence of the three steps: initiation, propagation and termination. The *initiation* step involves two reactions. The first is the production of free radicals by the homolytic dissociation of an initiator species I to yield a pair of initiator radicals R•

$$\mathrm{I} \xrightarrow{k_d} 2\mathrm{R}\bullet \qquad 1.1$$

where k_d is the rate constant for the initiator dissociation and it follows the Arrhenius equation. The rate law is generally first-order (i.e. rate of initiator decomposition)

$$r_i = -k_d\,[I] \qquad 1.2$$

Normally, not all the initiator radicals contribute to the initiation of polymerization; in some cases the initiator is attacked by a propagating chain prior to its decomposition. So instead of an increase in the radical concentration (two radicals being generated), it remains unchanged (dead chain and one radical). In other cases, the radicals formed in the primary decomposition undergo reactions to form neutral molecules instead of initiating the polymerization. Therefore, an *efficiency* term f is sometimes included in the rate law leading to the rate of initiation (r_i) (i.e. generation of radicals)

$$r_i = 2f k_d\,[I] \qquad 1.3$$

The *cage effect* is also another source that wastes the radials; in this case the radicals are confined in a close space (e.g. monomer, inert, polymer) for a period of time; the lifetime of the cage is affected by its nature.

The second part of the initiation step involves the addition of this radical to the first monomer molecule to produce the chain-initiating radical $M_1\bullet$

$$R\bullet + M \xrightarrow{k_i} M_1\bullet \qquad 1.4$$

It should be noticed that the rate limiting step is Eq 1.1 (Seymour, 2000), so the overall rate of initiation is 1.3.

Propagation consists of the growth of $M_1\bullet$ by the addition of large numbers (several thousands) of monomer molecules. Each addition creates a new radical at the end of the polymer chain that has the same identity of the previous one.

$$\begin{aligned} M_1\bullet + M &\xrightarrow{k_p} M_2\bullet \\ M_2\bullet + M &\xrightarrow{k_p} M_3\bullet \\ M_3\bullet + M &\xrightarrow{k_p} M_4\bullet \end{aligned} \qquad 1.5$$

or in general terms

$$M_n\bullet + M \xrightarrow{k_p} M_{n+1}\bullet \qquad 1.6$$

where k_p is the rate constant for propagation and it is considered independent of chain length; the rate of propagation (r_p) takes the following form

$$r_p = k_p [M\bullet][M] \qquad 1.7$$

where [M•] is the sum of the concentrations of all chain radicals.

At some point, the propagating polymer chain stops growing and terminates. *Termination* results from the annihilation of the active centers; it occurs by two routes: combination and disproportionation of the radicals. In *combination* (*known as coupling*) two radical chains are destroyed when they react with each other leading to one inactive chain. *Disproportionation termination* takes place when a radical chain strips a hydrogen atom from another radical chain; a carbon-carbon double bond takes the place of the missing hydrogen. Disproportionation leaves two inactive chains.

$$\begin{aligned} M_n\bullet + M_m\bullet &\xrightarrow{k_{tc}} M_{n+m} && \textit{(combination)} \\ M_n\bullet + M_m\bullet &\xrightarrow{k_{td}} M_n + M_m && \textit{(disproportionation)} \end{aligned} \qquad 1.8$$

where k_{tc} and k_{td} are the rate constants for termination by coupling and disproportionation; respectively. The rate of termination (r_t) is then

$$r_t = 2\, k_t\, [M\bullet]^2 \qquad 1.9$$

where $k_t = k_{tc} + k_{td}$ (Ebwele, 2000). The factor 2 was introduced because at each incidence two radicals disappear.

Figure 1.1 illustrates the initiation and propagation steps of polystyrene, at the beginning an initiator radical reacts with a styrene molecule producing a styrene radical, this new radical continues to react with other styrene molecules generating a long chain of styrene molecules (polystyrene). A discussion covering the homogeneous chain copolymerization will follow.

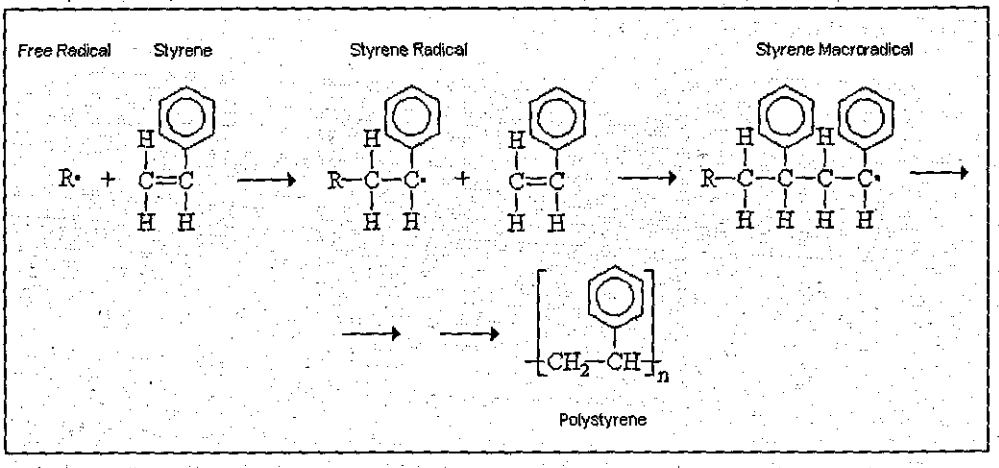

Figure 1.1 Schematic diagram of the initiation and propagation steps for polystyrene
(source: Polymer Science and Technology, Ebewele, p. 27-30)

1.2. Chain Copolymerization

Usually *homopolymers* (polymers made from one monomer) have properties suited to a certain application but are deficient to a wider range of applications. A copolymer with only a small proportion of a second monomer often possesses the desirable properties of the parent homopolymer, while the other component provides the properties formerly lacking. For instance; the homopolymer of acrylonitrile (synthetic fiber) has excellent resistance to weathering and chemicals but poor affinity for dyes. Copolymerization of acrylonitrile with small amounts of other monomers

(e.g. 10% of methyl methacrylate) yields the desirable properties of the homopolymer and the advantage of dyeability.

Chain polymerizations can be carried out with mixtures of two monomers to form a polymer with two different structures in the polymer chain. This process in which two monomers are simultaneously polymerized is called a *copolymerization*, and the product is a *copolymer*. It is important to note that the copolymer is not a mixture or a blend of two homopolymers but contains units of both monomers incorporated into each copolymer molecule. The two monomers enter into the copolymer in overall amounts determined by their relative concentrations and reactivities. The process can be illustrated as

$$M_1+M_2 \rightarrow \sim M_1M_2M_1M_1M_2M_1M_2M_2M_2M_1M_1M_2 \sim$$

There are four types of copolymers: *random copolymers* in which the monomers are arranged along the polymer chain in a random fashion similar to the above illustration, *alternating copolymers* in which there is a regular order of M1 and M2 (e.g. ~M1M2M1M2M1M2M1M2~), *block copolymers* in which there are long sequences of the same repeating unit in the chain (e.g. ~M1M1M1M1M2M2M2M1M1M1M2M2M2~), and last *graft copolymers* in which one monomer forms the main chain, and the second monomer forms side extensions as branches.

Copolymerization allows the synthesis of an almost unlimited number of different products by variations in the nature and relative amounts of the two monomer units in the copolymer product. An obvious example of the importance of the copolymerization process is the case of polystyrene. The United States produces millions of tons per year of polystyrene products, and only about one-third of the total is styrene homopolymer. Copolymerization as well as blending overcomes the brittleness and low impact strength of Polystyrene (Odian, 2004).

The inclusion of a second monomer however complicates the reaction kinetics and brings additional requirements; the most important requirement is the need to understand how differences in monomer reactivity affect copolymer composition and the sequence distribution of the different repeat units in the copolymer chains. Since the most reactive monomer is incorporated preferentially into the copolymer chains, the copolymer molecules formed can have compositions which significantly differ from the initial comonomer mixture composition.

1.2.1. Kinetics of Copolymerization (The Terminal Model)

The composition of a copolymer cannot be determined simply from knowledge of the homopolymerization rates of the two monomers. The copolymerization of the two monomers (M_1 and M_2) leads to two types of propagating species: one with $M_1\bullet$ at the propagating end and the other with $M_2\bullet$ (the "•" represents a radical as the propagating species). The *first order Markov* or *terminal model* of copolymerization assumes that the reactivity of the propagating species is dependent only on the monomer unit at the end of the chain (referred to as the end or ultimate unit); four propagation reactions are then possible. Monomers M_1 and M_2 can each add either to a propagating chain ending in M_1 or to one ending in M_2, that is,

$$\begin{aligned} M_1\bullet + M_1 &\xrightarrow{k_{11}} M_1\bullet \\ M_1\bullet + M_2 &\xrightarrow{k_{12}} M_2\bullet \\ M_2\bullet + M_1 &\xrightarrow{k_{21}} M_1\bullet \\ M_2\bullet + M_2 &\xrightarrow{k_{22}} M_2\bullet \end{aligned} \qquad 1.10$$

where k_{ij} is the rate constant for a propagating chain ending in M_i adding to monomer M_j. All propagation reactions are assumed to be irreversible. For the *homogeneous copolymerization in a batch reactor* the rates of disappearance of the two monomers are given by

$$\frac{-d[M_1]}{dt}=k_{11}[M_1\bullet][M_1]+k_{21}[M_2\bullet][M_1] \qquad 1.11$$

$$\frac{-d[M_2]}{dt}=k_{12}[M_1\bullet][M_2]+k_{22}[M_2\bullet][M_2] \qquad 1.12$$

where $[M_i\bullet]$ denotes the concentration of all the species ending with $M_i\bullet$. Dividing both equations yields the ratio of the rates at which the monomers enter the copolymer, that is, the *copolymer instantaneous composition*

$$\frac{-d[M_1]}{-d[M_2]}=\frac{k_{11}[M_1\bullet][M_1]+k_{21}[M_2\bullet][M_1]}{k_{12}[M_1\bullet][M_2]+k_{22}[M_2\bullet][M_2]} \qquad 1.13$$

Eq 1.13 can be transformed into

$$\frac{-d[M_1]}{-d[M_2]}=\frac{k_{11}\frac{[M_1\bullet]}{[M_2\bullet]}+k_{21}}{k_{12}\frac{[M_1\bullet]}{[M_2\bullet]}+k_{22}} \qquad 1.14$$

An expression for the ratio $[M_1\bullet]/[M_2\bullet]$ is obtained by applying the steady state approximation to the concentrations $[M_1\bullet]$ and $[M_2\bullet]$ (rate of generation and consumption of these radicals are constant), that is

$$\frac{d[M_1\bullet]}{dt}=0 \quad \& \quad \frac{d[M_2\bullet]}{dt}=0 \qquad 1.15$$

For the $[M_1\bullet]$ and $[M_2\bullet]$ to remain constant, their rates of interconversion must be equal (rate of conversion of $M_1\bullet$ to $M_2\bullet$ is equal to the conversion of $M_2\bullet$ to $M_1\bullet$), that is

$$k_{12}[M_1\bullet][M_2]=k_{21}[M_2\bullet][M_1]\Rightarrow\frac{[M_1\bullet]}{[M_2\bullet]}=\frac{k_{21}[M_1]}{k_{12}[M_2]} \qquad 1.16$$

Combining 1.14 and 1.16 and simplifying yields the *copolymerization equation* (Mayo-Lewis equation)

$$\frac{d[M_1]}{d[M_2]}=\frac{[M_1](r_1[M_1]+[M_2])}{[M_2]([M_1]+r_2[M_2])} \qquad 1.17$$

where $d[M_1]/d[M_2]$ is the molar ratio of the two monomers being added to the copolymer, and the parameters r_1 and r_2 are the monomer reactivity ratios

$$r_1=\frac{k_{11}}{k_{12}},\ r_2=\frac{k_{22}}{k_{21}} \qquad 1.18$$

The copolymerization equation can also be expressed in terms of mole fractions instead of concentrations. If f_1 and f_2 are the mole fractions of monomers M_1 and M_2 in the feed, and F_1 and F_2 are the mole fractions of M_1 and M_2 in the copolymer formed at any instant, then the copolymerization equation becomes more convenient and takes this form

$$\frac{F_1}{F_2}=\frac{f_1(r_1f_1+f_2)}{f_2(r_2f_2+f_1)} \qquad 1.19$$

1.2.2. Monomer Reactivity Ratios

The *monomer reactivity ratio* (r) is the ratio of the rate constant for a given radical adding to its own type of monomer to the rate constant for its addition of the other monomer (Eq 1.18). Table 1.1 provides a list of pairs of monomers reactivities. The data assists in estimating the extent of copolymerization of two monomers. In the system styrene(M_1)-n-butyl acrylate(M_2), for example, the reactivity ratios are r_1=0.7

and r_2=0.20. Since the rate of consumption of styrene (M1) is faster than that of butyl acrylate (M2), the composition of the feed would change rapidly if styrene were not added to prevent a change in its composition i.e. a phenomenon knows as composition drift (§1.2.3). It should be noted that there are some discrepancies in the literature regarding the reported reactivity values. Dubé et al. (1990) explained that this is due to improper experimental design or due to inaccurate copolymer composition analysis methods. However, Garcia et al. (2000) reported that differences between the apparent reactivity ratios determined by means of solution and bulk polymerizations are due to the polarity of the solvent. An increase in the polarity of the solvent increases the reactivity ratios.

The possibility of two monomers to copolymerize is noted by r values between zero and unity. An r_1 value greater than one means that M_1• preferentially adds M_1 instead of M_2, while an r_1 value less than one means that M_1• preferentially adds M_2. An r_1 value of zero would mean that M_1 is incapable of undergoing homopolymerization.

M_1	M_2	r_1	r_2	$r_1 r_2$
Methyl methacrylate	Styrene	0.5	0.5	0.25
	Vinyl acetate	20	0.015	0.30
	Butyl acrylate	2.86	0.12	0.34
Styrene	p-Chlorostyrene	0.74	1.025	0.76
	Vinyl acetate	55	0.01	0.55
	Butyl acrylate	0.7	0.2	0.14
Vinyl acetate	Butyl acrylate	0.02	3.48	0.07
	Vinyl laurate	1.4	0.7	0.98

Table 1.1 Typical free radical chain copolymerization reactivity ratios
(source: Polymer Handbook, 1999)

The reactivity ratios are experimentally determined by polymerization to low conversion for different feed compositions. After measuring the copolymer

composition, the copolymer equation (1.13) is solved for one of the reactivity ratios where it gives a straight line. Several runs provide several straight lines; plotting those lines on an r_1 vs. r_2 graph provides a region where those lines intersect, this region of intersections provides information about the reactivity ratios and the precision of the experiments.

If $r_1 > 1$, then monomer M_1 tends to produce homopolymers, or block copolymers. Preference for reaction with a different monomer occurs when $r_1 < 1$. When both r_1 and r_2 are approximately equal to 1, the conditions are said to be *ideal*, and a *random copolymer* is produced (*The term ideal copolymerization does not mean a desirable process*). When r_1 and r_2 are approximately equal to zero an *alternating copolymer* is produced. In general, there will be a shift toward alternating when the product of r_1 r_2 approaches zero. On the other hand, if the values of r_1 and r_2 are similar and the product r_1 r_2 approaches 1, the product will be more likely a random copolymer. The value of r_1 r_2 for most copolymerizations is between 1 and 0, and it might be used with discretion for estimating the randomness in a copolymer.

1.2.3. Copolymer Composition Drift

Due to different reactivities and solubilities (see *chapter 3*) of many monomers used in copolymerization, the instantaneous chemical composition of the copolymer is different from the chemical composition of the monomer in the reaction mixture. As a consequence the chemical composition of a copolymer formed gradually changes during the reaction. This phenomenon is known as *copolymer composition drift*.

In *batch systems* for a given pair of comonomers, M_1 and M_2, the mole fraction of monomer M_1 repeat units in the copolymer formed early in the reaction (F_1) is determined by the M_1 mole fraction initial value in the comonomer mixture (f_1). For most copolymerizations $F_1 \neq f_1$ and one monomer is consumed preferentially causing f_1 to change as the overall monomer conversion increases. This change in f_1 gives rise to a variation in F_1 with conversion leading to copolymers which consist of

copolymer molecules with significantly different compositions. This broadening of the distribution of copolymer composition clearly becomes more significant as the overall monomer conversion increases.

In $r_1 > 1$, $r_2 < 1$ copolymerizations f_1 decreases with conversion as M_1 is consumed preferentially. Eventually M_1 is consumed completely leaving some unreacted M_2 (i.e. f_1 becomes zero) and so thereafter the homopolymer of monomer M_2 is formed. In $r_1 < 1$, $r_2 < 1$ or $r_1 > 1$, $r_2 > 1$ copolymerizations f_1 changes with conversion until it becomes equal to either zero or unity and the corresponding homopolymer is formed from then onwards. When $r_1 >> r_2$ (i.e. $r_1>>1$ and $r_2<<1$) both propagating species ($M_1\bullet$ and $M_2\bullet$) preferentially add M_1 until it is consumed, afterward M_2 will homopolymerize.

Over the years different methods have been suggested to overcome the composition drift problem; a common feature was the usage of the continuous processes (e.g. semi-batch) instead of the batch process. The gradual addition of monomer should lead to control of the reaction due to an enhanced ratio of exchange reaction (independent of monomer concentration) to propagation reaction (dependent on monomer concentration). When the monomer is charged in a single shot, the polymer particles will be saturated with monomer, favoring the propagation reaction over the exchange reaction, consequently leading to composition drift. On the other hand, when the monomer is gradually charged, the particles will tend to be monomer-starved, favoring the exchange reaction that leads to control of the composition (Rivera et al., 2005).

The control addition of the comonomers to the reactor and preventing monomers buildup in the reactor (*known as starved conditions*) help to control the copolymer composition and leads to the creation of copolymer compositions at the desired levels. Keeping the monomers at minimum concentrations in the reaction vessel leads to the instantaneous conversion (>90% conversion) of the added monomers upon entering the reactor; hence the copolymer formed must have the same

overall composition as that of the comonomer mixture added. More discussion about this scenario is given in section 3.4.

1.2.4. Azeotropic Copolymerization

Figure 1.2 shows several curves for non-ideal cases of feed f versus instantaneous composition F. The curves will cross the line $F_1 = f_1$; at the point of intersection the polymerization proceeds without a change in the composition of either the feed or the copolymer. This is known as *azeotropic copolymerization.*

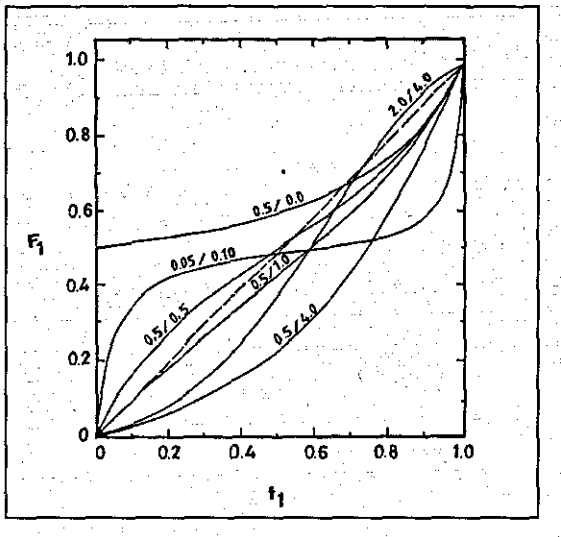

Figure 1.2 Instantaneous composition of copolymer (F_1) as a function of monomer composition (f_1) for different reactivity ratios (r_1/r_2)
(source: Ebewele , 2000)

Applying $F_1 = f_1$ in Eq 1.19 yields the critical composition of the azeotrope

$$(f_1)_c = \frac{1-r_2}{2-r_1-r_2} \qquad 1.20$$

or solving Eq 1.17 with $d[M_1] / d[M_2] = [M_1] / [M_2]$ gives

$$\frac{[M_1]}{[M_2]} = \frac{1-r_2}{1-r_1} \qquad 1.21$$

Next the emulsion polymerization process will be discussed; some fundamentals related to this process and the different components used in this system and their role will be carefully explained. It should be noted that the discussion of the copolymerization rate behavior is given at the end of chapter two instead of chapter one and the reason for this is the fact that the copolymerization rate is affected by the emulsion components and the nucleation process; obviously discussing those aspects should be done prior to the copolymerization rate.

2. Emulsion Polymerization

Emulsion polymerization is a heterogeneous polymerization that takes place in an emulsion typically incorporating water, monomer, surfactant, and initiator. The most common type of emulsion polymerization is an oil-in-water emulsion, in which droplets of monomer (the oil) are emulsified (with surfactants) in a continuous phase of water. The major developments in emulsion polymerization started around the Second World War for producing synthetic rubbers from 1,3-butadiene and styrene (styrene-butadiene rubber).

The emulsion polymerization process has several advantages. The continuous water phase is an excellent conductor of heat and allows the exothermic heat of reaction to be removed from the system. The final product, referred to as *latex*, can be used as is and does not generally need to be altered or processed. Moreover, there is one very significant advantage for emulsion polymerization. The molecular weight of a polymer can be controlled without altering the polymerization rate by using chain-transfer agents. In other polymerization processes, this cannot be done without altering the polymerization rate.

Emulsion polymerization is presently the predominant process for the commercial polymerizations of vinyl acetate, methacrylates, chloroprene, and various acrylate copolymerizations. Such applications include paints, coatings, finishes, and floor polishes.

2.1. Typical Ingredients and their Role

The main components of emulsion polymerization are the monomer(s), dispersing medium, emulsifier, and initiator.

2.1.1. Dispersing Medium

The *dispersing medium* is the liquid in which the various components are dispersed by means of the emulsifier. This medium is usually water in an attempt to

avoid the hazards associated with solvent-based emulsions. The quality of the water used in emulsion polymerization is important. De-ionized water may be used since the presence of foreign ions can interfere with both the initiation process and the action of the emulsifier. However, because oxygen is a free-radical scavenger which might delay the polymerization, the water should be deoxygenated, by purging with nitrogen (N_2) for instance. The usual ratio of water to monomer(s) is generally in the range 70/30 to 40/60 on a molar basis (Araujo et al., 2001).

2.1.2. Emulsifier

Emulsifiers (known as *surfactants or soaps*) are the key formulation ingredients in the emulsion polymerization process. The surfactants' main roles are to stabilize the monomer droplets to prevent coalescence, serve as the site for nucleation of particles, and stabilize the latex particles and the growing polymer particles to prevent agglomeration.

The action of the emulsifier is due to its molecules having both hydrophilic and hydrophobic ends and therefore they will be attracted to the surface of the polar water phase. Surfactants first will line up along the surface of the polar phase, and when that is completely filled up (corresponding to the *critical micelle concentration*, CMC), they will begin to form grouping of surfactant molecules where either the hydrophobic (in a polar continuous phase) or the hydrophilic (in a non-polar continuous phase) ends cluster inward to escape the continuous phase. Those groupings are known by *micelles*, and they are of different shapes and size, depending on the surfactant concentration and the nature of the surfactant molecules.

Anionic surfactants such as sodium lauryl (dodecyl) sulfate (SLS, $C_{12}H_{25}NaO_4S$) and sodium dodecylbenzene sulfonate are the most commonly used surfactants in emulsion polymerization. The sulfates and sulfonates group emulsifiers are useful for polymerization in acidic media (§2.1.5). *Non-ionic surfactants* such as poly(ethylene oxide), poly (vinyl alcohol) and hydroxyethyl cellulose are of use where the final polymer latex should be insensitive to changes in pH over a wide

range. Nonionic surfactants are only infrequently used alone, since their efficiency in producing stable emulsions is less than that of the anionic surfactants. Anionic and nonionic surfactants could have some effects on the initiator efficiency; more discussion is given in section 3.1. *Cationic surfactants* such as dodecylammonium chloride and cetyltrimethylammonium bromide are much less frequently used than anionic surfactants because of their inefficient emulsifying action, undesirable effects on initiator decomposition, and their cost compared to the anionic surfactants.

Increasing the surfactants' concentration increases the polymer particle number and decreases the particle size. However, the delayed addition of surfactant after the nucleation stage improves particle stability and does not affect the particle number, size, and size distribution.

Typical values of CMC	0.001 – 0.1 mol L^{-1}
Typical micelles dimensions	2-10 nm
Number of surfactant molecules in a micelle (i.e. aggregation number)	50-150
Micelle concentration	10^{19}-10^{21} L^{-1}
Concentration of monomer drops	10^{12} – 10^{14} L^{-1}
Monomer drops diameters	1-100 μm

Table 2.1 Typical values associated with emulsion polymerization
(source: Odian, 2004)

Typical values of CMC are between 0.001-0.1 mol/L (Table 2.1); and most of surfactants having values in the lower end; for instance, the CMC of SLS is 0.0081 mol/L (Araujo et al., 2001). The *aggregation number* for most surfactants lies between 50-150 surfactant molecules/micelle; for SLS, the aggregation number is in fact 80 molecules/micelle.

The concentration of the micelle is basically estimated with the help of the aggregation number, and the amount of surfactant in the recipe. Yet it should be noted

that the CMC and the aggregation number are markedly affected by the reaction medium. Corrin and Harkins (1947) reported that the addition of a small quantity of electrolyte to the system (e.g Potassium persulfate, $K_2S_2O_8$) reduces the CMC of the surfactant (anionic and cationic), but the effect becomes less with increasing the electrolyte concentration.

Stigter and Mysels (1955) demonstrated that the aggregation number of SDS increased with increasing NaCl concentration. Increasing the NaCl concentration from 0M to 0.1M increased the aggregation number of SDS from 80 to 112. Blackly (1975) explains that the reduction in the CMC will not affect the number of micelles; it will make the micelles larger and increase their effective ionic charge. However, others (e.g. Kamath, 1973) reported that the extra surfactant will generate more micelles leading to higher polymerization rates. Full et al. (1996) reported that smaller particles are achieved with increasing the electrolytes (e.g. K_2SO_4) concentrations (Carillo et al., 2007). In addition, CMC is also affected by the presence of some hydrophobic monomers (e.g. Styrene) leading to larger values (Gilbert, 1995).

2.1.3. Monomers

The water solubilities of most *monomers* are quite low (Table 2.2). When a water-insoluble or slightly water-soluble monomer is added, a very small fraction dissolves in the continuous aqueous phase.

Monomer	Solubility (g/100 g water)
Acrylic acid	Total
Butadiene	0.081
Butyl acrylate	0.16 (25°C)
Ethylene	0.9 (80°C, 4500 psig)
Methyl methacrylate	1.59 (20°C)
Styrene	0.027 (25°C)
Vinyl acetate	2.4 (20°C)

Table 2.2 Water-solubilities of some common monomers
(source: Araujo et al., 2001)

The amount of monomer in micelles compared to that in solution is much greater for the water-insoluble, non-polar monomers; it might reach up to 40-fold depending on the monomer type (Odian, 2004). The largest portion of the monomer (>95%) is dispersed as monomer droplets which are stabilized by surfactant molecules absorbed on to their surfaces. The droplets size depends on the agitation intensity and they usually vary between 1-100 μm. Comparing the droplets sizes to the monomer-containing micelles (Table 2.1), it is clear that the monomer droplets are much larger than the monomer-containing micelles. Consequently, the number concentration of micelles is more than the number concentration of monomer droplets, and the total surface area of the micelles is larger than that of the droplets by more than two orders of magnitude.

2.1.4. Initiators

The most commonly used water-soluble *initiators* are ammonium and potassium persulfate, which dissociates in the aqueous phase into two sulfate radical anions which can initiate the polymerization (Fig 2.1). Redox initiators, typically a mixture of an oxidizing agent and a reducing agent, whose reactions generate radicals (such as succinic acid peroxide) have also been used (Lovell and El-Aasser, 1997). They are typically useful for polymerization at low temperatures to produce high molar mass polymers with lower degree of branching.

Previously, it was demonstrated that the existence of electrolyte in the system (e.g. Potassium persulfate, $K_2S_2O_8$) reduces the CMC of the surfactant. In addition, the persulfate decomposition produces bisulfate anion leading to a drop in the pH of the medium during the course of the decomposition. Therefore, reactions are usually carried out in buffer solutions (e.g. $NaHCO_3$, §2.1.5) so that the pH remains constant (Blackly, 1975).

Under acidic conditions (pH<3), Kolthof and Miller (1951) reported that the rate coefficient of $K_2S_2O_8$ increases sharply which in return reduces the half-life of the initiator (i.e. time for the concentration of the initiator to decrease to one half its

original value). This effect could be a result of the dissociation of the oxygen from the persulfate ion in strongly acidic solution, whereas in alkaline or neutral media the source of the oxygen is the water.

$$K_2S_2O_8 + H_2O \rightarrow 2KHSO_4 + \frac{1}{2} O_2 \qquad 2.1$$

The *half-life* of $K_2S_2O_8$ was reduced from over 110 hours at pH>3 to less than 20 hours at pH=1. The initiator half-life ($t_{1/2}$) is calculated using the following equation

$$t_{1/2} = 0.693 / k_d \qquad 2.2$$

Where k_d is the initiator decomposition rate constant (s^{-1}).

Another important property is the *initiator efficiency*. Performing material balance on the amount of initiator that is decomposed during a polymerization and compared with that which initiates polymerization, it was found that initiator was inefficiently used. Dunn and Taylor (1965) concluded that 60% of the persulfate radicals were effective in initiating polymerizations.

2.1.5. Other Components

Various other components may also be present in the emulsion system. A variety of *chain-transfer agents* (CTAs), such as mercaptans, are used primarily to control the molar mass of the polymer. CTAs have the ability to stop the growth of a molecular chain by yielding an atom to the active radical at the end of the growing chain; however the CTA in turn is left as a radical which can initiate the growth of a new chain.

Buffers such as sodium bicarbonate ($NaHCO_3$) are often added to the formulation to control the pH of the reacting system. Some monomers undergo hydrolysis reactions at elevated pH values, while they remain stable at lower pH. In addition, under acidic conditions (§2.1.4) the decomposition of persulfate initiators

increases leading to a reduction in the number of free radicals in the polymerizing system. Consequently, the conversion will decrease.

2.2. Particle Nucleation

2.2.1. Heterogeneous (Micellar) Nucleation

The type of initiator used distinguishes emulsion polymerization from other types of polymerization. Oil-soluble initiators are used in suspension polymerization and the reaction occurs in the monomer droplets, whereas in emulsion polymerization, the initiator used is *water-soluble initiator*, so the initiator is present in the aqueous phase where it dissociates generating radicals.

In Smith-Ewart theory (§2.4), the site of polymerization is not the monomer droplets since the initiators employed are insoluble in the organic monomer. Instead, polymerization takes place almost exclusively in the micelles. Most of the radicals produced are captured by the micelles since the total surface area of the micelles is much larger than that of the monomer droplets. Although polymerization of the monomer in solution can take place, it does not contribute significantly to the overall conversion since the monomer concentration is low.

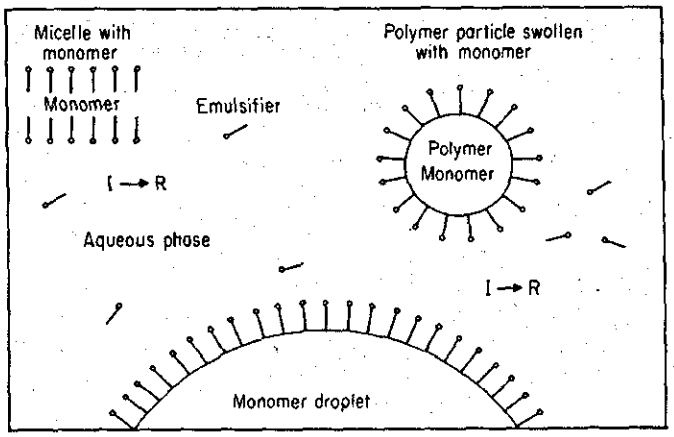

Figure 2.1 Simplified representation of an emulsion polymerization system
(source: Odian, 2004)

The micelles are rich with monomer compared to the monomer in solution; therefore they act as a meeting place for the organic (oil-soluble) monomer and the water-soluble initiator. As polymerization proceeds, the micelles grow by the addition of monomer from the aqueous solution, whose concentration is replaced by dissolution of monomer from the monomer droplets.

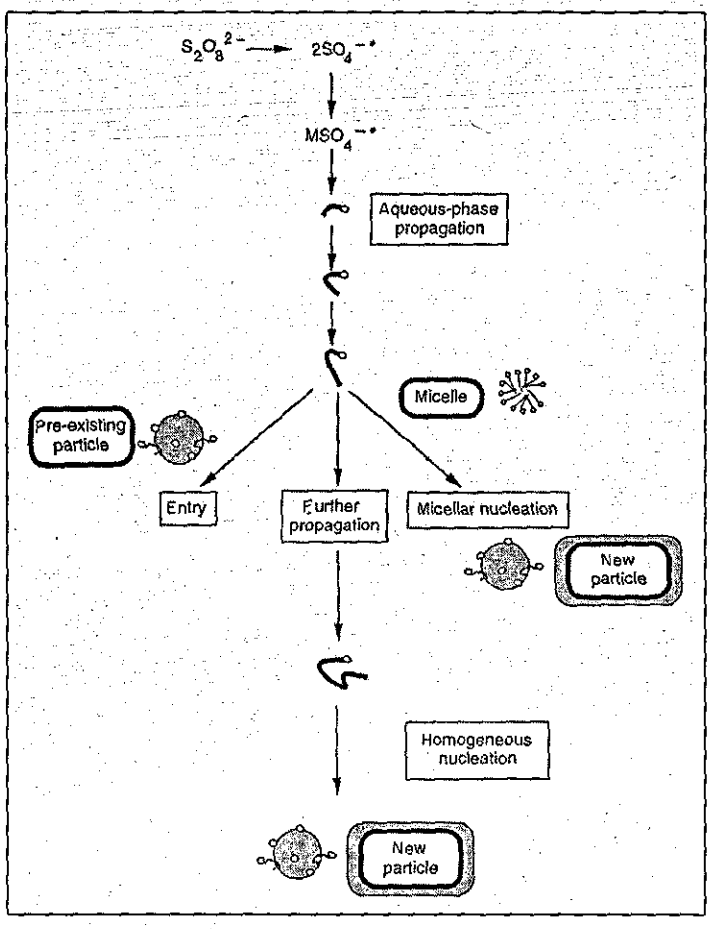

Figure 2.2 Simplified illustration of the emulsion polymerization homogeneous and heterogeneous nucleation (taken from Gilbert, 1995)

The emulsion polymerization system (Fig 2.1) consists of three types of particles: monomer droplets, inactive micelles in which polymerization is not occurring, and active micelles in which polymerization is occurring (referred to as

polymer particles). In the figure, an emulsifier molecule is shown as o— to indicate one end (o) is polar or hydrophilic and the other end (—) non-polar or hydrophobic.

Next, the sequence of events that leads to the formation of the polymeric particles in emulsion polymerization will be discussed. An illustration of this process is given in figure 2.2. At first, the initiator (e.g. potassium persulphate) starts to decompose at high temperatures (low temperatures in the case of some redox initiators) in the continuous phase (e.g. aqueous solution) producing initiator radicals. Due to high number of micelles and greater surface area, the initiator radicals are captured by the surfactant micelles.

Monomer which exists in the monomer drops dissolve in the water, and transfers to the hydrophobic environments provided by the micelles. When an initiator radical enters monomer-swollen micelle, it activates the micelle and polymerization starts; the micelle is now classified as polymer particle. The radical within the micelle reacts with the monomer producing monomeric radicals and continues propagating converting the monomer within the particles in to polymer. The monomer that is being converted in to polymer is continuously replaced by monomer mass-transfer from the monomer drops to the polymer particles.

When all the monomer in the drops is consumed, the drops disappear and the system starts to consume the dissolved monomer. As propagating continues, the monomer mass fraction in the particles is decreasing in favor of the polymer mass fraction. This could lead to an increase in the viscosity inside the particles.

When a radical enters a growing particle, it could react with a growing polymeric chain leading to an instant termination, or if a growing chain does not exist due to previous termination, then the radical might start a new chain. The increase in the viscosity inside the particles could lead to a reduction in the termination process due to the fact that the mobility of the chains is affected by the increase in the viscosity reducing the rate at which the radicals terminating the growing chains

(*known as autoacceleration or gel effect, §2.3*). The process of terminating growing chains and starting new ones will eventually lead to large number of dead chains in the polymeric particles. The molecular mass of these chains could be of the order 10^6 (Gilbert, 1995).

2.2.2. Homogeneous Nucleation

Homogeneous particle nucleation occurs when radicals generated in the aqueous phase propagate by adding monomer units to form water-soluble short-chain radicals (*known as oligomers*). When the oligomeric-radicals reach the limit of their solubility in the water they start to precipitate out of solution. The precipitated oligomeric radicals form primary particles which stabilize by absorbing surfactant (from solution, monomer droplets, and micelles) allowing further propagation and growth by absorbing monomer, polymerization, and by coagulation. The subsequent absorption of monomer is equivalent to micellar nucleation.

The extent of homogeneous nucleation is affected by the solubility of the monomers and the concentration of the surfactant in the continuous phase. More soluble monomers are more likely to undergo homogeneous nucleation more than less soluble monomers. Araujo et al. (2001) investigated several copolymerization systems and revealed that the number of particles increased with the solubility of the monomers.

When the surfactant concentration is well above the CMC, micellar nucleation is the predominant nucleation process. Around the CMC, homogeneous nucleation is present, but micellar nucleation is still the predominant process of nucleation. Working below the CMC, micelles are absent and only homogeneous nucleation occurs.

2.3. Polymerization Rate Behavior

In emulsion polymerizations, the polymerization rate behavior depends on the particle number density N_p (the concentration of polymer particles in units of number

of particles per litre) and the existence of monomer droplets in the reaction vessel. In *batch systems*, three intervals (I, II, III) can be observed (Figures 2.3 and 2.4). There is a separate monomer phase in intervals I and II but not in III. The particle number increases with time in interval I and then remains constant during intervals II and III.

Interval I: The main ingredient that controls this step is the *surfactant*. Particle nucleation occurs in this interval, with the polymerization rate increasing with time as the polymer particle number builds up.

As explained earlier, the monomer transfers from the monomer droplets to the aqueous phase, and then diffuses into the polymer particles to replace that which has reacted. As the polymer particles grow in size and contain polymer as well as monomer, in order to maintain stability they absorb more and more surfactant from that in solution. When the surfactant concentration in solution falls below its CMC, the inactive micelles become unstable and disappear.

By the end of interval I almost all of the surfactant in the system has been adsorbed by the growing polymer particles leading to a relatively unstable monomer droplets which will coalesce if agitation is stopped. The duration of this interval depends on the initiation rates and the solubility of monomers.

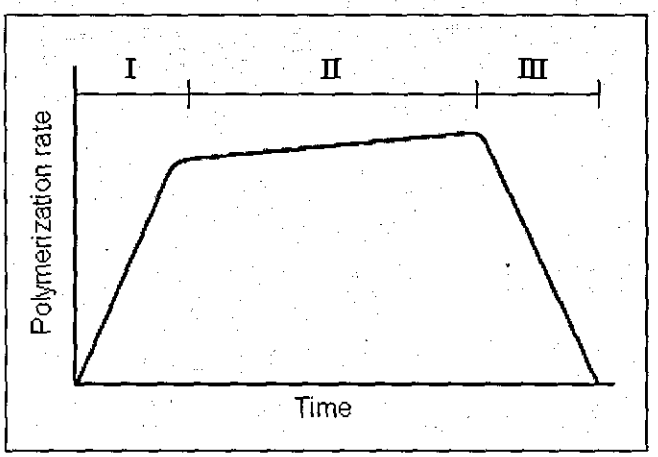

Figure 2.3 Polymerization rate stages in emulsion polymerization
(source: Ebewele, 2000)

Low initiation rates lead to a longer Interval I since more time is needed to attain the steady-state particle number, on the other hand, the more water-soluble monomers tend to complete interval I faster as a consequence of the existence of homogeneous nucleation occurring simultaneously with micellar nucleation, resulting in achieving the steady-state particle number sooner. Usually this interval counts for 5-20% conversion.

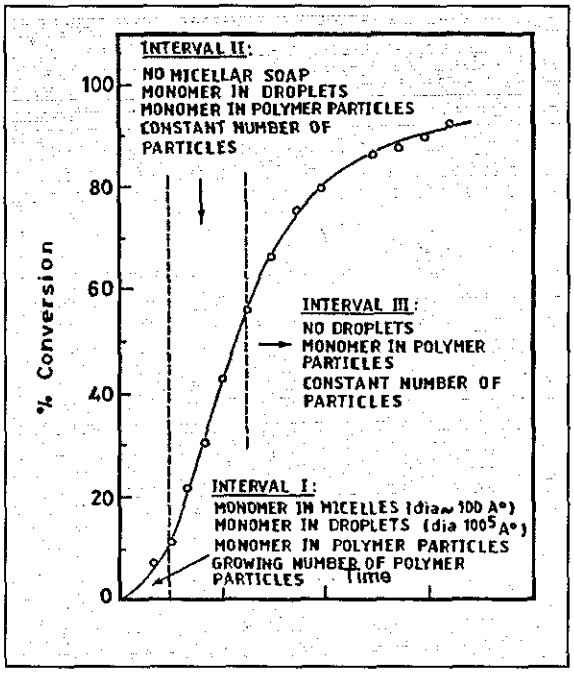

Figure 2.4 Conversion stages in a batch emulsion polymerization
(source: Ebewele, 2000)

Interval II: The existence of *monomer droplets* is the main feature of this interval. Polymerization proceeds in the polymer particles as the monomer concentration in the particles is maintained at the equilibrium (saturation) level by diffusion of monomer from solution, which in turn is maintained at the saturation level by dissolution of monomer from the monomer droplets. The polymerization rate is either constant due to constant number of particles or increases slightly with time as a consequence of the gel effect (*known as Trommsdorff or autoacceleration effect*).

The *gel effect* is due to an increase in the viscosity of the reaction mixture inside the polymer particles as the polymer chains form (§2.2.1). This high viscosity hinders the diffusion of chains because of entanglements, so the rate of termination slows considerably. However, the diffusion of small molecular monomers is hardly affected by viscosity, so propagation proceeds as before. In addition, initiator continues to add more free radicals to the system, chains grow without termination, so the conversion is rapid and the Molecular Weight (MW) is high. In this interval, the polymer particles increase in size as the monomer droplet sizes decrease.

Interval II ends when the monomer droplets disappear. The duration of this interval is controlled by the mass transfer limitations and the water solubility of the monomers. If the water solubility is high interval II could end at lower conversions since the drop in the total monomer contained in the droplets is quick, causing the transition at lower conversions. Low mass transfer rates of monomer from the monomer droplets to the aqueous phase increases the duration of this step.

Interval III: The particle number remains the same in interval III as in interval II, but the monomer concentration in the system decreases with time, since *monomer droplets are no longer present* to replace what is being absorbed by the polymer particles. The decrease in the concentration is slower with the more water-soluble monomers as the monomer in solution acts as a reservoir. The presence of a gel effect continues in interval III. Polymerization rate gradually decreases as the monomer concentration in the polymer particles decreases. Final conversions of 100% are usually achieved. The final polymer particles, spherical in shape, usually have diameters of 50–300 nm.

The discussion of the *polymerization rate behavior for a semi-batch system* is almost similar to the previous one. The semi-batch systems behavior is solely based on the chosen recipe and the addition procedure. If the surfactant is being added along the course of reaction and the concentration of the surfactant is maintained above the CMC, interval I will not end until the surfactant feed is stopped and it is fully

consumed. If monomers are added to the system, interval II will be longer. If the system is operated at the end in a batch mode to achieve 100% conversion, behaviour similar to figures 2.3 and 2.4 is expected during the batch region.

2.4. Polymerization Rate (Smith-Ewart Kinetics)

2.4.1. Homopolymerization

The *batch emulsion polymerization rate* differs in the three intervals. Micelles and polymer particles exist at interval I, and only polymer particles exist in intervals II, and III. So in the beginning, considering the polymerization rate of a single polymer particle –active micelle– (r_p), r_p depends on the propagation rate constant (k_p) and the monomer concentration $[M]_p$ in the particle

$$r_p = k_p [M]_p \qquad 2.1$$

The rate of polymerization (R_p) at any instant is given by the product of the concentration of active particles [P•] and the rate of propagation in a single particle

$$R_p = k_p [M]_p [P\bullet] \qquad 2.2$$

Since micelles and polymer particles exist at interval I, and only polymer particles exist in intervals II and III, [P•] can be expressed as

$$[P\bullet] = ([m] + [P]) \bar{n} / N_A \qquad 2.3$$

where [m] and [P] are the concentrations of micelles and particles (L^{-1}), $\bar{n}$ is the average number of radicals per micelle plus particle, and N_A is Avogadro number introduced to express [P•] in molar units (mol/L). Therefore, the polymerization rate expression can be expressed as

$$R_p = k_p [M]_p ([m]+[P]) \bar{n} / N_A \qquad 2.4$$

where R_p is expressed in mol L^{-1} s^{-1}. Most of the monomer conversion to polymer takes place in intervals II, and III. So eliminating the concentration of micelles leads to

$$R_p = k_p [M]_p [P] \bar{n} / N_A \qquad 2.5$$

Clearly from the previous discussion, the average number of radicals per particle ($\bar{n}$) is important in determining the polymerization rate. Smith-Ewart (1948) considers three different situations for $\bar{n}$. *Case 1* where the average number of growing chains per reaction locus is very small relative to unity, *case 2* where the average number of growing chains per reaction locus equals 0.5, and *case 3* where the average number of growing chains per reaction locus is large relative to unity (Blackly, 1975).

Case 1 ($\bar{n}$ < 0.5): If the radical desorption from particles is high and the radical termination in the aqueous phase is not negligible, $\bar{n}$ is considered < 0.5. Other factors such as small particle sizes, low initiation rates, and monomers with high water solubility also contribute to a decrease in $\bar{n}$. Vinyl acetate follows this case.

Case 2 ($\bar{n}$ = 0.5): Many systems are believed to conform to this case (Odian, 2004). If the rate of radical desorption does not occur or negligible compared to the rate of radicals entering particles (absorption), and if the particle size is too small to contain more than one radical (valid for D[4,3] ≤ 120 nm; Blackly, 1975), the trapped radical undergoes propagation until another radical enters and instantaneously terminates the reaction. For this system $\bar{n}$ is given a value = 0.5 and it is known as "zero–one system" since the polymer particles contain one radical and are growing, or contain no radicals and are inactive. This suggests that at any given moment half the polymer particles are active and growing, and the other half are dead. This assumption is noticeably assumed in the texts; however others (Gilbert, 1995) argued that this is not actually happening and $\bar{n}$ is actually ≤0.5.

Case 3 ($\bar{n} > 0.5$): When the particle size is large such that two or more radicals can coexist in a polymer particle without instantaneous termination, if the initiation rate is high, and if the termination rate in the aqueous phase and desorption are both negligible; $\bar{n}$ is considered > 0.5. This effect is more likely to occur as the particle size and percent conversion increase and due to gel effect (§2.2.1 and §2.3).

Araujo et al. (2001) demonstrated that the systems Sty/MMA (70/30), Sty/MMA (30/70), and the system Sty-BuA (70/30) follow Smith-Ewart case 2 ($\bar{n}$= 0.5) at low conversions, and increase at higher conversions due to gel-effect. Increasing the acrylate monomer composition led to an apparent increase in the n at lower conversions (30/70 Sty-MMA).

2.4.2. Homogeneous Copolymerization

Copolymerization models were used to predict the overall propagation rate, and the composition of the resulting copolymer. One of the early and straightforward models is the one called *terminal model* (*known as Mayo-Lewis* or *first order Markov*); in this model it is assumed that the reactivity of the propagation reaction is dominated by the nature of the terminal unit of the polymer radical.

This model was widely accepted as the bases of the copolymerization kinetics and thought to be able to describe most of copolymerization systems, and the systems which did not follow this model were thought to be exceptions. Fukuda et al. in 1985 and others have demonstrated that almost general failure of the terminal model to describe both the propagation rate and the composition in the free-radical copolymerization simultaneously. Therefore, other earlier models (*penultimate or second order Markov*) started to get more considerations.

A popular model is the *implicit penultimate model* where it was assumed that both the terminal and the penultimate units of the polymer radical affect its reactivity, but only the terminal unit affects its selectivity. Another model is the *explicit (or complete) penultimate model* where it was suggested that both the terminal and the

penultimate units of the polymer radical affect the reactivity and the selectivity. Next, the kinetics of those models will be presented.

The homogeneous rate of copolymerization (R_p) for a batch process can be expressed as follows (Ma et al., 2001)

$$R_p = (\bar{k}_p / \bar{k}_t^{1/2})\, R_i^{1/2}\, [M] \qquad 2.6$$

where [M] is the concentration of the monomers, $\bar{k}_p$ and $\bar{k}_t$ are the average propagation and termination rate constants (§1.1.1), and R_i is the rate of initiation expressed as

$$R_i = 2 f k_d\, [I] \qquad 2.7$$

where f is a factor which expresses the efficiency of the initiator (§1.1.1), k_d is the *initiator dissociation rate constant, and [I] is the initiator concentration.*

The average termination rate constant ($\bar{k}_t$) is taken as the average of the homopolymerization termination rate constants (k_{t1} and k_{t2}), each weighed on the basis of the copolymer composition in mole fraction (F) and it takes the following form (Fukuda et al., 1985)

$$\bar{k}_t = F_1\, k_{t1} + F_2\, k_{t2} \qquad 2.8$$

The average propagation rate constant based on the terminal model can be expressed as (Fukuda et al., 1985)

$$\bar{k}_p = \frac{r_1 f_1^2 + 2 f_1 f_2 + r_2 f_2^2}{(r_1 f_1 / k_{11}) + (r_2 f_2 / k_{22})} \qquad 2.9$$

where r_i is the reactivity ratio, k_{ii} is the rate constant for radical i to add monomer i, and f is the comonomer feed composition. Fukuda and coworkers reported that the failure of the terminal model is expected for most systems (Table 2.3).

Comonomers	Temp, °C	Terminal model predicts $\bar{k}_p$
STY/MMA	17.9 – 57.2	No
MMA/BMA	30	Yes
STY/BA	25, 50	No
MMA/BA	20, 60	No

Table 2.3 Various copolymer systems tested for terminal model
STY = styrene; MMA = methyl methacrylate; BMA = butyl methacrylate; BA = butyl acrylate

The *explicit penultimate model* describes the average propagation rate as

$$\bar{k}_p = \frac{\bar{r}_1 f_1^2 + 2 f_1 f_2 + \bar{r}_2 f_2^2}{\left(\bar{r}_1 f_1 / \bar{k}_{11}\right) + \left(\bar{r}_2 f_2 / \bar{k}_{22}\right)} \qquad 2.10$$

where the adjusted parameters $\bar{r}_i$ and $\bar{k}_{ii}$ are expressed as follows

$$\bar{r}_i = r_i' \frac{\left(f_i\ r_i + f_j\right)}{\left(f_i\ r_i' + f_j\right)} \qquad 2.11$$

$$\bar{k}_{ii} = k_{iii} \frac{\left(f_i\ r_i + f_j\right)}{\left(f_i\ r_i + f_j / s_j\right)} \qquad 2.12$$

and the four different monomer reactivity ratios (r_i and r_i') and the two radical reactivity ratios (s_i) are calculated as follows

$$r_i = k_{iii} / k_{iij},\ r_i' = k_{jii} / k_{jij},\ \text{and}\ s_i = k_{jii} / k_{iii} \qquad 2.13$$

where $i, j = 1$ or 2 and $i \neq j$, and k_{ijm} is the rate constant for the penultimate (i), the terminal (j), and the monomer (m) units. This model was fully described by Fukuda et al. in 1987 and it replaced their original *implicit penultimate model*

The *implicit penultimate model* (Fukuda et al., 1985) was proposed for the copolymerizations where the terminal model successfully describes the copolymer composition, but fails to describe the propagation rate and rate constants. Ma et al. in 2001 studied the system styrene (M1) and diethyl fumarate (M2), and their system conforms to this model (Figures 2.5 and 2.6).

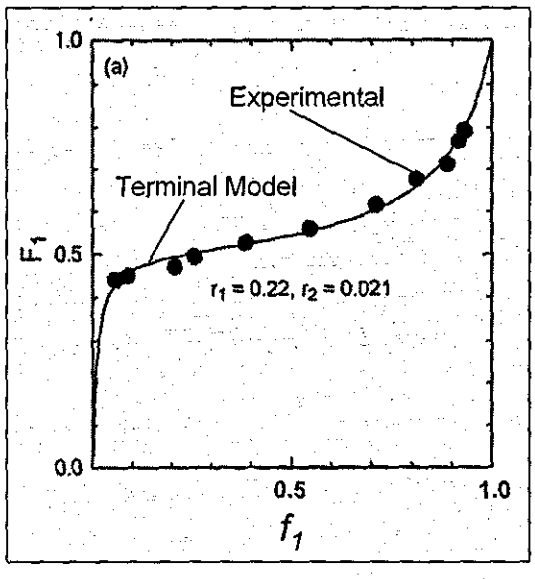

Figure 2.5 Copolymer composition (F_1) vs. feed composition (f_1) for the copolymer styrene (M1) diethyl fumarate (M2)
(Source: Ma et al., 2001)

Garcia et al. (1999) confirmed that like the majority of the Sty/alkyl acrylate systems, the system Sty/BuA can be modeled by the implicit penultimate model. It should be noticed that the main assumption in this model was (based on the composition data) that the penultimate unit affects the reactivity but not the selectivity (i.e. $r_i = r_i'$) so only s_i is the unknown. This assumption simplified 2.11 into the form (Coote and Davis, 1999)

$$\overline{r_i} = k_{ii} / k_{ij} \qquad 2.14$$

where $i, j = 1$ or 2 and $i \neq j$.

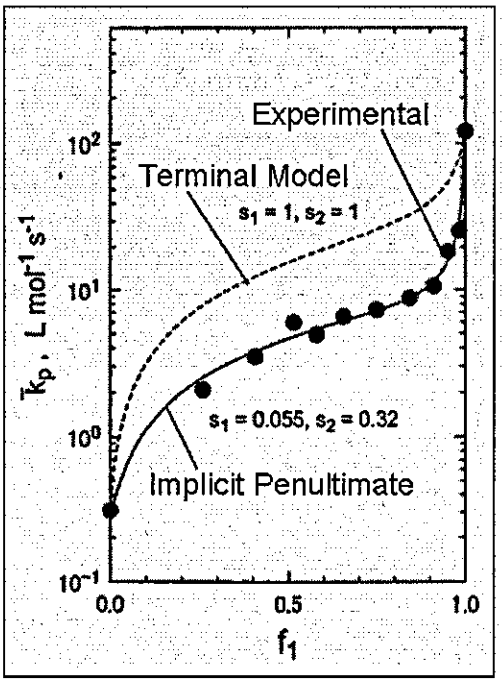

Figure 2.6 Propagation rate constant vs. feed composition (f_1) for the copolymer styrene (M1) diethyl fumarate (M2)
(Source, Ma et al., 2001)

In summary, the *terminal model for copolymerization* gives expressions for copolymer composition (Eqs. 1.17 and 1.19), propagation rate constant (Eq. 2.9), and polymerization rate (Eq. 2.6). The *explicit penultimate model* gives expressions for copolymer composition (Eqs. 1.17 and 1.19) where $\bar{r}_i$ is calculated according to 2.11 (i.e. penultimate effect on the reactivity), propagation rate constant (Eq. 2.10) where $\bar{k}_{ii}$ is calculated according to 2.12 (i.e. penultimate effect on the propagation), and polymerization rate (Eq. 2.6). The *implicit penultimate model* gives expressions for copolymer composition (Eqs. 1.17 and 1.19) where $\bar{r}_i = r_i = r_i'$ (i.e. there is no penultimate effect on the reactivity), propagation rate constant (Eq. 2.10) where $\bar{k}_{ii}$ is calculated according to 2.12 (i.e. penultimate effect on the propagation), and polymerization rate (Eq. 2.6).

Finally, several workers concluded that the *explicit penultimate model* should be considered the base model for the copolymerization kinetics (Coote and Davis, 1999) although other models are being developed and investigated.

2.5. Number of Polymer Particles

From the polymerization equation, it is apparent that the number density of polymer particles (N_p) is of critical importance in determining the polymerization rate (R_p). In the Smith-Ewart theory, where the micelles are the main sites of polymerization, the number of polymer particles is given by

$$N_p = \chi\,(\rho/\mu)^{0.4}\,(\omega \cdot S)^{0.6} \qquad 2.15$$

where ρ is the rate of radical generation, μ is the rate of particle volume growth, ω is the area occupied by a surfactant molecule, S is the surfactant concentration in the micelles neglecting the dissolved surfactant, and χ is a constant whose value is between 0.53 and 0.37 (Blackley, 1975).

Equation 2.15 is valid for Smith-Ewart case 2 ($\bar{n}$=0.5, §2.4.1). It should be noted that Smith-Ewart made several assumptions to simplify the problem. For instance, it was assumed that micellar nucleation is the only nucleation process, the transfer out of the particles does not occur, and that the entry of a second radical leads to an instant termination.

Nomura et al. in 1976 considered the chain transfer of radicals to monomer and the radicals absorption/desorption/re-absorption during interval I and came up with this equation

$$N_p = \chi\,(\rho/\mu)^{1-z}\,(\omega \cdot S)^{z} \qquad 2.16$$

where 0.6< z <1.0 and depends on the chain transfer constant and water solubility of the monomer.

Smith-Ewart theory predicts that the relations between the final number of polymer particles and the concentrations of the surfactant (figure 2.7) and the initiator take the flowing forms respectively

$$N_p \propto [S]^{0.6} \qquad 2.17$$

$$N_p \propto [I]^{0.4} \qquad 2.18$$

It should be noted that minor modifications of the Smith-Ewart assumptions will drive the exponent values from 0.4 and 0.6. Actually, Nomura et al. (1976) has shown that radical desorption from the particles increases the order of dependence exponent on the surfactant concentration from 0.6 to 1.0 and decreases the initiator dependence exponent from 0.4 to 0.

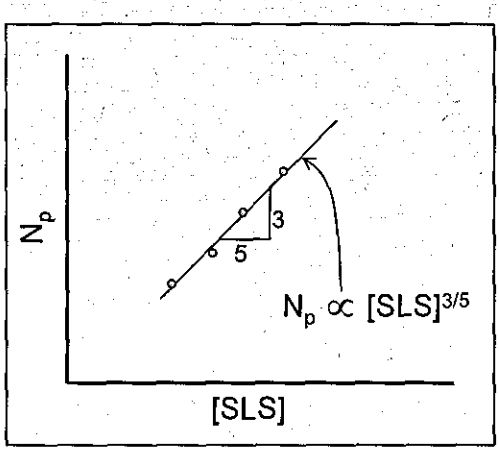

Figure 2.7 Dependence of the final number of polymer particles on the surfactant concentration (Smith-Ewart case 2)

The number of polymer particles based on the conversion and the size of the particles takes the following form (Araujo et al., 2001)

$$N_p = \frac{6M_T x_m}{\rho_p \pi d_p^3} \qquad 2.19$$

where M_T is the initial total monomer concentration (g/cm^3 of water), ρ_p is the polymer density (g/cm^3), d_p is the average particle diameter (cm), and x_m is the total weight conversion. This formula assumes that the particles contain only polymer.

2.6. Monomer Partitioning

2.6.1. Models for Estimation of Monomer Concentrations in Different Phases

In homogeneous polymerization (i.e. bulk or solution), the reactions occur in a single phase whereas in heterogeneous polymerization (i.e. emulsion or suspension), the reactions are affected by the existence of several phases in the reactor (e.g. micelles, monomer drops, polymer particles, and the suspension medium). Previously (§2.2) it was demonstrated that in emulsion systems, polymerization takes place almost exclusively in the micelles (Smith-Ewart). Therefore, estimating the concentration of the monomers in the particles is of a great importance to understand the polymerization rate, copolymer composition, and the polymer microstructure.

The rate of mass transfer of monomer between the different phases of the system is high enough for thermodynamic equilibrium of monomers between the phases to be achieved. Therefore, it is widely accepted that the monomer concentration inside the particles is controlled by thermodynamic considerations only (Gilbert, 1995)

Morton et al. (1954) monomer partition model is considered the most complete description of the monomer partitioning; therefore other models predictions are usually compared to the predictions by the Morton model (Gugliotta et al., 1995). Urretabizkaia and Asua implemented a simple monomer partition model (i.e. constant partition coefficients model, CPC) which is inspired by a method proposed by Omi et

al. (Urretabizkaia and Asua, 1994). Gugliotta et al. (1995) investigated the predictions of this model and was compared to Morton et al. and Maxwell and coworkers models

The main advantage of the CPC model (Appendix C) over Maxwell and Morton models is that most of the parameters that are required to solve Morton and Maxwell models are not required to solve the equations of this model. For instance, the CPC model does not depend on the existence of the monomers drops, therefore systematically checking the existence of the monomer drops is not a requirement to solve the equations .

Gugliotta et al. (1995) investigated the behavior of the system BuA (A) and Sty (B) copolymerization in a batch reactor by the three aforementioned. Figures 1, 2, and 3 illustrates the predictions of the instantaneous conversion of monomers A and B (xA, xB), the overall conversion (x), and the cumulative (YA) and instantaneous molar copolymer compositions (YA,inst). It should be noted that subscript A refers to the BuA monomer.

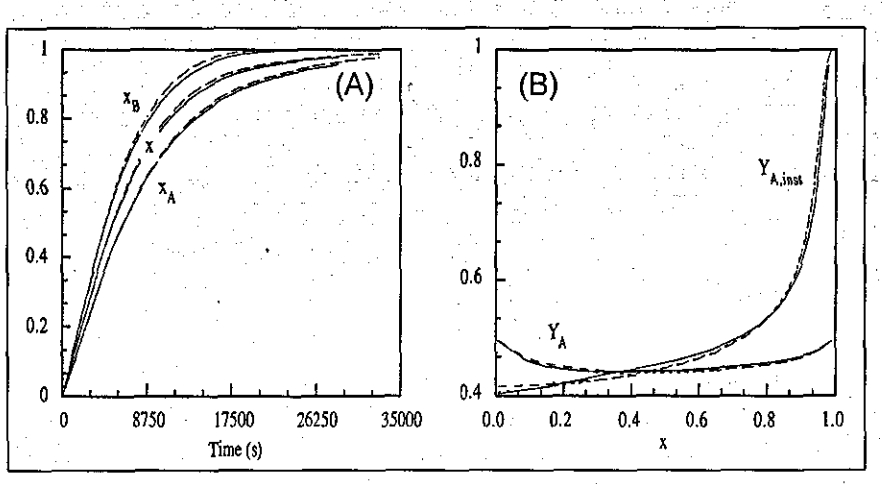

Figure 2.8 Conversions (A) and copolymer compositions (B) data calculated by the three different partitioning models of BuA/Sty with 30 wt% solids content and seed/monomer ratio of 0.1 (——) Morton, (------) Maxwell, and (----) CPC
(source: Gugliotta et al.; 1995)

Figure 2.8 illustrates that the three methods were able to give similar results when the seed/monomer ratio was 0.1 and the solids content was 30%. The authors

reported that the small differences between the methods are within the experimental error. Figure 2.9 illustrates that when the solids content is reduced to 10%, the predictions by Maxwell and the CPC models were similar but different from the ones obtained by Morton model. Figure 2.10 demonstrates the seed/monomer ratio on the predictions of the model. Reducing the seed ratio to the levels of the unseeded systems led to some differences between the Morton model and the Maxwell and CPC models.

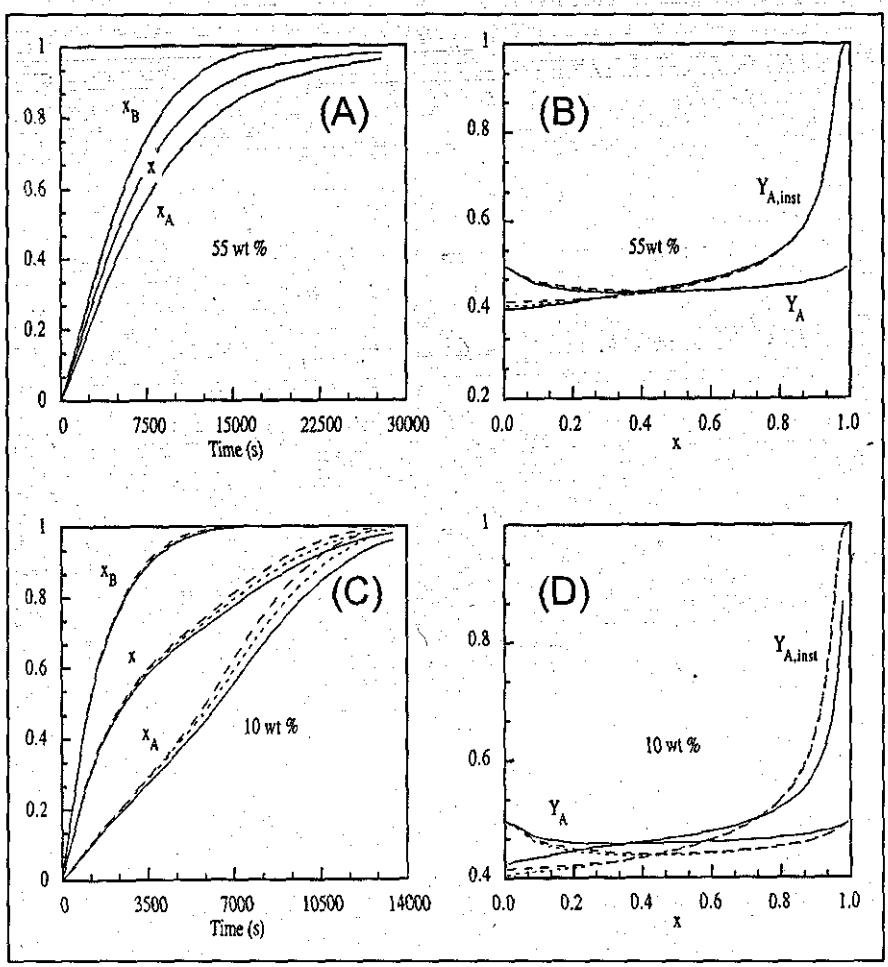

Figure 2.9 Effects of solids content on the three partitioning models for Sty/BuA copolymerization (——) Morton, (———) Maxwell, and (- - - -) CPC
(source: Gugliotta et al.; 1995)

Gugliotta et al. concluded that for high solids content systems (50 wt %), the predictions by the three models are independent of the model that is used. For medium solids content (30 wt %), the predictions were independent of the model when significant amounts of seed polymers were used (>10%).

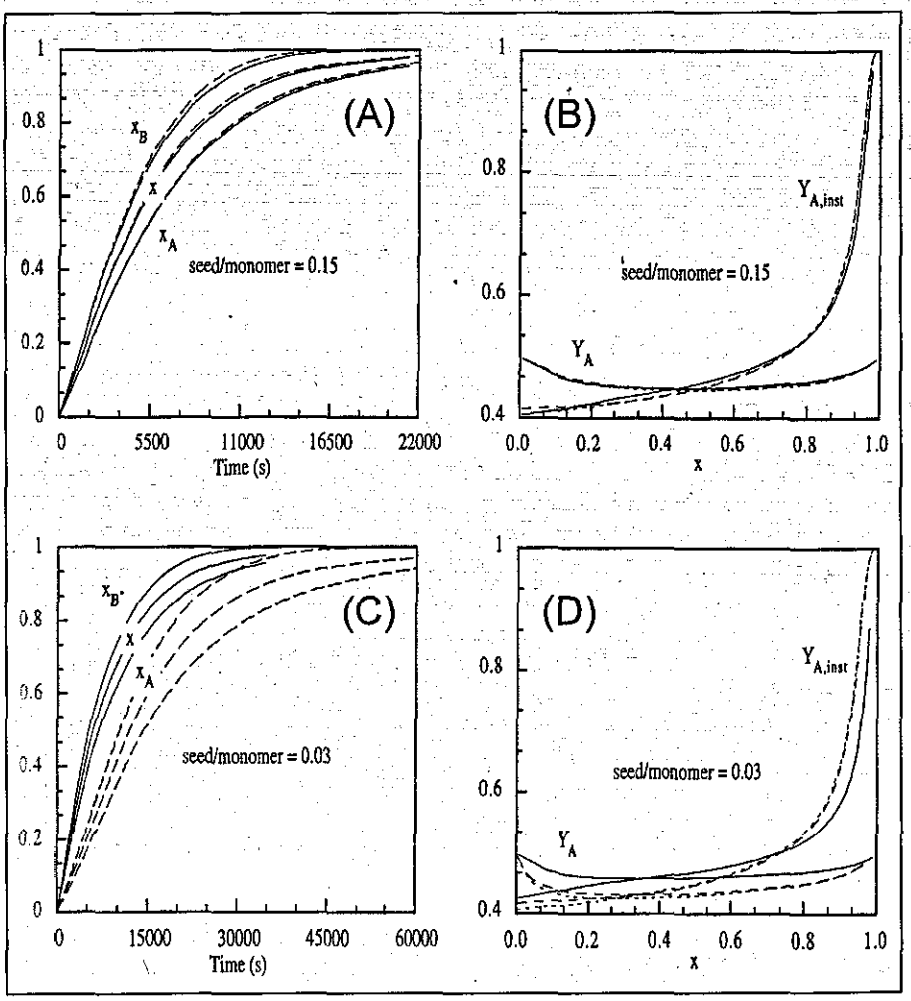

Figure 2.10 Effects of seed/monomer ratio on the three partitioning models for Sty/BuA copolymerization (—) Morton, (——) Maxwell, and (- - -) CPC
(source: Gugliotta et al.; 1995)

Low solids systems showed big differences between Morton model and the other models. It should be noted that the CPC model predictions were similar to the

Maxwell model in all the studied cases. Further details of the CPC model is given in the next section.

2.6.2. Constant Partition Coefficients Model

This model is basically an iterative algorithm for estimating the monomers concentration between the different phases. Gugliotta et al. (1995) explains that it was inspired by a method proposed by Omi et al.

For the estimation of the monomer concentrations in the different phases (i.e. continuous phase, polymer particles, and monomer drops) the overall material balances for the monomers must be solved with the equilibrium equations. Assuming that the volume change by mixing is negligible, the overall material balances (i.e. volume balances) can be written as follows

$$V_i = V_i^d + V_i^p + V_i^{aq}, \quad i = A, B \qquad 2.20$$

$$V^d = V_A^d + V_B^d \qquad 2.21$$

$$V^p = V^{pol} + V_A^p + V_B^p \qquad 2.22$$

$$V^{aq} = V^w + V_A^{aq} + V_B^{aq} \qquad 2.23$$

where V_i is the total volume of monomer i; V_i^d, V_i^p, V_i^{aq} are the total volumes of monomer i in the monomer drops, polymer particles, and aqueous phase, respectively; V^d, V^p, and V^{aq} represent the total volumes of the of the monomer drops, polymer particles, and aqueous phase, respectively; V^{pol} and V^w represent the total volume of the polymer and the water phase, respectively.

The equilibrium equations for the constant partition coefficients model are defined by

$$k_i^j = \frac{\phi_i^j}{\phi_i^{aq}}, \; i = A, B \text{ and } j = p, d \qquad 2.24$$

$$\phi_i^j = \frac{V_i^j}{V^j} \qquad 2.25$$

where k_i^j is the partition coefficient of monomer i between the phase j and aqueous phase, and ϕ_i^j is the volume fraction of component i in phase j. From 2.24 and 2.25 k_i^d and k_i^p can be written in the following form

$$k_i^d = \frac{V_i^d / V^d}{V_i^{aq} / V^{aq}} \qquad 2.26$$

$$k_i^p = \frac{V_i^p / V^p}{V_i^{aq} / V^{aq}} \qquad 2.27$$

V_i^d and V_i^{aq} can be obtained from eqs. 2.26 and 2.27, respectively, as follows

$$V_i^d = \frac{k_i^d V_i^{aq} V^d}{V^{aq}} \qquad 2.28$$

$$V_i^{aq} = \frac{V_i^p V^{aq}}{k_i^p V^p} \qquad 2.29$$

Combining 2.20, 2.28, and 2.29 V_i^p takes the following form

$$V_i^p = \frac{V_i}{1 + \frac{V^{aq}}{V^p k_i^p} + \frac{V^d k_i^d}{V^p k_i^p}} \qquad 2.30$$

The procedure to estimate the monomer concentrations in the different phases is as follows (source: Urretabizkaia and Asua, 1994):

1. Given V_i, V^{pol}, V^w, k_i^d, and k_i^p, guess V^d, V^p, V^{aq}

Where,

V_i	Volume of monomer i (cm^3)
V^{pol}	Volume of polymer (cm^3)
V^w	Volume of water in the reactor (cm^3)

k_i^d Partition coefficient of monomer *i* between the drops and the aqueous phase (Sty = 2714, BuA = 724)

k_i^p Partition coefficient of monomer *i* between the particles and the aqueous phase (Sty = 1629, BuA = 471)

V^d Volume of the monomer drops (cm^3)

V^p Volume of the monomer-swollen polymer particles (cm^3)

V^{aq} Volume of the aqueous phase (cm^3)

2. Calculate V_i^p using equation 2.30

Where,

V_i^p Volume of monomer *i* in the polymer particles (cm^3)

3. Calculate V_i^{aq} using equation 2.29

Where,

V_i^{aq} Volume of monomer *i* in the aqueous phase (cm^3)

4. Calculate V_i^d using equation 2.28

Where,

V_i^d Volume of monomer *i* in the drops (cm^3)

5. Calculate new V^d, V^p, and V^{aq} using equations 2.21, 2.22, and 2.23, respectively

6. Iterate until convergence in V^d, V^p, and V^{aq} is obtained

7. After convergence, calculate the concentrations of the monomers in the different phases according to this equation

$$[i]_j = V_i^j / \left(V_j \cdot \tilde{V}_i\right)$$

Where,

$[i]_j$ Concentration of monomer *i* in phase *j* (mol/ cm^3)

V_i^j Volume of monomer *i* in phase *j* (cm^3)

V_j Volume of phase *j* (cm^3)

$\tilde{V}_i$ Molar volume of monomer *i* (cm^3/mol)

This model that converges quickly is able to handle intervals II and III (i.e. presence and absence of monomer drops) without any change in the equations of the model. This is one of the main advantages of this model compared to the other models since the existence of monomer drops –especially for semicontinuous processes– has not to be systematically checked.

The model was successfully implemented by MATLAB®. The code extracts the required data from an EXCEL® sheet and writes the output back to the same sheet. The fully commented code and a sample of the EXCEL® sheet are given in appendix C.

3. Styrene-Butyl Acrylate Emulsion Copolymerization

Most commercial latexes are copolymers formed by the simultaneous copolymerization of two or more monomers. Copolymerization processes are very relevant to the industrial environment because they allow the preparation of polymers with a wide range of properties (Odian, 2004). The final latex properties are determined by factors such as the copolymer composition, molecular weight distribution (MWD), and morphology of particles. To control these properties different operational variables can be used (temperature, initiator, chain transfer agent (CTA), and comonomer), as well as different reactors (batch, semi-batch, and continuous) and also different control strategies (for example, feeding strategy and agitation intensity) (Leiza et al., 1997).

In the following sections a literature review of the copolymerization of Sty/BuA will be presented. The factors which affect the polymerization rate, molecular weight distributions, particles formation rate, and copolymer composition will be discussed.

3.1. Polymerization Rate

3.1.1. Agitation Effects

Zubitur and Asua (2001) investigated the effects of agitation on the copolymerization of Sty and BuA in a reactor operated for three hours semi-batch, and one hour batch. The effects of feeding neat (i.e. not mixed with other substances) and pre-emulsified monomers with and without chain transfer agents (CTA, §2.1.5) on the polymerization rate and molecular weight distribution (MWD) were studied. A summary of the experimental procedures from the literature is given in appendix B.

The authors reported that increasing the anchor type agitator speed up to 150 rpm (i.e. corresponds to power input = 0.1 KW/m^3) led to an increase in the polymerization rate when neat monomers were used. The power input was measured

using torque tables. Zubitur and Asua (2001) explained that this increase was related to a higher mass-transfer rate of monomer from the monomer droplets seeing as the agitation intensity did not affect the particles number. The authors reported that those results seem to be in agreement with Nomura et al.'s (1972) findings that the diffusion from the droplets to the aqueous phase can represent the main resistance to monomer transport.

It is apparent that the authors are suggesting that increasing the agitation speed increased the mass-tarnsfer of the monomer to the polymer particles. Zubitur and Asua (2001) explained that monomer diffusion from droplets to the aqueous phase depends on both the mass-transfer coefficient and the total area of the monomer droplets. When the agitation intensity is low, the monomer droplets coalesce and the interfacial area is small, leading to slow monomer diffusion rates from the droplets to the aqueous phase.

Feeding a mixture of neat monomers and water-insoluble CTA (mercaptans) led to a conversion evolution similar to the same mixture without CTA, this indicates that the presence of a highly water-insoluble CTA in the monomers feed did not retard the monomers diffusion and it is also an indication that the radicals formed by chain transfer are not significantly less active than are the monomer radicals. It should be noted that the CTA should affect the MWD only since its primary role is to terminate a propagating chain and to start a new one by donating a radical.

It was also illustrated that the pre-emulsification of the monomers led to an improvement in the instantaneous conversion (i.e. the ratio between the polymer in the reactor and the monomer fed up until the sampling time). The authors explained that this improvement was not related to an increase in the particle numbers but to an increase in the rate of mass-transfer from the droplets to the aqueous phase.

Ozdeger et al. (1998) studied the effects of the agitation speed and impeller type (Rushton and A310 fluidfoil) on the kinetics of a batch emulsion

copolymerization of Sty and BuA. They reported that the effects of solids content were more pronounced than the type and speed of the impeller used.

The solids content (given as percentage by mass) is an estimate of the solids in the reactor if the monomers were totally converted to polymer. It is desirable to have a high solids content in the final latex, mainly due to economical considerations, however the quality of the polymer produced is affected by other factors such as the composition drift (§1.2.3) and particle size distribution (PSD). Studying the heat of reaction (Q_r) and number of polymer particles (N_p) evolutions with time, the authors observed a reduction in the initial polymerization rate with increasing agitation intensity, and after the initial period the impeller speed did not affect the polymerization rate.

It should be noted that the authors were comparing the speed of the agitation of the two different impellers although the Rushton and A310 have different power numbers. The power input for the Rushton impeller is higher than the fluidfoil impeller at the same agitation speed, therefore comparison should be between power input (P/V) and not the impeller speed. The reduction in the initial number of particles with increasing agitation intensity is expected, since increasing the impeller speed leads to smaller and greater number of monomer droplets being created. Those monomer droplets will absorb more surfactant, causing a reduction in the surfactant available in the aqueous phase for nucleating the polymer particles, hence, the number of particles and the rate of polymerization will decrease with increasing agitation intensity. Ozdeger et al. (1998) reported that

In addition, Ozdeger et al. (1998) demonstrated that the impeller type did not affect the polymerization kinetics significantly indicating that there are no mass-transfer limitations. On the other hand, the polymerization rates at 30% solids content were higher than 50% solids. This result might be a consequence of more surfactant is associated with the oil phase at higher monomer-water ratios, leading to initially less

free surfactant available for the nucleation of particles; therefore the polymerization rate will decrease.

3.1.2. BuA Composition Effects

Guillaume et al. (1990) studied the emulsifier-free batch emulsion copolymerization of styrene with butyl acrylate. By operating the reactor without emulsifier, homogeneous nucleation is the only nucleation process and the kinetics are widely affected by the solubility of the monomers in the aqueous phase.

Conversion-time curves showed a strong increase of the polymerization rate with increasing the fraction of BuA in the recipe. Santos and Coutinho (1992) and Yang and Yang (1997) reported similar observations. An autoacceleration (Gel effect) period was observed after 50% conversion for the Sty homopolymerization and starts sooner with increasing the BuA content. It was indeed reported (e.g. Billmeyer, 1984) that the gel effect is more pronounced for pure acrylate (e.g. methyl methacrylate). Theoretically, the gel effect is due to an increase in the viscosity of the reaction mixture as the polymer chains form. This high viscosity hinders the diffusion of chains because of entanglements, so the rate of termination slows considerably. However, the diffusion of small molecular monomers is hardly affected by viscosity, so propagation proceeds as before. In addition, initiator continues to add more free radicals to the system, chains grow without termination, so the conversion is rapid and the Molecular Weight (MW) is high.

Moreover, a limiting conversion is found to appear at lower percentage conversion with increasing BuA content in the recipe. This limiting conversion happens when the glass transition temperature (T_g) of the composition of the polymer-rich phase corresponds to the polymerization temperature, as the reaction will be completely frozen.

The particle number does not change drastically upon variation of the BuA content. Elimination of the particle number effect leaves only one cause for this

increase in the polymerization rate which is the decrease in the termination rate constant due to gel effect.

3.1.3. Effects of Reaction Temperature

Santos and Coutinho (1992) studied the ideal batch time of reaction (the time for the conversion to reach a plateau), the effect of initiator concentration, the temperature, and comonomer composition in the emulsion copolymerization of styrene and butyl acrylate.

At lower temperatures, the authors observed a limited overall conversion (40% conversion at 60°C) and a large induction time; increasing the temperature reduced the induction times and improved the overall conversions. An explanation for this phenomenon was not provided but it is possible to suggest that the reduction in the induction period is related to an increase in the rate of radical generation as a consequence of increasing the temperature, so the polymerization starts sooner at higher temperatures. The improvement in the overall conversion with increasing the temperature is an indication that the T_g did not exceed the reaction temperature, so the reaction did not freeze and the conversion continued to higher values.

Santos and Coutinho (1992) concluded that 85°C gave the highest overall conversion with 150 minutes ideal batch time of reaction. It is important to note that high-conversion polymerizations produce broader MW distributions, which are not desirable from a practical viewpoint, since most polymer properties show optimum values at specific molecular weights (Odian, 2004).

Yang and Yang (1997) studied the effects of initiator concentrations, Sty/BuA ratio, reaction temperature, agitation rate, and emulsifier concentration on the polymerization rate, particle size, and molecular weight distribution in a batch system. Using a statistical method (Fractional Factorial Method) the authors were able to isolate the effects of the Sty/BuA ratio, reaction temperature, and surfactant concentration as the key variables influencing the conversion.

They reported that the polymerization rate increases with increasing temperature. The temperature increase leads to an increase in the initiator radicals' generation rate, which causes an increase in the propagation rate and number of particles (Odian, 2004).

3.1.4. Surfactant and Initiator Effects

Yang and Yang (1997) reported that the polymerization rate increases with increasing surfactant and the initiator concentrations. Increasing the surfactant concentration leads to an increase in the number of particles generated and this will cause higher polymerization rates. Increasing the initiator concentration increases the free radicals concentration, leading to an increase in the polymerization rate.

Chrastova et al. (1999) investigated the role of the anionic (Mersol H.) and non-ionic (Slovasol 2430) emulsifiers, initiated by potassium peroxodisulfate with and without activator ($Na_2S_2O_4$) on the batch emulsion copolymerization of Sty with BuA. The redox initiation system (such as $K_2S_2O_8/Na_2S_2O_4$) helps to generate free radicals at lower temperatures. One of the reasons to work at low polymerization temperatures is to obtain a high molecular weight polymer. However, at low temperatures an activator (Sodium dithionite dehydrate, $Na_2S_2O_4$) was required to achieve higher polymerization rates, due to the low dissociation rate constants of the initiator.

Several authors (e.g. Brooks, 1981) reported that emulsifier can take part in the reaction of peroxides decomposition; others reported that ionic emulsifier (Sodium dodecyl sulphate) in the micellar state does not contribute to the acceleration of the decomposition of $K_2S_2O_8$. Chrastova et al. (1999) demonstrated that the rate of copolymerization is higher for the systems emulsified with non-ionic emulsifier (Slovasol 2430).

Non-ionic emulsifier accelerates the decomposition of $K_2S_2O_8$, but low $K_2S_2O_8$ decomposition was observed when the Slovasol 2430 concentration is above

1.45×10^{-2} M, so probably the main influence of the non-ionic emulsifier on the rate of copolymerization will be only to a small extent the consequence of its acceleration of $K_2S_2O_8$ decomposition, the main influence might be its ability to influence colloidal characteristics of emulsion.

3.1.5. Solubility Effects

Araujo et al. (2001) investigated the conversion, particle size, copolymer composition, and gel content by varying polymerisation temperature, monomer composition, water to monomer ratio, initiator, and emulsifier concentrations for different binary and ternary systems including the copolymerization of Sty and BuA. Investigating the copolymerization rate revealed a possible correlation between the monomer solubility in water and the polymerization rate.

More water soluble monomers have higher polymerization rates. The authors did not explain this relation, but it could be related to Nomura et al's (1972) findings that monomer diffusion from droplets to the aqueous phase is the limiting step; so more soluble monomers have low mass-transfer effect leading to higher polymerization rates. However, no information about the agitation was provided. Therefore, it is not clear if the agitation was high enough when the mass-transfer limitation was observed.

3.2. Molecular Weight

Cruzrivera et al. (1989) performed a series of Sty/BuA copolymer latexes by emulsion copolymerization in the presence of a blend of emulsifiers and with $K_2S_2O_8$ as initiator. Different copolymerization feed strategies were tested (composition-controlled copolymerization (CC), azeotropic batch (AB), core-shell copolymerization (CS), and Multistage polymerization (ML)). An explanation of those strategies is provided in appendix B.

Since the polymerization ingredients and temperature in the aforementioned methods were exactly the same, it is obvious that the observed differences in the MW (Table 3.1) which was obtained by Size Exclusion Chromatography (SEC) were related to the different feed strategies. The azeotropic batch and the CC processes gave higher MW than the ML and CS processes, which were explained by the difference in the monomer concentration in the reaction loci, regardless of the monomer composition in the feed.

Code	Composition (mol% BuA)	MW $\times (10^{-3})$	M_n $\times (10^{-3})$	MW/M_n
PS Seed	-	1204	362	3.3
CC1	72	2435	716	3.4
CC2	50	1305	241	5.4
B3	24.7	1726	384	4.5
CS1	68.6	402	35	11.6
CS2	48.9	835	69	12.1
CS3	28	885	112	7.9
ML1	70	467	44	10.6
ML2	50.5	630	113	5.5
ML3	28.6	858	115	7.4

Table 3.1 MW characteristics of different Sty/BuA copolymer latexes
Mw = Weight average molecular weight, Mn = Number average molecular weight, Mw/Mn = Polydispersity index, CC = composition-controlled copolymerization, AB = azeotropic batch, CS = core-shell copolymerization, ML = Multistage polymerization, PS = Polystyrene

Moreover, the polydispersity indices (i.e. *the ratio of the number average molecular weight (M_n) to the weight average molecular weight (Mw), which is a measure of the broadness of a molecular weight distribution*) for the CC and the batch processes were less than the CS and ML since the latter processes consist of different MW species (e.g. ML composites contain three different MW polymers from PS seed, copolymer intermediate layer, and PBuA final layer).

Zubitur and Asua (2001) reported that the average MW in the neat monomer addition case increased with increasing the stirrer speed up to 150 rpm; increasing the stirrer speed above 150 rpm did not affect the MW. They explained that this is due to a mass transfer effect where higher monomer concentration exist in the latex particles at higher agitation speeds up to 150 rpm; above this speed the monomer concentration in the polymer particles was at the thermodynamic equilibrium values. Consequently, increasing the agitation speed above 150 rpm had no effect on the monomer concentration and the molecular weight. This finding is consistent with their observation on the affect of the stirrer speed on the instantaneous conversion where the transfer from the monomer droplets to the aqueous phase is the limiting step.

The presence of a highly water-insoluble CTA (mercaptans) in the monomer droplets led to a decrease in the average MW, and increasing the agitation intensity led to a further decrease which is likely due to an improvement in the mass-transfer rate; this result suggests that the polymerization of water-insoluble monomers can be very sensitive to agitation, increasing the stirrer speed, increases the monomer droplets, increases the surface area, increases the mass-transfer of the monomer and CTA leading to a reduction in the MW.

The authors also tested the effects of feeding pre-emulsified monomers on the MW, and they did not observe any changes, which suggest that the monomer concentrations were at the thermodynamic equilibrium values. Pre-emulsifying the monomers led to a decrease in the resistance to CTA mass-transfer; this will lead to a further decrease in the MW. The authors did not observe any agitation effects on the particle size distribution.

Yang and Yang (1997) studied the molecular weight and polydispersity of the Sty/BuA copolymerization final latex. They observed an increase in the number average molecular weight (M_n) as a result of surfactant concentration increase, initiator concentration and temperature decrease. Reducing the reaction temperature

reduces the rate of radical generation and often reduces the chain transfer to monomer leading to larger MW values.

Increasing the Sty/BuA ratio leads to a decrease in M_n; the authors explained that the monomers of low Sty/BuA ratio are easily propagated to obtain a polymer of higher molecular weight. An explanation was not provided, but it could be related to the fact that increasing the BuA composition, leads to gel effect. Consequently, the termination rate will decrease leading to higher MW since the chains are propagating and not terminating. Further statistical investigations isolated the surfactant concentration as the dominating factor affecting the M_n.

The polydispersity of the system increased with the polymerization time increase; the polydispersity increase is larger for a surfactant-free system. These results are due to the fact that many molecules with different molecular weights were generated at the BuA rich stage of polymerization (later stage), and that the larger polydispersity exists in the system of larger particles size. Decreasing the Sty/BuA ratio led to an increase in the polydispersity; this is believed to be related to more gel effect (autoacceleration) exists in the BuA-rich comonomers, leading to a wider molecular weight distribution. On the other hand, increasing surfactant concentration reduced the polydispersity, and it is thought to be due to a decrease in the particle size induced by the addition of the surfactant, which can be regarded as case II of the Smith-Ewart theory (§2.4) where $\bar{n} = 0.5$; such a decrease in the particle size leads to increasing the termination rate (r_t) compared to the propagation rate (r_p).

3.3. Particle Formation

Araujo et al. (2001) reported that the experimentally observed particle concentration is less than what was numerically expected (based on the micelle aggregation number and the surfactant concentration in the system), which confirms that not all the initial micelles were nucleated. This is due to the fact that as soon as new particles are nucleated and start growing, emulsifier molecules from the remaining micelles are used to cover the surface of the growing particles. They

observed that hydrophilic monomers (water-soluble) polymerized with low solubility comonomers promote particle formation, and due to the large number of particles they will grow to smaller sizes at comparable amounts of surfactant. This might be related to the fact that water-soluble monomers promote homogeneous nucleation.

The behavior of the number of particles with increasing fractional conversion indicates a role for the solubility. The particle concentration in the systems copolymerized with Sty (low water-solubility) became almost constant after a given conversion, but this behavior was not present in the systems copolymerized with MMA (moderately soluble monomer). This could be a result of the MMA tendency for homogeneous nucleation in comparison to Styrene.

Yang and Yang (1997) reported that the particle size increased with conversion in copolymerizations with and without surfactants, and it approached a constant diameter when the monomers were used up. The presence of surfactants leads to smaller particles (Chui et al., 1991). Moreover, a unimodal distribution exists in surfactant-free copolymerization, and a bimodal existed in with-surfactant copolymerization system.

Fitch et al. (1983) explained that the nucleation time is short relative to reaction time in the surfactant-free system, which leads to uniformly sized particles, and that the nucleation time is long in with-surfactant system leading to a bimodal size distribution of particles. The statistical design method revealed that the key variable influencing particle size is the surfactant concentration. An increase in the particle size corresponds to a decrease in the surfactant concentration, which is attributable to fewer particles being generated in surfactant-free emulsion polymerization.

Ozdeger et al (1998) observed some differences in the particle number data between the A310 fluidfoil and Rushton impellers when operated at 1000 rpm, but due to insufficient data, the authors could not conclude whether the differences were

significant. At the lower solids contents, unimodal latex particle size distributions were obtained, that is not the case at the higher solids which is evident by the skewness at smaller particle sizes. This is likely to be due to surfactant partitioning to the aqueous phase.

At higher solids, more surfactant is associated initially with the oil phase, leading to free surfactant in the later stages of polymerization, which is used partly for stabilizing the existing particles, and the rest for creating new particles. The authors also stated that it is possible at higher solids contents, the initial conditions correspond to surfactant levels below the CMC, leading to homogeneous nucleation, followed by micellar nucleation when enough surfactant is partitioned.

3.4. Copolymer Composition

Canu et al. (1994, b) suggested an optimal monomer feed policy for producing a polymer with constant composition (§1.2.3), in the minimum reaction time and with complete depletion of both monomers (Appendix B).

This feeding policy overcomes the irreproducibilities which affect the system behaviour in terms of conversion vs. time, thus involving changes in the concentrations of emulsifier, initiator, or buffer agents. Other less frequent irreproducibilities such as the ones affecting the monomers partitioning are not taken care of. The proposed procedure for determining the optimal monomer policy for producing a given amount of polymer with constant composition is summarized in appendix B. The performance of this approach was validated by applying this procedure to the Sty/BuA copolymerization in a batch and semi-batch reactors. The polymer compositions were at the desired values.

Cruzrivera et al. (1989) used the composition-controlled (CC) method to produce a quasi-homogeneous copolymer where most of the total amount of monomers is added before starting the reaction, and only the remaining Sty (the most reactive monomer) is fed dropwise to avoid compositional drift. Another way to

obtain homogeneous copolymer was to apply the copolymerization equation 1.17. For a binary system where both reactivity ratios are less than one (r_{ij} <1) an azeotropic feed composition (§1.2.4) calculated according to the polymerization equation 1.11, with Sty/BuA = $(1-r_2)/(1-r_1)$ = 2.72, would be expected. Such a composition was chosen so it was not necessary to use a controlled process to produce a homogeneous copolymer.

Zubitur and Asua (2001) reported that the cumulative copolymer composition was initially richer with Sty than the feed composition at higher agitation rates (220 rpm), and eventually the copolymer composition approached the feed composition when starved conditions were reached. At lower stirrer speed (70 rpm), the Sty composition was lower than the feed and remained lower. This is believed to be a mass-transfer effect. Sty is more water-insoluble than is BuA, increasing the impeller speed will generate more Sty droplets. Therefore more Sty will diffuse to the aqueous phase and become available to the polymer particles, and since the reactivity ratios of the Sty is higher than the BuA it will dominate the composition of the polymer particles.

Ozdeger et al. (1998) reported some differences in the copolymer compositions obtained at various agitation speeds; these are not considered to be significant. The results were in agreement with Zubitur and Asua (2001) since the copolymer was rich with Sty at the early stages only. Ozdeger et al. (1998) reported that some differences in the copolymer composition between the two impellers at early stages of the polymerization at 400 rpm impeller speed. However, due to insufficient data, the authors could not conclude whether those differences were significant or not. Moreover, a role for the solids contents on the copolymer composition was also detected; unfortunately the data presented were also insufficient to come to a firm conclusion.

Sun et al. (2007) investigated the solution semi-batch RAFT copolymerization of Sty-BuA and demonstrated the possibility of controlling the composition of the

copolymer by feeding the more reactive monomer (Sty) according to Mayo-Lewis equation (1.19). The least reactive monomer (i.e. BuA) was totally fed initially along with part of the Sty monomer. The semibatch feed consisted of Sty monomer that was fed by means of a programmed metering pump and the feed rate was according to a mathematical model (i.e. Mayo-Lewis).

3.5. Conclusion

In this chapter a literature review covering the Sty/BuA copolymerization was offered. The copolymerization behaviour is affected by many variables such as the reaction temperature, agitation intensity, and the solubility of the monomers.

The effects of mass-transfer from the monomers droplets to the continuous phase were found to play a role in controlling polymerization rate. Increasing the agitation intensity, pre-emulsifying the monomers, and increasing the surfactant concentration helped to increase the rate at which the monomers transfer to the aqueous phase and hence increasing the polymerization rate. The average molecular weight of the copolymer was mainly affected by the reaction temperature and the BuA contents. Increasing the reaction temperature increases the termination rate, and lowering the BuA content in the recipe reduces the gel effect, leading as well to low MW. The polymer particles, as expected, were found to be affected mainly by the concentration of the emulsifier and the agitation intensity. The successful control of the copolymer composition requires a controlled feeding strategy; one of the recommended methods was to feed the more reactive monomer (Sty) along the course of the reaction (semi-batch) which minimized the composition drift. More variables and explanations are provided in the abovementioned table.

4. Experimental Procedure

The starting point in the proposed work will be based on Zubitur and Ausa (2001) published work. The exact published recipe for the neat monomer without CTA case will be used (Table 4.1), and after reproducing their results the proposed experiments will be applied where different reactor start-up procedures will be investigated to verify their effects on the overall behavior of the reactor.

Component	Initial Charge (g)	Stream 1 (g)	Stream 2 (g)
Styrene	–	–	329.7
Butyl acrylate	–	–	270.3
Sodium Lauryl Sulfate	9.0	3.0	–
Potassium Persulfate	1.0	–	–
Sodium Bicarbonate	1.0	–	–
Deionised Water	1050.0	150.0	–
Flow Rate (g/min)	–	0.85	3.33

Table 4.1 Recipe used in the copolymerization of Sty/BuA
(source: Zubitur and Ausa (2001))

Based on the physical data of the reagents (Appendix A), the Sty/BuA ratio was found to be 60/40 on molar bases, and the surfactant's volumetric flow rate was 0.85 cm^3/min. Since only the overall flow rate of the styrene and butyl acrylate was provided, and based on the fact that the authors adjusted the feed rate to complete the semi-batch mode in 3 hours, it was possible to calculate the individual volumetric flow rates which were found to be 2.01 and 1.68 cc/min for the styrene and the butyl acrylate feeds respectively.

The reaction's temperature was 70°C, and different agitation speeds were tested. Based on their observations the proper speed was found to be 150 rpm (power input 0.1 KW/m^3) (§3.1). Table 4.2 is a list of the reported agitation speeds, the

corresponding Reynolds numbers at the beginning and at the end of the experiments, and the power input reported by the authors.

Impeller Speed (rpm)	Reynolds Number		Initial Power Input (kW/m^3)
	Beginning	End	
70	9450	380	0.005
100	13500	540	0.01
150	20250	810	0.1
220	29700	1190	0.3

Table 4.2 Agitation speeds and their corresponding Reynolds numbers and power inputs (source: Zubitur and Ausa (2001))

4.1. Apparatus, Procedure, and Reagents

4.1.1. Apparatus

Reactions were performed in a jacketed 1L glass reactor (figure 4.1). Water, heated up to the desired reaction temperature was pumped through the jacket and the temperature was monitored by a thermocouple inside the reactor. This method was tested and found to be sufficient to control the reaction temperature within ±1.0 °C. The reactor is equipped with four baffle plates, an overhead reflux condenser cooled by tap water, and a radial 4 blade stirrer (diameter = 6 cm). A displacement pump with three heads was used to feed the various ingredients to the reactor.

The reactants were purged with N_2 for 30-45 minutes in 3 glass bottles; each bottle was connected to one of the displacement pump heads by high-density polyethylene or Teflon tubing. Three separate streams were fed to the reactor, two streams for the styrene and the butyl acrylate, and the third one will be for the surfactant solution or a mixture of surfactant and other ingredients selected according to the recipe and the feeding procedure. The flow rates of the pump heads were adjusted at the desired levels before the experiment and were verified before and after each experiment by measuring the feed rate; the average flow rate was recorded. The

precision of the pump was found to be acceptable based on the observed constant flow rates. A schematic of the apparatus is given in figure 4.1.

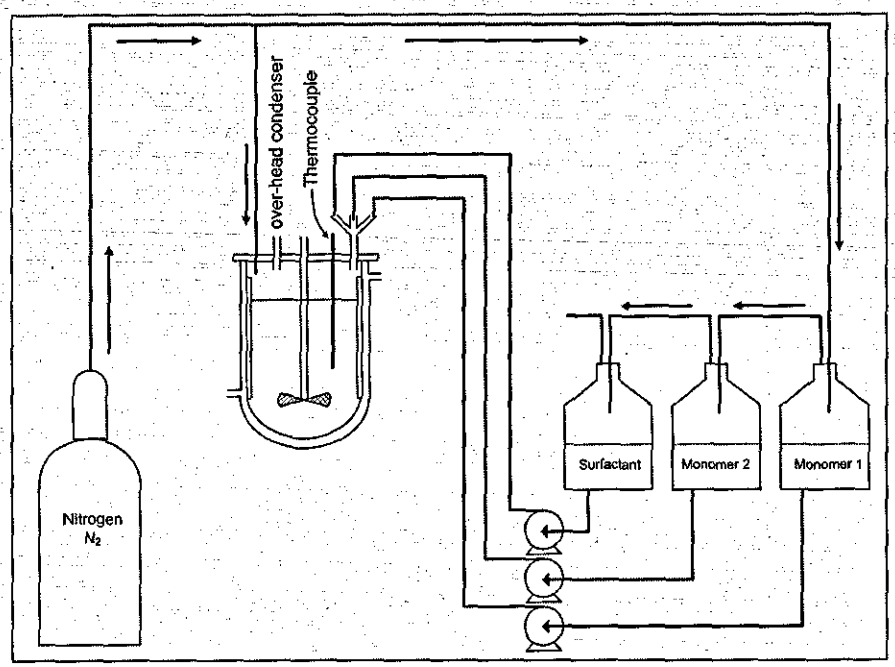

Figure 4.1 Schematic diagram illustrates the apparatus

4.1.2. Procedure

At the beginning, the reactor is filled with the predetermined initial charge, and then it was heated to the desired reaction temperature while being stirred and purged with N_2 for at least 30 minutes. While purging the reactor, the other ingredients of the recipe (i.e. subsequent feed) were purged for 30-45 minutes with N_2. The initiator was dissolved in 100 cm^3 deionised water. The initiator solution was purged with N_2 and heated to the polymerization reaction temperature. The reactor and the subsequent feed were kept under a blanket of N_2 during the experiment. Using a gas bubbler, the rate of the N_2 flow rate was monitored and kept low to minimize foaming and evaporation. Finally, the experiment starts by adding the initiator solution and starting the pump. Samples were removed at the desired time intervals

(*10 minutes*); aliquots of 3-4 g latex were withdrawn by clean glass pipettes; some of the latex will be used for gravimetric calculations and the rest for the particle size measurements and the copolymer composition analysis.

4.1.3. Reagents

Styrene (99%, Stabilized with 10-15 ppm p-tert-butylcatechol) and Butyl acrylate (99+%, stabilized with 20 ppm MEHQ) were obtained from Fisher Scientific. Both were distilled under vacuum (< 20 mmHg) at 65°C to remove the inhibitors. The monomers were then kept in dark glass bottles, sealed with plastic bags, and then stored at about -20°C to prevent any further polymerization. The initiator, potassium persulfate (KPS), the emulsifier, sodium lauryl sulfate (SLS), and the buffer, Sodium bicarbonate ($NaHCO_3$) were obtained from different sources and were used as received. Full information about the chemicals is given in appendix A.

4.2. Analysis

4.2.1. Conversion

The conversion was monitored by the gravimetric method. Using clean glass pipettes, aliquots of 3-4 g latex were withdrawn at the desired time interval. These samples were added to pre-weighed foil containers and the new weight was recorded. Then an inhibitor consisting of a mixture of methanol and hydroquinone (95/5 w/w) was added to the latex to kill any further polymerization, and then the new weight was recorded. The samples were left overnight at room temperature to dry, and then were further dried in a vacuum oven for another night at ~60°C. The dried polymer was weighed to calculate the monomers instantaneous conversion based on the following mass balance for the semi-batch process:

$$\text{Instantaneous Conversion} = \frac{\textit{Weight of Dry Sample - Weight of Solids}}{\textit{Weight of Monomers}} \quad 4.1$$

$$\text{Weight of dry sample} = \textit{Weight of sample} - \textit{Weight of the holding container} \quad 4.2$$

$$\text{Weight of solids} = \textit{Weight of solids initially in the reactor} + \textit{Weight of the additional solids through the feed} - \textit{Weight of solids extracted through sampling} \quad 4.3$$

$$\text{Weight of monomers} = \textit{Weight of monomers initially in the reactor} + \textit{Weight of the additional monomers through the feed} - \textit{Weight of monomers extracted through sampling} \quad 4.4$$

Where the solids are the surfactant (*SLS*), the initiator ($K_2S_2O_8$), the buffer ($NaHCO_3$), and the inhibitor (*hydroquinone*).

4.2.2. Particle Size

The latex particles size was measured in some experiments using Malvern® Mastersizer which was later replaced by Malvern® Zetasizer 3000 because it offers smaller size ranges. The Zetasizer 3000 uses the full *Mie* theory which gives accurate results over the range 0.02-2000 μm. The Zetasizer 3000 calculates the z-average from the intensity of scattered light according to the cumulants analysis. The measurements were done at 25°C using a scattering angle of 90°. For each sample drawn for the gravimetric calculations, some of it kept in a test tube for the particle size measurement. Before conducting each measurement, a clean disposable glass syringe was used to transfer a very small amount of the concentrated latex from the test tube to a cuvette and diluted with deionised water, and then the measurement was conducted. The measurement was done twice on some of the samples to check the accuracy of the instrument, and the difference between two consecutive runs on one sample was found to be ±4%.

4.2.3. Composition

Fourier transform infrared (FT-IR) spectroscopy was used to analyze the copolymer samples composition. Further discussion of this technique is given in chapter 6.

4.2.4. Number of polymer particles (N_p)

Araujo et al. I (2001) reported that the number of polymer particles per cm^3 of water takes the following form (Araujo et al. I, 2001)

$$N_p = \frac{6M_T x_m}{\rho_p \pi d_p^3} \qquad 4.5$$

Where M_T is the initial total monomer concentration (g/cm^3 of water), ρ_p is the polymer density (g/cm^3), d_p is the average particle diameter (cm), and x_m is the total weight conversion. This formula assumes that the particles contain only polymer.

4.2.5. Surface Tension Measurement

In order to estimate the CMC, surface tension measurements were conducted using DuNouy Tensiometer. Previously (§2.1.2) it was demonstrated that the CMC is affected by the reaction medium. The presence of electrolytes or hydrophobic monomers affects the CMC. Therefore, surface tension measurements were conducted on solutions of deionised water saturated with Sty and BuA monomers.

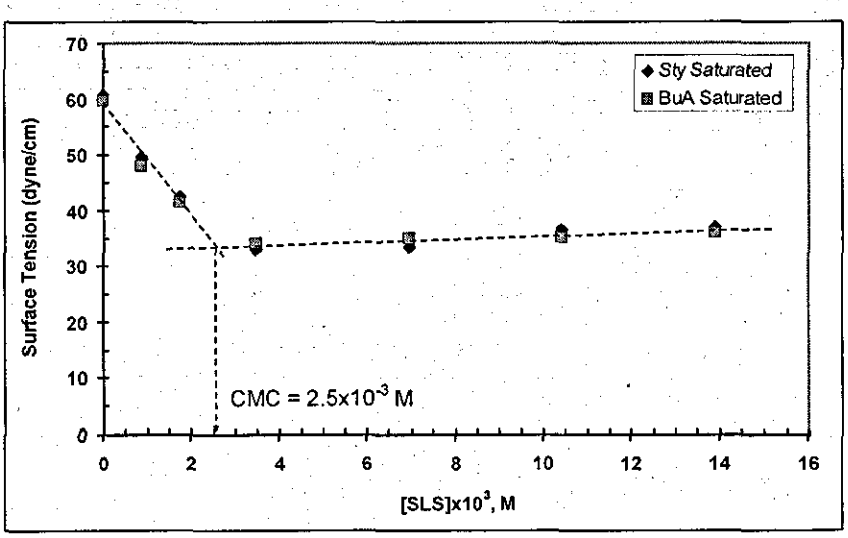

Figure 4.2 Surface tension evolutions with surfactant concentration of water saturated with BuA and Sty monomers at 70 °C

In order to recreate the reaction conditions, initiator ($K_2S_2O_8$) and buffer ($NaHCO_3$) were added to the solutions and the temperature of the solutions was raised to 70 °C. Figure 4.2 illustrates that the CMC is 2.5×10^{-3} M, which is identical to what is reported in the literature (Gilbert, 1995). It also demonstrates that the type of the monomer did not affect the CMC. The CMC values for the solutions saturated with Sty or BuA were identical.

5. Preliminary Experiments

5.1. Experimental Setup Testing

Several experiments were conducted to test the system. For the test runs, two streams of styrene and butyl acrylate were fed to the system in a semi-batch mode, and all the other ingredients (i.e. SLS, KPS, and $NaHCO_3$) were initially charged to the reactor. The recipe is exactly 50% of the recipe implemented by Zubitur and Asua (2001) and is given in table 5.1. The reactor was operated in semi-batch mode for 3 hours, and then 1 hour in a batch mode; so the total duration of the experiments was 4 hours. The average volumetric flow rates of the Sty and the BuA were at 1.0 and 0.86 cm^3/min respectively, and the molar ratio of the monomers (Sty/BuA) was 60/40. The agitation intensity and the reaction temperature were 150 rpm and 70°C respectively. It should be noted that a full reproducibility and error propagation study is given in appendix D.

Component	Initial Charge (g)	Stream 1 (g)	Stream 2 (g)	Stream 3 (g)
Styrene	–	–	164.85	–
Butyl acrylate	–	–	–	135.15
Sodium Lauryl Sulfate	6.0	–	–	–
Potassium Persulfate	0.5	–	–	–
Sodium Bicarbonate	0.5	–	–	–
Deionised Water	600.0	–	–	–
Flow Rate (g/min)	–	–	0.92	0.75

Table 5.1 Test experiments recipe and feeding strategy

Figure 5.1 illustrates a comparison between the instantaneous conversion evolution with time of one of the test runs and the data reported by Zubitur and Asua (2001). It is noticeable that the overall behavior of the conversion is comparable to Asua's results. The ultimate conversion was lower than the original data by 5% only.

This difference could be related to the effects on the rate of polymerization by the agitation intensity. Next a discussion of the agitation effects on the polymerization rate and the polymer particles will be given.

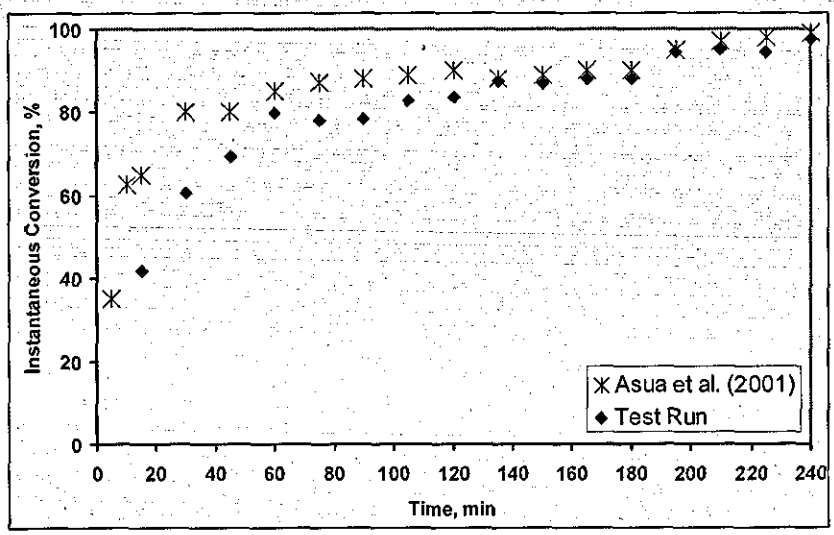

Figure 5.1 Instantaneous conversion evolution with time compared with the data from Zubitur and Asua (2001)

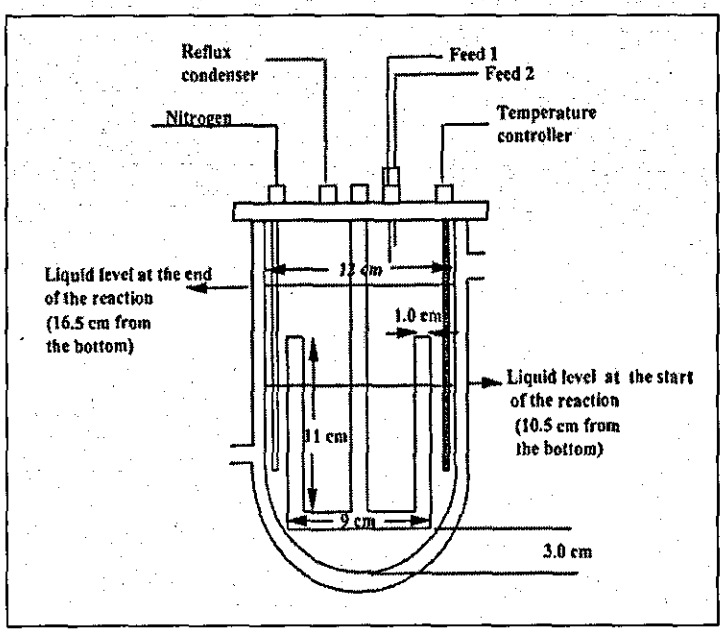

Figure 5.2 Schematic of the reactor used by Zubitur and Asua (2001)
(source: Zubitur and Asua, 2001)

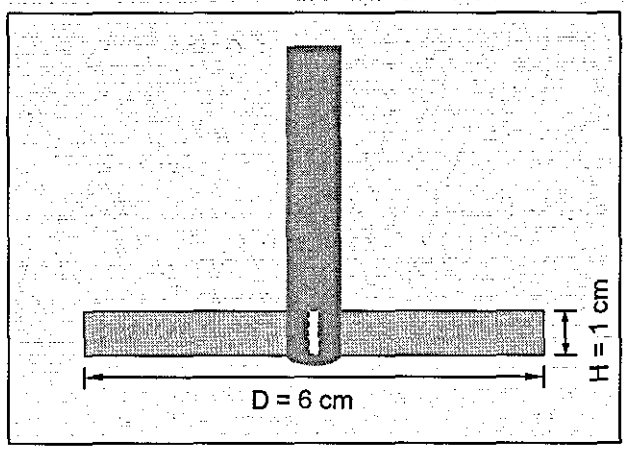

Figure 5.3 Front view schematic of 4-blades flat blade agitator

5.2. Agitation Effects

Figure 5.2 is a schematic of the reactor in the original work (Zubitur and Asua, 2001). Comparing the geometry of the impeller in figure 5.2 to our impeller (figure 5.3), clearly the power input in the original work is higher compared to our setup at the same agitation speed, so operating at similar agitation speed does not provide similar agitation conditions.

Zubitur and Asua (2001) reported that the corresponding Reynolds numbers for 150 rpm agitation speed were 20,250 at the beginning of the reaction, and 810 at the end due to the increase in the viscosity; the power input was 0.1 kW/m^3 (Table 4.2).

The power requirements for an impeller can be calculated using following equation

$$P = N_p \rho D^5 N^3 \qquad 4.6$$

where P is power, N_p is power number, ρ is density, D is impeller diameter, and N is impeller speed. The power number is a function of Reynolds number for laminar and transition regime flow, and a constant for turbulent flow. In our setup, the stirrer is flat

blade where the power number is about 4; D = 6 cm and N=150 rpm, using those numbers in the aforementioned equation corresponds to 0.05 watts. Since the volume of the reactor is 1 L, the power input per unit volume is 0.05 kW/m^3. Clearly the current impeller speed provides only 50% power input compared to the original work.

In order to investigate the effects of the impeller speed on the system, two experiments were conducted similar to Zubitur and Asua (2001) published work, where three streams (styrene, butyl acrylate, and surfactant) were fed to the reactor. The experiments were scaled down to fit the apparatus; the recipe and the feeding strategy were as shown in table 5.2. The agitation speeds were 150 and 300 rpm and the temperature was held constant at 70°C. The average volumetric flow rates of the Sty, BuA, and SLS for the 150 and 300 rpm runs were at 1.02, 0.89, and 0.49 cm^3/min and 0.96, 0.86, and 0.5 cm^3/min; respectively.

Component	Initial Charge (g)	Stream 1 (g)	Stream 2 (g)	Stream 3 (g)
Styrene	–	–	190.06	–
Butyl acrylate	–	–	–	155.82
Sodium Lauryl Sulfate	5.19	1.73	–	–
Potassium Persulfate	0.58	–	–	–
Sodium Bicarbonate	0.58	–	–	–
Deionised Water	605.3	86.5	–	–
Flow Rate (g/min)	–	0.5	1.06	0.87

Table 5.2 Recipe and feeding strategy for the 150 and 300 rpm runs

The instantaneous conversion, the particle sizes, and the number of polymer particles are illustrated in figures 5.4 The shape of the conversion data in figure 5.4(A) is similar to the published work (Asua et al.; 2001); and increasing the agitation speed to 300 rpm did not lead to noticeable differences in the instantaneous conversions. It should be noted that 300 rpm impeller speed provides about 8 times

the power input compared to 150 rpm, yet the instantaneous conversion for the 300 rpm was comparable to the 150 rm.

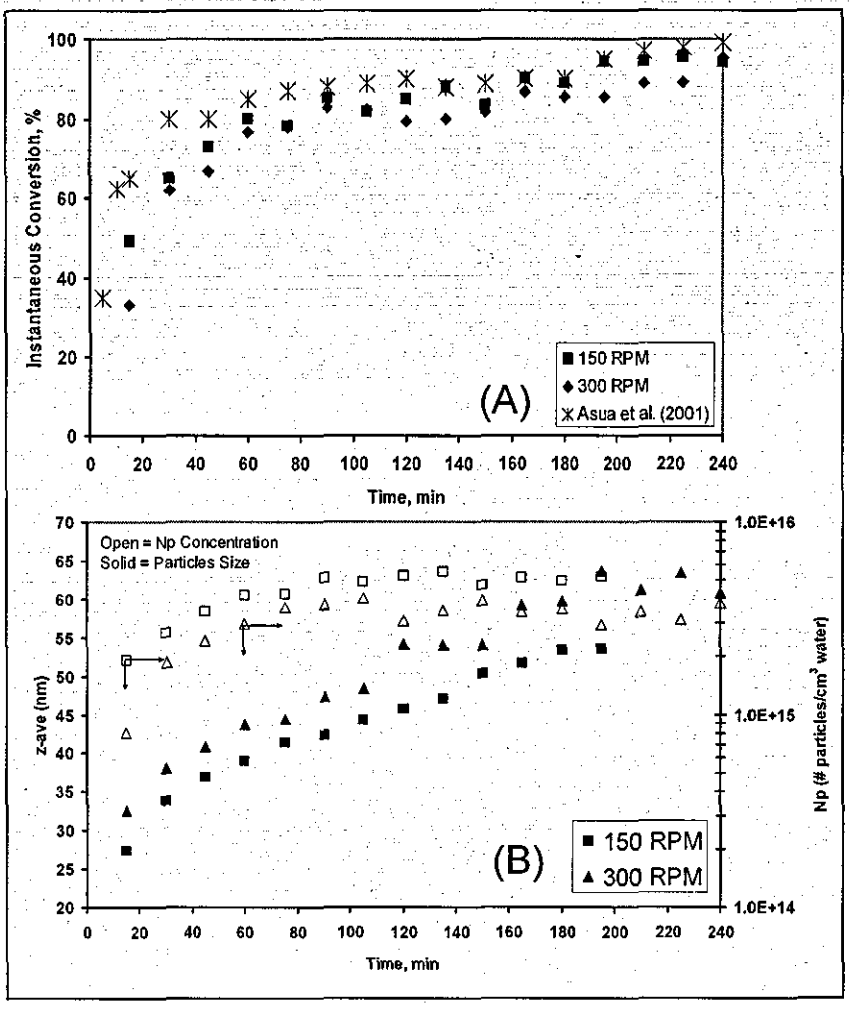

Figure 5.4 Time evolution of the instantaneous conversion (A) and the particle size and number of polymer particle (B) for the 150 and 300 rpm runs

However, the effects on the z-average and the number of polymer particles are clear. Increasing the agitation speed generated more monomer drops. Consequently this resulted in more surfactant being absorbed by the drops leading to smaller particle sizes and lower number of polymer particles since the amount of the surfactant that is available for nucleation was lower for higher speeds agitation; this is exactly what

figure 5.4(B) illustrates. The reduction in the number of polymer particles might explains the slight reduction in the conversion for the 300 rpm. The z-average samples kept increasing while the monomers were fed to the reactor, when the batch region started, the z-average started to level out since the monomers are vanishing from the reactor.

5.3. Conclusion

The experiments in this chapter serve as a starting point for the proposed research. It was found that the instantaneous conversion data is comparable to the published data by Zubitur and Asua (2001). Increasing the power input by a factor of 8 did not affect the instantaneous conversion markedly. The effects on the particles were obvious and expected.

6. Copolymer Composition Analysis

6.1. Introduction

The chemical composition of a polymer is one of the key factors that determine its properties. The determination of the polymer composition is also important for a better understanding of the chemistry, reactivity, adhesion, and polymer fabrication techniques. In the following paragraphs a brief review of some spectroscopic techniques which are used to determine the microstructure of a polymer is presented.

Mori (1989) investigated the styrene-methyl methacrylate copolymers composition by ultraviolet absorption spectrophotometry (UV), infrared absorption spectrophotometry (IR), and proton nuclear magnetic resonance spectrophotometry (^{1}H-NMR). The random copolymer PS-PMMA was prepared using solution polymerization. The monomers were mixed with equal volume of benzene (solvent), and azobis-iso-butylonitrile (AIBN, 0.4 g/L) was used as initiator. The mixture was heated up to 65°C under N_2 atmosphere and was left for 10 hours to polymerize. Yields of the copolymers were between 15-35%. In order to extract the copolymer, the solution was poured into a tenfold volume of methanol and the copolymer was recovered by precipitation. An extra step was used to purify the copolymer by reprecipitation from chloroform-methanol, and finally it was dried at 55°C under reduced pressure. The conversion was at a low degree in order to achieve a statistical monomer sequence distribution (i.e. random copolymer). This helped the authors to isolate the IR absorption bands that are sequence-distribution-dependent from the bands that are sequence-distribution-independent; the latter can be used to determine the copolymer composition.

The following is a brief description of the procedures used to analyze the samples prepared using the aforementioned techniques. The IR spectra were obtained by dissolving the copolymers in chloroform ($CHCl_3$) and recording the IR spectra in the regions of the carbonyl band (i.e. C=O) around 1730 cm^{-1} and the phenyl band

(i.e. C=C) band around 1600 cm^{-1}. The solution cell was a NaCl window cell of 0.5 mm path length, and the IR resolution was 2 cm^{-1}.

In the UV analysis technique, the copolymers and the PS homopolymer were dissolved in $CHCl_3$. Quartz cells of 1-cm path length were used to conduct the analysis where the resolution was selected as 0.1 nm. The UV calibration curve was constructed using the absorbance at 260 nm and the PS concentration.

For the NMR analysis, deuterated chloroform ($CDCl_3$) was used as a solvent with tetramethylsilane (TMS) as an internal standard. The composition of the copolymers was measured from the integrated area of the phenyl peak to the integrated total proton peak area as follows:

$$Styrene\ (mol\ \%) = \frac{8\ (phenyl\ peak\ area)}{5\ (total\ peak\ area)} \times 100 \qquad 6.1$$

Mori (1989) explained that the correlations among the data as obtained by the different techniques were examined by plotting one vs. the other. For instance, when the X-axis was styrene content as obtained by NMR then the Y-axis was the methyl metharcylate content as obtained by UV and IR (i.e. 1730 cm-1). Similarly, when the X-axis was styrene content as obtained by the IR (i.e. 1600 cm-1) then the Y-axis was the methyl metharcylate content as obtained by the other methods.

The compositions of the copolymers obtained by the three techniques are listed in Table 6.1. The data are in good agreement except for the IR results of the phenyl band at 1600 cm^{-1}. The phenyl band was weak compared to the carbonyl band at 1730 cm^{-1}, so a more concentrated solution (5 wt %) was required to conduct the IR analysis. The authors suggested that the deviation in the data was mainly a result from the instrumental error due to the low absorption coefficient. The relative standard deviations were 0.1-0.6%, 0.3-1.5%, 0.5-0.8%, and 5% for the UV, NMR, IR at 1730 cm^{-1}, and IR at 1600 cm^{-1}; respectively.

The IR absorption bands in the region 1100 and 1300 cm^{-1} in the PS-PMMA copolymer were mainly MMA-originated, and they were not additive to the IR spectra of both PS and PMMA homopolymers. The bands in this region changed in wavenumbers and absorption coefficients with composition. So those bands are sequence-distribution-dependent and therefore cannot be used to analyze the copolymer composition. The authors concluded that an UV absorption at 260 nm for a styrene unit, and an IR absorption band at 1730 cm^{-1} for a MMA unit are independent of the nature of the neighboring monomer units in a copolymer chain and could be used to validate the composition of the copolymer.

Copolymer	Styrene Feed (mol %)	Styrene (mol %)			
		UV	NMR	IR	
				1730 cm^{-1}	1600 cm^{-1}
I	90	85.5	84.2	87	76.8
III	70	65.7	66.3	67.4	63.4
V	50	48.7	49.8	51.9	43.6
VII	30	41.5	43.5	41.4	40.4
IX	10	15.2	14.3	11.2	6.6

Table 6.1 Copolymer composition as obtained by three independent analytical techniques (source: Mori, 1989)

Ghatzi et al. (1997) studied the system styrene/2-ethylhexyl acrylate (STY/2-EHA) using the elemental analysis (i.e. determines the amount of an element in a compound), UV, and FT-IR techniques. A batch reactor was used to prepare a series of different copolymer compositions, as well as a PS homopolymer in emulsion. The reaction was terminated at low conversion; the mole fraction of the residual monomer in the reactor was always less than 3%.

The elemental analysis is based on estimating the weight percentage of an element in a compound. The most common type of elemental analysis is for carbon,

hydrogen, and nitrogen (CHN analysis), which is widely used for organic compounds. So by estimating the weight percent of the carbon and hydrogen, the copolymer composition was determined. PS solutions in dichloromethane at a concentration range from 0.6-1.2 g/l together with PS solutions in dichloromethane and dioxane from the literature were used to prepare the calibration curve (figure 6.1). The maximum UV absorption values were at 260 nm. The resolution was set at 0.1 nm, and quartz cells of 1 cm path length were used for all measurements. The transmission IR absorption spectra were collected at room temperature in the range 450-4000 cm^{-1} and the resolution was 1 cm^{-1}. PS homopolymer and copolymer solutions in $CHCl_3$ at concentrations of 10-50 g/l were measured in a liquid cell of 0.2 mm path length equipped with KBr windows. Calibration curves were constructed based on the peak intensities.

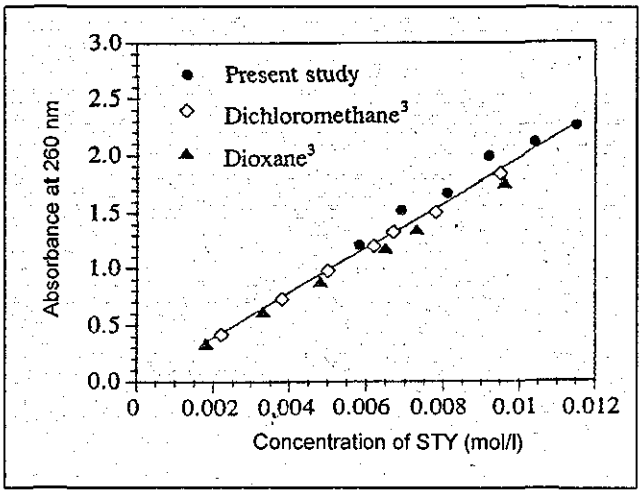

Figure 6.1 UV calibration curve (source: Ghatzi et al.; 1997)

Sequence-independent absorption bands have to be identified for determining copolymer composition through IR spectroscopy; especially for statistical copolymer systems (block copolymers do not exhibit such problems). On the other hand, sequence-dependent bands (exhibiting peak position and non-linear intensity changes with copolymer composition) can be used for determining the monomer sequence distribution.

Ghatzi et al. (1997) reported that the position of the styrene absorption band at 1602 cm^{-1} changed by less than 2 cm^{-1} to higher frequency as the styrene content in the copolymer increased which is considered a marginal shift (figure 6.2). In addition, the normalized peak height of this band (after correcting for the baseline) increases linearly with the styrene mole fraction content in the copolymer evaluated from the UV and elemental analysis. Those two facts suggest that the absorption band at 1602 cm^{-1} is a good representative of the PS content in the copolymer.

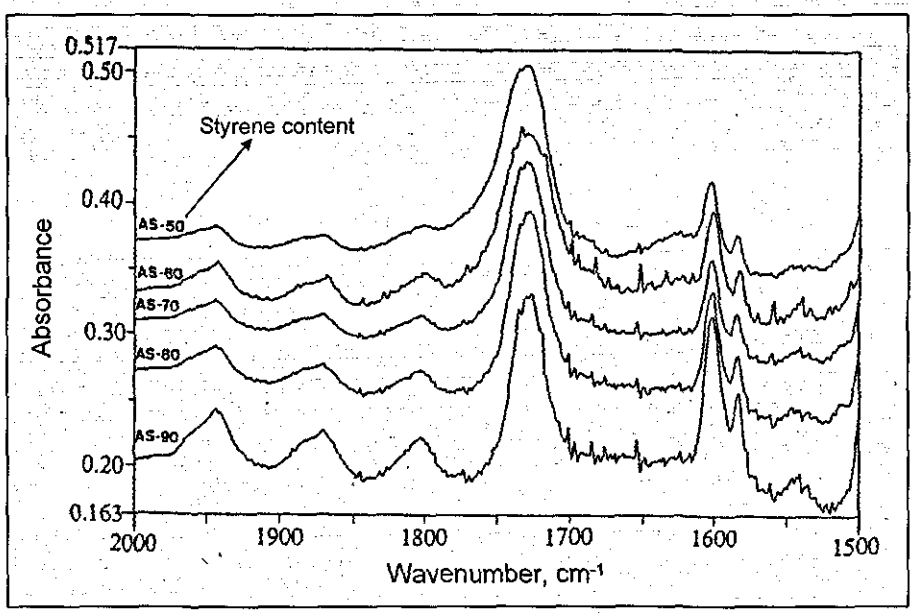

Figure 6.2 IR KBr transmission spectra of STY/2-EHA in the region 2000-1500 cm^{-1}
(source: Ghatzi et al.; 1997)

Close examination of the peak at 1730 cm^{-1} (figure 6.2), which can be assigned to the carbonyl stretching vibration of the acrylate component, revealed considerable variations in their shapes as the overall copolymer composition changed, and specifically, a broadening to higher wavenumbers as the 2-EHA content of the copolymer was increased. Moreover, a non-linear relationship was shown to exist when plotting the normalized intensities of the peak (after baseline correction), as a function of the acrylate mole fraction in the copolymer evaluated from UV and elemental analysis. Those two facts indicate that the carbonyl peak at 1730 cm^{-1} cannot be used to determine the copolymer composition.

Examining the ester peak at 1158 cm^{-1} associated with the acrylate in the copolymer (not shown) revealed a linear relationship between the intensity of this peak and the mole fraction of the acrylate in the copolymer evaluated using the aforementioned methods indicating that this peak can be considered a good representative of the copolymer composition.

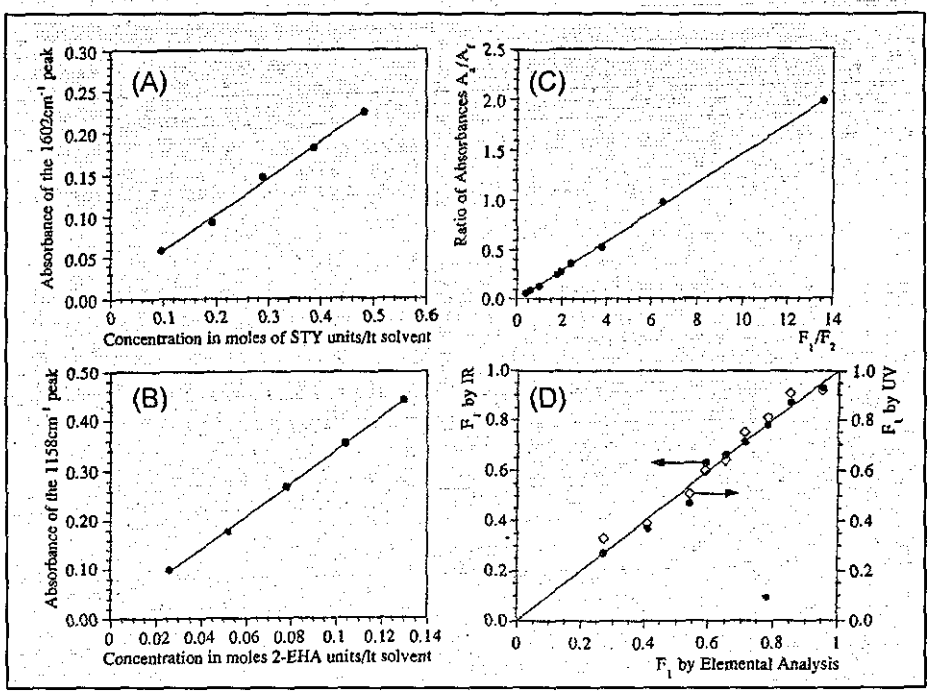

Figure 6.3 IR calibration curve based on the PS peak at 1602 cm^{-1} (A), IR calibration curve based on the 2-EHA peak at 1158 cm^{-1} (B), ratio of the absorbances of the bands 1602 and 1158 cm^{-1} as a function of the ratio of the monomer mole fraction in the copolymer (C), and comparison between the estimated values of copolymer composition based on the three independent techniques (D)
(source: Ghatzi et al.; 1997)

The IR calibration curves based on the peaks 1602 cm^{-1} and 1158 cm^{-1} are shown in figures 6.3(A-C), and a comparison between the estimated values of the copolymer composition based on the three different analytical methods is given in figure 6.3(D). A satisfactory agreement between the copolymer composition values obtained by the three techniques can be observed.

Vuluga et al. (2004) investigated the use and limits of FT-IR and Differential Scanning Calorimetry (DSC) to characterize the microstructure of a copolymer made from 1,3-dioxolane (DXL) and 1,3-dioxepane (DH). 1,3-dioxepane can readily be polymerized only by a cationic ring-opening mechanisms (Vuluga et al., 1999). However, cyclic acetals copolymerized using this method may be suspected of being blends of homopolymers.

DXL and DH homopolymers and copolymers were all prepared at the same conditions using cationic copolymerization. Homopolymer mixtures have been prepared by dissolving the corresponding amounts from each homopolymer in acetone, at a total concentration of 5% by weight. The samples have been evaporated and dried at 10^4 Pascal and 35 °C for 24 hours.

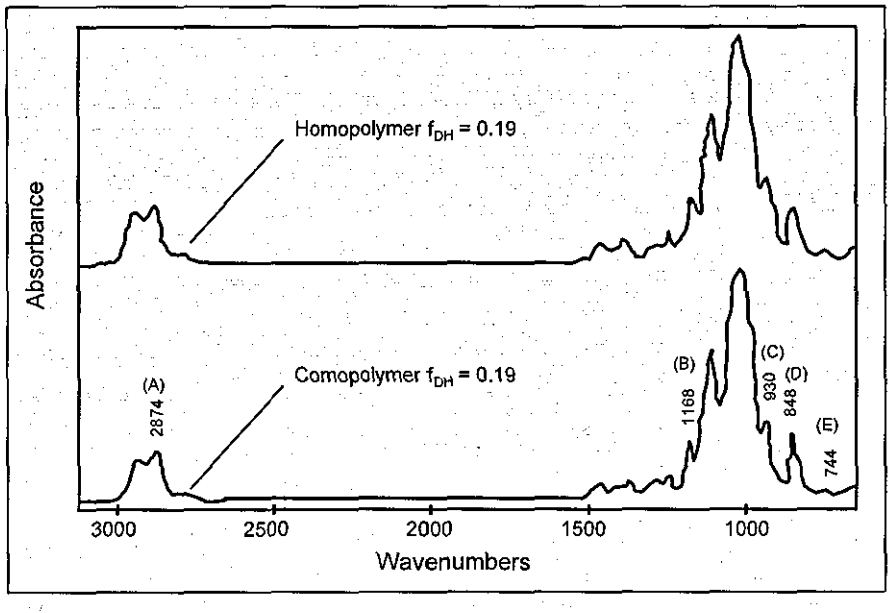

Figure 6.4 IR spectra of a mixture of DXL and DHL homopolymers and for a copolymer (source: Vuluga et al.; 2004)

The copolymer composition was measured by analyzing the concentration of the unreacted monomers through gas chromatography, as well as the initial monomer concentration. To assure uniformity of all samples, copolymer samples were also been

dissolved in acetone at 5% by weight and dried using the same technique as the homopolymers.

The authors did not observe any differences regarding the positions and intensities of peaks when they compared the FT-IR spectrum of a polymer mixture with that of a copolymer (figure 6.4) having the same total composition (DH=19%). This fact indicated that a calibration curve built using different composition homopolymer mixtures could be used to estimate the composition of the copolymer. Five peaks were used to prepare four calibration curves for a mixture of homopolymer blends at different compositions (figure 6.5). The copolymer composition is the average of the measured compositions resulting from the calibration curves.

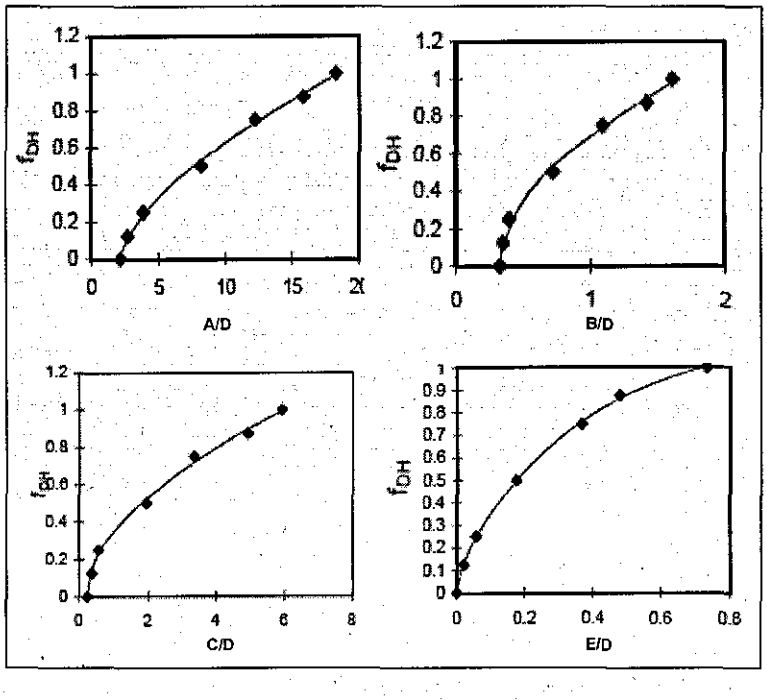

Figure 6.5 IR calibration curves between the molar fraction of DH units (f_{DH}) and selected IR peaks (source: Vuluga et al.; 2004)

DSC measurements have shown that for homopolymer mixtures, both, glass transition temperature (T_g) and melting temperature (T_m) are present in the thermograms. T_m disappears for copolymers with molar fraction of the comonomer

above 10%. T_g depends linearly upon copolymer composition (fig 6.6); considering the straight line equation, the glass transition temperature could be roughly used to estimate the composition of the copolymer.

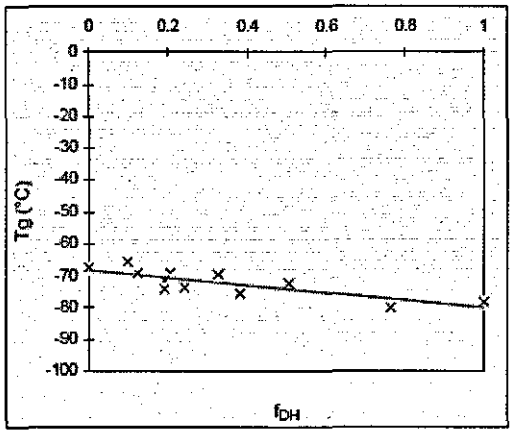

Figure 6.6 Variation of T_g with DH mole fraction in the copolymer
(source: Vuluga et al.; 2004)

Romero et al. (2005) demonstrated the possibility of constructing the FTIR calibration curve for the system Sty/BuA by measuring blends of PS and PBA in different well-know proportions.

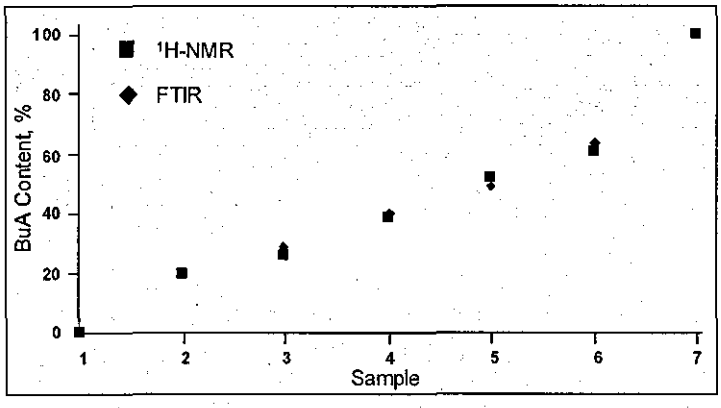

Figure 6.7 Comparison of BuA content as determined by ^{1}H-NMR and FTIR
(Source: Romero et al.; 2005)

From the FTIR spectra of the blends, the ratios of the absorption peaks at 700 cm^{-1} for the PS and 1727 cm^{-1} for the PBA determined and plotted against the PBA

content of the blend. The calibration curve was then used to calculate the BuA content in the copolymer. Romero et al. demonstrated a good agreement between the FTIR and the ^{1}H-NMR techniques (Fig 6.7).

Hua et al. (2004) monitored the copolymer Sty/BuA offline using an ATR-FTIR probe. The ATR-FTIR (Attenuated total reflectance infrared spectroscopy) is basically a FTIR instrument equipped with ATR accessory which allows samples to be examined directly in the solid or liquid state without further preparation. The conversion and the copolymer composition were determined by monitoring the monomer concentration. Hua et al. reported that the ATR-FTIR results agreed at 99% confidence level with the traditional gravimetric and ^{1}H-NMR spectroscopy.

In conclusion, several spectroscopic methods which are used to determine the composition and the microstructure of copolymers were reviewed. It was reported that FT-IR is an effective method for the determination of the copolymer composition, yet it suffers from some limitations when compared to the other spectroscopic techniques (i.e. NMR and UV).

The proper selection of FT-IR absorbance peaks which are sequence-distribution-independent is important for estimating the copolymer composition. Broadening of the IR peaks, and the shift in their positions with changing the copolymer composition are indications of sequence-distribution-dependent peaks. Sequence-distribution-dependent peaks should be avoided in estimating the composition of the copolymer. Constructing the calibration curve based on the IR spectra of homopolymer blends is an acceptable method. The UV and the NMR techniques are good alternatives, but they were either unavailable (NMR) or do not provide adequate information about the copolymer microstructure (UV).

6.2. Constructing the IR calibration curve

6.2.1. Preparation of homopolymers

The first step in constructing the calibration curve is to obtain homopolymers of polystyrene (PS) and polybutyl acrylate (PBA) and mix them at different compositions. The PS homopolymer was obtained from Fisher Scientific, and the PBA homopolymer was prepared by means of solution polymerization.

Homogeneous polymerization processes (i.e. Bulk and Solution) produce the minimum contamination of the polymer compared to heterogeneous processes (i.e. Emulsion, Suspension) due to the fact that just the fundamental ingredients exist in the homogeneous polymerization recipes. For instance, in bulk polymerization the monomer is heated up to certain temperature (50-70 °C) and then the initiator is added. However, bulk polymerization is highly exothermic and requires strong and elaborate stirring since the viscosity of the reaction system increases rapidly at relatively low conversion. The viscosity coupled with the exothermic effects make temperature control difficult.

Polymerizing of a monomer in a solvent (i.e. Solution Polymerization) overcomes many of the disadvantages of the bulk process. The solvent acts as diluent and helps in the transfer of the heat of polymerization, and also reduces the viscosity of the reaction mixture. On the other hand, the presence of solvent may present new difficulties. For instance, the purity of the polymer may be affected if there are difficulties in removing the solvent.

The recipe used to prepare the PBA polymer is given in table 6.2. First a mixture of the monomer (butyl acrylate) and the solvent (toluene) is heated up to 80 °C and purged with N_2 for half an hour, and then the initiator (lauryol Peroxide) was added at a concentration of 0.01 mol/l of the monomer. The mixture was left for 72 hours under a blanket of N_2. The rate of the N_2 flow rate was monitored and kept low to minimize evaporation.

Ingredient	Weight, gm	Density	Molecular Weight
Butyl acrylate	27	0.894	128.17
Toluene	170	0.8661	92.13
Lauryol Peroxide	0.11961	-	398.70

Table 6.2 Polybutyl acrylate solution polymerization recipe

To recover the PBA polymer, the reaction mixture was poured into a separating funnel containing around tenfold volume of methanol. And then the mixture was vigorously agitated and left for few hours. The precipitate (polymer and traces of toluene and possibly butyl acrylate monomer) was collected in a beaker and was dried under vacuum at 100 °C for at least 48 hours.

6.2.2. Obtaining the IR spectra

To conduct the FT-IR analysis, solutions of the homopolymers in THF at 5% w/w were prepared and casted on NaCl discs. To assure uniform films, the discs were rotated at high speeds (~500 rpm) for short times (~5-10 seconds). After drying the discs at room temperature for 24 hours, the FT-IR analysis was carried out; the IR spectra were recorded over the range 450-4000 cm^{-1} and the resolution was set to 1 cm^{-1}.

Prior to blending the homopolymer mixtures, the purity of the polymers should be confirmed (e.g. no traces of butyl acrylate monomer exist in the PBA polymer). This step was done by comparing the spectra of the polymers to published IR spectra of homopolymers and monomers (Fig 6.7). Observing the five peaks of Aldrich™ IR spectra for polystyrene and poly butylacrylate standards (6.7A and 6.7C) with the IR spectra of the polystyrene homopolymer (6.7B) and the poly butylacrylate homopolymer that is prepared in the lab (6.7D), it is clear that the spectra were similar; the frequencies of the transmittance bands were identical. The differences in the absolute transmittance were expected since the absolute transmittance increases with the thickness of the sample.

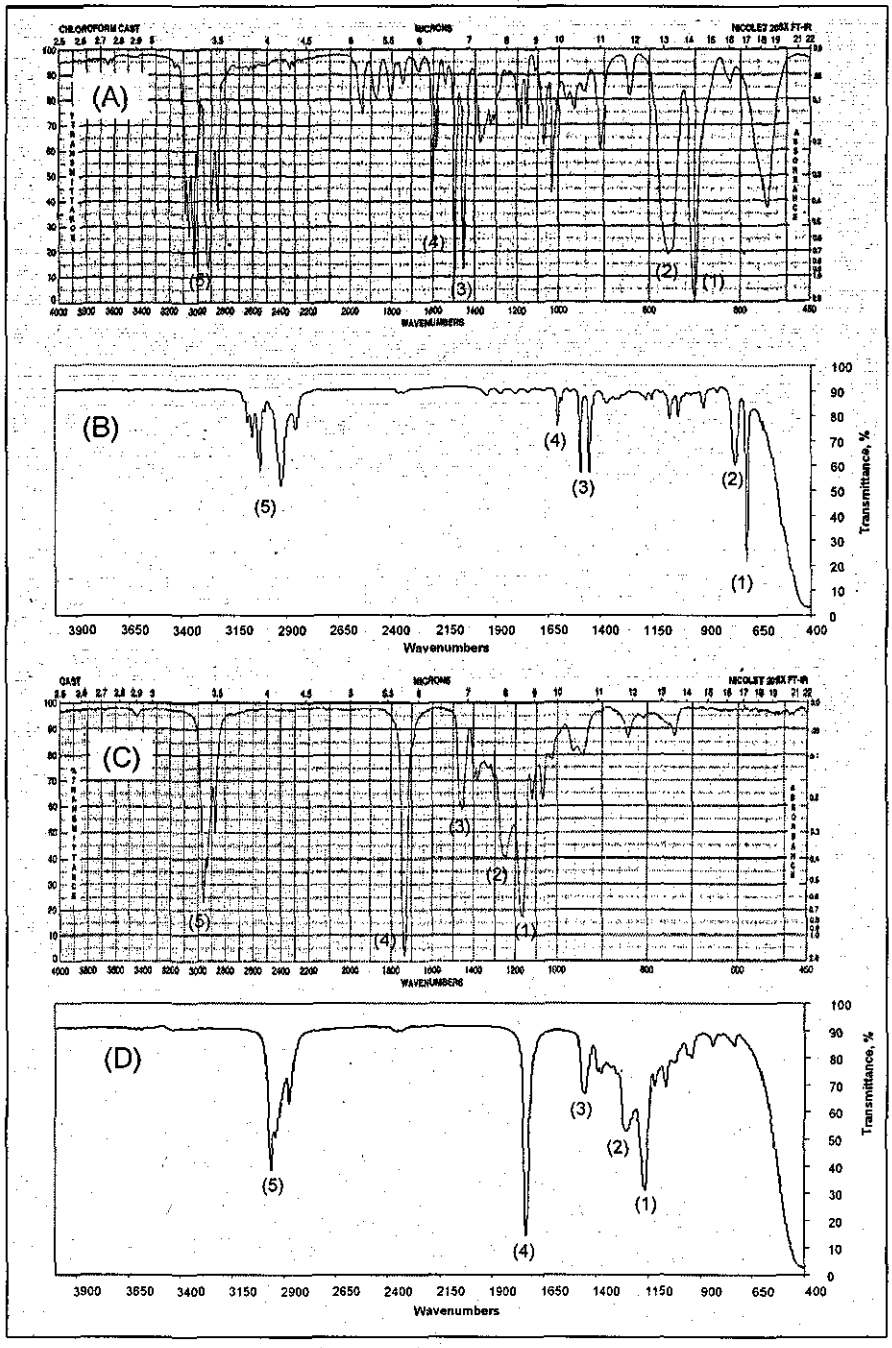

Figure 6.7 Aldrich™ IR spectra of PS (A) and PBA (C) homopolymers compared to the IR spectra of Fisher™ PS (B) homopolymer and PBA (D) homopolymer which is prepared by solution polymerization

Solutions of the PS and PBA homopolymers in THF at 5% w/w concentrations were prepared at different compositions (Table 6.3). The mixtures were prepared based on the monomers' molecular weights. For each composition, two films were cast on the NaCl discs using the same method explained earlier. Figure 6.8 illustrates the spectra of the different blends. Clearly, as the PBA concentration decreases some peaks which are associated with the PBA decrease, while others which are associated with the PS content in the blend started to increase.

PBA, g	PS, g	Molar fraction of PBA
0.2956	2.1614	0.1000
0.4496	1.4848	0.1975
0.3082	0.3933	0.3890
0.4439	0.2485	0.5921
0.6919	0.1523	0.7869
0.4853	0.045	0.8976

Table 6.3 Different PS-PBuA homopolymers blends based on the monomers molecular weights (BuA=128.17, Sty = 104.15)

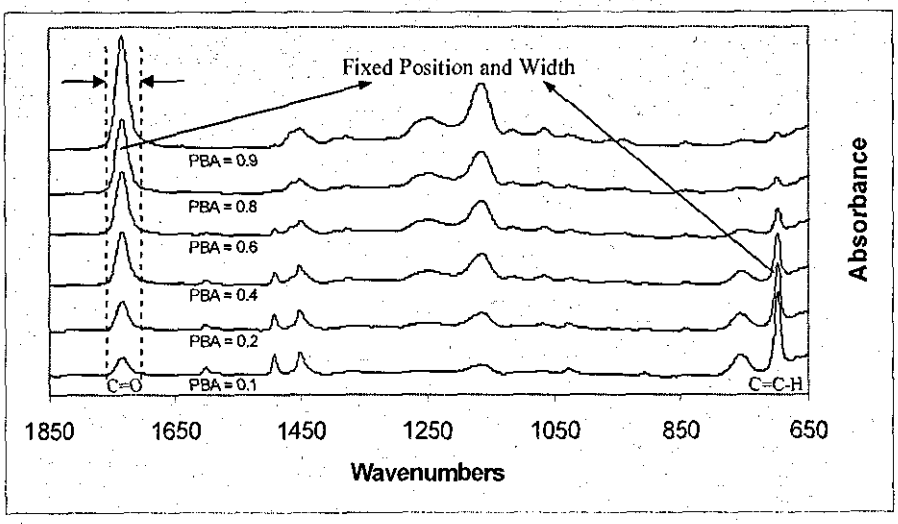

Figure 6.8 FT-IR spectra of different PS-PBuA blends

It should be noted that in quantitative infrared spectroscopy, baseline corrections should be implemented. The absorbance difference between the baseline and the top of the band is then used. Figure 6.9 is an illustration of this technique.

In creating the calibration curve, the ratio of the PBA carbonyl stretching C=O (i.e. peak at ~1730 cm^{-1}) to PS benzene ring bending C=C-H (i.e. peak at ~700 cm^{-1}) was chosen. The main reasons for choosing the peaks at 1730 cm^{-1} and 700 cm^{-1} is the fact that the peaks were present at the same position in all the different blends, and broadening was not detected with changing the composition, as illustrated in figure 6.8, hence these peaks are sequence-distribution-independent (§6.1) and can be used to estimate the copolymer composition.

The different absorbance values and molar ratios for the homopolymer blends are given in table 6.4. MATLAB® curve fitting tool box was used to fit the average absorbance ratio and the PBA molar content in the samples (figure 6.10). The butyl acrylate molar ratio in the samples can be estimated using this equation

$$\textit{Butyl acrylate content (mole fraction)} = \frac{-1.546\times10^{-4}x^{3}+5.595\times10^{-3}x^{2}+0.9252x-3.252\times10^{-2}}{x+1.699} \qquad 6.2$$

where x is the IR peak ratio, i.e. PBA carbonyl stretching (C=O) absorbance divided by the absorbance of the PS benzene ring bending (C=C-H).

It should be noted that the data in figure 6.10 were constructed based on homopolymer blends compositions that range from 0.1-0.9 by mole. Therefore, within this range it is expected that the calibration curve provides accurate estimates for the composition of the copolymer.

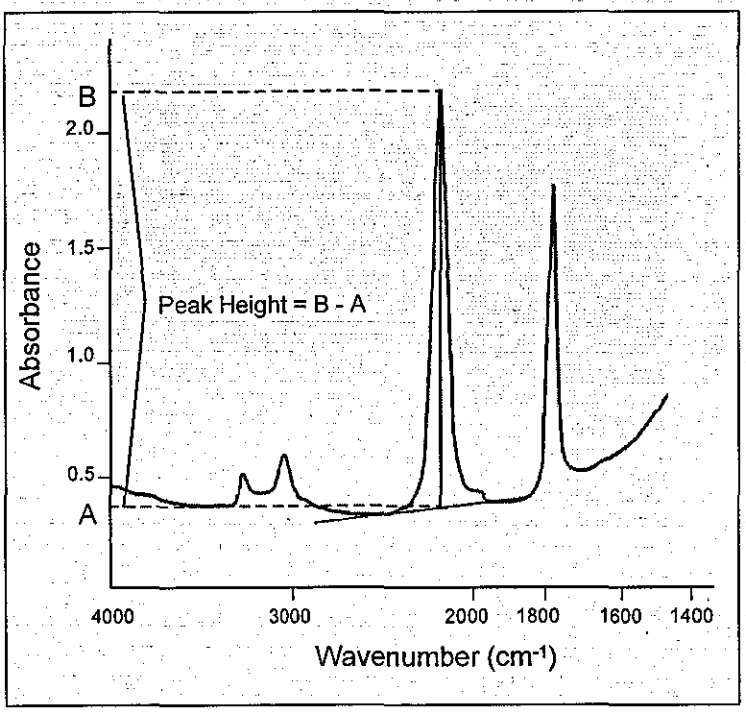

Figure 6.9 An illustration of IR baseline correction

PBA mole fraction	First set of films			Second set of films			Average abs. ratio
	PBA C=O	PS C=C-H	Abs. ratio	PBA C=O	PS C=C-H	Abs. ratio	
0.1000	0.1080	0.2348	0.2491	0.0999	0.2009	0.2404	0.2447
0.1975	0.1350	0.1929	0.5117	0.1259	0.1965	0.4976	0.5047
0.3890	0.1724	0.1588	1.2309	0.1625	0.1458	1.3220	1.2764
0.5921	0.1994	0.1108	3.0638	0.2002	0.1112	2.9017	2.9828
0.7869	0.2086	0.0756	7.4630	0.2275	0.0821	8.3781	7.9205
0.8976	0.2930	0.0736	20.9224	0.2511	0.0695	19.2404	20.0814

Table 6.4 FT-IR absorbance ratios of different homopolymer blends

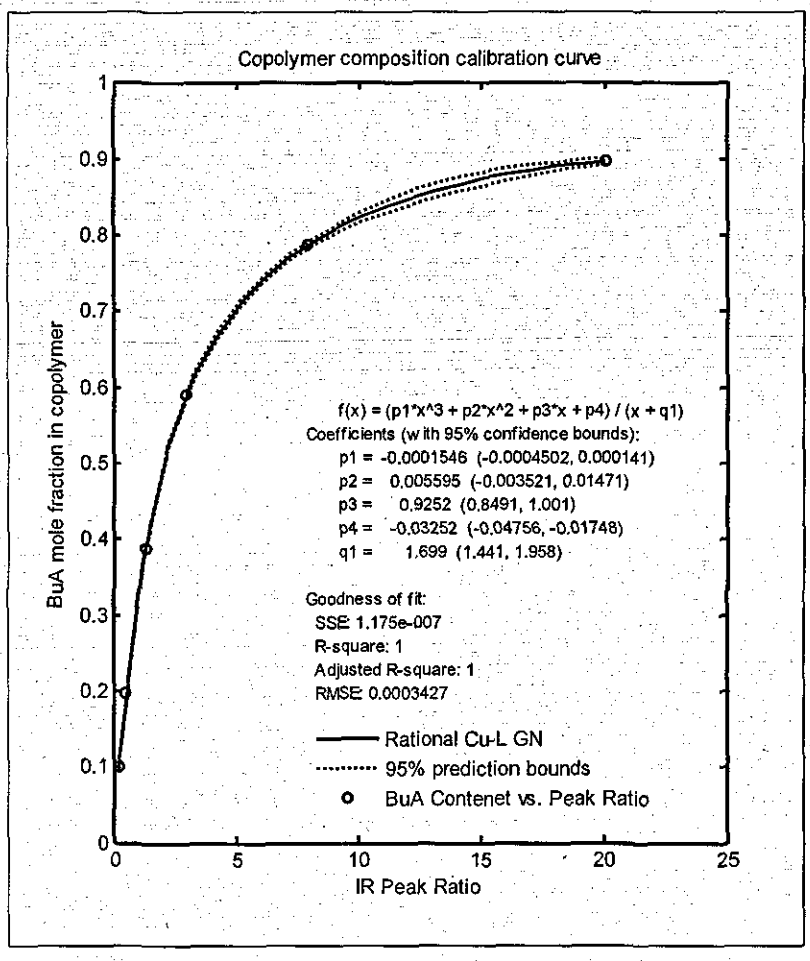

Figure 6.10 FT-IR calibration curves

6.3. Validating the calibration curve

Previously (§6.1) it was demonstrated how some IR absorbance bands are affected by the type of the neighboring units and those bands should not be used to estimate the copolymer composition. In order to study this, another analysis method can be used to estimate the composition (e.g. NMR, UV, GC) and then check whether the absorbance obtained from the IR for a certain peak changes linearly or not with composition estimated using the other method. The fact that the change is linear, coupled with no differences in the peak's frequency and no broadening is detected,

then this confirms that this peak is a good representative of the copolymer composition.

Another method to test the IR accuracy is to prepare a copolymer at low conversion (10-30%) and estimate its composition using a method other than the IR, and at the same time obtains IR spectra of this copolymer. Next homopolymer blends can be prepared where the composition is equivalent to the copolymer composition analyzed earlier, and analyze the blend with FT-IR. By comparing both spectra it is possible to isolate the peaks that have similar frequency and absolute absorbance and use them to estimate the composition.

Both methods require other analysis instruments which were not available, and also both require a technique of obtaining exactly equal film thicknesses for the IR analysis or using an IR solution cell with fixed width since the absolute absorbance is affected by the thickness of the sample. However, another method was implemented successfully to verify the calibration curve by means of an azeotropic copolymerization.

Wall (1944) explained that although the composition of a copolymer which is forming at any time is generally different from that of the monomer mixture, there can be particular compositions for which the copolymerization equation (Eq. 6.3) holds even though the reactivity ratios of the monomers are not equal to one ($r_1 \neq r_2 \neq 1$)

$$\frac{F_1}{F_2} = \frac{f_1(r_1 f_1 + f_2)}{f_2(r_2 f_2 + f_1)} \qquad 6.3$$

F_i and f_i are the instantaneous copolymer and feed compositions; respectively. By setting $F_1 = f_1$, Eq 6.4 transforms into

$$(f_1)_c = \frac{1-r_2}{2-r_1-r_2} \qquad 6.4$$

This indicated that if the composition of the monomer mixture in the reactor is based on Eq. 6.4, then the system forms a constant polymerizing mixture. In other words, the copolymer produced will be of a uniform composition given by the azeotropic monomer ratio.

Preparing azeotropic copolymers using homogeneous polymerizations (i.e. bulk and solution polymerizations) is possible. But for heterogeneous systems (e.g. emulsion) since polymerization occurs in the particles, it is not simple to guarantee that the monomer mixture in the particles is equivalent to the azeotropic monomer ratio.

Cruzrivera et al. (1989) demonstrated the possibility of preparing Sty-BuA azeotropic copolymer when the Sty/BuA molar ratio = 2.72. The molar ratio of the Sty should be 0.73 and the BuA molar ratio should be 0.27. Applying those numbers in 6.3 reveals that the reactivity ratios of the styrene and butyl acrylate are 0.7, and 0.2; respectively.

Next two azeotropic copolymerization experiments will be discussed. The first one is a solution copolymerization, and the second one is an emulsion copolymerization. The solution copolymerization recipe is given in table 6.5, and it was performed similarly to the preparation of the PBA homopolymer explained earlier.

FT-IR analysis was carried out on two solution copolymer samples, and by dividing the absolute absorbance of the C=O peak by the absolute absorbance of C=C-H peak, the absorbance ratios 0.810, and 0.814 were obtained. Applying those numbers to Eq. 6.2, the estimated butyl acrylate content in the copolymer was found

to be 29% which is identical to the butyl acrylate content in the actual recipe (figure 6.5).

Component	Weight (g)	Density (g/cm^3)	Molecular Weight	Mole Fraction
Butyl acrylate	9.0	0.8940	128.17	0.29
Styrene	18.0	0.9090	104.15	0.71
Toluene	130.0	0.8661	92.13	-
Lauryol Peroxide	0.12	-	398.70	-

Table 6.5 Recipe of azeotropic copolymerization of Sty-BuA in solution

Component	Weight, g
Surfactant (SLS)	6
Initiator (KPS)	0.5
Buffer ($NaHCO_3$)	0.5
Deionized Water	600
Styrene	114
Butyl acrylate	52

Table 6.6 Recipe of azeotropic copolymerization of Sty-BuA in emulsion

The second experiment was an azeotropic batch emulsion copolymerization run (table 6.6) which was carried out in a 1 L jacketed batch reactor. The polymerization temperature was 70 °C, and the reaction mixture was purged with N_2 while agitating at 300 rpm prior to the addition of the initiator. Samples were collected every 2-3 minutes in the first 15 minutes, and then every 30 minutes. The duration of the experiment was four hours.

The instantaneous conversion and the butyl acrylate content in the copolymer determined by the FT-IR and the calibration curve (figure 6.10) evolution with time

are given in figure 6.11(A), and the particle sizes (z-average) and number of polymer particles evolution with time is illustrated in figure 6.11(B).

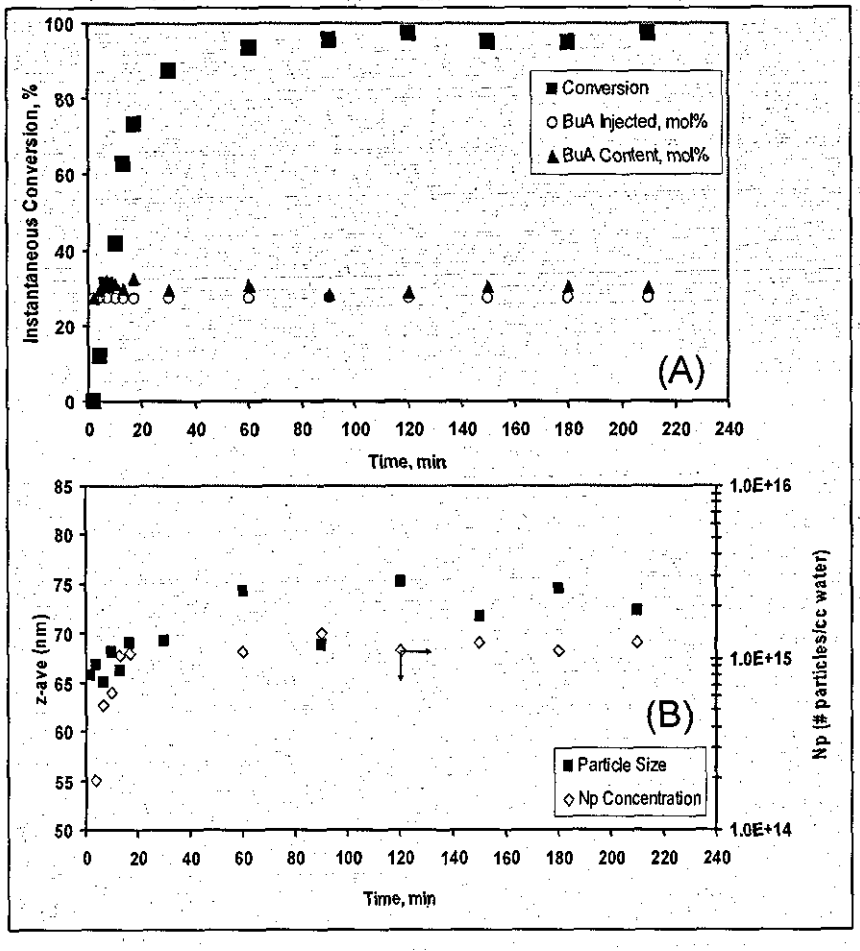

Figure 6.11 Instantaneous conversion and butyl acrylate content (A) and the z-average and number of polymer particles (B) evolution with time for the azeotropic batch emulsion copolymerization

Figure 6.11(A) illustrates the usual behavior of the conversion evolution in a batch reactor. In the beginning, the system exhibits a sharp increase in the conversion (interval 1); particle nucleation occurs in this interval, with the polymerization rate increasing with time as the polymer particle number builds up. In interval two the number of polymer particles is constant, and the monomer diffuses from the monomer drops to the polymer particles; the polymerization rate is slower in this interval. The

third and last interval starts when the monomer drops disappear and the system starts to consume the dissolved monomer; noticeably the polymerization rate is much slower in this interval.

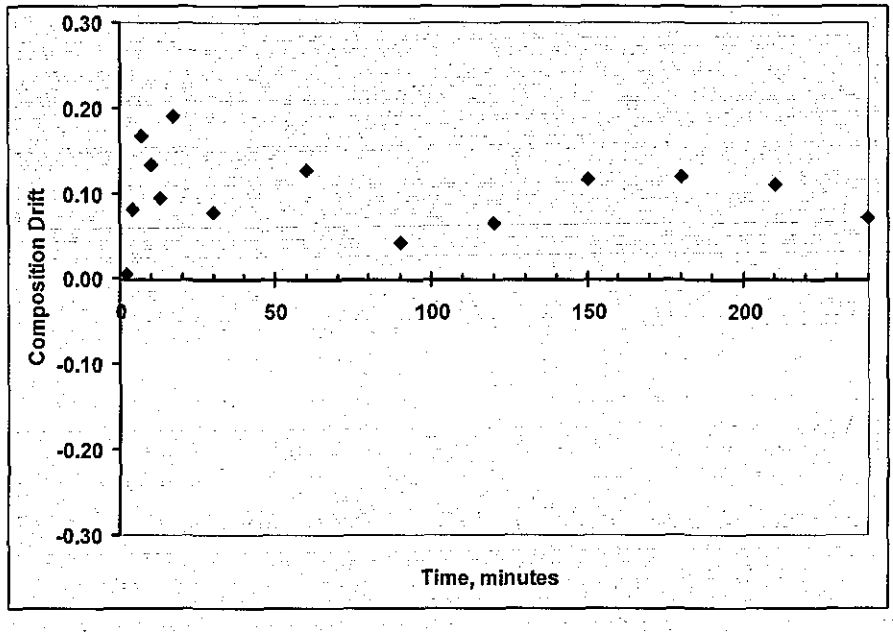

Figure 6.12 The composition drift of the azeotropic batch emulsion copolymerization

Most of the polymerization occurs in the first 30 minutes, which is also indicated by the increase in the z-average in figure 6.11(B). After the first 30 minutes, the particle size slightly increases and remained constant at the end. Once more, this behaviour is also expected since most of the monomers were consumed and very little is available (~10%), so the size does not change greatly.

The composition drift (i.e. the ratio between the BuA content in the copolymer and the BuA injected to the reaction vessel) is illustrated in figure 6.12. A value of 0.0 represents the ideal case where no composition drift is occurring, a negative value indicates that the BuA content in the sample is less than the BuA content in the reactor, and a positive value indicates the reverse. It should be noted that the reported

composition in figures 6.11 and 6.12 is the average composition of the polymer particles, not the instantaneous composition of the copolymer just formed.

Observing figure 6.11, the first sample extracted after two minutes showed a butyl acrylate content of 28% and after 30 minutes the BuA content was 28% as well. The butyl acrylate content in the extracted samples remained constant and varied between 27% and 30% for the remaining of the experiment. Figure 6.12 demonstrates that the copolymer composition was nearly constant and minimal composition drift was detected. This result is in agreement with Cruzrivera et al. (1989).

The data from the azeotropic solution and emulsion copolymerizations demonstrate that the calibration curve was able to give accurate estimates of the copolymer composition and confirms the validity of the FT-IR technique.

6.4. Conclusion

A brief literature review focused on the analysis of the copolymer composition using the spectroscopic techniques was presented. The investigated spectroscopic techniques (i.e. NMR, UV, and FT-IR) were confirmed to be adequate in studying the copolymer microstructure, and were able to provide precise estimates of the copolymer composition. The NMR and UV do not suffer from some of the limitations that are associated with the FT-IR technique. Due to the lack of NMR instrument and the inadequacy of the UV technique, the FT-IR technique was selected since it provides information about the copolymer microstructure and composition. The FT-IR spectroscopic technique was applied successfully.

Copolymer samples with accurate compositions which could serve as standards for building the FT-IR calibration curve are not available; therefore blends of homopolymers were used to construct the FT-IR calibration curve. The FT-IR spectra show several IR absorption bands (peaks); some of those bands are sequence-distribution-dependent and some are sequence-distribution-independent; the latter are

the ones used for building the calibration curve and estimating the overall copolymer composition.

For the copolymer styrene-butyl acrylate, it was demonstrated that absolute peak ratios for PBA carbonyl stretching (i.e. C=O peak at ~1730 cm^{-1}) and the PS benzene ring bending (i.e. C=C-H at ~700 cm^{-1}) could be used to estimate the composition of the copolymer. Homopolymer blends of PBA and PS were used to construct a calibration curve, which was validated by a set of azeotropic copolymerization experiments in solution and in emulsion.

7. Effects of Monomer Feeding Policy

7.1. Introduction

In this chapter a detailed presentation of the experiments conducted to investigate the effects of distributing the monomers between the initial charge and the subsequent feed on the composition of the copolymer styrene-butyl acrylate will be given. The evolutions of the instantaneous and the overall conversion, the particle size, the number of polymer particles, the composition of the copolymer, and the concentration of the monomers in the different phases with time will be discussed. A detailed discussion of the work that was conducted on this particular copolymer in the literature was given in chapter three.

7.2. Monomers distribution effects

Several runs were made where the flow rate of the monomers and the total mass of styrene and butyl acrylate in the feed and in the initial charge were varied. The recipes of the experiments are given in table 7.1.

There are two stages for each experiment, in the first stage the experiment was conducted in a semibatch mode, and in the second stage the experiment was operated in a batch mode. The total duration for both stages does not exceed four hours (240 minutes), and the duration of the second stage (i.e. batch stage) depends on the duration of the first stage (i.e. semibatch stage). The first stage duration was varied between 90 and 180 minutes, so the remaining time to complete the four hours reaction time will be for the batch stage.

The masses of the initiator, deionized water, surfactant, and the buffer were all kept constant. The reaction temperature was also kept constant at or near 70° C, and the monomers flow rate was adjusted to completely transfer the monomers in either 90 or 180 minutes. The total mass that exists in the reactor at the end of each experiment and the solids content (i.e. mass ratio of the polymer to everything else in

the reactor if all the monomers got converted) were kept constants at around 1100 cc and an average of 32% respectively.

Run	Monomers in I.C., g		Monomers Transferred, g		Feeding Time, minutes	Monomers Mole Ratio %, Sty/BuA
	Sty	BuA	Sty	BuA		
1	194.53	0.00	0.00	163.65	180	59/41
2	0.00	160.00	199.62	0.00	180	61/39
3	96.97	0.00	98.17	164.14	180	59/41
4	0.00	80.00	196.34	80.46	180	60/40
5	194.00	0.00	0.00	160.92	90	60/40
6	0.00	160.00	199.62	0.00	90	61/39
7	97.00	0.00	101.44	159.31	90	61/39
8	0.00	80.00	197.98	84.48	90	60/40
9	0.00	0.00	245.43	76.44	90	80/20
10	0.00	0.00	43.36	185.06	90	22/78
11	0.00	0.00	171.80	138.39	90	60/40
12	0.00	0.00	71.99	211.61	90	30/70
Other Ingredients		Surfactant (SLS)			7.1 g	
		Initiator (KPS)			0.6 g	
		Buffer ($NaHCO_3$)			0.6 g	
		Deionised Water			700 g	
		Final Volume			1100 cm^3	
		Solids Content			32%	
		Temperature			70° C	

Table 7.1 The recipes of the experiments related to the study of the monomers effects on the copolymer

Next a discussion of the observed effects on the instantaneous and overall conversion, the composition of the copolymer, and the particles will be presented.

7.2.1. Instantaneous and overall conversion evolutions

Figures 7.1 and 7.2 illustrate the instantaneous (§3.1.1) and the overall conversion evolutions with time for experiments R1-R8.

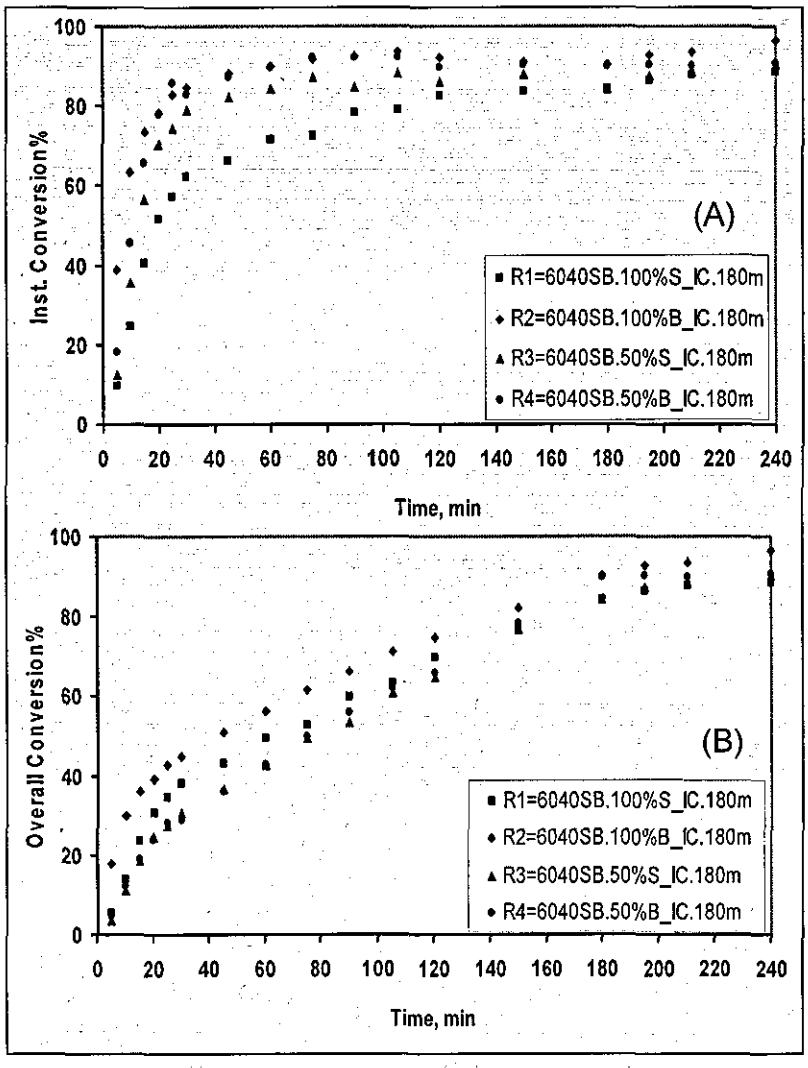

Figure 7.1 The time evolution of the instantaneous (A) and the overall (B) conversions for the experiments R1-R4

The duration of the semibatch stage for the experiments in figure 7.1 is 180 minutes, whereas the semibatch stage duration for the runs in figure 7.2 is 90 minutes.

The total reaction time for all the experiments (i.e. semibatch and batch stages) is 240 minutes.

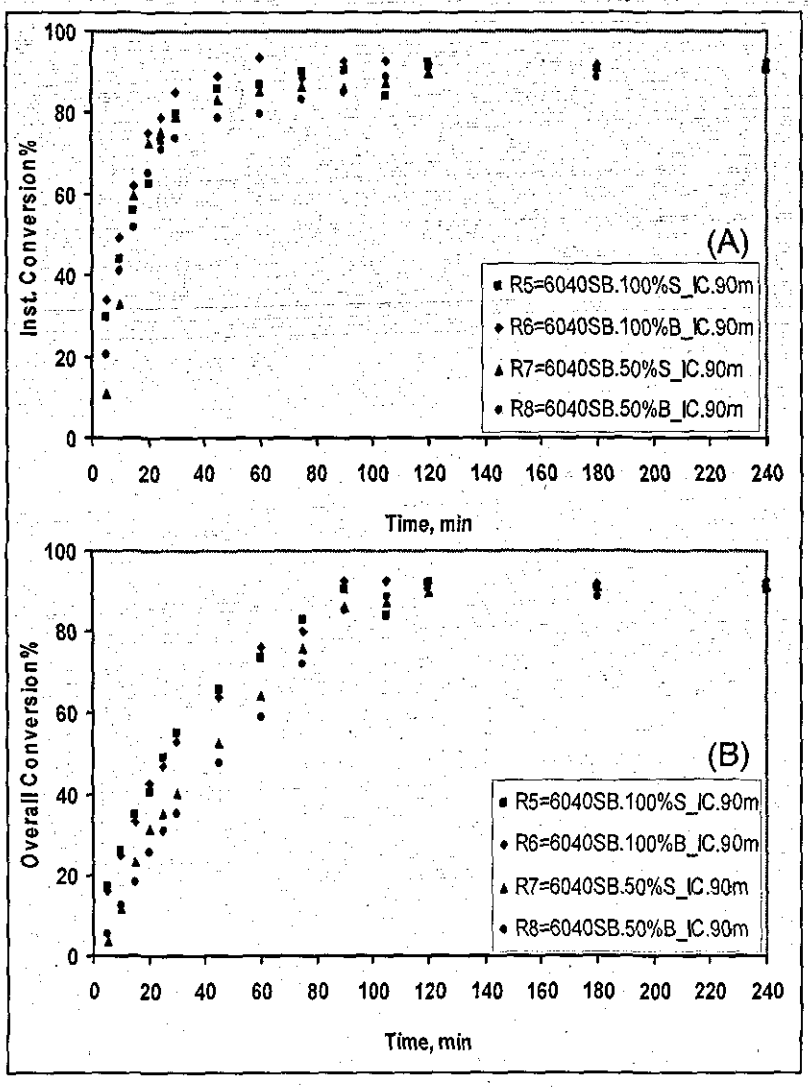

Figure 7.2 The time evolution of the instantaneous (A) and the overall (B) conversions for the experiments R5-R8

The code which appears in the legend of the above figures explains the Sty/BuA molar ratio in the recipe, the mass fraction of one of the monomer in the initial charge, and the duration of the semibatch stage. For instance in figure 7.2, R8=6040SB.50%B_IC.90m indicates that the Sty/BuA molar ratio in the recipe was

60/40, 50% of the BuA existed in the initial charge, and that the duration of the semibatch stage was 90 minutes. This format will be used throughout the next chapters.

In §3.1 the instantaneous conversion was defined as the ratio between the polymer in the reactor and the monomer fed up until the sampling time. However, the overall conversion is the ratio between the polymer in the reactor and the total monomer in the recipe.

The instantaneous conversion curves in figures 7.1(A) and 7.2(A) illustrate an expected behavior which is comparable to figure 5.1 (Zubitur and Asua, 2001); where at an early stage the system exhibits a sharp increase in the polymerization rate due to nucleation. At this stage (i.e. interval 1, §2.3) most of the micelles are activated by initiator radicals leading to a sharp increase in the polymerization rate. This interval ends when all the micelles are activated and free surfactant is not available in the system. As more monomer gets converted, the instantaneous conversion slightly increases until the end of the semibatch stage. This interval is denoted as interval 2, and it ceases when the monomer drops vanish. During the batch stage the remaining monomers are consumed and since no further monomer is added, then there is no monomer accumulation. Hence there is a noticeable increase in the instantaneous conversion in the batch stage, as might be expected.

The overall conversion profiles in figures 7.1(B) and 7.2(B) illustrate that starting with one of the monomers fully charged in the beginning (i.e. R1, R2, R5, and R6) gives higher overall conversions when compared to the other feeding scenarios (i.e. R3, R4, R7, and R8). Starting with monomer in the initial charge implies that this monomer will be available in the reaction medium to polymerize for longer times when compared to feeding the monomer along the course of the reaction, this will eventually lead to higher conversions. As a result, increasing the amount of the monomer in the initial charge leads to higher overall conversions as shown in the aforementioned figures.

The recipe for the experiments R1-R8 was kept unaltered (Table 7.1), and yet it should be noted that this is a binary system where the monomers have different molar masses (Sty=104.15, BuA=128.17) and that the molar ratio of the monomers in the recipe is 60/40 (i.e. Sty/BuA molar ratio). As a result, starting with 100% or 50% of one particular monomer, and feeding the remaining during the semibatch stage will eventually lead to the injection of the same amount of monomer as shown in figures 7.3(A) and 7.4(A) but only at the end of the semibatch stage, and not before that.

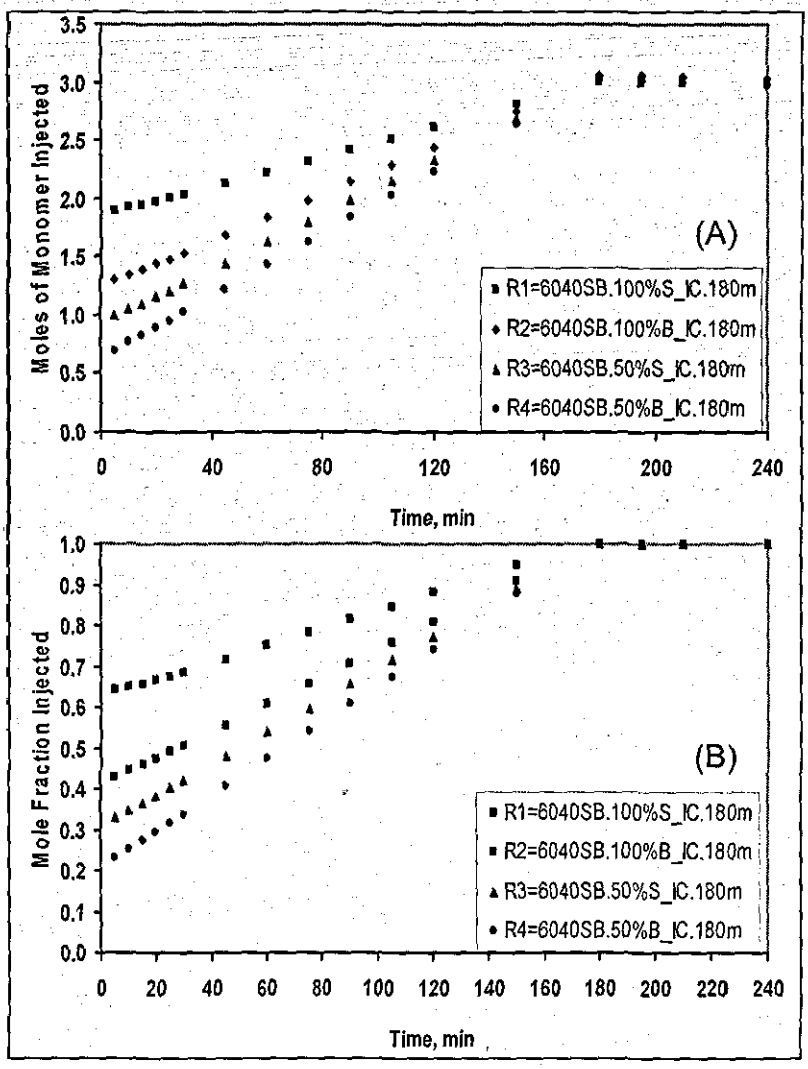

Figure 7.3 The total moles (A) and overall mole fraction (B) of injected monomers for the experiments R1-R4

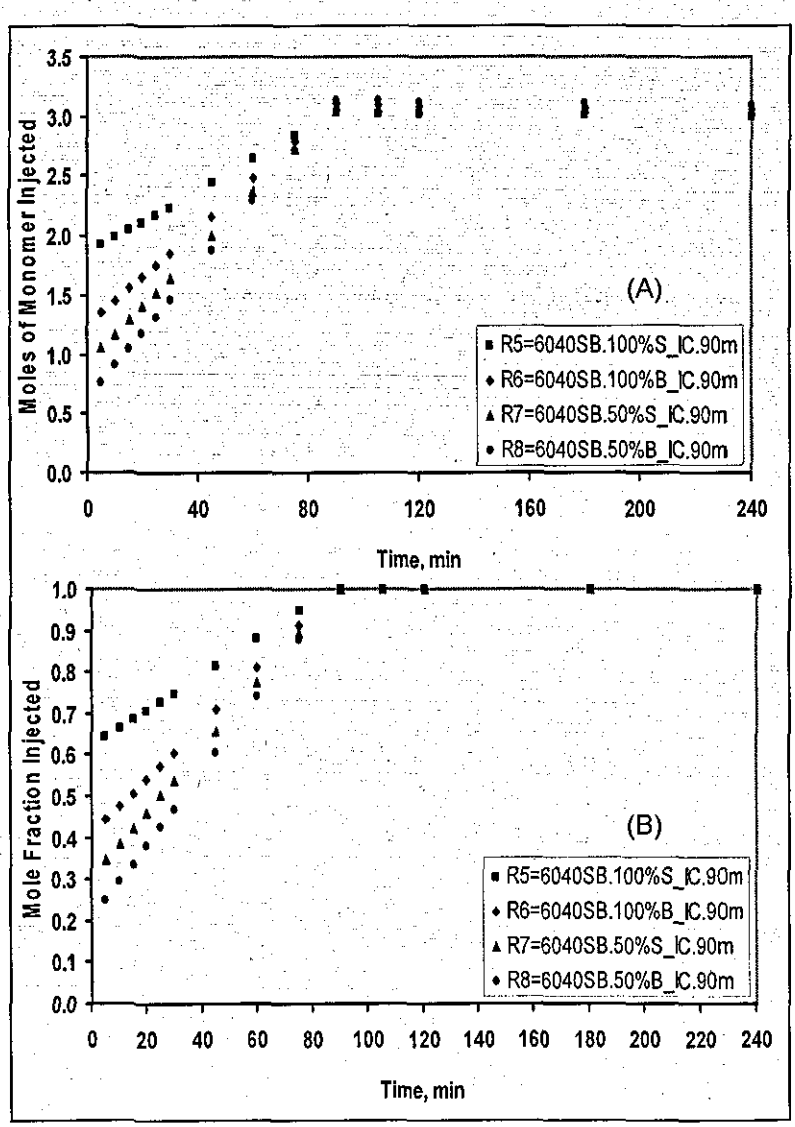

Figure 7.4 The total moles (A) and overall mole fraction (B) of injected monomers for the experiments R5-R8

This could be further explained by examining figures 7.3 and 7.4 which illustrate the time evolution of the total moles of monomers that were injected to the reactor, and the overall fraction of the monomer in the reactor (i.e. mole ratio of monomer injected to the total moles of monomer in the recipe). At the end of the semibatch stage three moles of monomer were fed in all the experiments. But in the

beginning of the experiments, the amount of the monomer in the initial charge varies according to the feeding scenario of each experiment.

Further investigation of figures 7.1(A) and 7.2(A) one can observe that the runs where the BuA existed in the initial charge exhibited higher conversions compared to the runs where the Sty was in the initial charge. For instance, the instantaneous conversion for R4 was higher than R3, this was apparent even at an early stage of the reaction. In addition, R5 and R6 demonstrated the same result.

As explained in §2.4.1, the rate of polymerization in emulsion polymerizations is given by equation 2.5. Considering the facts that the reactivity of the Sty is higher than the BuA, the respective k_p values for the BuA = 127 l mol^{-1} s^{-1} and for the Sty = 376 l mol^{-1} s^{-1} (deArbina et al., 1996) and since starting with 100% or 50% of the Sty in the initial charge provides more monomer than starting with the BuA (figures 7.3 and 7.4). All these facts suggest higher polymerization rates when the Sty exists in the reactor and not the other way around.

Investigating the effects of starting with one monomer or the other on the overall conversion (Figure 7.1 and 7.2), it is noticeable that the overall conversion for R2 was higher than R1; R4 and R3 demonstrated the same behavior where starting with 50% BuA in the initial charge leads to higher overall conversions. R5 and R6 showed similar overall conversion behavior, and since the monomer content in R5 is more than R6 this confirms that R6 polymerization rate was higher. In runs R7 and R8, starting with the 50% Sty in the initial charge gave slightly higher overall conversions. These results clearly indicate that the polymerization rate increases with increasing the BuA content in the recipe.

Nomura et al. (1972) reported that monomer diffusion from droplets to the aqueous phase can be the limiting step; so more soluble monomers have higher mass-transfer rate leading to higher polymerization rates. Zubitur and Asua (2001) reported that increasing the stirring speed will overcome the limitations reported by Nomura et

al. since reducing the size of the drops will increase the surface area leading to higher mass-transfer rates. However, it should be noted that earlier (§5.2) it was shown that increasing the stirrer speed did not increase the polymerization rates. Furthermore, the constant partition coefficient model predicted that monomer drops vanished after the first 10 minutes. These two facts indicate that the solubility in the water did not play a role in increasing the polymerization rate, and this is in agreement with other reports (Flory, 1953; Brooks, 1970).

Some researchers (Piirma and Chen; 1979) reported that the polarity of the polymer affects the effective molecular area of a surfactant molecule on the particle surface (i.e. area occupied by each surfactant molecule on a particle). They reported that as the polarity of the copolymer increases due to composition change, the affinity between the surfactant molecules and the polymer particle is becoming less than the affinity between the surfactant molecules themselves. Therefore, the area occupied by each surfactant molecule on a particle (A_m) is increasing due to the polymer particles being partially covered.

Polystyrene is non-polar and polybutyl acrylate is a polar polymer, thus, it is expected that as the butyl acrylate in the composition increases, A_m increases, leading to more free surfactant molecules being available in the system. These excess surfactant molecules could lead to more micelles which could increase the polymerization rates. This will be investigated in §7.2.3.

Araujo et al. (2001) revealed a possible correlation between the monomer solubility in water and the polymerization rate, they suggested that homogeneous nucleation for water soluble monomers could increase the number of polymer particles leading to an increase in the polymerization rate (§3.1).

It was also reported that increasing the BuA in the recipe leads to an increase in the polymerization rate. Yang and Yang (1998) reported that increasing the Sty ratio retarded the reaction rate. Guillaume et al. (1990) suggested that the increase in

the polymerization rate when the BuA ratio was increased could be caused by an increase of the average number of radicals per particle ($\bar{n}$) in the case of rich BuA copolymerizations, and this behavior was attributed to gel effect (§2.2.1 and §2.3).

Plessis et al. (2001) reported that the addition of small amounts of Sty to the reaction mixture in the seeded semi-batch emulsion copolymerization of Sty/BuA reduced the level of branching and reduced the gel effect. Gilbert et al. (2005) explains that branching occurs via two reactions: a bimolecular reaction, intermolecular chain transfer by hydrogen atom abstraction (long chain branching, LCB), and a unimolecular reaction, intramolecular "backbiting" (short chain branching, SCB). The Sty monomer does not branch and it reduces the PBuA ends, consequently reducing the SCB effect.

It should be noted that increasing the BuA content in the polymer beyond 40% increased the cross-linking. This finding was detected while dissolving the samples in THF for the composition study. The increase in the cross-linking could be an indication of an increase in the gel effect leading to higher polymerization rates for the BuA rich initial charge runs.

Figures 7.5 and 7.6 demonstrate the time evolution of the calculated monomer mass fraction in the particles (Appendix C). It is noticeable that both monomers showed similar concentration in the particles. For instance, the Sty mass fraction in R1 (figure 7.5A) and the BuA mass fraction in R2 (figure 7.5B) were similar (i.e. ~0.55), this is an indication that the solubility of the monomers did not affect the monomer mass transfer to the particles. R5 in figure 7.6B shows that after 60 minutes the Sty monomer vanished from the particles; consequently the polymerization rate after the first hour is driven by the added BuA. Similarly, R6 in figure 7.6A showed that it took the BuA 45 minutes to fully polymerize. It should be noted that on molar bases, R5 contained initially 22% more monomer than R6. R2 in figure 7.5B showed a behavior similar to the previous ones; whereas the result in R1 demonstrates that the Sty rate of depletion was low compared to the other cases, which is a sign of low

polymerization rate for this particular case. This result is analogous to the instantaneous conversion evolution result (R1, figure 7.1A).

In experiments R3, R4, R7, and R8 50% of one particular monomer was injected initially, and the remaining was fed during the semibatch stage. So it was expected to observe that both monomers existed in the particles at least until the end of the semibatch stage, and this is exactly what figures 7.5 and 7.6 demonstrate.

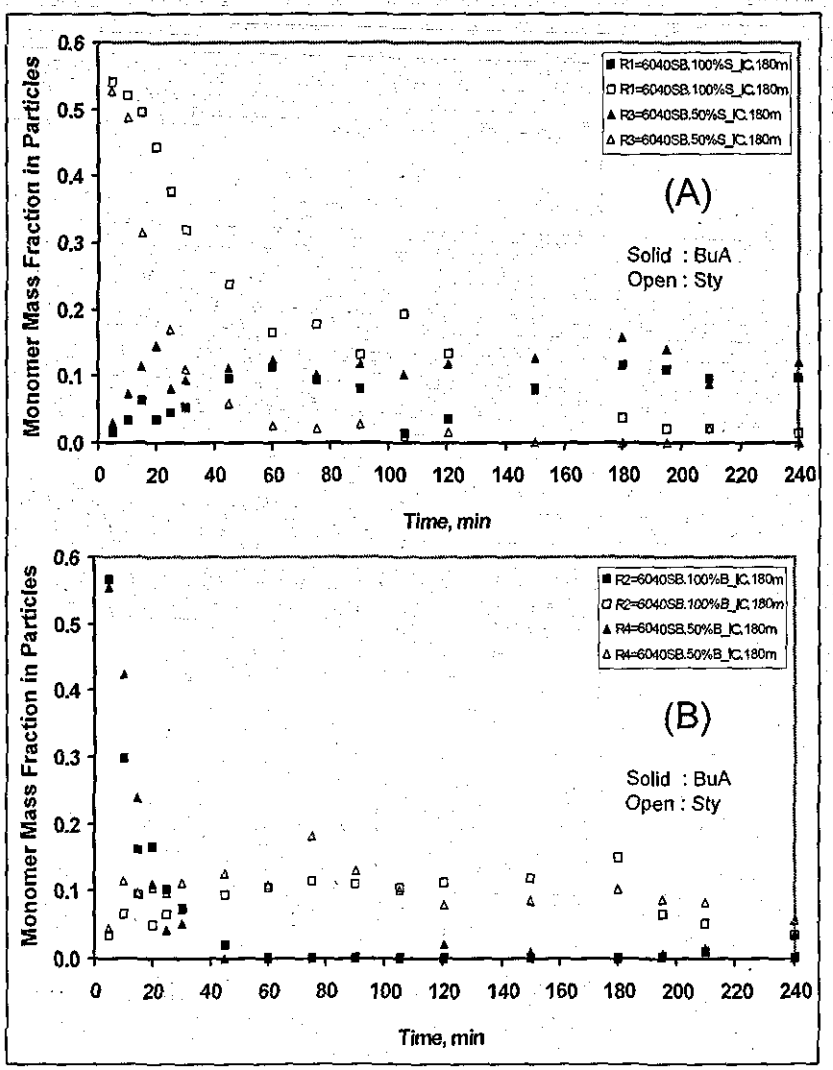

Figure 7.5 The time evolution of the monomers mass fraction in the polymer particles for 180 minutes feeding time experiments

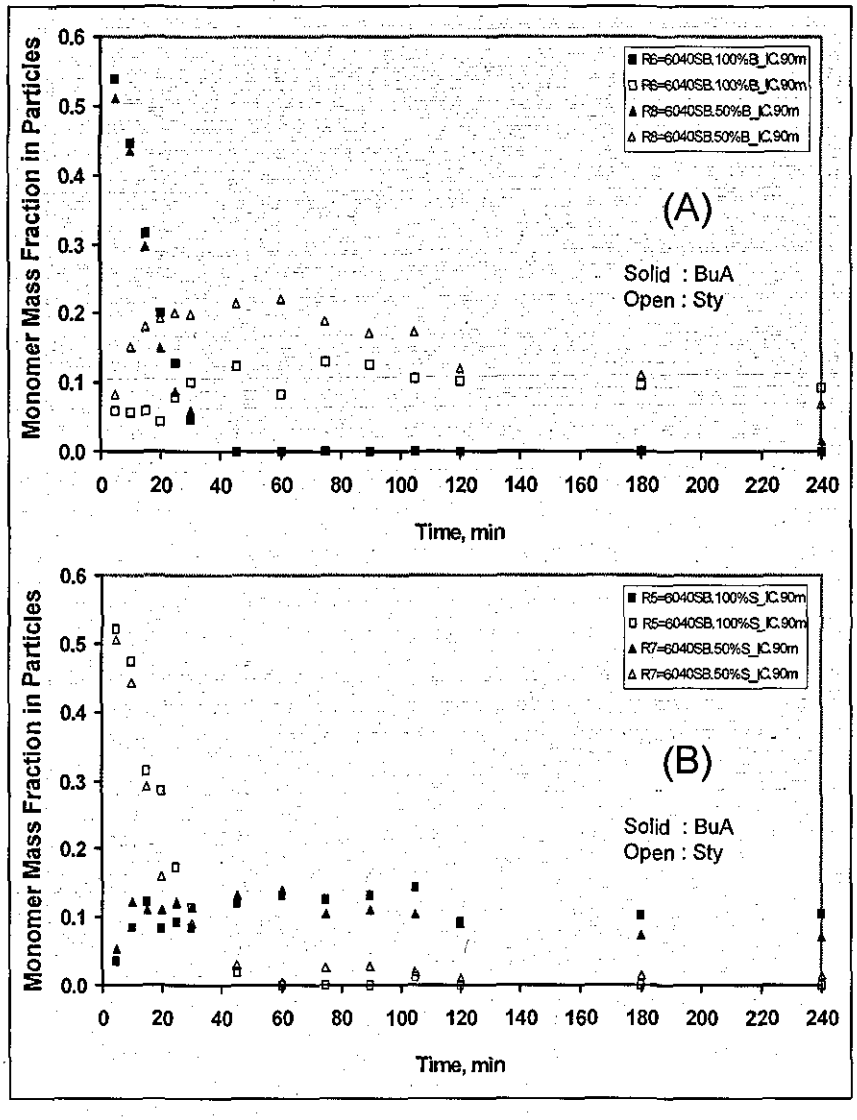

Figure 7.6 The time evolution of the monomers mass fraction in the polymer particles for 90 minutes feeding time experiments

These results suggest that starting the reaction with the BuA in the initial charge leads to higher polymerization rates; the overall and the instantaneous conversions were higher for the runs containing BuA in the initial charge. It is also noticeable that the differences in the solubility in the aqueous solvent between the monomers did not affect the mass fraction of the monomers in the particles; the

monomer concentrations were similar. The rate of depletion of both monomers was almost identical for most of the cases. R1 showed a slow polymerization rate which is apparent in the instantaneous conversion evolution (Figure 7.1A) and the Sty mass fraction in the particles (Figure 7.5A).

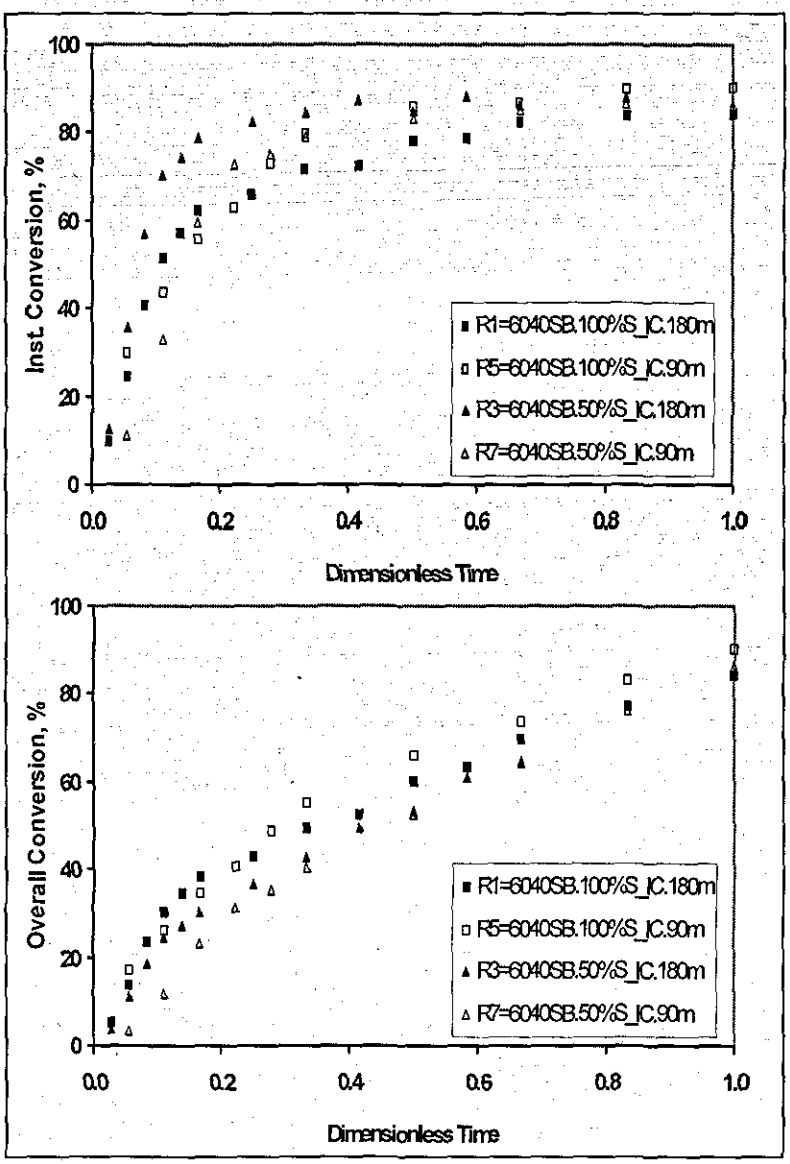

Figure 7.7 Feeding time effect on the instantaneous (A) and overall (B) conversions for Sty rich initial charge experiments

Figures 7.7 and 7.8 illustrate the feeding time effect on the conversion throughout the semibatch stage. It should be noted that the x-axis represents the ratio between the sampling time and the duration of the semibatch stage. The instantaneous conversion results (figures 7.7A and 7.8A) indicate that increasing the feeding rate decreases the instantaneous conversion, consequently increasing the monomer accumulation in the reactor.

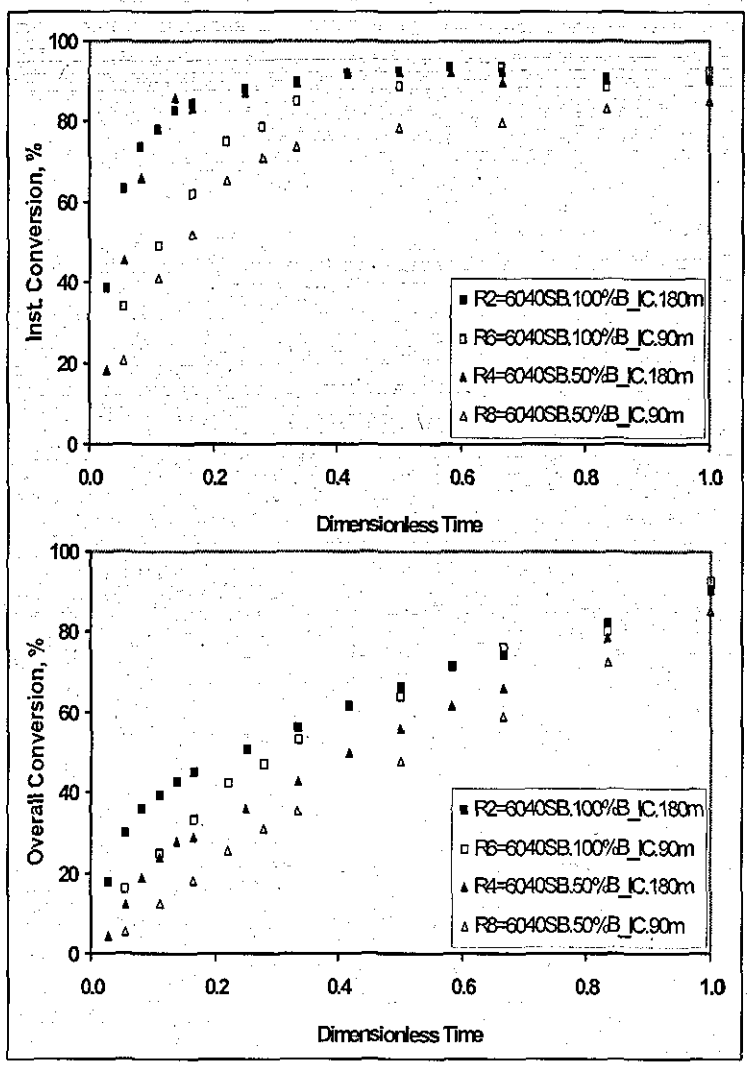

Figure 7.8 Feeding time effect on the instantaneous (A) and overall (B) conversions for BuA rich initial charge experiments

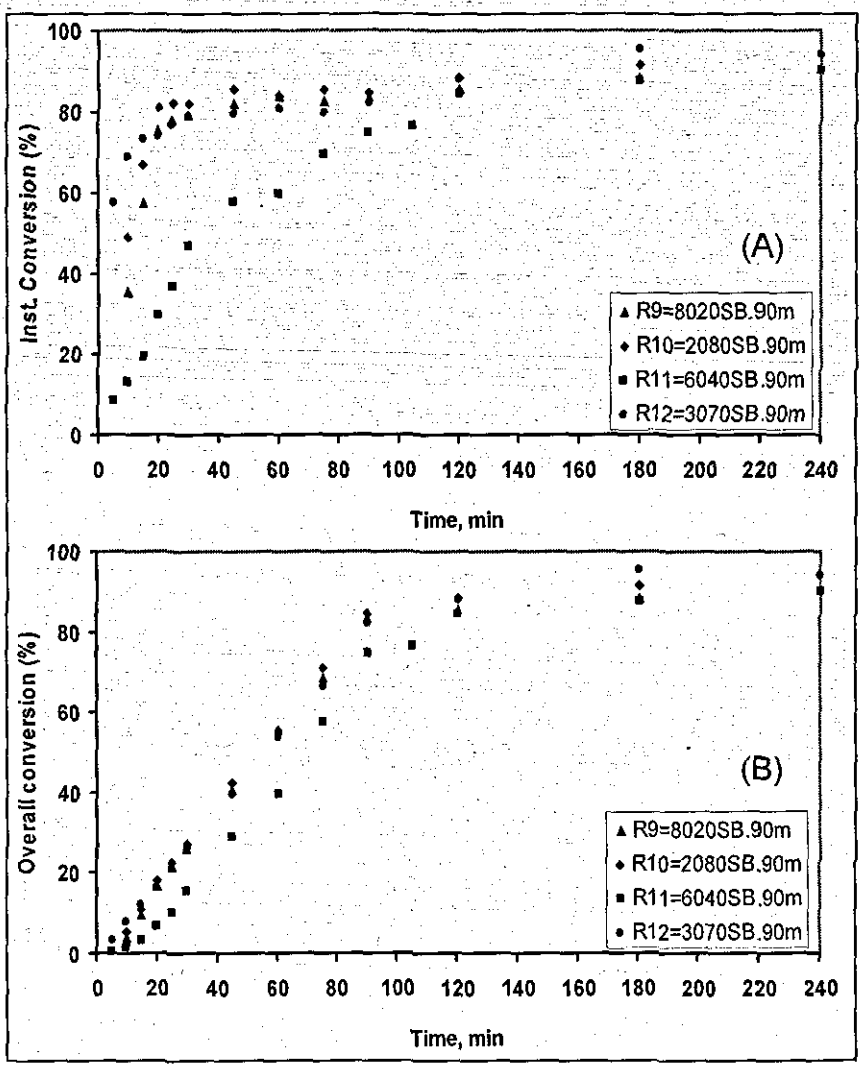

Figure 7.9 The time evolution of the instantaneous (A) and the overall (B) conversions for the experiments R9-R12

Figures 7.9, 7.10, and 7.11 demonstrate the conversion, the time evolution of the monomers fed to the reactor and the monomer mass fraction in the particles for the experiments R9-R12, respectively. The recipes in these experiments were not identical. The solids content and the Sty/BuA ratios were varied in order to investigate their effects on the kinetics of the reaction and the physical properties of the copolymer. The total moles of monomers transferred to the reactor were between 1.7

and 2.7 moles (figure 7.10), and in these runs the initial charge did not contain monomers. All the monomers in the recipe were fed during the semibatch stage which lasted for 90 minutes (Table 7.1).

Observing the instantaneous conversion curves (figure 7.9A); some differences between the experiments are observed. R12 exhibited the highest initial instantaneous conversion, and R11 was the lowest. The overall conversion results indicate that R9, R10, and R12 exhibited similar conversion profiles during the semibatch stage, and then R12 gave higher conversions in the batch stage. It should be noted that R12 recipe, on molar bases, contain more monomer than the other runs.

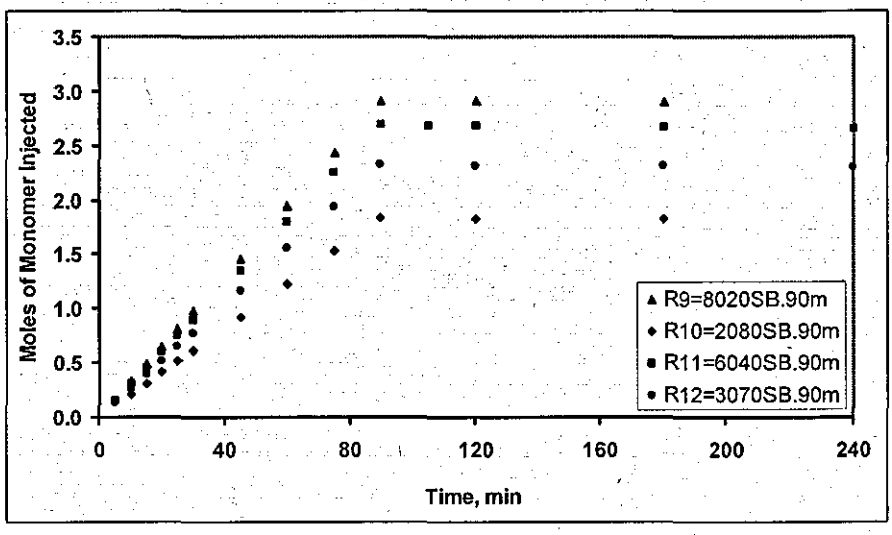

Figure 7.10 The time evolution for the total moles of monomer injected to the reactor for the experiments R9-R12

Figure 7.11 demonstrates an interesting fact; it is noticeable that the particles were initially rich with BuA monomer even when the recipe was dominated by the Sty monomer. For instance, in R9, the Sty/BuA ratio was 80/20, yet the BuA mass fraction was slightly higher than the Sty mass fraction. The BuA in the recipes of the experiments R10 and R12 was richer than the Sty, so it was expected to notice the differences in the particles. The BuA depletion rate was noticeable in R9, R10, and R12, whereas the Sty concentration seems constant, as if its rate of accumulation in

the particles is close to its rate of depletion. As the conversion increases, the monomer mass fraction in the particles becomes similar.

Figure 7.11 illustrates that the monomers concentration in the particles in R11 were similar; the fact that 60/40 Sty/BuA molar ratio is near the azeotropic composition (i.e. Sty/BuA=70/30) could play a role in the monomers mass fraction in the reactor since the differences in molar mass between the two monomers is not large.

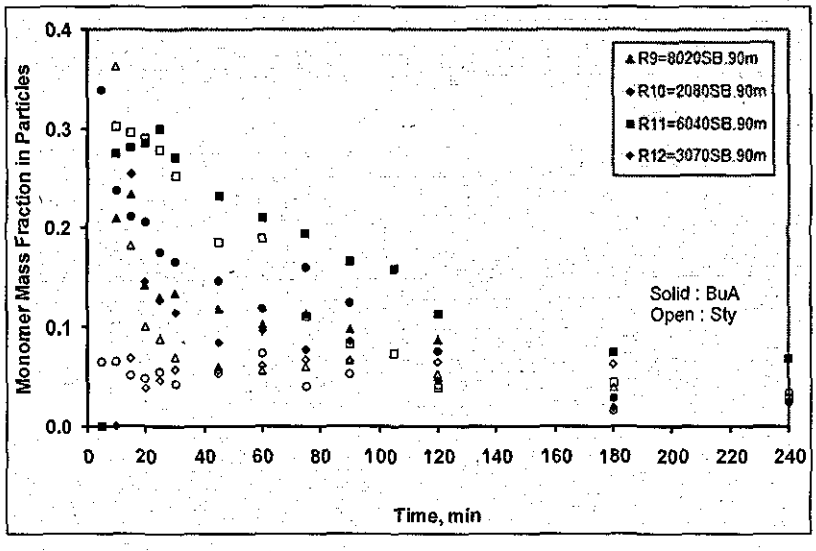

Figure 7.11 The time evolution of the monomers mass fraction in the polymer particles for the experiments R9-R12

In conclusion, it was demonstrated that starting the reaction with the BuA in the initial charge led to higher polymerization rates when compared to starting the reaction with the Sty; the effects were apparent on both the overall and the instantaneous conversions.

Researchers proposed several theories; in contrast to other work (Flory, 1953; Brooks, 1970), Nomura et al. (1972) and Zubitur and Asua (2001) suggested that the solubility of the monomers in the water has an effect on the mass transfer rate of the

monomers to the particles; this is not a valid justification since it was previously shown that the speed of the agitation in the reactor did not affect the polymerization rate (§5.2). Moreover, the constant partition coefficient model (§2.6) predicted that monomer drops vanished within the first ten minutes and that both monomers showed similar mass fraction in the particles. These facts suggest that although the solubility of the BuA is six times the Sty solubility in the water, yet that did not play a role in affecting its concentration in the particles. Consequently, the BuA solubility in the water did not play a role in increasing the polymerization rate.

The increase in the polymerization rate when the initial charge is rich with BuA could be also attributed to the nucleation in the system. There are some reports proposing that the BuA is affecting the nucleation in the system; these effects could be related to the polarity of the BuA or its solubility in the water. Piirma and Chen (1979) demonstrated that as the content of a polar monomer increases in the copolymer, the area occupied by the surfactant molecules on the particles increases. This might lead to the generation of more particles which in return will increase the polymerization rate. Araujo et al. (2001) suggested that more soluble monomers increase the homogeneous nucleation leading to an increase in the polymerization rates. The effects of the BuA on the nucleation will be discussed thoroughly in §7.2.3.

Guillaume et al. (2001) suggested that the increase in the polymerization rate could be a result of gel effect in the system which occurs at higher BuA concentrations. Since it was detected that cross-linking occurs when the BuA content increases, there is a possibility that gel effect is one of the factors that lead to this increase in the polymerization rate.

Feeding the monomers at higher rates leads to a reduction in the instantaneous conversion. The effects on the other properties of the copolymer will be discussed in the next sections.

7.2.2. Copolymer composition evolution

In this section, the main effects of the strategy implemented in feeding the monomers to the reaction vessel on the overall copolymer composition will be discussed.

Figures 7.12 and 7.13 illustrate the time evolution of the copolymer composition and the composition drift respectively.

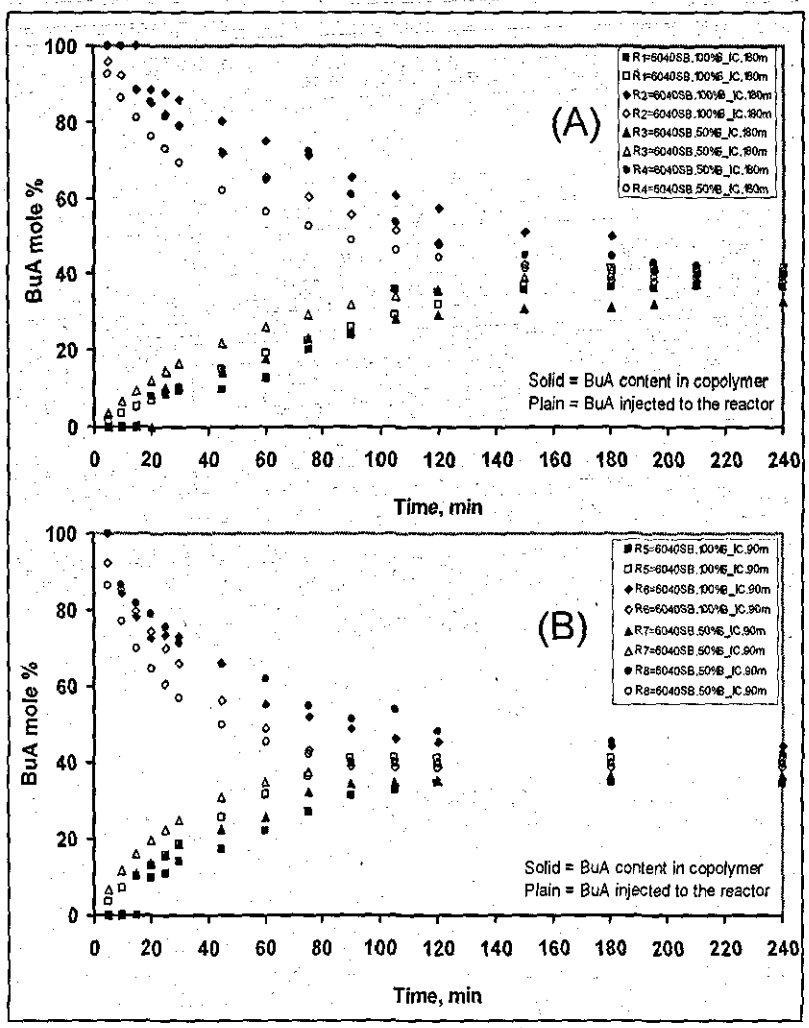

Figure 7.12 The time evolution of the copolymer composition for the experiments R1-R8

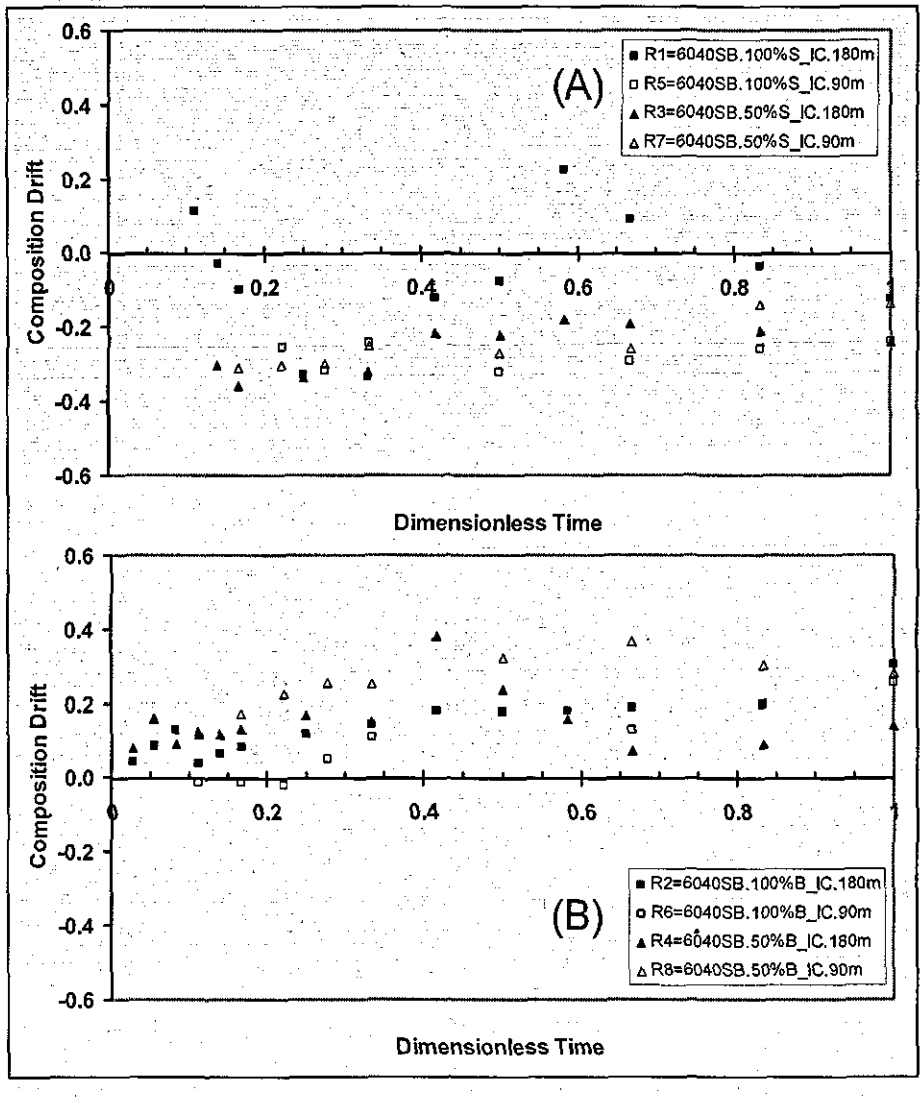

Figure 7.13 The time evolution of the composition drift during the semibatch stage for the experiments R1-R8

The composition drift is defined as the ratio between the BuA content in the copolymer and the BuA injected to the reaction vessel; the x-axis in figure 7.13 represents the ratio between the sampling time and the total duration of the semibatch stage. A value of 0.0 represents the ideal case where no composition drift is occurring, a negative value indicates that the BuA content in the sample is less than the BuA

content in the reactor, and a positive value indicates the reverse. It should be noted that the reported composition in the figures is the overall composition of the copolymer samples extracted from the reactor at any given time and it does not represent the change in the composition between the time intervals.

Examining figure 7.12, it is noticeable that initially the copolymer is rich with the monomer which was fed in the initial charge (i.e. the first monomer). It is also noticeable that in the extreme cases where the initial charge contained 100% of one of the monomers (i.e. R1, R2, R5, and R6); it was possible to detect the other monomer (i.e. second monomer) that is being fed to the reactor in the copolymer composition even at an early stage of the reaction (i.e. 10 minutes). The detection of the second monomer after short time shows that it was possible for the second monomer to dissolve in the water and transfer to the particles which were rich with polymer and the first monomer rapidly. The fact that the aqueous phase was rich with the first monomer did not show an effect on the mass transfer to the particles. Both monomers were able to dissolve in the saturated aqueous phase and were able to reach the particles although that the monomers solubilities in the different media were different.

Previously (Figures 7.7A and 7.8A) it was demonstrated that reducing the semibatch stage duration lowered the instantaneous conversion; examining this effect on the composition drift (figure 7.13), it is noticeable that reducing the duration of the semibatch stage did not show a major effect on the composition drift. The composition drift in 7.13A (i.e. Sty rich initial charge) was between -0.4 and -0.2, and in 7.13B (i.e. BuA rich initial charge) it was between +0.05 and +0.2, which illustrates that the drift in the composition is affected by the monomer type in the initial charge, and it also demonstrates that BuA rich initial charge minimized the drift in the composition.

The role of the rich BuA initial charge in minimizing the drift in the composition was not surprising and several authors have reported similar results. Canegallo et al. (1994, b) proposed a procedure to control the composition of the

copolymer; their procedure requires the continuous monitoring of the conversion by means of online tools. At first, the critical monomer (i.e. the least reactive monomer; BuA) is identified, and is totally injected in the beginning, similar to R2 and R6 experiments. The more reactive monomer (i.e. Sty) is fed in a semibatch mode. The Sty feed rate during the semibatch stage (§3.4) is adjusted throughout the experiment according to the conversion and a mathematical model to guarantee the production of a homogeneous copolymer. However, it should be noted that Canegallo et al. feeding scenario was not linear (i.e. Sty feed rate was not constant), whereas in R2 and R6 the Sty feed rate was linear with time. Canegallo et al. showed that a homogeneous copolymer was successfully produced throughout the experiment and that the BuA weight fraction in the copolymer was constant at 0.5 (i.e. mole fraction = 0.45).

Cruzrivera et al. (1989) demonstrated a minimal composition drift by applying a procedure similar to R2 and R6; the BuA was fed initially and the Sty was fed in the subsequent feed. The decision to inject the BuA monomer initially and to incorporate the Sty in the subsequent feed was made according to the reactivity of the monomers (i.e. BuA reactivity < Sty reactivity).

Figures 7.14 and 7.15 demonstrate the copolymer composition evolution and the composition drift for the runs R9-R12. The monomer mixture of R9 and R11 was richer with the Sty monomer. Observing R9 and R11 (figure 7.14), it is noticeable that the BuA content in the copolymer was slowly increasing with time; this slow increase is analogous to the BuA monomer slow depletion in the particles (figure 7.11). Observing figure 7.15, it is noticeable that R9 and R11 exhibited the highest composition drift in which the copolymer was rich with the Sty; this drift was decreasing with time until the composition of the copolymer approached the composition of the feed monomer mixture at the end of the experiments (figure 7.14).

Zubitur and Asua (2001) reported that the cumulative copolymer composition was initially richer with Sty than the feed composition. They stated that there is a correlation between the agitation intensity and the composition of the copolymer in

which increasing the agitation intensity reduced the monomer drops size which in return helped the Sty to overcome its limited solubility in the water and dissolves quickly, and therefore the copolymer was initially richer with the Styrene. However, Plessis et al. (2001) reported that the amount of Sty in the copolymer Sty/BuA was larger than the feed composition. They attributed that to be due to the reactivity of the Styrene.

It should be noted that previously it was shown that the agitation intensity did not affect the reaction kinetics (§5.2). It was also demonstrated that the monomer drops vanished early in the experiments, and that both monomers showed similar concentrations in the particles although their solubilities in the water were different (figures 7.5 and 7.6). All these facts indicate that the observed increase in the Sty content in the copolymer could be related to other factors.

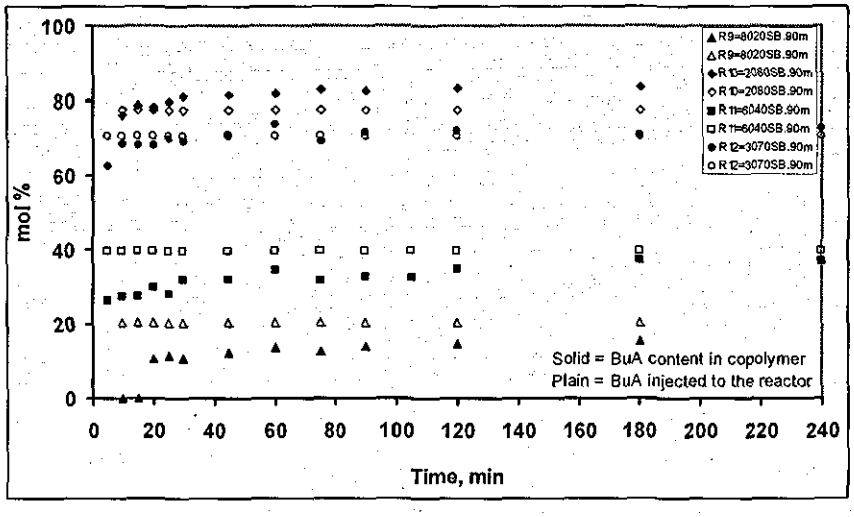

Figure 7.14 The time evolution of the copolymer composition for the experiments R9-R12 (no monomer in initial charge)

Ozdeger et al. (1998) demonstrated similar results where the copolymer was initially richer with the Sty than the BuA and then it approached the composition of the mixture at the end; the Sty/BuA molar ratio was 55/45.

Figure 7.11 demonstrates that the rate at which the Sty is depleting from the particles is higher than the rate of the BuA depletion, leading to this composition drift. It was demonstrated earlier that the water solubility effect on the reaction kinetics was not apparent; it is more likely that this effect is related to the Sty reactivity and not its solubility in the solvent. The BuA content in the monomer mixture of the experiments R10 and R12 was higher than the Sty, and these two runs demonstrated lower composition drift as can be seen in figures 7.15. The fact that the Sty content in the monomer mixture was low could be the main reason in minimizing the drift in the composition. The reactivity of the Sty coupled with rich Sty monomer mixture leads to composition drift. Therefore, minimizing the content of the Sty in the monomer mixture leads to a reduction in the composition drift.

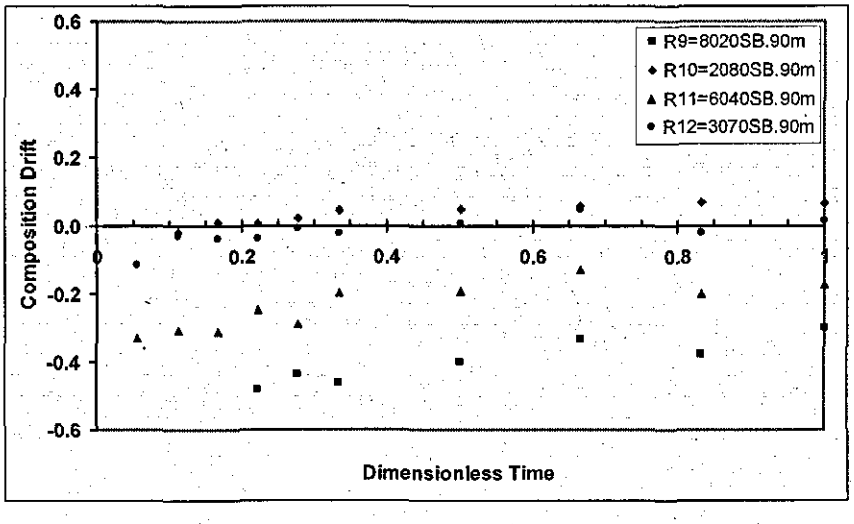

Figure 7.15 The time evolution of the composition drift during the semibatch stage for the experiments R9-R12 (no monomer in initial charge)

Finally, it was demonstrated in this section that monomer rich aqueous phase did not affect the dissolution of the monomer that is being fed to the reactor. Both monomers (i.e. Sty and BuA) were able to polymerize and emerge in the copolymer composition even after a short period of time (figures 7.5 and 7.6). In addition, feeding the monomers at twice the feed rate in order to reduce the semibatch stage duration did not affect the composition although its effect on the instantaneous

conversion was demonstrated earlier (i.e. increasing the feed rate reduced the instantaneous conversion). The resulting copolymer composition approached the monomer mixture composition in all the studied cases, and this approach was at higher rates when the feeding rate was higher (i.e. 90 minutes semibatch stage).

Starting with the BuA (i.e. least reactive monomer) in the initial charge and feeding the Sty in the subsequent feed minimized the composition drift, the same finding was reported by other researchers (Canegallo et al., 1994(b); Cruzrivera et al., 1989). Feeding the more reactive monomer (i.e. Sty) overcame the effects which are related to the differences in reactivities of the monomers.

It was also demonstrated that Sty rich monomer mixture increases the copolymer composition drift. This was also reported in the literature, but contrary to the others findings (i.e. Zubitur and Asua; 2001) the solubility was not the main cause of the drift; the reactivities of the monomers could be the main reason for this drift.

7.2.3. Copolymer particles evolution

In this section the evolution of the particles size and number of polymer particles will be discussed.

Figures 7.16 and 7.17 demonstrate the time evolution of the z-average and number of polymer particles for the experiments R1-R8. Clearly, some differences in the size between the runs at early and later stages can be observed. The experiments in which the BuA content in the initial charge was high gave initially smaller particles, and this effect was also apparent on the final particles size.

Previously (§7.2.1), it was demonstrated that on molar bases, the experiments in which the initial charge contains BuA (i.e. R2, R4, R6, and R8) initially contain lesser amount of monomer than the Sty runs (figures 7.3 and 7.4), however the same amount of monomer is fed at the end of the semibatch stage. Therefore, since feeding the same amount of monomer did not produce similar final particles size (figure 7.16), this clearly confirms that the initial conditions of the reactor did show an impact on the polymer; otherwise all the runs should exhibit similar final z-average since the amount of SLS and the ultimate monomer concentration in the recipes were constant.

Observing figure 7.17, it is noticeable that the runs which exhibited smaller particles showed higher number of polymer particles when compared to the runs with the bigger particles. In emulsion polymerization, the increase in the number of polymer particles is an indication of a decrease in the size of the particles. However what makes this result interesting is that this increase in the number of polymer particles can be detected even at the initial stage where the number of moles was different. Reducing the monomer amount at constant SLS concentrations should lead to smaller particles and smaller number of polymer particles; we noticed the first but not the latter.

In summary, these findings suggest that the experiments where the initial charge contain the monomer BuA exhibited smaller particles and higher number of

polymer particles when compared to the runs where the initial charge contains Sty monomer.

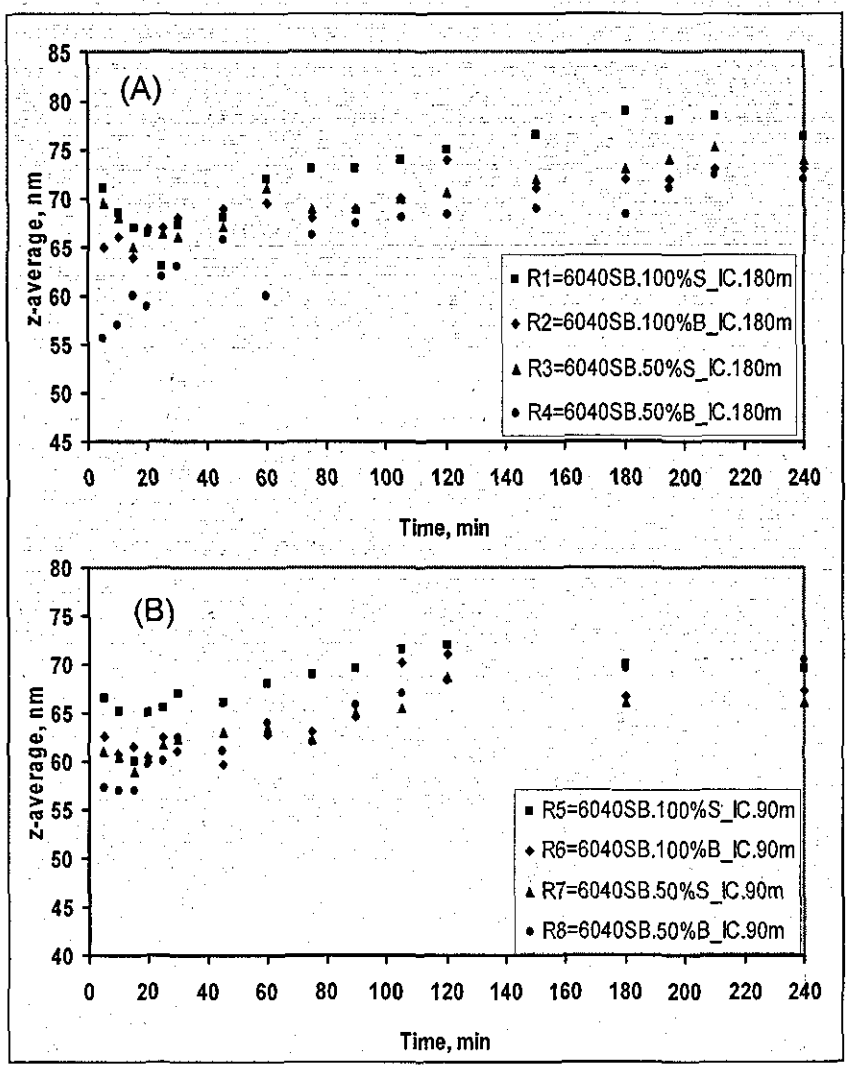

Figure 7.16 The time evolution of the particle sizes for the experiments R1-R8

In emulsion polymerization, monomers that show signs of higher solubility in water might promote homogeneous nucleation (Lovell and El-Aasser, 1997). In return, larger number of small particles will be generated which will eventually result in a smaller average particles size in the final product. BuA solubility in water is six

times the solubility of the Sty monomer, so the increase in the number of particles and the reduction in the particles size could be related to this fact.

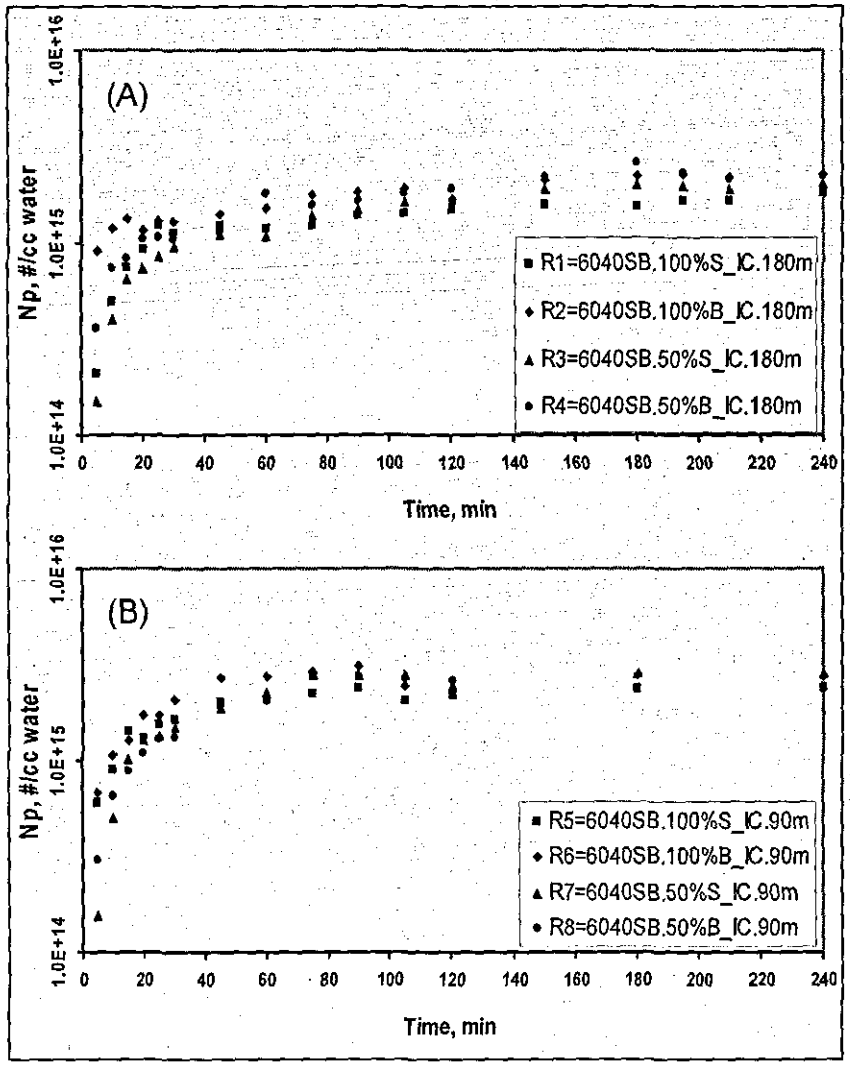

Figure 7.17 The time evolution of the number of polymer particles for the experiments R1-R8

Araujo et al. (2001) observed a role for the monomers solubility in the solvent. They reported that hydrophilic monomers (i.e. water-soluble) if polymerized with low solubility comonomers promotes particle formation, and due to the large number of particles they will grow to smaller sizes for similar amounts of surfactant. They

explained that this could be related to fact that water-soluble monomers encourage homogeneous nucleation.

In addition, taking into account the BuA solubility effects on the particles suggests that feeding BuA to the system during the semibatch stage could lead to longer nucleation periods since particles are being generated due to homogeneous nucleation. However, Figure 7.17 demonstrates an interesting result where it is apparent that polymer particles build up continued at least for the first 40 minutes for the experiments R1-R8. If the solubility of the BuA is the only effect, in that case the increase in the number of particles should cease sooner for the runs R2 and R6 since Sty (less water-soluble than BuA) is the monomer that is being fed and it is known that Sty does not promote homogeneous nucleation. This observation suggests that the solubility of the BuA is not the only factor affecting the number of the polymer particles and the particles size.

Ozdeger et al (1998) suggested that at higher solids, more surfactant is associated initially with the oil phase, leading to free surfactant in the later stages of polymerization, which is used partly for stabilizing the existing particles, and the rest for creating new particles. It should be noted that the constant partition coefficient model predicted that monomer drops vanished within the first ten minutes from the reactor for the experiments R1-R12.

Piirma and Chen (1979) investigated the factors affecting the number of surfactant molecules on the surface of the polymer particles (§7.2.1). They investigated the effects of the particles size, reaction temperature, electrolyte concentration, the swelling of the particles, and the polarity of the polymer on the area occupied by each surfactant molecule on a particle (i.e. under saturation conditions, effective molecular area of a surfactant molecule on the particle surface, $(A_m)_{sat}$).

In summary, they demonstrated that $(A_m)_{sat}$ is constant at 0.47 nm^2 if the average particles size was in the range of 70-150 nm, $(A_m)_{sat}$ was reduced to 0.36 nm^2

at 45 nm particle size. Raising the temperature from 22 °C to 47 °C increased $(A_m)_{sat}$ from 0.47 to 0.52 nm^2, considering that the temperature was raised by a factor of 2, the temperature effect can be considered minimal. $(A_m)_{sat}$ = 0.47 nm^2 at 0M electrolyte concentration, and it became 0.35 nm^2 when the electrolyte concentration was raised up to 0.9M, once again it is possible to consider this effect to be minimal. Swelling the PS-PMMA copolymer particles with benzene up to twice the original unswelled volume reduced A_{sat} by 10%. Finally, PMMA is a polar polymer, and increasing its content in the copolymer showed big effects on the $(A_m)_{sat}$ as can be seen in the figure (7.18).

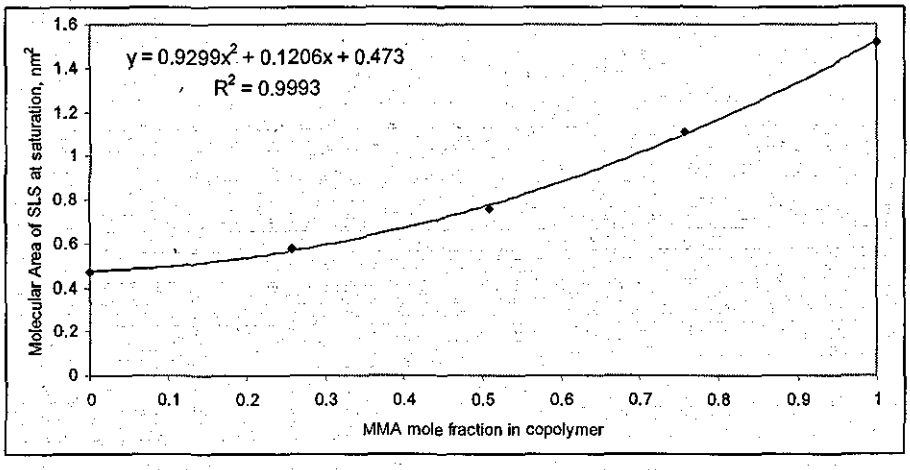

Figure 7.18 The evolution of molecular area of SLS at saturation on the polymer particle with MMA content in the copolymer

SLS molecules concentration in the reactor	2.12×10^{19} molecules/cm^3 water
Expected initial number of micelles	2.65×10^{17} micelles/cm^3 water
Final SLS molecules concentration in the reactor	2.10×10^{19} molecules/cm^3 water

Table 7.2 Concentration of SLS in the reactor

Table 7.2 provides some data concerning the SLS surfactant in the reactor for the experiments R1-R8. The aggregation number for SLS (i.e. 80 molecules/micelle,

§2.1.2) was used to estimate the expected initial number of micelles. Experiments R1-R8 showed similar final concentration of SLS molecules in the reactor, and it was estimated by subtracting the experimental final number of polymer particles from the expected initial micelles and multiplying by the aggregation number.

The observed number of polymer particles in figure 7.17 is lower than the initially available micelles (Table 7.2); this comes in agreement with Araujo et al. (2001) findings. They reported that not all the initial micelles are nucleated, and they explained that this is due to the fact that as soon as new particles are nucleated and start growing, the particles will absorb some of the available surfactant to cover the surface of the growing particles.

In order to investigate the particles coverage with SLS molecules, it will be assumed that Piirma and Chen (1979) data for PS-PMMA are similar to the copolymer Sty-BuA. Moreover, since the biggest effect was reported to be related to the change in the polarity of the copolymer, all the other factors (e.g. temperature) will be ignored given that their effect on $(A_m)_{sat}$ were minimal (Piirma and Chen, 1979).

Figures 7.19 and 7.20 illustrate the theoretical particle coverage with SLS molecules at saturation (A) and the unadsorbed SLS molecules (i.e. inactive micelles and free SLS molecules) in the reactor at any given time (B) for the experiments R1-R8.

To calculate the theoretical coverage at saturation (i.e. Total SLS molecules that are required to fully saturate the particles according to Piirma's findings), a second degree polynomial was generated to estimate $(A_m)_{sat}$ for the copolymer Sty-BuA (figure 7.18). Then using the experimental z-average and number of polymer particles data, the required total SLS molecules to cover the surface of the particles at saturation was estimated. The numbers of the unadsorbed SLS molecules at saturation

were estimated from the difference between the total amount of SLS in the reactor and the theoretical coverage.

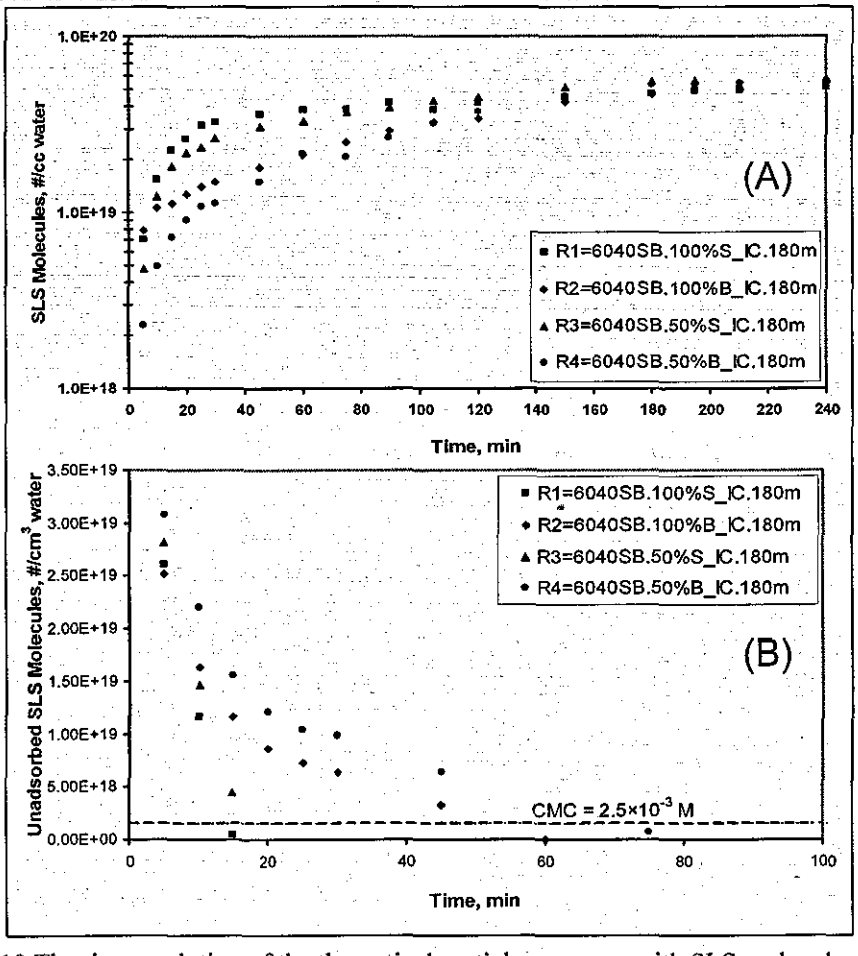

7.19 The time evolution of the theoretical particle coverage with SLS molecules at saturation (A) and the unadsorbed SLS molecules in the reactor (B) for the experiments R1-R4

Figure 7.19 illustrates that based on the reported $(A_m)_{sat}$ figures in the literature, assuming that the particles are fully saturated with SLS molecules (i.e. extreme case) the amount of the unadsorbed SLS exceeds the CMC for longer periods. This could be one of the reasons that led to the observed extended nucleation periods in the system. It is also noticeable that the amount of SLS that is required to fully saturate the particles is initially higher for the runs where the initial charge was

rich with the Sty. In addition, the rate at which the SLS depletes from the system is higher for the Sty rich initial charge runs when compared to the BuA rich initial charge runs. After the first 20 minutes for the experiments R1 and R3, and after 60 minutes for R2 and R4, the amount of SLS that is required to fully saturate the particles exceeds the SLS that is available in the system. Figure 7.20 demonstrates something similar, but the times were shorter after increasing the feed rates.

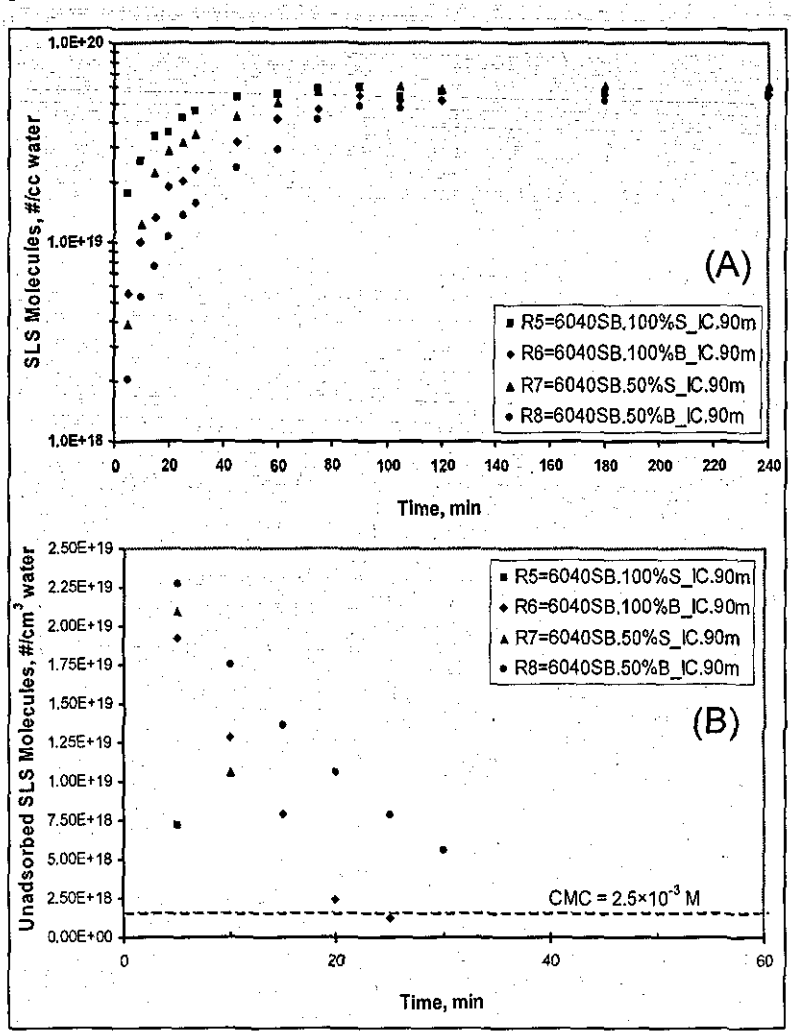

7.20 The time evolution of the theoretical particle coverage with SLS molecules at saturation (A) and the unadsorbed SLS molecules in the reactor (B) for the experiments R5-R8

This finding indicates that the particles are not fully saturated with SLS molecules at the end of the runs since the amount of SLS is not sufficient. Yet this lack of SLS molecules to fully saturate the particles did not lead to polymer coagulation in the system.

Figures 7.19 and 7.20 also demonstrate that when the initial charge is rich with the BuA monomer, the amount of SLS molecules that is required to saturate the particles was lesser than the Sty rich initial charge runs. This observation indicates that when the initial charge is richer with BuA, additional free surfactant is available in the system. This could lead to the generation of more polymer particles and in return could lead to the observed increase in the polymerization rate for BuA rich runs (figures 7.1 and 7.2).

It should be noted that these findings are for the extreme case where the particles are fully saturated initially. Yet this serves as an indication that even if the particles are not fully saturated and unadsorbed SLS is available for all the runs (i.e. Sty and BuA rich runs), the amount of SLS that is available for nucleation will be at larger quantities for the BuA rich runs when compared to the Sty rich runs, hence leading to more polymer particles and an increase in the polymerization rates.

Experiment	A_m, nm^2	Experiment	A_m, nm^2
R1	1.58	R5	1.71
R2	1.78	R6	1.84
R3	1.66	R7	1.85
R4	1.71	R8	1.76

Table 7.3 Effective molecular area of SLS molecule on polymer particle at 60/40 Sty/BuA

Based on the available SLS in the system at the end of each experiment, and assuming that all the SLS molecules are adsorbed by the polymer particles, it is possible to estimate A_m for the runs R1-R8, the results are demonstrated in table 7.3.

Once more, table 7.3 shows that according to Piirma et al. findings the polymer particles at the end of experiments R1-R8 were not fully saturated with the SLS molecules since the expected A_m value was 0.7 nm^2 (figure 7.18)

Figure 7.21 demonstrates the z-average and the number of polymer particles evolutions with time for the runs R9-R12. It should be noted that that these runs were conducted without monomer in the initial charge, all the monomer was fed during the semibatch stage, and that the monomer ratio in the recipes was variable (Table 7.1).

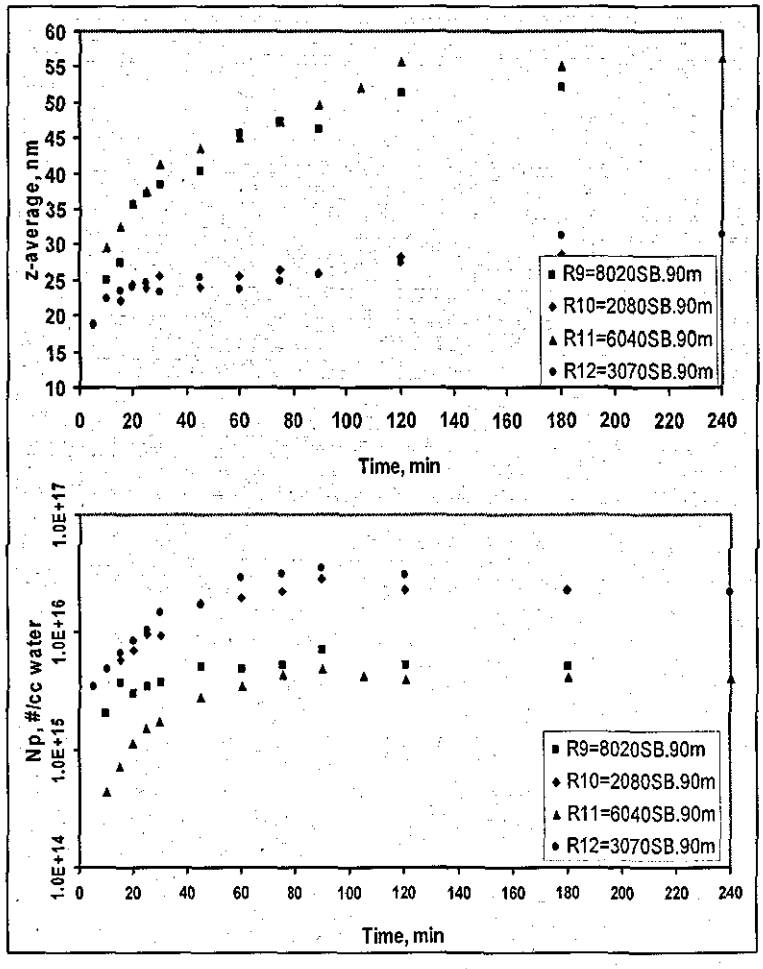

Figure 7.21 The time evolution of the particle sizes (A) and the number of polymer particles (B) for the experiments R9-12

Observing figure 7.21(A), it is noticeable that R10 and R12 gave very small sizes compared to R9 and R11. These differences in the size are an indication of the differences in the number of polymer particles which can be observed in 7.21(B). It should be noted that R9 and R11 contain more Sty than BuA, and did contain more monomer by mole compared to R10 and R12. Therefore, it was expected that R9 and R11 exhibit bigger particles since the SLS concentration is constant in R9-R12 and the monomer concentration in R9 and R11 is higher than R10 and R12. In addition, increasing the Sty concentration in the recipe leads to bigger particles as demonstrated earlier (figures 7.16 and 7.17).

In conclusion, it was demonstrated in this section that rich BuA initial charge leads to smaller particle sizes and larger number of polymer particles. Some researchers (Araujo et al., 2001) suggested that homogeneous nucleation for water soluble monomers could play a role in increasing the number of particles leading to a reduction in the average particles size.

Ozdeger et al. (1998) suggested that SLS that is used to stabilize the oil phase could become available at a later stage when the oil drops vanish. This excess SLS could partially be used to generate new particles. It should be noted that monomer drops vanished early in the experiments.

Applying Piirma and Chen (1979) data on the Sty-BuA copolymer demonstrated that the polymer particles were not saturated with SLS molecules, and that when the initial charge is BuA rich, more unadsorbed SLS is available in the system. This excess SLS could be used to generate new particles leading to the observed increase in the polymerization rate for BuA rich initial charge experiments. It should be noted that coagulation was not detected in the system.

7.3. Conclusion

In this chapter it was demonstrated that distributing the monomers between the initial charge and the subsequent feed showed various effects on the polymerization rate, the particles evolution, and the composition of the copolymer.

Starting the reaction with the BuA in the initial charge led to higher polymerization rates, smaller polymer particles, and minimized the composition drift. Investigating the nucleation in the system and applying Piirma's findings revealed that the polymer particles are not saturated with SLS molecules, and that the unadsorbed SLS was at higher quantities when the initial charge was rich with the BuA monomer. This could explain the increase in the polymerization rate for the BuA rich initial charge runs and the reductions in the particles size. Since cross-linking was also detected in the system, there is a possibility that gel effect is one of the factors that led to this increase in the polymerization rate (Guillaume et al., 2001).

Moreover, it was also demonstrated that considering the extreme case and that is if the particles are fully saturated with surfactant molecules, it was found that unadsorbed SLS existed in the reactor at concentrations higher than the CMC for up to 60 minutes in some experiments which could explain the extended nucleation periods. It was also demonstrated that when the initial charge is Sty rich the quantity of the unadsorbed SLS was lesser than the BuA rich initial charge runs.

The constant partition coefficient model (§2.6 and appendix C) predicted that monomer drops vanished within the first ten minutes and that the initial BuA monomer mass fraction in the particles for the case when the initial charge is rich with this monomer is similar to the Sty mass fraction when the Sty is richer in the initial charge. These results are supported by the composition results where it was demonstrated that monomer rich aqueous phase did not affect the dissolution of the second monomer that is being fed to the reactor. Both monomers (i.e. Sty and BuA) were able to polymerize and emerge in the copolymer composition even after a short period of time although their solubilities in the water were different. These results

coupled with the agitation tests indicate that in contrast to Nomura et al. (1972) and Zubitur and Asua (2001), the monomer partitioning is controlled by thermodynamic laws and that the mass-transfer of the monomers to the particles is not the rate limiting step.

Starting with the BuA in the initial charge and feeding the Sty in the subsequent feed minimized the composition drift. This finding was reported by other researchers (Canegallo et al., 1994(b); Cruzrivera et al., 1989). Feeding the more reactive monomer (i.e. Sty) overcame the effects which are related to the differences in reactivities of the monomers. It was also demonstrated that Sty rich monomer mixture increases the copolymer composition drift. This was also reported in the literature, but contrary to the others findings (i.e. Zubitur and Asua; 2001) the solubility was not the main cause of the drift; the reactivities of the monomers could be the main reason for this drift.

Feeding the monomers at higher rates led to a reduction in the instantaneous conversion but did not affect the composition of the copolymer or the particles evolution. The copolymer composition approached the monomer mixture composition in all the studied cases, and this approach was at higher rates when the feeding rate was higher.

In summary, BuA rich initial charge leads to higher polymerization rates, minimal composition drift, larger number of polymer particles, and smaller particle sizes. Minimizing the reaction time by increasing the monomer feed rate lowered the instantaneous conversion but did not influence the composition or the particles evolution.

8. Effects of Surfactant and Initiator on the Copolymer

8.1. Introduction

In this chapter a detailed discussion of the experiments conducted to investigate the effects of distributing the surfactant and the initiator between the initial charge and the subsequent feed on the composition of the copolymer styrene-butyl acrylate will be presented. The evolutions of the instantaneous and the overall conversion, the particle size, the number of polymer particles, the composition of the copolymer, and the concentration of the monomers in the different phases with time will be discussed. This will lead to a better understanding of the effects of the surfactant and the initiator on the overall behavior in the reactor and the effects on the composition of the Sty-BuA copolymer

8.2. Surfactant distribution effects

Several runs were made where the amount of SLS in the feed and in the initial charge was varied. The recipes of the experiments are given in table 8.1.

These experiments were conducted similarly to the runs R1-R11. There were two stages for each experiment. The first was the semibatch stage, and the second was the batch stage. The total duration of both stages was four hours, and the semibatch stage duration was 90 minutes for all the runs. In table 8.1 the masses of the other ingredients (i.e. the initiator, deionized water, buffer, and the monomers) were kept unaltered. Hence, the total mass and the solids content were constant. The reaction temperature was at or near 70° C.

8.2.1. Effects of surfactant concentration in the initial charge

In experiments R13-R16, the initial concentration of the surfactant was varied between 25% and 200%; the initial charge did not contain monomers. The subsequent feed consists of monomers only, and no further surfactant was added to the system.

In order to isolate the effects of the initial surfactant concentration on the kinetics and the properties of the Sty-BuA copolymer, all the other ingredients of the recipe were not changed in the experiments shown in table 8.1.

Figure 8.1 illustrates the instantaneous conversion (A) and the overall conversion (B) evolutions with time for the experiments R13-R16. A correlation between the SLS concentration and the conversion can be observed in which decreasing the SLS concentration lowered the polymerization rate.

Run	Surfactant Conc. SLS (g) / Water (cm^3)		Monomers Transferred, g		Feeding Time, minutes	Monomers Mole Ratio %, Sty/BuA
	I.C.	Feed	Sty	BuA		
13	14/700	0.0/0.0	71	210	90	30/70
14	7.1/700	0.0/0.0	72	212	90	30/70
15	3.5/700	0.0/0.0	71	210	90	30/70
16	1.8/700	0.0/0.0	77	214	90	30/70
17	3.5/350	3.5/350	74	220	90	30/70
18	1.8/175	5.3/525	71	210	90	30/70
Other Ingredients		Initiator (KPS)			0.6 g	
		Buffer ($NaHCO_3$)			0.6 g	
		Final Volume			1000 cm^3	
		Solids Content			30%	
		Temperature			70° C	

Table 8.1 The recipes of the experiments related to the study of the surfactant effects on the copolymer

It is noticeable that run R16 showed the lowest instantaneous conversion compared to the other runs, whereas runs R13 and R14 exhibited the highest instantaneous conversion. This effect is also apparent on the overall conversion (figure 8.1B) where R16 gave the lowest overall conversion. Reducing the initial surfactant concentration primarily leads to a reduction in the number of micelles in

the system, and since the micelles are the locus of the polymerization reaction, any change in their numbers will eventually have an impact on the kinetics of the system. Thus, a reduction in the number of micelles leads to a reduction in the polymerization rate.

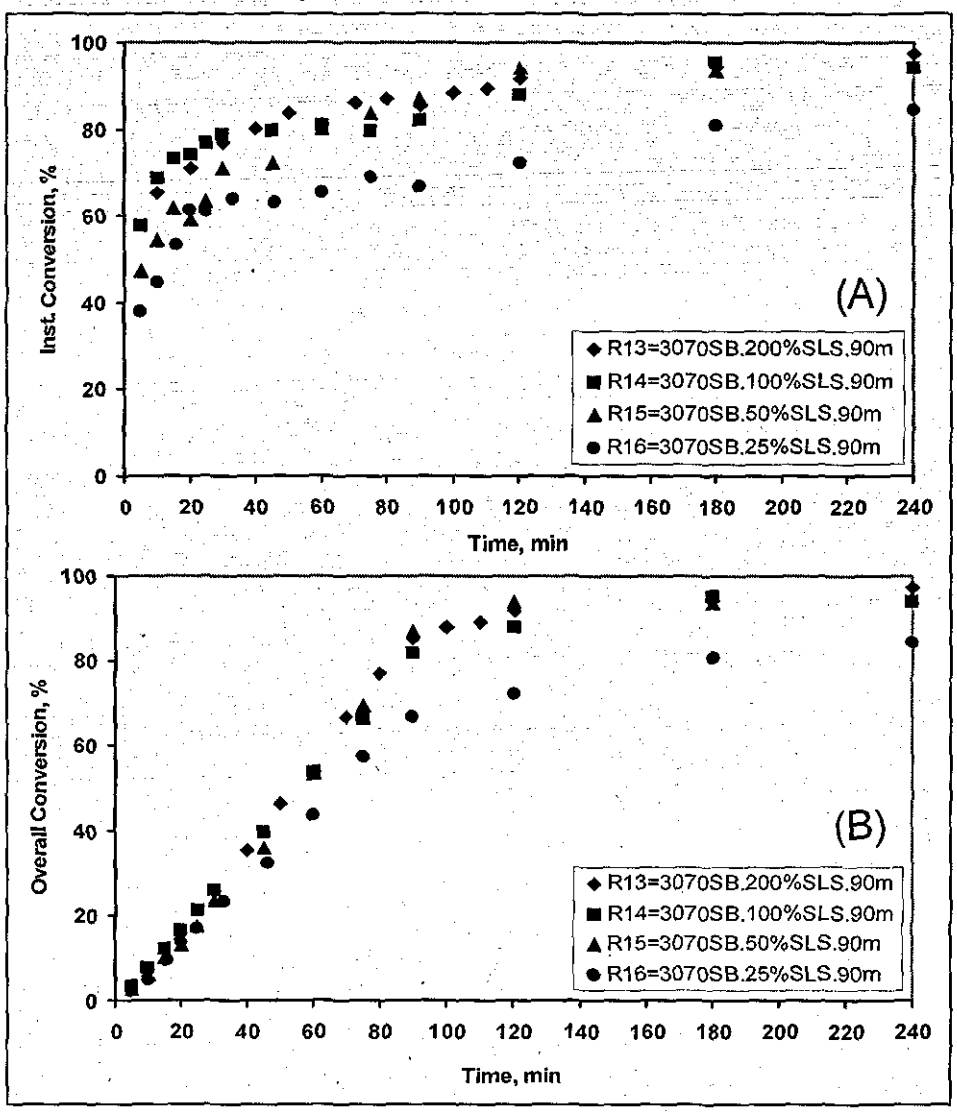

Figure 8.1 The time evolution of the instantaneous (A) and overall (B) conversions for the experiments R13-R16

R16 instantaneous and overall conversions were increasing in the batch stage at lower rate, which suggests that the R16 final conversion could be comparable to R13-R15, but it will take longer to reach that level.

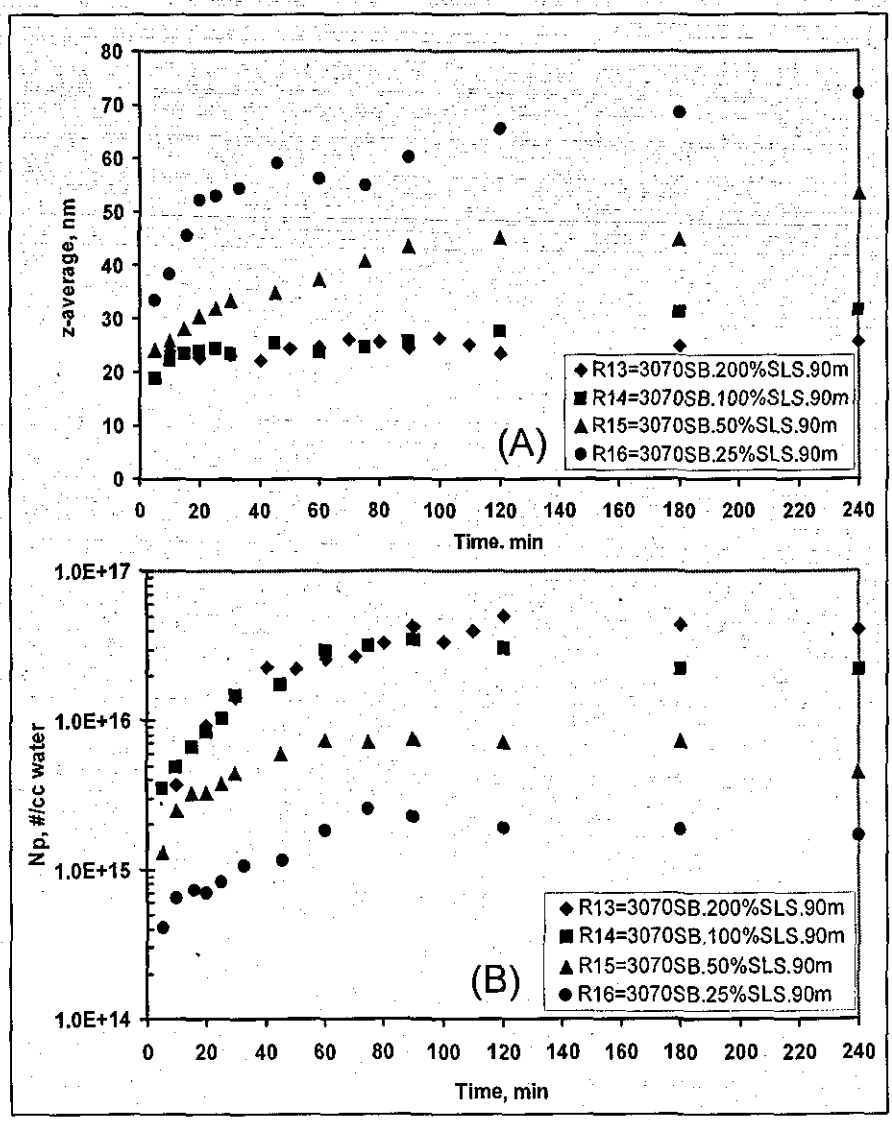

Figure 8.2 The time evolution of the particle sizes (A) and number of polymer particles (B) for the experiments R13-R16

Figure 8.2 demonstrates the SLS concentration effects on the z-average (A) and the number of polymer particles (B). Reducing the SLS concentration led to a

reduction in the number of polymer particles and since the monomers diffuse into a fewer number of particles, this will lead to an increase in the average particle sizes (figure 8.2A).

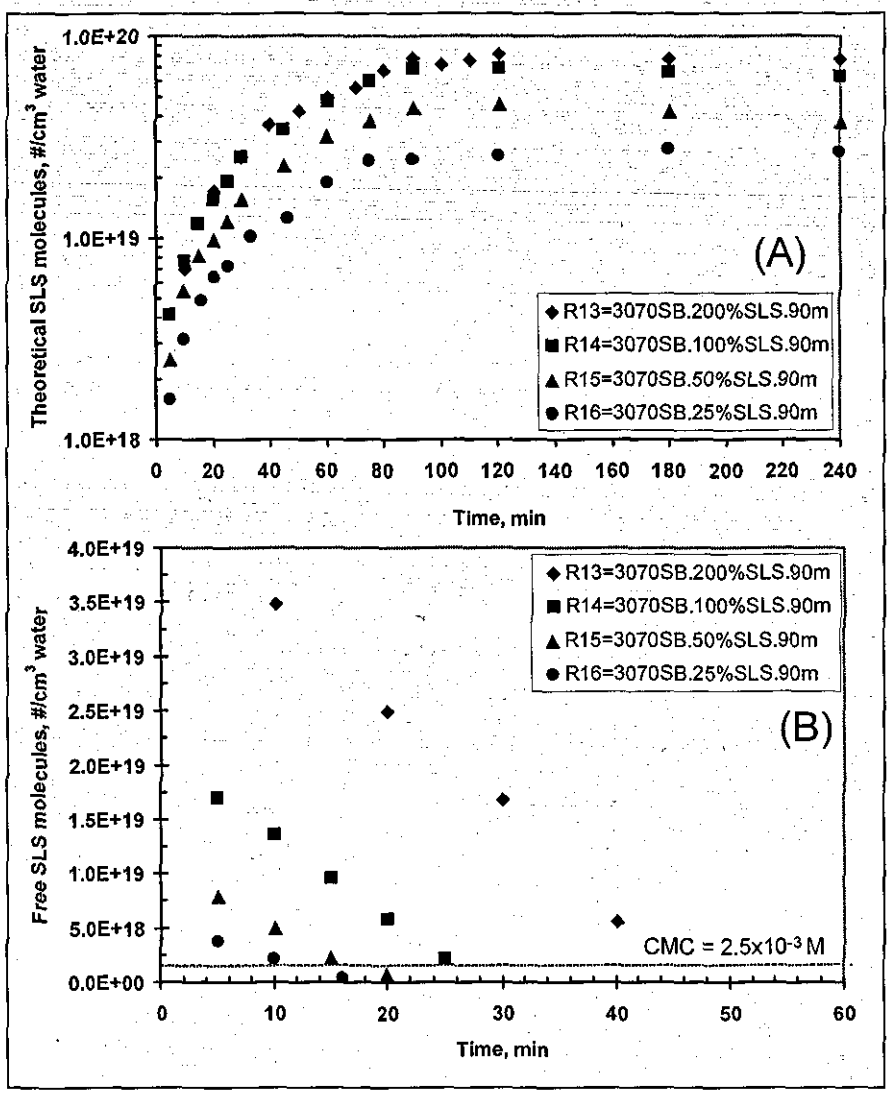

Figure 8.3 The time evolution of the theoretical particle coverage with SLS molecules at saturation (A) and the unadsorbed SLS molecules in the reactor (B) for the experiments R13-R16

It should be noted that Yang and Yang (1997) reported that the statistical design method revealed that the key variable influencing particle size is the surfactant concentration. An increase in the particle size corresponds to a decrease in the surfactant concentration.

The results of figures 8.1 and 8.2 show that increasing the SLS concentration beyond 100% (i.e. 7.1 SLS g/700 cm^3 water) did not show an effect on the system. In general, increasing the surfactant concentration increases the number of polymer particles and leads to higher polymerization rates. This was not detected and the runs R13 and R14 exhibited similar kinetics.

Figure 8.3 illustrates the theoretical number of SLS molecules which are required to fully saturate the polymer particles (A) and the free SLS molecules in the system (B) that are not adsorbed onto the particles if the polymer particles were fully saturated. It should be noted that runs R13 and R14 exhibited similar particle sizes and number of particles, so it was expected that both runs theoretically show similar demand for SLS molecules to saturate the particles. This is exactly what figure 8.3A demonstrates. Figure 8.3B shows that even if the particles were fully saturated in the system, the remaining free SLS in the system for R13 and R14 was above the CMC for at least 40 and 20 minutes respectively. Therefore, micelles were available in R13 but apparently they were not activated (§2.2.1) and did not transform in to polymer particles.

Observing the monomer mass fraction in the particles (figure 8.4); it is noticeable that the particles were rich with BuA since the recipe is rich with this monomer. It is also apparent that the effects of SLS concentration on both monomers were similar. If a run exhibited a reduction in the BuA concentration in the particles, it exhibits a reduction in the Sty monomer mass fraction in the particles as well.

Previously, it was demonstrated that the system is not affected by the solubility of the monomers in the water (§5.2; §7.2.1), and this result is another

indication of that finding since increasing the number of particles provides more surface area and will allow the more soluble monomer to diffuse at higher rates. Clearly this did not occur, and the monomer solubility in the water did not affect the kinetics of the reaction indicating the system was in equilibrium.

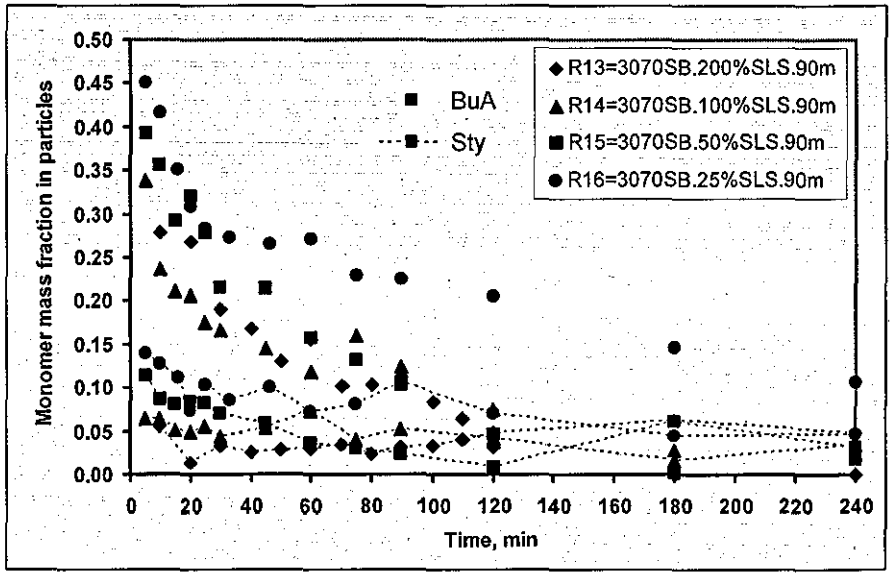

Figure 8.4 The time evolution of the monomers mass fraction in the polymer particles for the experiments R13-R16

Figure 8.5 illustrates the evolution of the composition (A) and the composition drift (B) of the experiments R13-R16. There are no apparent effects of the SLS concentration on the composition of the copolymer. All the runs exhibited only a small composition drift which was not affected by the change in the SLS concentration in the initial charge. This finding is in agreement with what was observed previously and that is there is no apparent effect for the SLS concentration on the monomer mass fraction in the particles.

Previously (§2.5), it was demonstrated that Smith-Ewart case 2 predicts that the order of dependence of the number of polymer particles on the surfactant concentration is 0.6 for batch reactors. Figure 8.6 illustrates that varying the surfactant

concentration from 25% to 200% shows that the final order of dependence for the semibatch emulsion copolymerization of Sty-BuA was 1.62 which is higher than Smith-Ewart predictions for batch systems.

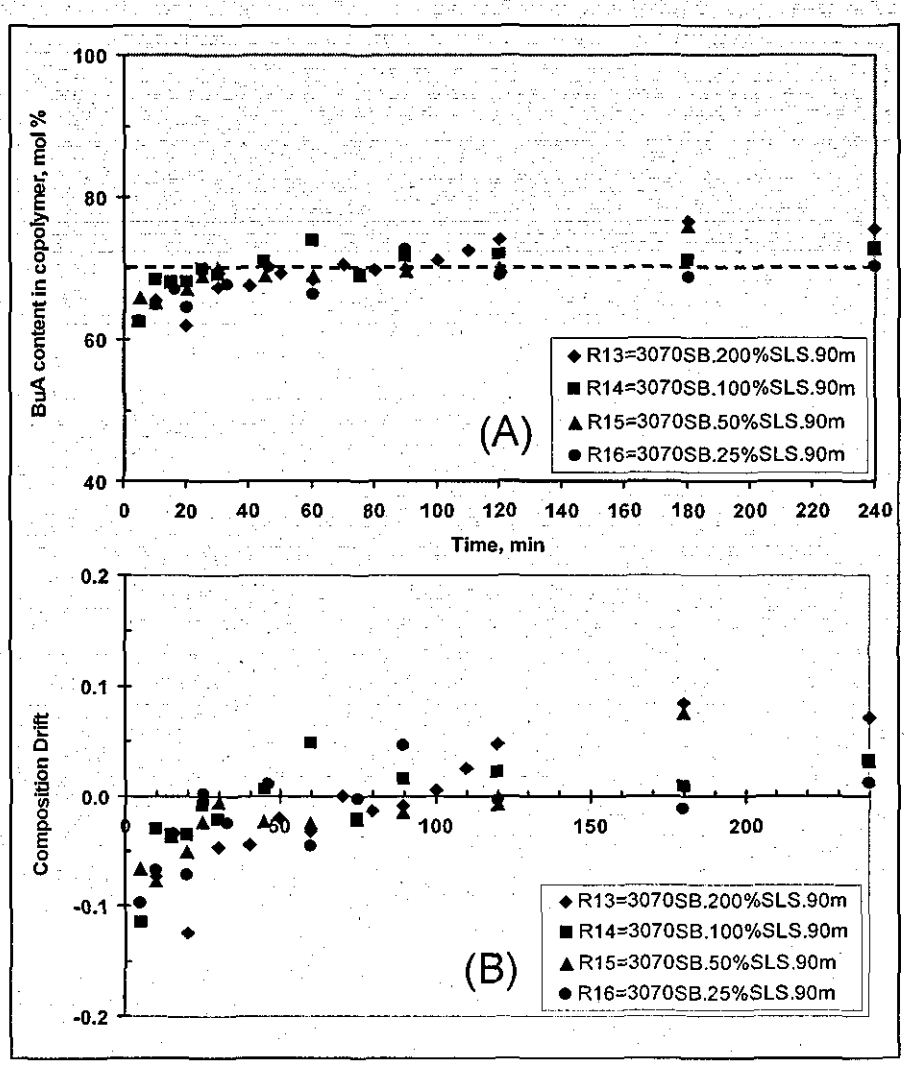

Figure 8.5 The time evolution of the copolymer composition (A) and composition drift (B) for the experiments R13-R16

It should be noticed that several researchers (e.g. Nomura et al., 1976) demonstrated that minor modifications to Smith-Ewart kinetics could produce different orders of dependence. For instance, the rate of particle volume growth (μ;

§2.5) is not constant at monomer-starved conditions (Sajjadi and Brooks, 1999). The particle growth rate decreases leading to higher numbers of polymer particles.

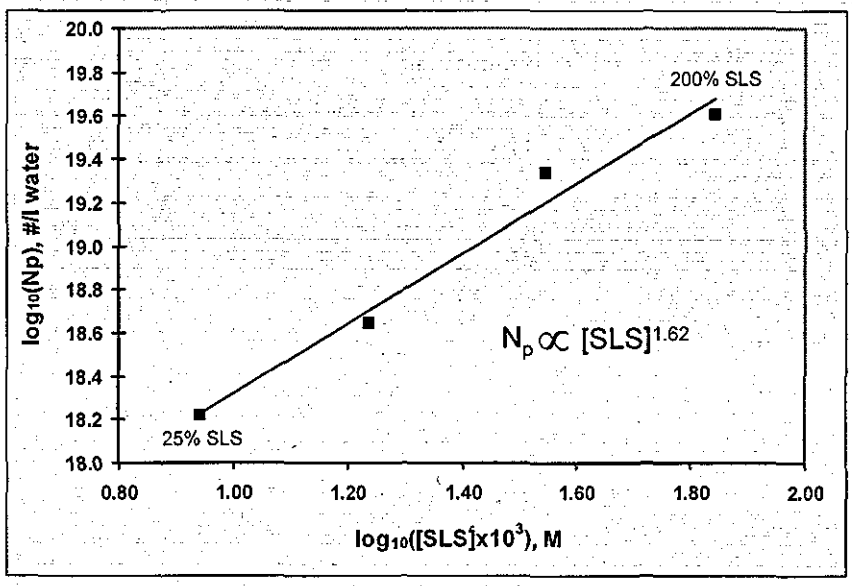

Figure 8.6 The order of dependence of the number of polymer particles on the surfactant concentration for the runs R13-R16

Finally, in this section a thorough study of the effects related to reducing the SLS concentration in the recipe on the kinetics of the Sty-BuA copolymerization was presented. Reducing the surfactant concentration led to a reduction in the number of polymer particles and in return this resulted in a reduction in the polymerization rate. Increasing the surfactant concentration beyond 100% did not affect the polymerization rate or the number of polymer particles, although free non-adsorbed surfactant molecules above the CMC were available in the system. The real cause of this behavior will be looked at in the next sections.

Changing the SLS concentration did not show an effect on the copolymer composition and the composition drift. This suggests that the reduction or the increase in the number of polymer particles does not affect the monomer concentration in the particles. This was proven experimentally using the composition data, and by

estimating the concentration of the monomers in the particles numerically by means of the constant partition coefficient model (§2.6 and appendix C).

8.2.2. Distribution of the surfactant between the initial charge and the subsequent feed

The experiments R17 and R18 were conducted to investigate the effects distributing the surfactant between the initial charge and the subsequent feed on the Sty-BuA copolymerization. A solution of deinonised water and surfactant was fed during the semibatch stage. It should be noted that the surfactant concentration in the initial charge and in the subsequent feed was kept constant (i.e. 3.47×10^{-2} M). However, the mass of the initial charge was varied according to table 8.1.

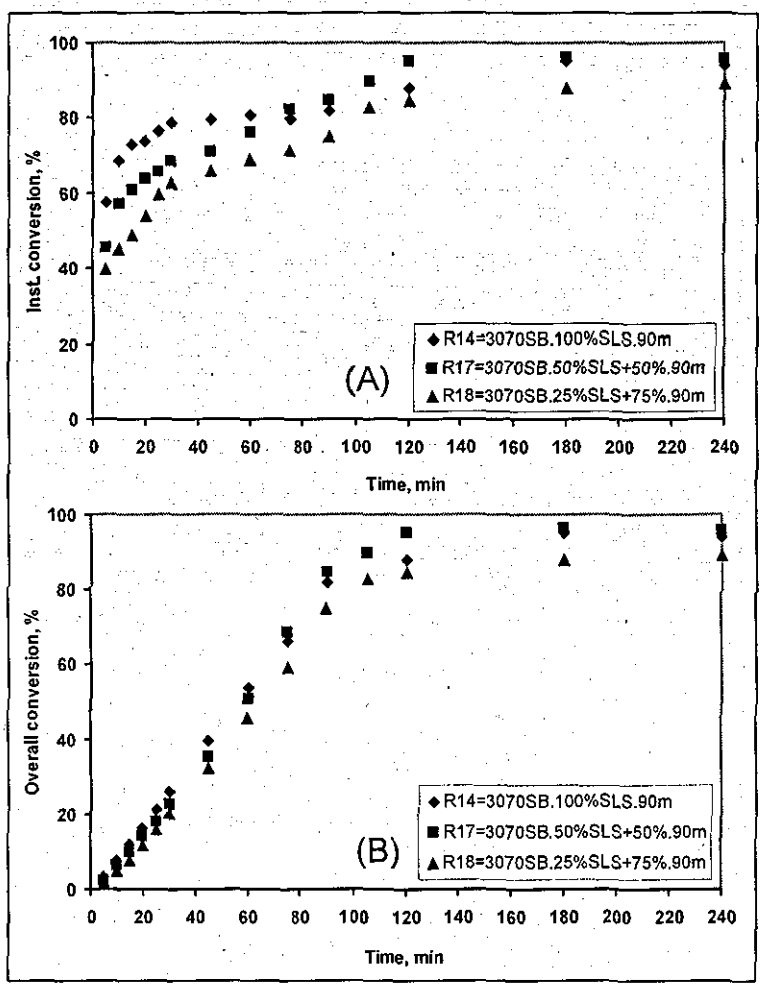

Figure 8.7 The effects of the SLS feed on the instantaneous (A) and overall (B) conversions for the experiments R14, R17, and R18

The supplied semibatch surfactant feed brought the final volume in the reactor for all the runs to the same level (~1000 cm^3). This approach will help in identifying the role of the extra surfactant added during the semibatch stage, and whether this role was stabilizing the existing particles, or generating new particles.

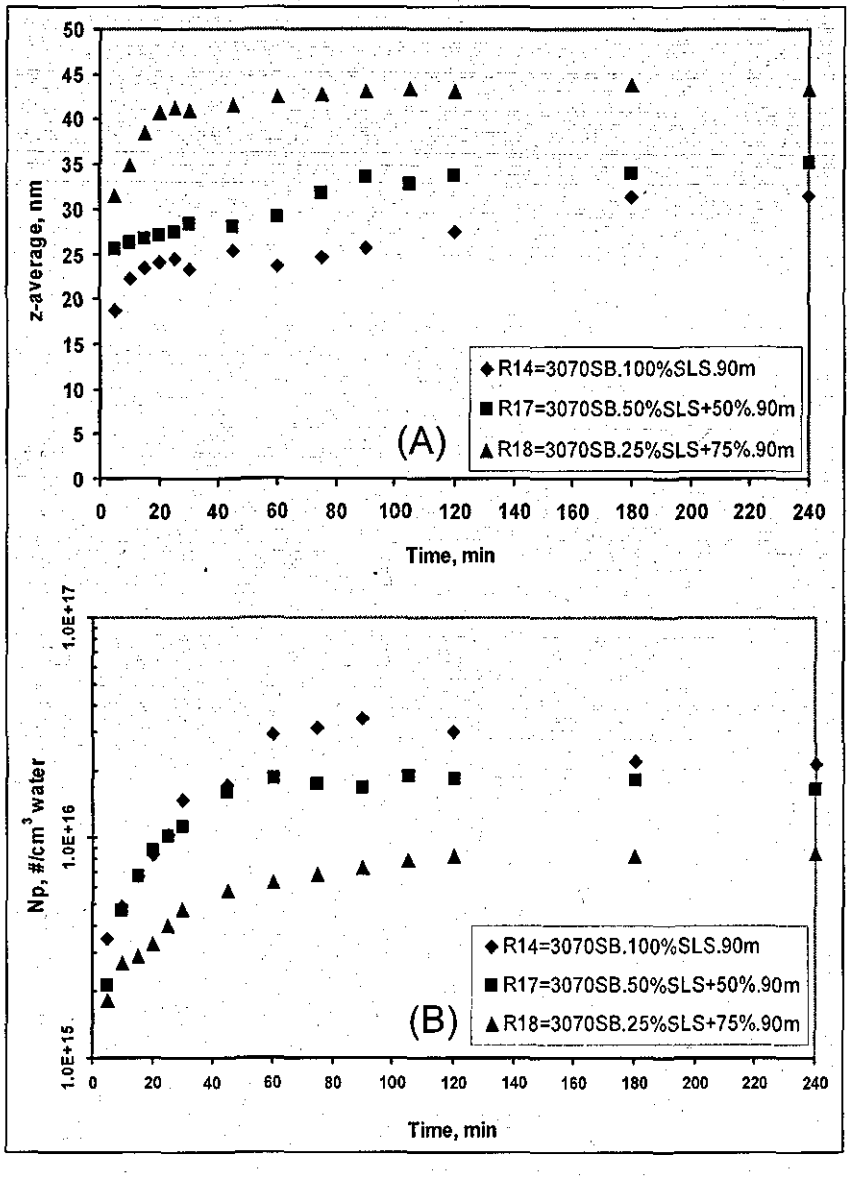

Figure 8.8 The effects of the SLS feed on the particle sizes (A) and number of polymer particles (B) for the experiments R14, R17, and R18

Figure 8.7 illustrates the instantaneous (A) and the overall (B) conversions evolution with time. It is apparent that reducing the mass of the initial charge reduced the polymerization rate. The reduction in the polymerization rate could be attributed to the fact that reducing the mass of the initial charge led to an increase in the agitation intensity and in return increased the number of monomer drops and reduced their sizes. As a result, due to the increase in the surface area the monomer drops will absorb more surfactant leading to a reduction in the number of micelles and reducing the polymerization rate. This effect was apparent on the initial and the final polymerization rate.

Figure 8.8 demonstrates that the semibatch SLS feed did not raise the number of particles in R18 and R17 to the same level of R14. This could suggest that part of the additional SLS surfactant was used to stabilize the existing particles or the monomer drops. Therefore, its effect on the polymerization rate was limited.

Figures 8.9 demonstrate the effects of the SLS in the initial charge on the overall number of particles and particle sizes. The polymer particles and particle sizes were plotted against the overall surfactant ratio in the reactor (i.e. the ratio between the surfactant in the reactor and the total surfactant in the recipe) for the runs R17 and R18. Figure 8.9 clearly demonstrates that at the same surfactant quantity, different particle sizes and number of polymer particles were obtained. For instance, at 0.7 SLS overall ratio the reactor contains 5 g of SLS surfactant, yet R17 and R18 exhibited different z-average and number of polymer particles.

Figure 8.10 illustrates the evolution of the mass fraction of the monomers in the particles with time (A) and with the overall SLS ratio (B). There is no apparent correlation between the surfactant and the monomer concentration in the particles. It is clear from figure 8.10B that similar ratios gave similar monomer mass fractions, which confirms the previous finding (§8.2.1) where it was demonstrated that there is no role for the SLS on the composition and the monomer concentration in the particles (figure 8.11).

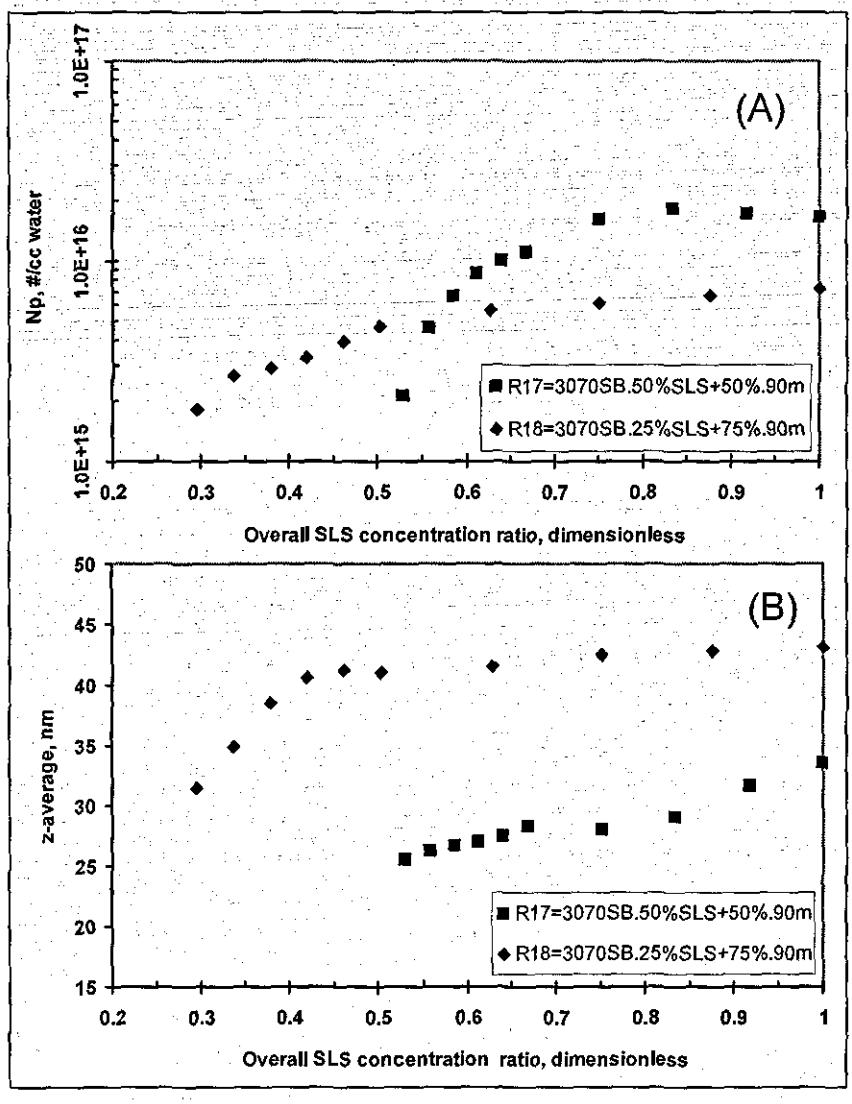

Figure 8.9 The evolution of the number of polymer particles (A) and particle sizes (B) with overall SLS ratio

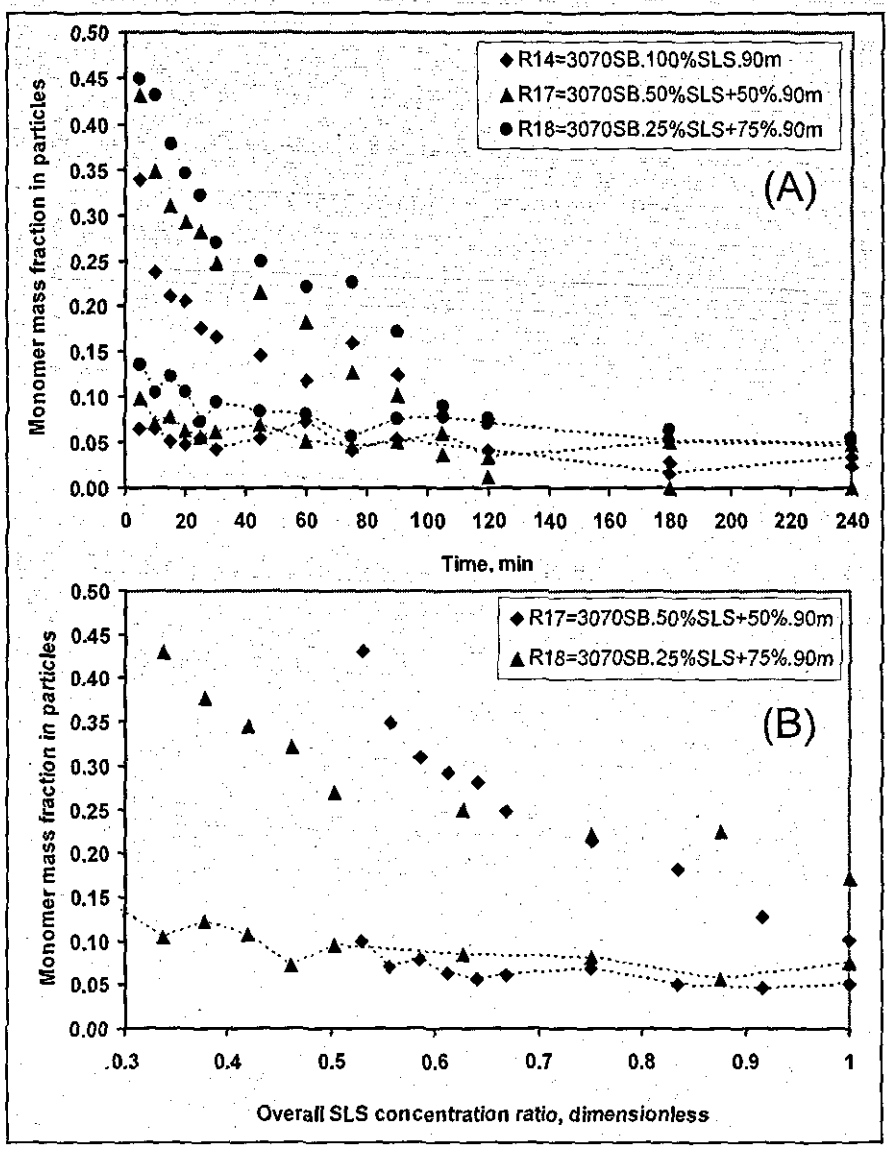

Figure 8.10 The time evolution of the monomers mass fraction in particles (A) and SLS overall ratio (B) for the experiments R17 and R18

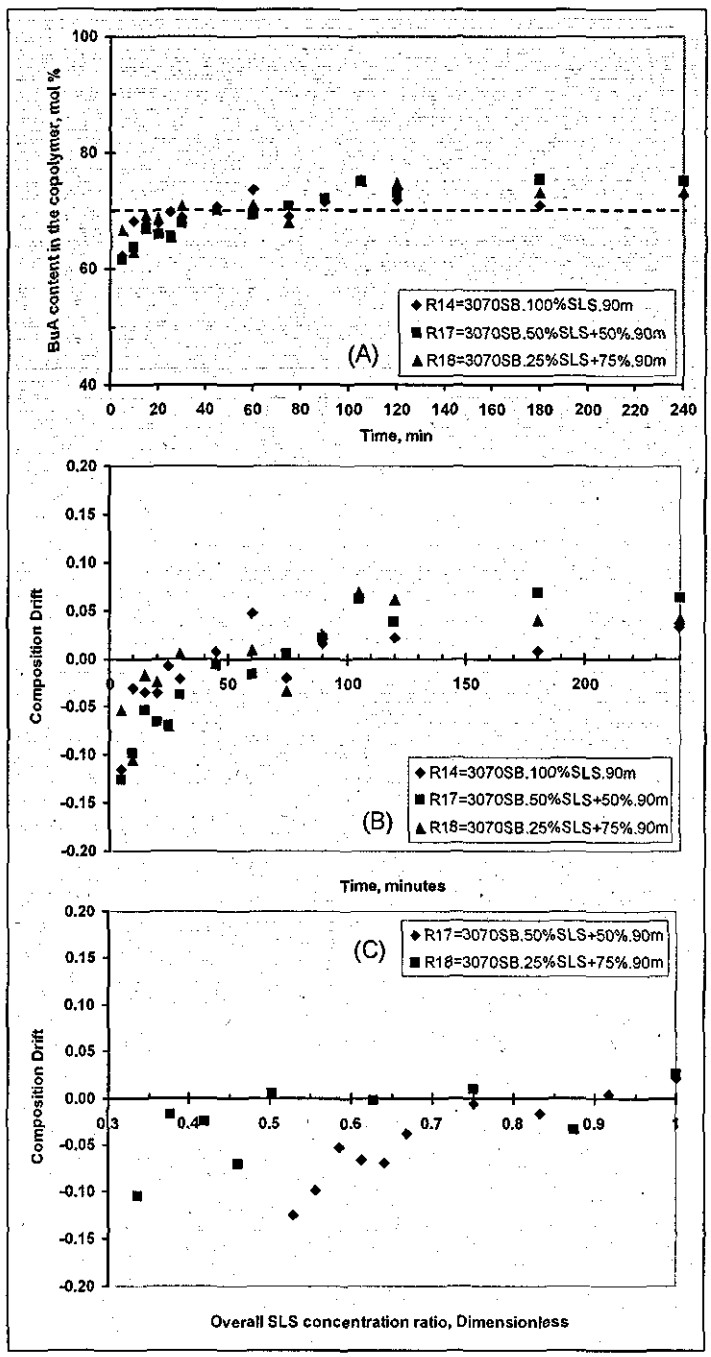

Figure 8.11 The time evolution of the copolymer composition (A) composition drift (B) and the effects of the SLS overall ratio in the reactor on the evolution of the composition drift (C) for the experiments R14, R17, and R18

Figure 8.11 illustrates the time evolutions of the copolymer composition (A), composition drift (B), and the effect of the overall SLS ratio on the evolution of the composition drift (C). Since the monomer concentration in the particles was independent of the SLS concentration, it was expected to observe the same behaviour for the copolymer composition and the composition drift. This is exactly what figure 8.11 illustrates. The SLS concentration did not show an effect on the composition of the copolymer; R14, R17, and R18 exhibited similar composition evolution behavior.

In conclusion, feeding the surfactant during the semibatch stage led to a reduction in the number of polymer particles causing lower polymerization rates. The semibatch SLS feed did not generate new micelles and it was used to stabilize the existing particles. Since the concentration of the surfactant in the initial charge and in the semibatch surfactant feed was constant, it is concluded that the main effect that led to the drop in the polymerization rate and the number of polymer particles was the agitation intensity. Reducing the mass of the initial charge led to higher agitation intensities causing smaller monomer drops. Consequently, the drops will absorb more surfactant leading to a reduction in the micelles and in the polymerization rate. The reduction in the number of micelles produced bigger particles since the monomer diffuse in to fewer micelles.

The Sty-BuA copolymer composition was not affected by the change in the particle sizes and the number of polymer particles. The composition drift was independent of the factors that affected the particles and the polymerization rate.

8.3. Initiator distribution effects

Several runs were conducted where the amounts of the KPS in the semibatch feed and in the initial charge were varied. The recipes of the experiments are given in table 8.2.

Run	Initiator Conc. KPS (g) / Water (cm^3)		Monomers Transferred, g		Feeding Time, minutes	Monomers Mole Ratio %, Sty/BuA
	I.C.	Feed	Sty	BuA		
19	1.2/700	0.00/0.0	68	205	90	30/70
20	0.60/700	0.00/0.0	71	211	90	30/70
21	0.30/700	0.00/0.0	72	214	90	30/70
22	0.15/700	0.00/0.0	73	215	90	30/70
23	0.30/350	0.30/350	74	213	90	30/70
24	0.15/175	0.45/525	74	220	90	30/70
25*	1.2/700	0.00/0.0	72	212	90	30/70
26*	0.6/700	0.00/0.0	71	210	90	30/70
Other Ingredients		Surfactant (SLS)			7.0 g	
		Buffer ($NaHCO_3$)			0.6 g	
		Final Volume			1000 cc	
		Solids Content			30%	
		Temperature			70° C	

(*) SLS = 200% (i.e. 14 g)

Table 8.2 The recipes of the experiments related to the study of the initiator effects on the copolymer

These experiments were conducted similarly to the previous runs. The polymerization was performed in two different stages. First, a semibatch stage which lasted for 90 minutes, and then a subsequent 150 minutes batch stage. The total duration of both stages was four hours.

The masses of the other ingredients (i.e. the SLS, deionized water, buffer, and the monomers) were kept unaltered except in two runs (i.e. R25 an R26) where the SLS concentration was twice the usual concentration (i.e. 200% SLS = 14 g). The total mass and the solids content were constant. The reaction temperature was at or near 70° C.

8.3.1. Effects of initiator concentration in the initial charge

In experiments R19-R22, the concentration of the KPS in the recipe was varied between 25% and 200%; the initial charge did not contain monomers. All the other ingredients of the recipes were kept unaltered (table 8.2). The subsequent feed was a mixture of the monomers only, and no further initiator was fed to the system.

Figure 8.12 illustrates the evolutions of the instantaneous (A) and the overall (B) conversions with time for the experiments R19-R22. A relationship between the KPS concentration and the conversion can be observed in which lower polymerization rates were obtained when the KPS concentration in the initial charge was reduced. Experiment R21 exhibited the lowest polymerization rate compared to the other runs. Reducing the initial KPS concentration causes a reduction in the concentration of the initiator radicals in the system.

Previously (§2.2.1), it was demonstrated that the initiator radicals start the polymerization reaction initially in the micelles and later in the polymer particles. Consequently, the change in the initiator concentration will affect the kinetics of the system in which a reduction in the KPS concentration is expected to lead to a reduction in the polymerization rate. Run R22 overall conversion is increasing with time in the batch stage, but this increase is of a lower rate indicating that the system might eventually reach higher conversions, but that will be after longer times compared to the other runs.

It is also noticeable that runs R19 and R20 exhibited similar kinetics although the KPS concentration in R19 is twice the concentration in R20.

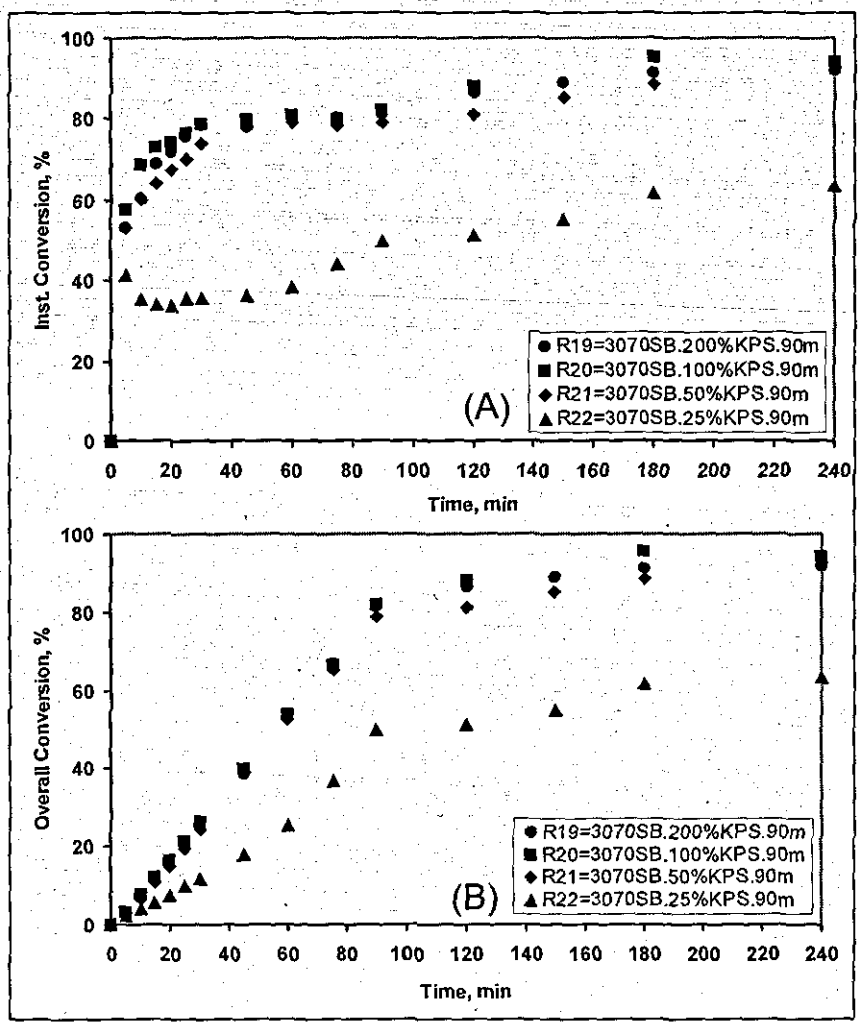

Figure 8.12 The time evolution of the instantaneous (A) and overall (B) conversions for the experiments R19-R22

Figure 8.13 demonstrates the KPS concentration effects on the particle sizes (A) and the number of polymer particles (B). Reducing the KPS concentration led to a reduction in the number of polymer particles and an apparent increase in the particle sizes. These two consequences could be attributed to the fact that reducing the KPS concentration leads to fewer numbers of active micelles, as a result, the monomers

diffuse in to smaller number of micelles or polymer particles, and this will lead to an increase in the average particle sizes (figure 8.13A).

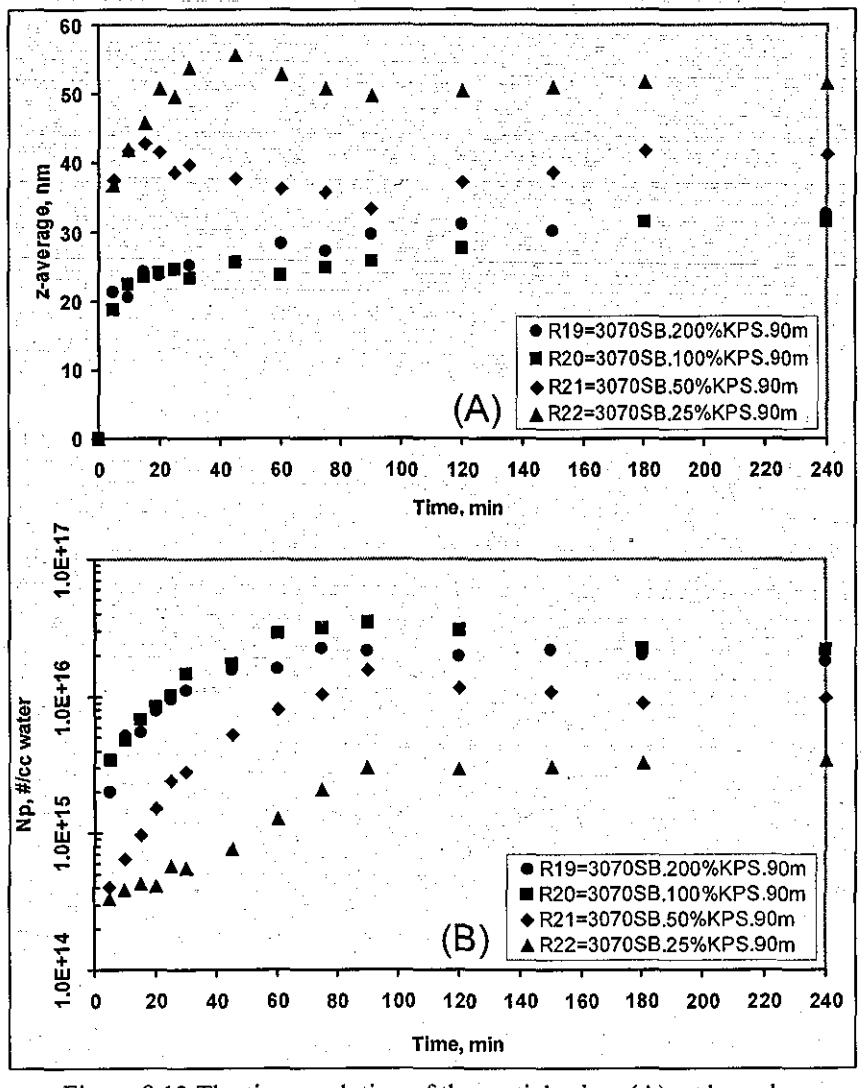

Figure 8.13 The time evolution of the particle sizes (A) and number of polymer particles (B) for the experiments R19-R22

Figure 8.14 illustrates the composition and the composition drift. Similar to the SLS, there were no apparent KPS effects on the composition of the copolymer. Although the KPS concentration affected the number of polymer particles and the particle sizes which in return affected the total surface area of the particles. Yet this

did not result in noticeable effects on the composition of the copolymer. Once more this suggests that the solubility of the monomers in the water is not playing a role in the system. Similar findings can be interpreted from figure 8.15. It illustrates that the monomer mass fraction was independent of the KPS effects on the system. This was expected since the KPS did not affect the composition in the system.

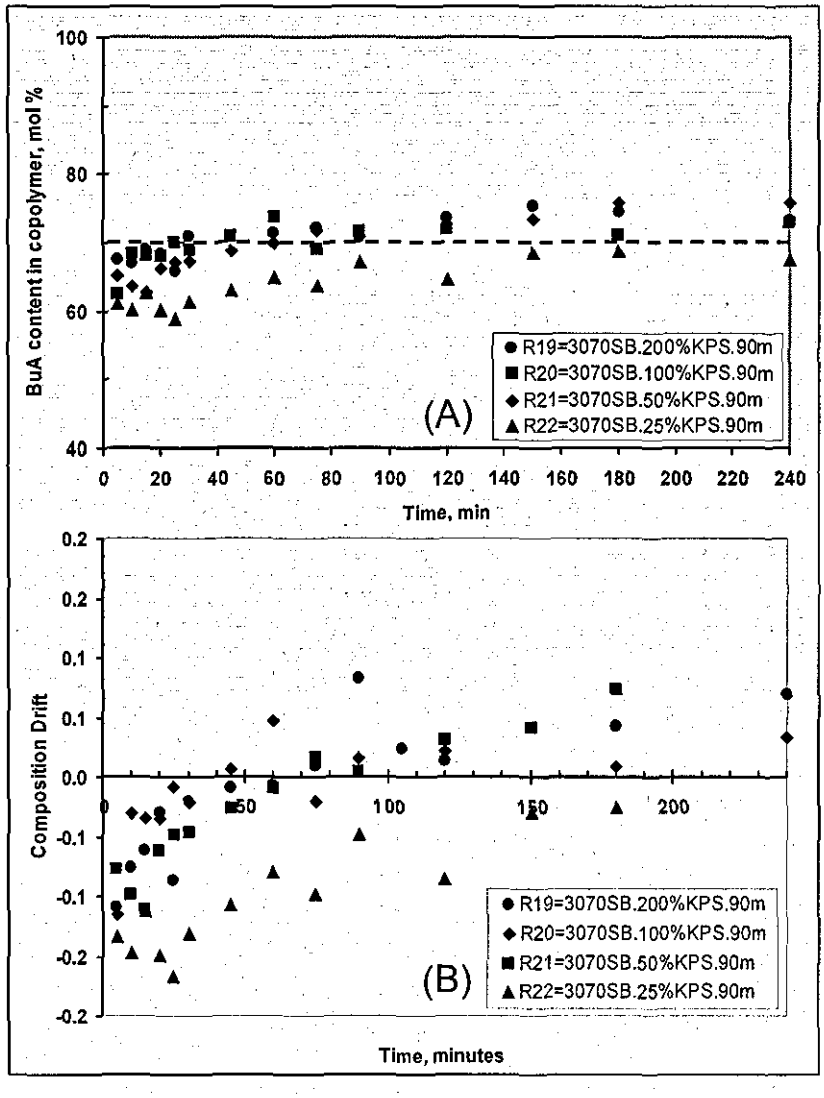

Figure 8.14 The time evolution of the copolymer composition (A) and composition drift (B) for the experiments R19-R22

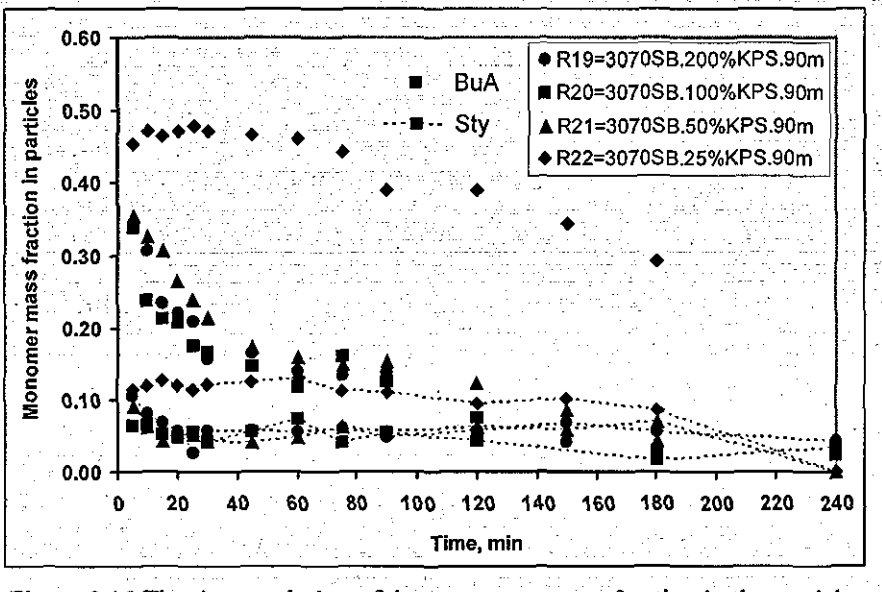

Figure 8.15 The time evolution of the monomers mass fraction in the particles for the experiments R19-R22

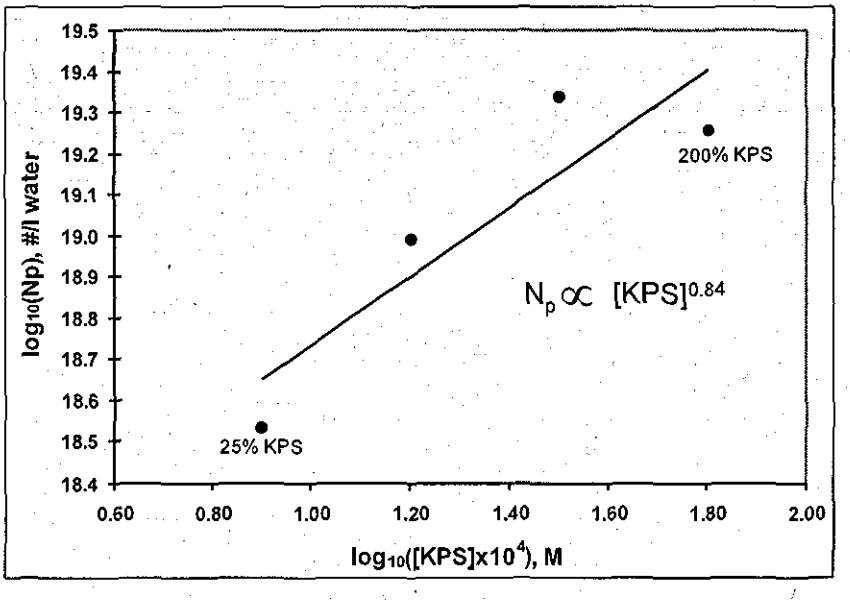

Figure 8.16 The order of dependence of number of polymer particles on the initiator concentration for the runs R19-R22

Previously (§8.2.1), it was demonstrated that the power dependence of the number of polymer particles on the surfactant concentration was higher than Smith-Ewart case 2 predictions. Figure 8.16 illustrates the power dependence of the number of polymer particles on the initiator concentration. Smith-Ewart kinetics predicts a value of 0.4, but figure 8.16 suggests a value of 0.84. Once more, the obtained value is higher than Smith-Ewart case 2 predictions, which could indicate that some of the assumptions of case 2 such as the constant growth rate of the particles are not valid for the semibatch emulsion copolymerization of Sty-BuA (Sajjadi and Brooks, 1999).

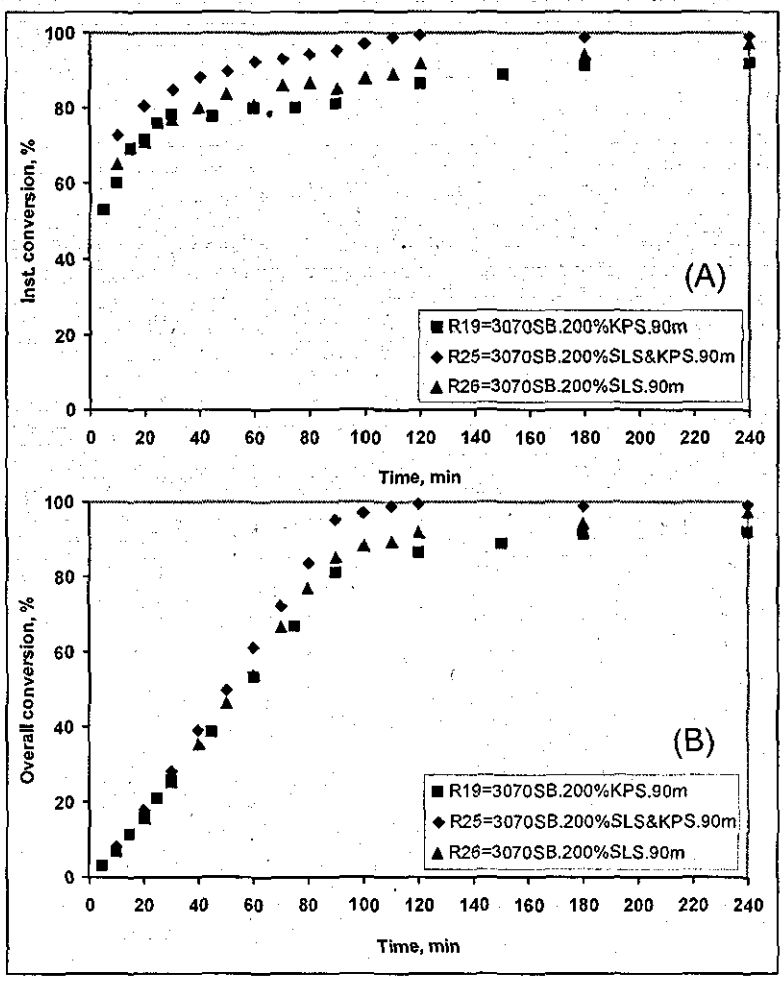

Figure 8.17 The time evolution of the instantaneous (A) and overall (B) conversions for the experiments R19, R25, and R26

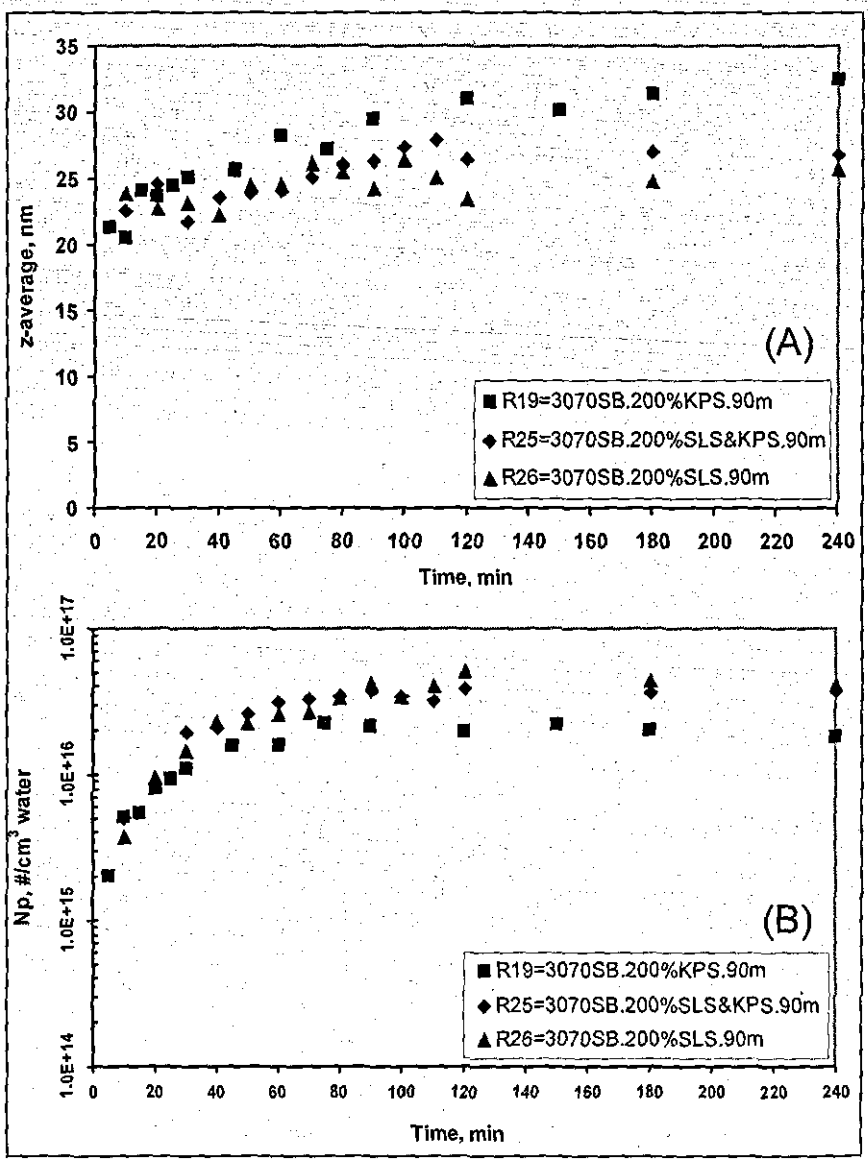

Figure 8.18 The time evolution of the particle sizes (A) and number of polymer particles (B) for the experiments R19, R25, and R26

Previously (§8.2.1 and §8.3.1) it was demonstrated that increasing the SLS or the KPS concentrations in the initial charge beyond 100% did not show effects on the kinetics of the system. An attempt to understand this behaviour was made by

increasing the KPS and the SLS concentrations in the initial charge to 200% simultaneously.

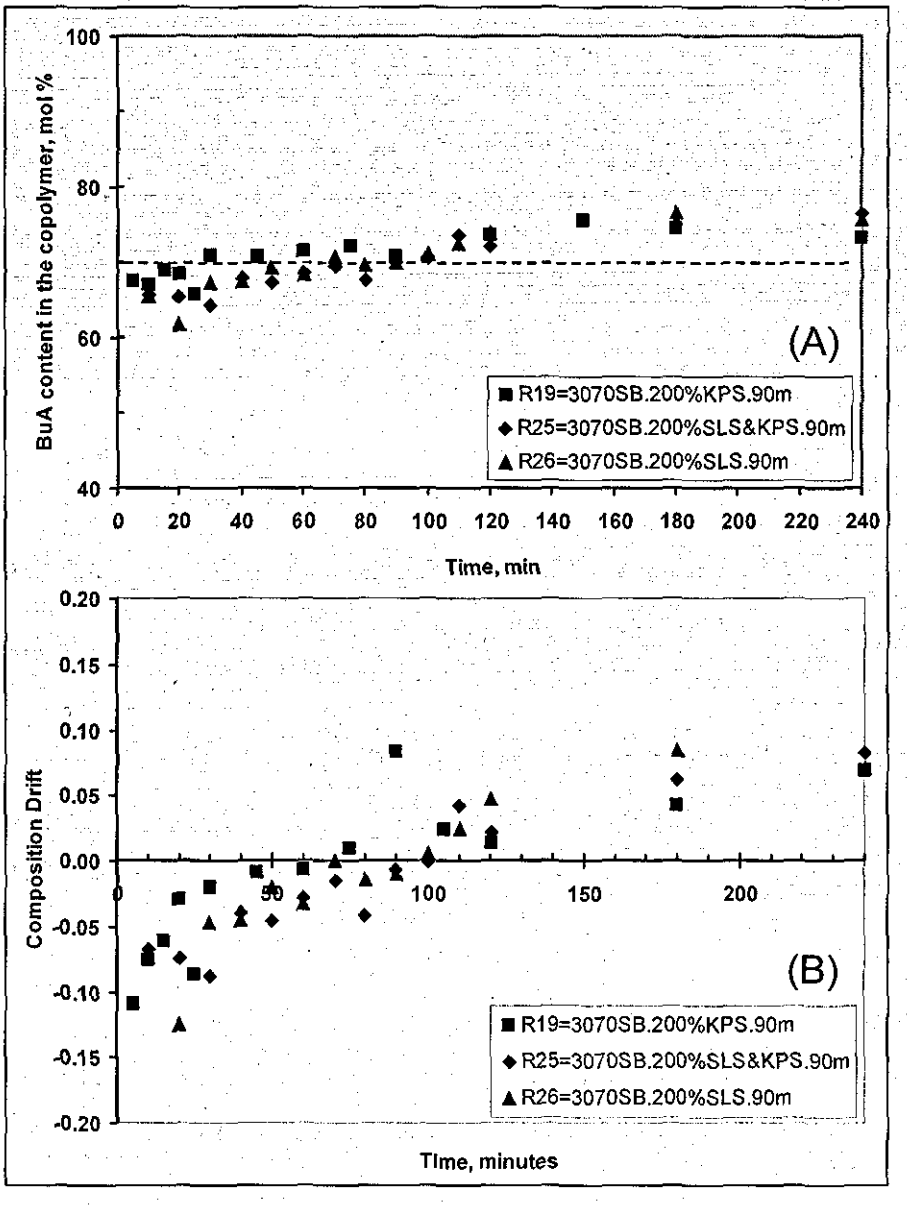

Figure 8.19 The time evolution of the composition (A) and composition drift (B) for the experiments R19, R25, and R26

Figures 8.17-8.19 demonstrate the effects on the conversion, the particles, and the composition evolutions with time. Figure 8.17 illustrates that the instantaneous

and the overall conversions (R25) slightly increased due to the simultaneous increase of KPS and the SLS concentrations. This change is not apparent in R19 and R26. An effect on the number of polymer particles and the particle sizes is not noticeable in figure 8.18. There is a chance that the simultaneous increase of the SLS and the KPS led to the activation of more micelles and in return led to this increase in the polymerization rate. But this is not evident by the number of particles in the system (figure 8.18). Once more, the composition and the composition drift were not affected and all the runs exhibited similar behaviours (figure 8.19).

In conclusion, it was found that reducing the initiator concentration reduces the initiator radicals in the system leading to a reduction in the polymerization rate. Similar effect was detected on the number of polymer particles in which the number of particles was reduced with reducing the initiator concentration. The reduction in the number of polymer particles indicates that lower initiator concentration activated fewer micelles leading to smaller number of polymer particles. Consequently, the polymerization rate in the system was reduced. Lower number of particles led to larger particle sizes since the monomer transfers to smaller number of particles.

Feeding the initiator beyond certain limit (100% KPS) did not affect the system kinetics until it was coupled with an increase in the SLS concentration. This could be related to the fact that the excess KPS activated more micelles upon increasing the SLS concentration.

Although the polymerization rate and the number of polymer particles were affected by the change in the initiator concentration, the overall composition and the composition drift were independent of the initiator effects.

8.3.2. Distribution of the initiator between the initial charge and the subsequent feed

Runs 23 and 24 were conducted to study the effects of distributing the initiator between the initial charge and the semibatch feed on the Sty-BuA copolymer.

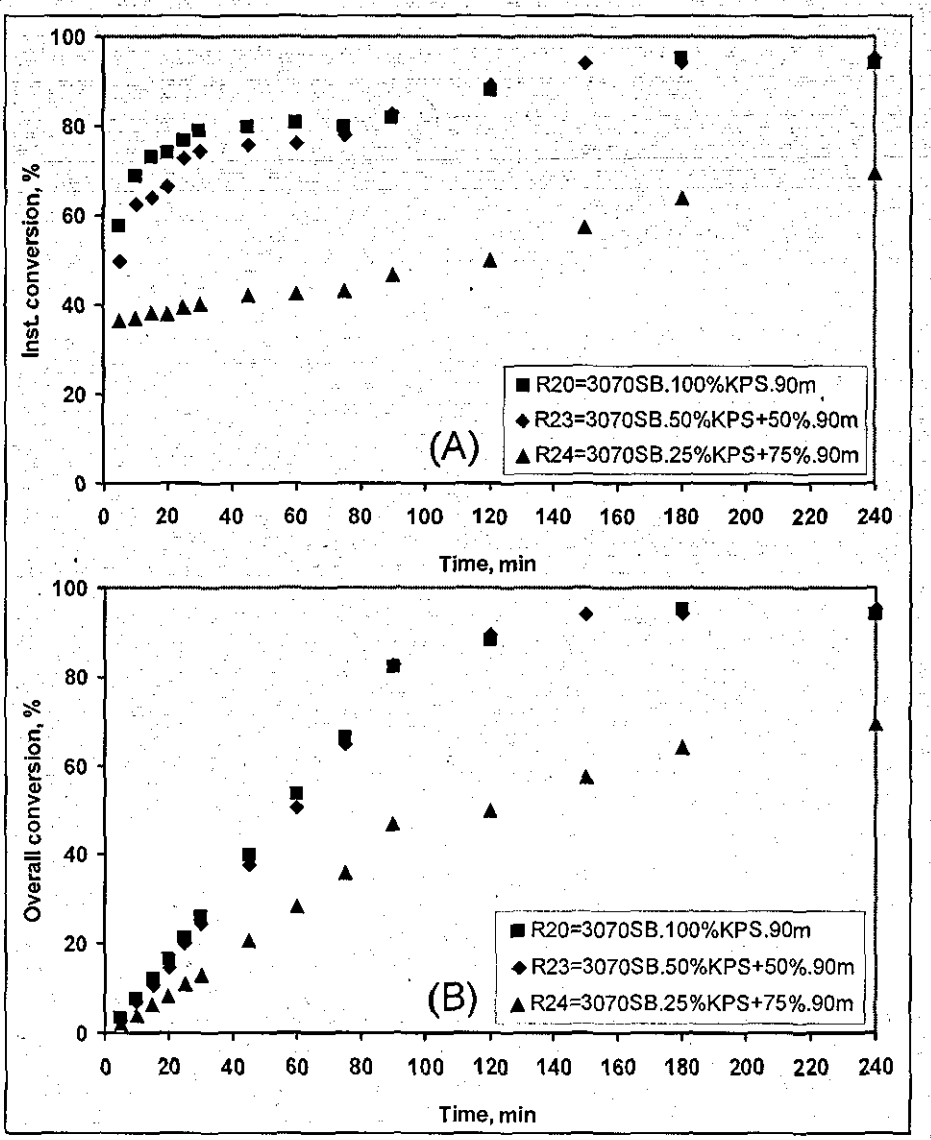

Figure 8.20 The effects of initiator feed on the instantaneous (A) and overall (B) conversions for the experiments R20, R23, and R24

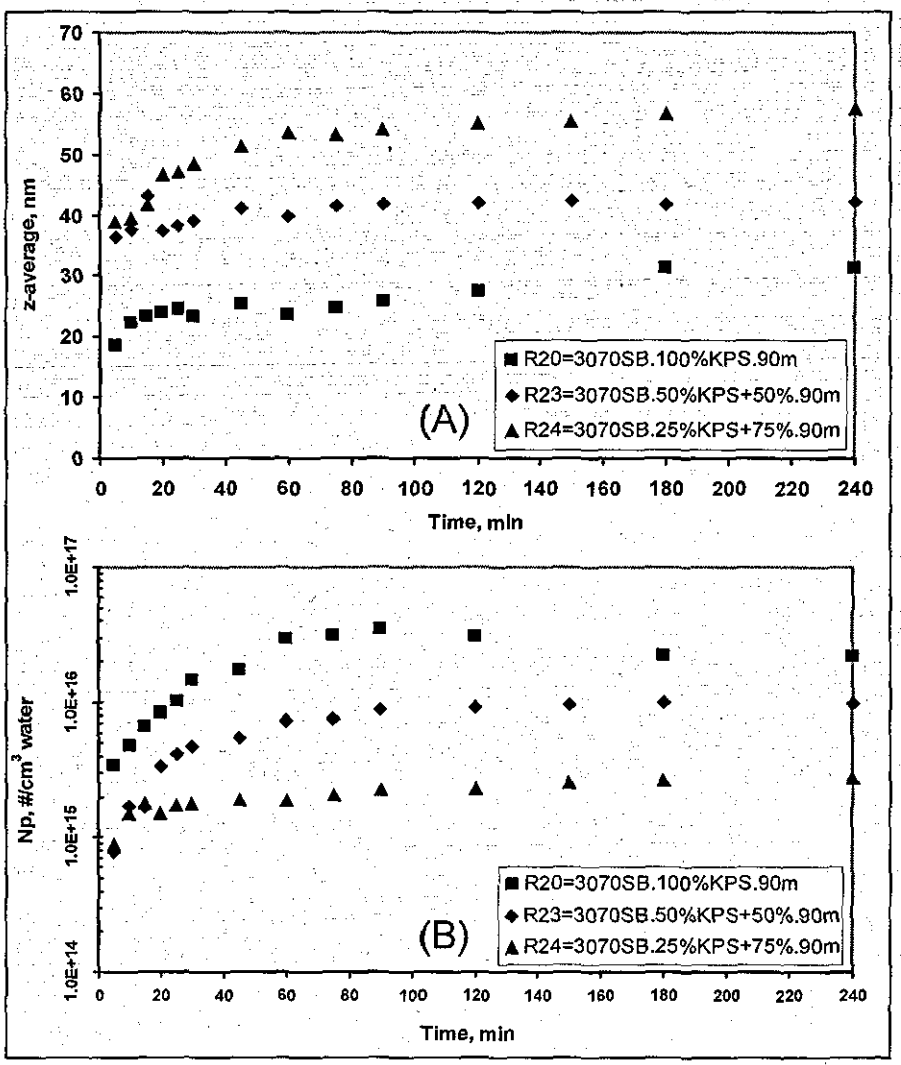

Figure 8.21 The effects of initiator feed on the particle sizes (A) and number of polymer particles (B) for the experiments R20, R23, and R24

The volume of the initial charge in runs 23 and 24 was 50% and 25% of the usual volume (100% initial charge volume = ~700 cm^3). The initiator concentration was constant in the initial charge and in the semibatch feed (i.e. 3.18×10^{-3} M). The initial charge does not contain monomers. Separate streams of the monomers and the initiator fed the reactor during the semibatch stage. The semibatch feeds brought the

reactor final volume up to the usual level (i.e. ~1000 cm^3) at the end of the semibatch stage.

Figure 8.20 illustrates the evolutions of the instantaneous (A) and the overall (B) conversions with time for the runs R20, R23, and R24. Although the concentration of the initiator is constant, noticeable differences between the runs in the polymerization rate is observed. It seems that there was a negative effect on the polymerization rate when the mass of the initial charge was reduced and the initiator was fed during the semibatch stage.

This effect is also apparent in figure 8.21 where it is clear that there was a reduction in the number of polymer particles as a result of reducing the mass of the initial charge. This could be explained by the fact that reducing the initial volume leads to initially higher agitation intensities; consequently leading to smaller monomer drops. The smaller monomer drops will absorb more surfactant compared to the bigger monomer drops.

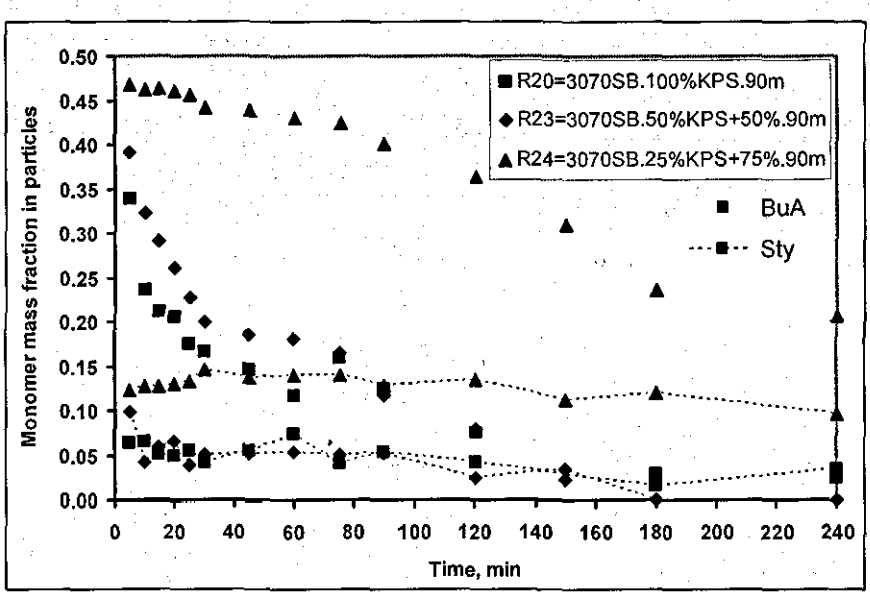

Figure 8.22 The effects of initiator feed on the monomers mass fraction in the particles for the experiments R20, R23, and R24

This reduction in the surfactant could lead to a reduction in the polymerization rate and an increase in the particle sizes since the monomer will diffuse in to fewer number of polymer particles.

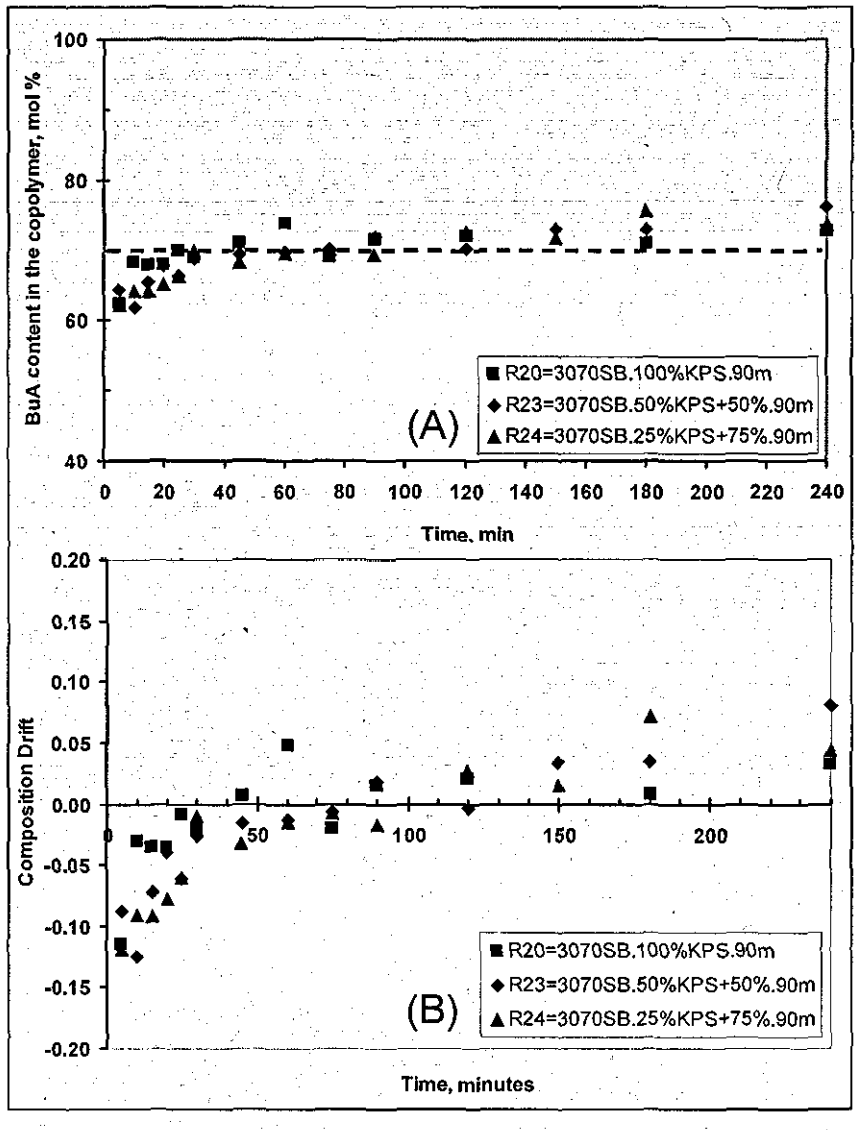

Figure 8.23 The effects of initiator feed on the copolymer composition (A) and composition drift (B) for the experiments R20, R23, and R24

The mass fraction of the monomers in the particles (figure 8.22) and the composition and the composition drift (figure 8.23) data confirmed that the discrepancies in the particles and the polymerization rate did not show major effects on the composition of the copolymer.

In conclusion, the semibatch initiator feed showed negative effects on the polymerization rate. The initiator concentration in the semibatch feed and in the initial charge was constant, yet lower polymerization rates were obtained when the semibatch initiator feed was supplied. This effect could be related to the higher agitation intensities since the reduction in the initial charge volume led to smaller monomer drops. Consequently, more surfactant was absorbed by the monomer drops leading to a reduction in the micelles and the polymerization rate.

The reduction in the number of micelles led to a reduction in the number of polymer particles and an increase in the particle sizes. The composition and the composition drift were not affected by the changes in the system kinetics.

8.4. Surface tension evolution

To investigate the surfactant evolution in the reactor, an attempt was made to extract samples from the reactor and to conduct surface tension measurements. Figure 8.24 is an illustration of the surface tension evolution of an experiment where the recipe was identical to R14.

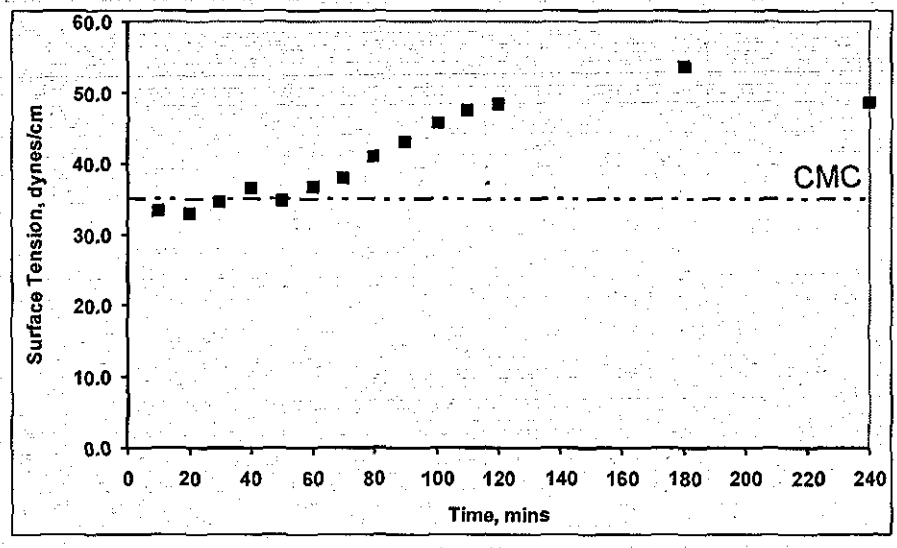

Figure 8.24 The time evolution of the surface tension for 100% SLS and KPS in the initial charge and semibatch feed of monomers

It should be noted that this method suffers from some limitations. For instance, due to the volume of the samples that were extracted from the reactor (20-30 cm^3 / sample) it is expected that the behavior of the reactor might be affected by the reduction in the volume. Moreover, inhibitor solution was not added to the samples since it might alter the conditions of the samples, this might indicates that the samples may exhibited further polymerization since the temperature was kept high at or near 70 °C.

Figure 8.24 illustrates that the surface tension for R14 varied between 33 and 35 dynes/cm for the first 20 minutes and then it started to increase. This suggests that the SLS concentration was below the CMC after the first 20 minutes. Observing

figure 8.2, it is clear that the nucleation continued for 40-60 minutes. The fact that nucleation continued further than 20 minutes does not necessarily mean that homogeneous nucleation was occurring. This could be a result of smaller particle sizes that were not detected until later times, or the surface tension measurements do not represent the actual conditions in the reactor due to the aforementioned limitations.

8.5. Conclusion

In this chapter, a detailed study of the effects of distributing the surfactant and the initiator between the initial charge and the semibatch subsequent feed on the kinetics of the Sty-BuA semibatch emulsion copolymerization was presented.

It was not surprising to find that reducing the surfactant content in the initial charge reduces number of polymer particles in the system leading to larger particle sizes. This reduction in the number of polymer particles caused a reduction in the polymerization rate of the system.

No apparent effects were detected on the composition and the composition drift. This indicates that the diffusion of the monomers to the particles and the monomers mass fraction in the particles were not affected by the changes related to the surfactant concentration. It was also found that the system did not follow Smith-Ewart predictions. The power dependence of the number of polymer particles on the surfactant concentration was 1.62 which is higher than Smith-Ewart case 2 predictions (i.e. 0.6).

Distributing the surfactant concentration between the initial charge and the subsequent feed showed major effects on the polymer particles and subsequently the polymerization rate. The surfactant concentration in the initial charge and the semibatch feed was constant (i.e. 3.47×10^{-2} M), yet it was found that reducing the volume of the initial charge, and supplying surfactant feed during the semibatch stage led to a reduction in the polymerization rate and the number of polymer particles. This caused larger particle sizes.

Reducing the volume of the initial charge leads to higher power input by the impeller. The increase in the power input could lead to smaller monomer drops and an increase in their numbers. The increase in the total surface area of the monomer drops will lead to more surfactant being absorbed by the monomer drops causing a

reduction in the amount of the surfactant that is available for the micelles. This reduction in the number of micelles will eventually leads to a reduction in the number of polymer particles, an increase in the particle sizes, and a decrease in the polymerization rates.

The composition and the composition drift of the Sty-BuA copolymer were independent of the variations in the number of particles and the polymerization rates. Once more, this indicates that that the composition of the system and the mass fraction of the monomers in the particles were independent of the effects related to the surfactant or the agitation intensity.

Studying the initiator concentration in the initial charge revealed predictable results. Reducing the initiator concentration in the initial charge reduced the polymerization rate. This was a result of the reduction in the initiator radicals in the system which led to lower numbers of polymer particles and larger particle sizes. The power dependence of the number of polymer particles on the initiator concentration was 0.84, which is higher than the 0.4 value which is predicted by Smith-Ewart case 2.

However, the copolymer composition and composition drift were not affected by the initiator concentration although the effects on the rates of polymerization were obvious.

Distributing the initiator between the initial charge and the semibatch subsequent feed demonstrated a behavior similar to the surfactant distribution. Lowering the volume of the initial charge led to a reduction in the polymerization rate and the number of polymer particles although the initiator concentration was kept constant (i.e. 3.18×10^{-3} M) in the initial charge and in the semibatch feed. Once more, this could be attributed the decrease in the size of the monomer drops and the increase in their numbers as a result of higher agitation intensities. The copolymer composition and composition drift were independent of these effects.

The simultaneous increase of the surfactant and the initiator concentrations led to higher polymerization rates when compared to the increase of one and not the other. This might indicates that the excess initiator radicals activated more micelles leading to higher polymerization rates. The effects on the number of particles were not apparent. The composition data were independent of the changes in the rates of the polymerizations.

In summary, reducing the surfactant or the initiator concentrations in the initial charge led to lower number of polymer particles, larger particle sizes, lower polymerization rates, and did not show any effects on the composition of the copolymer. Distributing the surfactant or the initiator between the initial charge and the semibatch feed led to a reduction in the polymerization rate as a result of a reduction in the number of polymer particles, but did not influence the copolymer composition. The surfactant feed did not generate more particles; it was mainly used to stabilize the existing particles.

9. General Conclusions

9.1. Conclusions

The main objective of this work was to study the effects of the distribution of the reaction ingredients between the initial reactor charge and the semibatch feed on the composition and the overall behavior of the emulsion copolymerization of styrene (Sty) and butyl acrylate (BuA) in a semibatch reactor. Sodium lauryl sulphate (SLS) and potassium persulphate (KPS) were used as surfactant and initiator respectively. The conversion, particle sizes, and the composition of the samples were analyzed using the gravimetric method, Malvern™ Zetasizer, and Fourier transform infrared spectroscopy (FT-IR) respectively. Computer modeling was applied to study the monomer concentration in the particles by means of the constant partition coefficient (CPC) model. The general conclusions derived from this work will be summarized in the next few sections.

9.1.1. Monomer effects on the Sty-BuA copolymer

It was found that the distribution of the monomers between the initial charge and the semibatch feed showed significant effects on the polymerization rate, the particle sizes and numbers, and the composition of the copolymer.

In general BuA rich initial charge when compared to Sty rich initial charge shows:

- Higher polymerization rates
- Smaller particle sizes
- Minimal composition drift

BuA is a polar monomer; BuA rich initial charge leads to less surfactant molecules that are adsorbed on the BuA rich polymer particles. It was demonstrated that the estimated additional unadsorbed SLS in the reactor for the BuA rich initial

charge case leads to an increase in the number of polymer particles and hence a reduction in the particle sizes. This will eventually lead to higher polymerization rates.

Cross-linking was detected when the BuA content in the copolymer exceeds 40%. This could indicate that gel effect led to lower termination rates due to the increase in the viscosity within the polymer particles and eventually caused the apparent increase in the polymerization rates for BuA rich initial charge experiments.

Investigating the free unadsorbed SLS molecules in the reactor based on Piirma and Chen results revealed that the SLS concentration in the reactor was above the CMC for up to 60 minutes. This information could explain the extended nucleation periods that were detected. The nucleation time increases when the system is BuA rich and decreases when it is Sty rich (i.e. polarity effects).

At high agitation intensities (0.4 kW/m^3) the number of polymer particles and the polymerization rate exhibited a slight decrease when compared to moderate agitation intensities (0.05 kW/m^3). This was linked to the increase in the number of monomer drops at higher agitation intensities which resulted in the absorption of more surfactant molecules by the monomer drops, in order to stabilize them, causing a decline in the number of micelles and affecting the rates of polymerization.

BuA rich initial charge experiments exhibited minimal composition drift. The reactivity of the Sty monomer is the main cause of the copolymer composition drift. Reducing the Sty monomer content in the initial charge in favour of the BuA monomer and feeding the Sty in the semibatch feed led to a reduction in the composition drift and the production of copolymers with Sty-BuA molar ratio that is comparable to that of the monomer mixture.

The solubilities of the monomers in the aqueous phase did not affect the monomer concentrations within the particles. The CPC model (§2.6 and appendix C)

illustrated that the Sty monomer mass fraction inside the particles for Sty rich initial charge runs is comparable to the BuA monomer mass fraction in the particles for BuA rich initial charge runs at the same reaction conditions. The fact that the BuA solubility in the aqueous phase is higher than the Sty did not reduce its concentration in the polymer particles in favor of the Sty monomer. Moreover, the composition results demonstrate that even when the aqueous phase and the polymer particles were rich with the first monomer (i.e. the monomer that is fed in the initial charge) that did not affect the dissolution of the second monomer (i.e. the monomer that is being fed to the reactor) and the second monomer was able to polymerize and emerge in the copolymer composition even after short periods of time. This demonstrates that the solubilities of the monomers in the aqueous phase did not affect the kinetics of the system.

Feeding the monomers at higher rates helps in reducing the reaction time. It was found that increasing the monomer feeding rates led to a reduction in the instantaneous conversion but did not affect the composition of the copolymer or the particles evolution. The copolymer composition approached the monomer mixture composition in all the studied cases, and this approach was at shorter times when the feeding rate was higher.

In general, increasing the BuA content in the initial charge demonstrates the best approach since it will reduce the reaction time and it will reduce the composition drift. However, this approach will lead to smaller particle sizes which can be increased by increasing the content of the Sty in the initial charge.

9.1.2. Surfactant effects on the Sty-BuA copolymer

It was found that the surfactant effects on the nucleation in the system were significant. As expected, reducing the SLS concentration in the initial charge led to a reduction in the number of polymer particles and an increase in the particle sizes. These effects led to a reduction in the polymerization rate.

The composition of the copolymer, the composition drift, and the monomers mass fraction in the particles were independent of the number of polymer particles and the particle sizes.

It was also found that the system did not follow Smith-Ewart predictions. The power dependence of the ultimate number of polymer particles on the surfactant concentration was 1.62 which is greater than Smith-Ewart case 2 predictions (i.e. 0.6). This could be related to some of Smith-Ewart case 2 assumptions, and in particular to the particles growth rate since it was assumed originally to be constant, however, this might not be the case in this work.

Distributing the surfactant between the initial charge and the subsequent feed while maintaining constant surfactant concentration in the system showed significant effects on the kinetics of the system. It was found that the reduction in the volume of the initial charge led to a reduction in the number of polymer particles and the polymerization rate. This was associated with the increase in the number of monomer drops as a result of the increase in the agitation intensity. The additional monomer drops absorb more surfactant reducing the total number of micelles in the system and the polymerization rate. Once more, the composition and the composition drift of the Sty-BuA copolymer were independent of the variations in the number of particles and the polymerization rates.

In general, feeding all the surfactant in the initial charge is the best approach since it overcomes the power input effects that were caused by the change in the volume, and it offers the possibility to estimate the final particle sizes. The irregularities in the number of polymer particles and the polymerization rate did not affect the Sty-BuA copolymer composition.

9.1.3. Initiator effects on the Sty-BuA copolymer

The effects related to the initiator concentration in the initial charge on the kinetics of the system were expected. The polymerization rate and the number of polymer particles were reduced when the initiator concentration in the system was reduced. The power dependence of the number of polymer particles on the initiator concentration was 0.84, which is greater than the 0.4 value which is given by the Smith-Ewart case 2. However, the copolymer composition and the composition drift were not affected by the initiator concentration and were independent of the effects on the rates of polymerization and the particles evolution. This finding is similar to the results from the surfactant concentration study.

The distributing of the initiator between the initial charge and the subsequent semibatch feed demonstrated a behavior similar to the surfactant distribution effects. Once more, it was found that the power input plays an important role and that lowering the volume of the initial charge led to a reduction in the polymerization rate and the number of polymer particles even at constant initiator concentrations. This was attributed to the decrease in the size of the monomer drops and the increase in their numbers as a result of higher agitation intensities. The copolymer composition and composition drift were independent of these effects.

Therefore, feeding all the initiator in the beginning is the best approach since it prevents any agitation intensity effects on the system that were caused by the change in the volume. Reducing the factors that could affect the system simplifies the process and improves the chances of controlling the system. The composition of the Sty-BuA copolymer was independent of any irregularities caused by the initiator and the power input.

9.2. Future work

Investigating the effects related to the distribution of the monomers, the surfactant, and the initiator in the initial charge and the semibatch feed improved the awareness of their effects on the polymerization rate, particles evolution, and the composition of the copolymer. This understanding made it possible to propose suggestions concerning the best approach to undertake the semibatch emulsion copolymerization of Sty-BuA process in order to minimize the reaction time, the financial cost, and to produce a copolymer with minimum composition drift.

However, it is recommended that the following tasks should be studied in order to expand the knowledge in this area:

- The molecular mass of the polymer is of prime importance since it affects the mechanical and the chemical properties of the polymer. The molecular mass is expected to be affected by the compositions of the initial charge and the subsequent feed, therefore studying the molecular mass should be considered.

- An investigation of the particle size distribution will help to widen the knowledge about the particles evolution in the reactor and might help in explaining the reasons that caused the drift from Smith-Ewart kinetics.

- It was demonstrated that the power input plays an important role and affects the particles evolution. A thorough investigation of the power input is another area that should be considered.

- Investigating the monomers concentrations in the particles by means of the constant partition coefficients model was successfully implemented in this work. The investigation of other mathematical models is another area that might be considered.

Appendices

Appendix A: Physical and chemical properties of the reaction components[1]

Component	Property	Value
Styrene (Monomer)	Chemical formula	C_8H_8
	Molecular mass	104.15
	Boiling point	145°C (760.0 mm Hg)
	Specific gravity	0.91
	Inhibitor	10-15 ppm p-Tert-Butylcatechol
	Solubility in water	0.027 g/100 g of water (20°C)
	k_{pii}[2]	376 l/mol/sec
Butyl acrylate (Monomer)	Chemical formula	$C_7H_{12}O_2$
	Molecular mass	128.17
	Boiling point	145°C (760.0 mm Hg)
	Specific gravity	0.89
	Inhibitor	20 ppm MEHQ
	Solubility in water	0.16 g/100 g of water (25°C)
	k_{pii}[2]	127 l/mol/sec
Potassium Persulfate (Initiator)	Chemical formula	$K_2S_2O_8$
	Molecular mass	270.3118
	Specific gravity	2.4770
	k_I[3]	5.78×10^{-6}
	Efficiency[3]	0.6
Sodium Bicarbonate (Buffer- pH regulator)	Chemical formula	$NaHCO_3$
	Molecular mass	83.995
	Specific gravity	2.16

Physical and chemical properties of the reaction components (Continued)

Component	Property	Value
Sodium Lauryl Sulphate (Emulsifier)	Chemical formula	$C_{12}H_{25}NaO_4S$
	Molecular mass	288.38
	Solubility	15 g/100 g of water (20°C)
Hydroquinone (Inhibitor)	Chemical formula	$C_6H_6O_2$
	Molecular mass	110.11
	Boiling point	285°C (760.0 mm Hg)

(1) Fisher Scientific MSDS data (2) Propagation rate constant; deArbina et al. (1996) (3) Blackley (1975)

Appendix B: Experimental Procedures from the Literature

Reference	Type of process	Ingredients		Notes
Zubitur & Asua (2001)	Semi-batch	Monomers	Sty/BuA(1)	Initial charge: SLS, $K_2S_2O_8$, $NaHCO_3$, and Water. Neat monomers run: • Stream 1: SLS, Water. • Stream 2: Sty, BuA, and CTA (if used). Pre-emulsified monomers run: Stream 1: Sty, BuA, SLS, Water, and CTA (if used)
		Emulsifier	SLS(2)	
		Initiator	$K_2S_2O_8$(3)	
		CTA(4)	$C_{12}H_{25}S$ (5)	
		Buffer	$NaHCO_3$ (6)	
Ozdeger et al. (1998)	Batch	Monomers	Sty/BuA	
		Emulsifier	Triton X-405	
		Initiator	$K_2S_2O_8$	
Yang and Yang (1997)	Batch	Monomers	Sty/BuA	
		Emulsifier	SLS	
		Initiator	$K_2S_2O_8$	

(1) Sty = Styrene, BuA = Butyl acrylate, (2) SLS = Sodium lauryl sulphate, (3) $K_2S_2O_8$ = Potassium persulfate, (4) CTA = Chain transfer agent, (5) $C_{12}H_{25}S$ = Dodecyl mercaptan
(6) $NaHCO_3$ = Sodium bicarbonate

Appendix B (Continued)

Reference	Type of process	Ingredients		Notes
Guillaume et al. (1990)	Batch	Monomers	Sty/BuA	
		Emulsifier	***	
		Initiator	$K_2S_2O_8$	
		Buffer	$NaHCO_3$	
Santos and Coutinho (1992)	Batch	Monomers	Sty/BuA	
		Emulsifier	SLS	
		Initiator	$H_8N_2O_8S_2$(1)	
Chrastova et al. (1998)	Batch	Monomers	Sty/BuA	Ionic emulsifier = Mersol H Non-ionic emulsifier = Slovasol 2430
		Emulsifier	Mersol H, and Slovasol 2430	
		Initiator	$K_2S_2O_8$	
		Activator	$Na_2S_2O_4$(2)	

(1) $H_8N_2O_8S_2$ = Ammonium persulphate, (2) $Na_2S_2O_4$ = Sodium dithionite dehydrate

Appendix B (Continued)

Reference	Type of process	Ingredients		Notes
Cruzrivera et al. (1989)	Semi-batch and Batch	Monomers	Sty/BuA	(Check the procedure at the end of this section)
		Emulsifier	Aerosol MA80 and 22N	
		Initiator	$K_2S_2O_8$	
		Buffer	$NaHCO_3$	
Araujo et al. (2001)	Batch	Monomers	Sty/BuA	
		Emulsifier	SLS	
		Initiator	$H_8N_2O_8S_2$	
Canu et al. II (1994)	Semi-batch and Batch	Monomers	Sty/BuA	
		Emulsifier	SLS	
		Initiator	$K_2S_2O_8$	

(1) $H_8N_2O_8S_2$ = Ammonium persulphate, (2) $Na_2S_2O_4$ = Sodium dithionite dehydrate

Cruzrivera et al. (1989) copolymerization strategies:

Composition-controlled copolymerization (CC):

- Initial charge: BuA + Part of Sty
- Sty was added stepwise based on the analysis of the unreacted monomer to keep the composition constant

Core-shell copolymerization (CS):

- Polystyrene seed was first prepared batchwise
- A buffer and half of the initiator were charged
- Monomer mixture was then added at starved conditions
- After 6 hours, the remaining initiator was added to reach near 100% conversion

Multistage polymerization (ML): similar to CS with two main differences

- Comonomer mixture was richer with Sty
- BuA was introduced in the third step

Azeotropic batch (AB):

- All the ingredients were initially charged, and the monomer mixture composition was calculated according to the polymerization equation

Canu et al. (1994) Copolymer Composition Control Policy in a Semi-batch Reactor:

Canu et al. proposed a procedure to produce a copolymer with a constant instantaneous composition. This procedure has been tested on binary and ternary copolymers and in all the cases the produced copolymer was at the desired composition (Canu et al. I & II, 1994). Here is a summary of the procedure for a binary system:

1. Identifying the critical monomer:

The *critical monomer* is entirely charged at the beginning, and it is identified as the one *exhibiting the minimum value of the parameter* A_i

$$A_i = \frac{Y_i \rho_c}{C_i \rho_i} \qquad \text{B.1}$$

where i stands for monomer i, Y_i is the copolymer weight composition, ρ_c is the copolymer density, C_i is the polymer-free volume fraction of monomer i in the polymer particles, and ρ_i is polymer i density. Y_i is determined by

$$Y_i = \frac{y_i MW_i}{\sum_j y_j MW_j} \qquad \text{B.2}$$

where y_i is the mole fraction of monomer i in the polymer, MW_i is the molecular weight of monomer i. And C_i is determined according to

$$\frac{y_1}{y_2} = \frac{\left(\frac{k_{p11} k_{p21} C_1 \tilde{\rho}_1}{k_{p21} C_1 \tilde{\rho}_1 + k_{p12} C_2 \tilde{\rho}_2} + \frac{k_{p21} k_{p12} C_2 \tilde{\rho}_2}{k_{p21} C_1 \tilde{\rho}_1 + k_{p12} C_2 \tilde{\rho}_2} \right) C_1 \tilde{\rho}_1}{\left(\frac{k_{p12} k_{p21} C_1 \tilde{\rho}_1}{k_{p21} C_1 \tilde{\rho}_1 + k_{p12} C_2 \tilde{\rho}_2} + \frac{k_{p22} k_{p12} C_2 \tilde{\rho}_2}{k_{p21} C_1 \tilde{\rho}_1 + k_{p12} C_2 \tilde{\rho}_2} \right) C_2 \tilde{\rho}_2} = \text{constant} \qquad \text{B.3}$$

where k_{pij} is the propagation rate constant of radical i with monomer j, and $\tilde{\rho}$ is the molar density. Considering $C_1+C_2=1$ reduces A.3.3 to a quadratic equation for C_1 or C_2, which can be solved easily.

2. Identifying the transition interval from flooded to starved conditions:

This is achieved by solving the following equation

$$M_C^* = \frac{M_c^f A_j - B_j \phi^*}{A_j + \frac{\phi^*}{1-\phi^*}} \qquad \text{B.4}$$

where the index j refers to the critical monomer, ϕ^* is the overall volume fraction of monomer species in polymer particles at saturation, M_c^f is the final amount of polymer produced , and B_j is a parameter related to the monomer water solubility determined according to

$$B_j = \frac{M_j^{w,*} \phi_c}{\phi^* \rho_j} \qquad \text{B.5}$$

where $M_j^{w,*}$ is the monomer concentration in the aqueous phase at saturation, ϕ_c is the monomer swelling ratio as a function of the amount of polymer produced (M_c) and it is obtained by solving

$$\phi = \frac{\left(A_j\left(M_c^f - M_c\right) + M_c + B_j\right) - \sqrt{\left(\left(A_j\left(M_c^f - M_c\right) + M_c + B_j\right) + 4B_j M_c\right)}}{2B_j} \qquad \text{B.6}$$

M_C^* values could be negative i.e. the critical monomer (j) is largely soluble in the aqueous phase (i.e. B_j is large). This means the reaction does not exhibit flooded interval, and it operates in the starved interval from the beginning.

3. Calculate the monomer feed flow rates:

Finally the flow rates for the flooded and starved intervals are determined according to the following two equations

Flooded Interval:

$$\hat{Q}_i\left(M_c\right) = \hat{Q}_i^f = \frac{Y_i}{A_i}\left(A_i - A_j\right) = \text{constant} \qquad \text{B.7}$$

Starved Interval:

$$\hat{Q}_i\left(M_c\right)=\hat{Q}_i^s=\frac{Y_i}{A_i}\left(B_i-M_c/(1-\phi)^2\right)\left(\frac{A_i+(\phi/(1-\phi))}{B_i+M_c/(1-\phi)^2}-\frac{A_j+(\phi/(1-\phi))}{B_j+M_c/(1-\phi)^2}\right)$$

B.8

Finally, it should be noted that the different numerical values used in the previous equations are obtained from different literature sources (e.g. $M_j^{w,*}$, k_{pij}, ρ_i, *and* ϕ_i^*). The data for the examined systems (e.g. styrene-butyl acrylate, methyl methacrylate-vinyl acetatae, and methyl methacrylate-vinyl acetate-butyl acrylate) are tabulated in the original reference (Canu et al. I & II, 1994).

Appendix C: MATLAB® Implementation of the Constant Partition Coefficients Model

```
function [result] =
monomer_conc(excel_file,sheet_number,number_of_samples,...
read_range,write_range)

% ****************************************************************
% * Definition: This MATLAB function will determine the monomers
% * concentration in the polymer particles according to the
% * constant partition coefficients model.
% *
% * Author      : M.A-Tamimi
% * Date        : June 15, 07 (1st version)
% ****************************************************************

% If the execution did not finish 0 will be returned, otherwise 1
% will be returned (check the last line)

result=0; %#ok<NASGU>

% *** Constants ***

% BuA, Sty, Pol, and Water densities

bua_density=0.894; sty_density=0.909; pol_density=1.1;
water_density=1;

% Mw of the monomers

Mw_bua=128.17; Mw_sty=104.15;

% Partition coefficient of monomer i between the drops and the
% aqueous phase

k_sty_d=2714; k_bua_d=724;

% Partition coefficient of monomer i between the particles and
% the aqueous phase

k_sty_p=1629; k_bua_p=471;
```

```
% *** Reading the required data from excel file  ***

% Preparing the range in which the data will be read from
% the excel file. readf: first cell, readl: last cell

readf=read_range; readl=read_range+number_of_samples-1;

% Converting the range to string variable (total 109 columns)

read_r=strcat('A',num2str(readf),':','DE',num2str(readl));

% Reading all the data in to 1 big matrix, and then the
% different columns will be assigned to different vectors

excel_data=xlsread(excel_file, sheet_number,read_r);

% Get the time (min) (i.e. 2nd column)

time=excel_data(:,2);

% Time difference between 2 samples (min) (i.e. 3rd column)
% time_difference=excel_data(:,3);

% Total mass of the unconverted monomers in the reactor (gm)
% (columns 58 and 60)

bua_reactor_gm=excel_data(:,58);
sty_reactor_gm=excel_data(:,60);

% Volume of the unconverted monomers in the reactor (cc)

v_bua_cc=bua_reactor_gm./bua_density;
v_sty_cc=sty_reactor_gm./sty_density;

% Molar volume of monomers (cc/mol)

v_bua_mol=v_bua_cc./(bua_reactor_gm./Mw_bua);
v_sty_mol=v_sty_cc./(sty_reactor_gm./Mw_sty);

% Total moles of converted monomer

bua_converted_mol=excel_data(:,54);
sty_converted_mol=excel_data(:,57);
```

```
% Polymerization rate for each monomer (mol/sec)

bua_pol_rate_mol_sec=bua_converted_mol./(time.*60);
sty_pol_rate_mol_sec=sty_converted_mol./(time.*60);

% Mass of polymer in the reactor (i.e. Mass of monomers
% converted, gm)

pol_reactor_gm=excel_data(:,51);

% Volume of polymer (cc)

v_pol_cc=pol_reactor_gm./pol_density;

% Mass of water in the reactor (gm)

water_reactor_gm=excel_data(:,16);

% Volume of water in the reactor (cc)

v_w_cc=water_reactor_gm./water_density;

% Particle sizes (z-zeverage, nm)

Z_ave_nm=excel_data(:,40);

% Particles concentration in the reactor (#/cc of water)

Np_per_cc=excel_data(:,64);

% Total number of polymer particles

Total_Np=Np_per_cc.*v_w_cc;

% Guess the volume of the particles (1st guess: assuming that each
% particle takes the shape of a sphere, and taking the z-average
% as the diameter find out the volume of each particle, and then
% multiply that by the total number of the particles

v_p_cc=4/3*pi.*(Z_ave_nm.*1e-7/2).^3.*Total_Np;

% Guess the volume of the aqueous phase (1st guess: it equals
% volume of the water)
```

```
v_aq_cc=v_w_cc;

% Guess the volume of the monomer drops (1st guess:
% Monomer mass in the reactor/sty density)

v_d_cc=(sty_reactor_gm+bua_reactor_gm)./sty_density;

% Initializing the vectors which will hold the volume of the
% monomers in the different phases (cc)

v_bua_p=zeros(size(v_aq_cc)); v_bua_d=zeros(size(v_aq_cc));
v_bua_aq=zeros(size(v_aq_cc));

v_sty_p=zeros(size(v_aq_cc)); v_sty_d=zeros(size(v_aq_cc));
v_sty_aq=zeros(size(v_aq_cc));

% This loop will read the data for each sample

    for ii=1:length(v_d_cc)

        % starting the trial and error procedure (2000 iterations
        % is the max)

        for rr=1:2000

          % Volume of monomers in the particles (cc)

          v_bua_p(ii)=v_bua_cc(ii)/(1+v_aq_cc(ii)/v_p_cc(ii)/...
          k_bua_p+v_d_cc(ii)*k_bua_d/v_p_cc(ii)/k_bua_p);

          v_sty_p(ii)=v_sty_cc(ii)/(1+v_aq_cc(ii)/v_p_cc(ii)/...
          k_sty_p+v_d_cc(ii)*k_sty_d/v_p_cc(ii)/k_sty_p);

          % Volume of the monomers in the aqueous phase (cc)

          v_bua_aq(ii)=v_bua_p(ii)*v_aq_cc(ii)/k_bua_p/v_p_cc(ii);
          v_sty_aq(ii)=v_sty_p(ii)*v_aq_cc(ii)/k_sty_p/v_p_cc(ii);

          % Volume of the monomers in the drops (cc)

          v_bua_d(ii)=k_bua_d*v_bua_aq(ii)*v_d_cc(ii)/v_aq_cc(ii);
          v_sty_d(ii)=k_sty_d*v_sty_aq(ii)*v_d_cc(ii)/v_aq_cc(ii);
```

```
        % Calculate new Vd, Vp, and Vaq and compare them to the
        % old values

        v_d_new=v_sty_d(ii)+v_bua_d(ii);
        v_p_new=v_pol_cc(ii)+v_sty_p(ii)+v_bua_p(ii);
        v_aq_new=v_w_cc(ii)+v_sty_aq(ii)+v_bua_aq(ii);

      chk1=abs(v_d_new-v_d_cc(ii)); chk2=abs(v_p_new-v_p_cc(ii));
      chk3=abs(v_aq_new-v_aq_cc(ii));

      % In case the difference between the old values and the new
      % ones is lower the 1e-4 break the loop. Otherwise, use the
      % new values and recalculate

          if ((chk1<1e-6) && (chk2<1e-6) && (chk3<1e-6))
              break;

          else
              v_d_cc(ii)=v_d_new;
              v_p_cc(ii)=v_p_new;
              v_aq_cc(ii)=v_aq_new;

          end % if statement

      end % iterations loop

      % This will produce a warning in case the data did not
      % converge

      if (rr==2000)
         sprintf('Warning! The data did not converge.\nSample...
         number%i, err1:%f    err2:%f err3:%f',ii,chk1,chk2,chk3)

      end %if statement

      % sprintf('Sample #: %i\tNo. of trials = %i',ii,rr)
      % sprintf('%i %f %f %f %f %f %f',ii, v_bua_p(ii),...
      % v_bua_aq(ii), v_bua_d(ii), v_sty_p(ii),...
      % v_sty_aq(ii), v_sty_d(ii))

    end % Samples loop

% Concentration of monomers in different phases (mol/cc)
```

```
bua_conc_p=v_bua_p./(v_p_cc.*v_bua_mol);
bua_conc_aq=v_bua_aq./(v_aq_cc.*v_bua_mol);
bua_conc_d=v_bua_d./(v_d_cc.*v_bua_mol);

sty_conc_p=v_sty_p./(v_p_cc.*v_sty_mol);
sty_conc_aq=v_sty_aq./(v_aq_cc.*v_sty_mol);
sty_conc_d=v_sty_d./(v_d_cc.*v_sty_mol);


% Writing the final results to the excel file

sample_number=1:number_of_samples;

volume_bua_in_system=v_bua_p+v_bua_aq+v_bua_d;
mass_of_bua_in_system=volume_bua_in_system.*bua_density;

% The difference between the calculated mass and the given mass

bua_error=mass_of_bua_in_system-bua_reactor_gm;

volume_sty_in_system=v_sty_p+v_sty_aq+v_sty_d;
mass_of_sty_in_system=volume_sty_in_system.*sty_density;
sty_error=mass_of_sty_in_system-sty_reactor_gm;

% Preparing the output. All the results will be merged in to
% 1 big matrix.

final_result=[sample_number', time, bua_conc_p, sty_conc_p,...
bua_conc_d,sty_conc_d, bua_conc_aq, sty_conc_aq, v_p_cc,...
v_d_cc, v_aq_cc, v_bua_p,v_sty_p, v_bua_d, v_sty_d,...
v_bua_aq,v_sty_aq,volume_bua_in_system,...
mass_of_bua_in_system,bua_error, volume_sty_in_system,...
mass_of_sty_in_system,sty_error, bua_pol_rate_mol_sec,...
sty_pol_rate_mol_sec];

% Writing the results.

write_r=strcat('A',num2str(write_range));

xlswrite(excel_file,final_result,sheet_number, write_r);
```

```
% return 1 to MATLAB to idicate that the code was executed
% successfully

result=1;

% ************************ END ****************************
```

Appendix D: Reproducibility and Error Propagation

There are many variables that could affect the reproducibility in a semibatch process. For instance, inefficient deoxygenating the reactor and contaminating the reactor through sampling both could affect the accuracy and the reproducibility. These effects could be avoided by following a strict experimental procedure. In addition, Errors in solid content analysis (e.g. sampling, weighing, and drying) could affect the reproducibility and could be avoided by careful treatment. Next, a discussion of the reproducibility and error propagation of two identical runs (Table D.1) will be presented.

Component	Initial Charge (g)	Stream 1 (g)	Stream 2 (g)	Stream 3 (g)
Styrene			164.85	
Butyl acrylate				135.15
Sodium Lauryl Sulfate	6.0			
Potassium Persulfate	0.5			
Sodium Bicarbonate	0.5			
Deionised Water	600.0			
Flow Rate (g/min)			0.92	0.75

Table D.1 Test experiments recipe and feeding strategy

D.1 Conversion

The instantaneous conversion was determined by means of the gravimetric method. This method relies on continuously weighing the samples during and after the experiment. An attempt was made to determine the uncertainty in the measurements by conducting repeated measurements of a known quantity. The uncertainty in the determination of the weight was found to be ±0.0003 g. The instantaneous conversion is calculated as follows:

$$x = \frac{W_d - W_c - W_s}{W_m} \qquad \text{D.1}$$

where W_d is the weight of the dry sample, W_c is the weight of the holding container, W_s is the weight of the solids, and W_m is the weight of the monomers. The

uncertainties δW_d, δW_c and δW_s were all taken = 3×10^{-4}. W_m is estimated from the monomer feed rate and δW_m will be assumed = 0.

The uncertainty in a function $f(x_1,\ldots,x_n)$ caused by the uncertainties in $x_1,\ldots,x_n$ (i.e. $\delta x_1,\ldots,\delta x_n$) can be determined as follows

$$\delta f = \sqrt{\left(\frac{\partial f}{\partial x_1}\delta x_1\right)^2 + \ldots + \left(\frac{\partial f}{\partial x_n}\delta x_n\right)^2} \qquad \text{D.2}$$

Applying Eq. D.2 on D.1 and differentiating yields the uncertainty in x

$$\delta x = \frac{3\times10^{-4}\sqrt{3}}{W_m} \qquad \text{D.3}$$

Tables D.2 and D.3 illustrate δx for both test runs. The error propagation due to the gravimetric method starts at ~0.5% and decreases down to ~0.1% at the end of the experiments.

Sample	W_c, g	W_d, g	W_s, g	W_m, g	x, %	δx, %
1	1.0233	1.3810	0.3135	0.0976	45.30	0.53
2	1.1141	1.5016	0.2973	0.1429	63.12	0.36
3	1.0150	1.5213	0.3255	0.2609	69.27	0.20
4	1.0033	1.5761	0.3150	0.3229	79.81	0.16
5	1.0531	1.5485	0.2333	0.3361	77.99	0.15
6	1.0530	1.8034	0.3232	0.5446	78.45	0.10
7	1.0162	1.6940	0.3442	0.4029	82.79	0.13
8	1.1628	1.9989	0.2816	0.6635	83.57	0.08
9	1.0341	1.6423	0.2604	0.3975	87.49	0.13
10	0.9931	1.8593	0.3032	0.6474	86.97	0.08
11	1.2008	2.1538	0.2692	0.7776	87.93	0.07
12	1.0238	2.0596	0.2996	0.8360	88.06	0.06
13	1.1517	2.2188	0.2620	0.8530	94.38	0.06
14	1.1816	2.2010	0.2655	0.7932	95.05	0.07
15	1.0218	2.1814	0.3186	0.8911	94.37	0.06
16	1.0122	2.3239	0.3015	1.0349	97.61	0.05

Table D.2 The propagation error in the instantaneous conversion of experiment 1

Sample	W_c, g	W_d, g	W_s, g	W_m, g	x, %	δx, %
1	1.0174	1.3719	0.2985	0.1137	49.24	0.46
2	1.1151	1.4582	0.2660	0.1185	65.09	0.44
3	1.1428	1.6610	0.3165	0.2758	73.13	0.19
4	1.1783	1.8031	0.2654	0.4632	77.60	0.11
5	1.0834	1.7420	0.2660	0.5017	78.24	0.10
6	1.0450	1.7947	0.2574	0.5953	82.69	0.09
7	1.1769	2.1191	0.2903	0.7969	81.80	0.07
8	1.1256	1.9804	0.2889	0.6643	85.18	0.08
9	1.2087	2.0298	0.2857	0.6086	87.97	0.09
10	1.0848	2.2752	0.2988	1.0684	83.45	0.05
11	1.0467	1.8413	0.2789	0.5729	90.01	0.09
12	1.1186	2.3714	0.3231	1.0456	88.92	0.05
13	1.1624	2.2433	0.3027	0.8229	94.56	0.06
14	1.1634	2.5895	0.2939	1.2001	94.34	0.04
15	1.0073	2.1140	0.2948	0.8488	95.65	0.06
16	1.0015	2.1458	0.3005	0.8950	94.28	0.06

Table D.3 The propagation error in the instantaneous conversion of experiment 2

Figure D.1 illustrates the reproducibility analysis of the conversion. A good agreement is observed for both runs and it is expected that the same agreement was obtained for all the runs in this work.

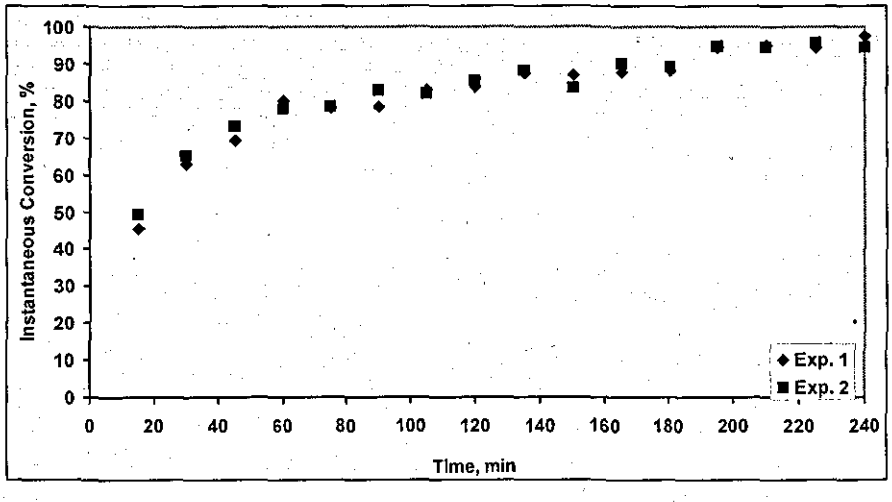

Figure D.1 The instantaneous conversion reproducibility

D.2 Particle Sizes and Number of Polymer Particles

The latex particles size was measured by Malvern® Zetasizer 3000. The average difference between consecutive runs on one sample was found to be ±4%. The number of polymer particles is determined according to the following equation

$$N_p = \frac{6M_T x}{\rho_p \pi d_p^3} \qquad \text{D.4}$$

where M_T is the initial total monomer concentration (g/cm^3 of water), ρ_p is the polymer density (g/cm^3), d_p is the average particle diameter (cm), and x is the total weight conversion. The average uncertainty for d_p is 4%, and ρ_p was taken = 1.1 g/cm^3. Ignoring δM_T and considering δx and δd_p, and applying D.2 on D.4 yields δN_p which takes the following form

$$\delta N_p = \frac{6M_T\sqrt{\delta x^2 \times d_p^{\,2} + 9x^2 \times \delta d_p^{\,2}}}{\pi d_p^{\,4} \rho_p} \qquad \text{D.5}$$

Sample	d_p, nm	δd_p	$d_p+\delta d_p$	$d_p-\delta d_p$	N_p, #/cm^3	δN_p	$N_p+\delta N_p$	$N_p-\delta N_p$
1	29.60	1.18	30.78	28.42	1.27E+15	1.53E+14	1.42E+15	1.11E+15
2	40.70	1.63	42.33	39.07	1.36E+15	1.63E+14	1.52E+15	1.20E+15
3	42.80	1.71	44.51	41.09	1.93E+15	2.31E+14	2.16E+15	1.70E+15
4	46.00	1.84	47.84	44.16	2.39E+15	2.87E+14	2.68E+15	2.10E+15
5	47.00	1.88	48.88	45.12	2.74E+15	3.29E+14	3.07E+15	2.41E+15
6	48.30	1.93	50.23	46.37	3.05E+15	3.66E+14	3.42E+15	2.69E+15
7	51.00	2.04	53.04	48.96	3.20E+15	3.84E+14	3.58E+15	2.81E+15
8	53.00	2.12	55.12	50.88	3.29E+15	3.95E+14	3.69E+15	2.90E+15
9	53.50	2.14	55.64	51.36	3.77E+15	4.53E+14	4.23E+15	3.32E+15
10	55.00	2.20	57.20	52.80	3.84E+15	4.61E+14	4.30E+15	3.38E+15
11	54.80	2.19	56.99	52.61	4.33E+15	5.19E+14	4.85E+15	3.81E+15
12	56.00	2.24	58.24	53.76	4.44E+15	5.32E+14	4.97E+15	3.90E+15
13	56.10	2.24	58.34	53.86	4.73E+15	5.67E+14	5.30E+15	4.16E+15
14	55.80	2.23	58.03	53.57	4.84E+15	5.81E+14	5.42E+15	4.26E+15
15	56.30	2.25	58.55	54.05	4.68E+15	5.61E+14	5.24E+15	4.12E+15
16	56.00	2.24	58.24	53.76	4.92E+15	5.90E+14	5.51E+15	4.33E+15

Table D.4 The propagation error in the number of polymer particles and particle sizes of experiment 1

Sample	d_p, nm	δd_p	$d_p+\delta d_p$	$d_p-\delta d_p$	N_p, #/cm³	δN_p	$N_p+\delta N_p$	$N_p-\delta N_p$
1	30.00	1.20	31.20	28.80	1.32E+15	1.59E+14	1.48E+15	1.16E+15
2	38.50	1.54	40.04	36.96	1.66E+15	1.99E+14	1.86E+15	1.46E+15
3	41.00	1.64	42.64	39.36	2.32E+15	2.78E+14	2.59E+15	2.04E+15
4	44.70	1.79	46.49	42.91	2.53E+15	3.04E+14	2.84E+15	2.23E+15
5	46.50	1.86	48.36	44.64	2.84E+15	3.41E+14	3.18E+15	2.50E+15
6	48.00	1.92	49.92	46.08	3.28E+15	3.94E+14	3.67E+15	2.89E+15
7	51.50	2.06	53.56	49.44	3.07E+15	3.69E+14	3.44E+15	2.70E+15
8	52.80	2.11	54.91	50.69	3.40E+15	4.08E+14	3.81E+15	2.99E+15
9	54.00	2.16	56.16	51.84	3.70E+15	4.44E+14	4.14E+15	3.26E+15
10	54.60	2.18	56.78	52.42	3.78E+15	4.54E+14	4.23E+15	3.33E+15
11	54.80	2.19	56.99	52.61	4.44E+15	5.33E+14	4.98E+15	3.91E+15
12	55.00	2.20	57.20	52.80	4.75E+15	5.69E+14	5.31E+15	4.18E+15
13	55.70	2.23	57.93	53.47	4.86E+15	5.83E+14	5.44E+15	4.28E+15
14	54.60	2.18	56.78	52.42	5.15E+15	6.18E+14	5.76E+15	4.53E+15
15	56.30	2.25	58.55	54.05	4.76E+15	5.71E+14	5.33E+15	4.19E+15
16	55.00	2.20	57.20	52.80	5.03E+15	6.04E+14	5.64E+15	4.43E+15

Table D.5 The propagation error in the number of polymer particles and particle sizes of experiment 2

Tables D.4 and D.5, and figures D.2 and D.3 demonstrate the error propagation in the number of polymer particles and the particle sizes of experiments 1 and 2. It is noticeable that δN_p increases with time although it was demonstrated earlier that δx decreases. This increase is a result of the increase in the average particle sizes (d_p) which leads to bigger values of δd_p, this indicates that δx effect on δN_p was minimal.

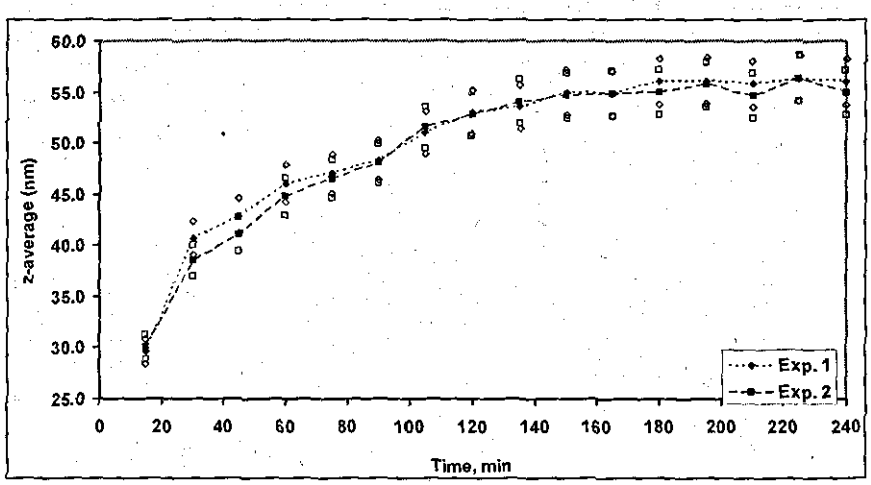

Figure D.2 The particle sizes reproducibility

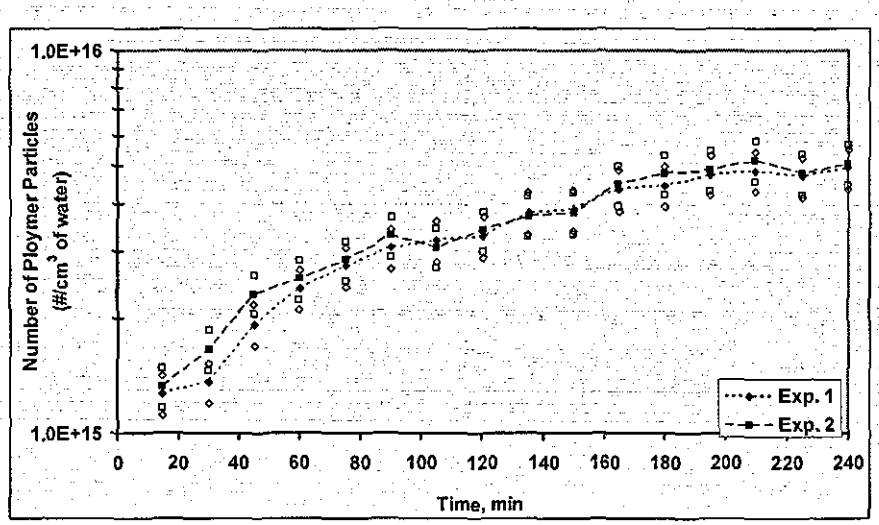

Figure D.3 The number of polymer particles reproducibility

D.3 Composition

The composition of the copolymer was determined by means of curve fitting (§6.2). The IR data were fit using MATLAB® curve fitting tool (i.e. cftool). The goodness of fit as reported by MATLAB® was as follows: The sum of squared errors (SSE) = 1.175×10^{-7}, the coefficient of determination R^2 = 1.0, and the root squared mean errors (RMSE) = 0.00003427.

r	*Lower f(r)*	*f(r)*	*Upper f(r)*
0.244711	0.093937	0.099895	0.105853
2.22838	0.517659	0.523232	0.528806
4.21205	0.662117	0.668528	0.67494
6.19572	0.73858	0.744442	0.750303
8.17939	0.78572	0.792036	0.798352
10.1631	0.816852	0.824907	0.832962
12.1467	0.839237	0.84886	0.858484
14.1304	0.856646	0.866791	0.876936
16.1141	0.871003	0.880304	0.889606
18.0977	0.883053	0.890363	0.897672

Table D.6 95% confidence bounds

The 95% confidence bounds are given in table D.6, where r = is the IR peak ratio —i.e. PBA carbonyl stretching (C=O) absorbance divided by the absorbance of the PS benzene ring bending (C=C-H)— and $f(r)$ is the composition as determined by the fit (§6.2).

References

References

ARAUJO, O., GIUDICI, R., SALDIVAR, E. and RAY, W.H., 2001. Modeling and experimental studies of emulsion copolymerization systems. I. Experimental results. *Journal of Applied Polymer Science,* **79**(13), pp. 2360-2379.

BILLMEYER, F.W., 1984. Textbook of polymer science. 3rd edn. New York ; Chichester: Wiley.

BLACKLEY, D.C., 1975. Emulsion polymerisation : theory and practice. London: Applied Science Publishers.

BRANDRUP, J., IMMERGUT, E.H. and GRULKE, E.A., 1999. Polymer handbook. 4th edn. New York ; Chichester: Wiley.

BROOKS, B.W., 1970. *British Polymer Journal,* **2**, pp. 197.

BROOKS, B.W. and MAKANJUOLA, B.O., 1981. The Rate of Persulfate Decomposition in the Presence of Polymer Lattices. *Makromolekulare Chemie-Rapid Communications,* **2**(1), pp. 69-73.

CANEGALLO, S., CANU, P., MORBIDELLI, M. and STORTI, G., 1994. Composition Control in Emulsion Copolymerization .2. Application to Binary and Ternary-Systems. *Journal of Applied Polymer Science,* **54**(12), pp. 1919-1935.

CANU, P., CANEGALLO, S., MORBIDELLI, M. and STORTI, G., 1994. Composition Control in Emulsion Copolymerization .1. Optimal Monomer Feed Policies. *Journal of Applied Polymer Science,* **54**(12), pp. 1899-1917.

CARRAHER, C.E. and SEYMOUR, R.B., 2000. SeymourCarraher's polymer chemistry. 5th , rev. and expand edn. New York: Marcel Dekker.

CHATZI, E.G., KAMMONA, O., KENTEPOZIDOU, A. and KIPARISSIDES, C., 1997. Infrared spectra and compositional analysis of styrene. *Macromolecular Chemistry and Physics,* **198**(8), pp. 2409-2420.

CHIU, W.Y., LAI, S.M., CHEN, L.W. and CHEN, C.C., 1991. Particle-Size Distribution and Molecular-Size Distribution of Polymers in Soap-Free Emulsion Polymerization of Styrene. *Journal of Applied Polymer Science,* **42**(10), pp. 2787-2793.

CHRASTOVA, V., DURACKOVA, S., MRENICA, J. and CERNAKOVA, L., 1999. Emulsifier and initiator effects on the emulsion copolymerization of styrene with butyl acrylate. *Chemical Papers-Chemicke Zvesti,* **53**(2), pp. 140-144.

COOTE, M.L. and DAVIS, T.P., 1999. The mechanism of the propagation step in free-radical copolymerisation. *Progress in Polymer Science,* **24**(9), pp. 1217-1251.

CORRIN, M.L. and HARKINS, W.D., 1947. The Effect of Salts on the Critical Concentration for the Formation of Micelles in Colloidal Electrolytes. *Journal of the American Chemical Society,* **69**(3), pp. 683-688.

CRUZRIVERA, A., RIOSGUERRERO, L., MONNET, C., SCHLUND, B., GUILLOT, J. and PICHOT, C., 1989. Structure Property Relationships in Styrene Butyl Acrylate Emulsion Copolymers .1. Preparation and Characterization of Latexes. *Polymer,* **30**(10), pp. 1872-1882.

DEARBINA, L.L., BARANDIARAN, M.J., GUGLIOTTA, L.M. and ASUA, J.M., 1997. Kinetics of the emulsion copolymerization of styrene and butyl acrylate. *Polymer,* **38**(1), pp. 143-148.

DUBE, M.A., PENLIDIS, A. and ODRISCOLL, K.F., 1990. A Kinetic Investigation of Styrene Butyl Acrylate Copolymerization. *Canadian Journal of Chemical Engineering,* **68**(6), pp. 974-987.

DUNN, A.S. and TAYLOR, P.A., 1965. Polymerization of Vinyl Acetate in Aqueous Solution Initiated by Potassium Persulphate at 60 Degrees C. *Makromolekulare Chemie,* **83**(APR), pp. 207-&.

EBEWELE, R.O., 2000. Polymer science and technology. Boca Raton ; London: Crc.

FERNANDEZ-GARCIA, M., FERNANDEZ-SANZ, M., MADRUGA, E.L., CUERVO-RODRIGUEZ, R., HERNANDEZ-GORDO, V. and FERNANDEZ-MONREAL, M.C., 2000. Solvent effects on the free-radical copolymerization of styrene with butyl acrylate. I. Monomer reactivity ratios. *Journal of Polymer Science Part A-Polymer Chemistry,* **38**(1), pp. 60-67.

FERNANDEZ-GARCIA, M., FERNANDEZ-SANZ, M., MADRUGA, E.L. and FERNANDEZ-MONREAL, C., 1999. A kinetic study of free radical copolymerization of styrene butyl acrylate. *Macromolecular Chemistry and Physics,* **200**(1), pp. 199-205.

FITCH, R.M., 1983. in Science and technology of polymer colloids. Boston; Hingham, MA: Nijhoff; Distributors for the U.S. and Canada, Kluwer Boston.

FLORY, P.J., 1953. Principles of polymer chemistry. Cornell U.P.

FUKUDA, T., MA, Y.D. and INAGAKI, H., 1985. Free-Radical Copolymerization .3. Determination of Rate Constants of Propagation and Termination for the Styrene Methyl-Methacrylate System - a Critical Test of Terminal-Model Kinetics. *Macromolecules,* **18**(1), pp. 17-26.

GILBERT, R.G., 1995. Emulsion polymerization : a mechanistic approach. London: Academic Press.

GUGLIOTTA, L.M., ARZAMENDI, G. and ASUA, J.M., 1995. Choice of Monomer Partition Model in Mathematical-Modeling of Emulsion Copolymerization Systems. *Journal of Applied Polymer Science,* **55**(7), pp. 1017-1039.

GUILLAUME, J.L., PICHOT, C. and GUILLOT, J., 1990. Emulsifier-Free Emulsion Copolymerization of Styrene and Butyl Acrylate .1. Kinetic-Studies in the Absence of Surfactant. *Journal of Polymer Science Part A-Polymer Chemistry,* **28**(1), pp. 119-136.

HUA, H., RIVARD, T. and DUBE, M.A., 2004. Off-line monitoring of styrene/butyl acrylate copolymerizations in toluene using ATR-FTIR spectroscopy. *Polymer,* **45**(2), pp. 345-354.

JASSO-GASTINEL, C.F., LOPEZ-URETA, L.C., GONZALEZ-ORTIZ, L.J., REYES-GONZALEZ, I., LOPEZ-DELLAMARY, F.A. and MANERO-BRITO, O., 2007. Synthesis and characterization of styrene-butyl acrylate polymers, varying feed composition in a semicontinuous emulsion process. *Journal of Applied Polymer Science,* **103**(6), pp. 3964-3971.

KAMATH, V.R., 1973. Emulsion polymerization of styrene: kinetics.

KOLTHOFF, I.M. and MILLER, I.K., 1951. The Chemistry of Persulfate .1. the Kinetics and Mechanism of the Decomposition of the Persulfate Ion in Aqueous Medium. *Journal of the American Chemical Society,* **73**(7), pp. 3055-3059.

LEIZA, J.R., SUDOI, E.D. and ELAASSER, M.S., 1997. Preparation of high solids content poly(n-butyl acrylate) latexes through miniemulsion polymerization. *Journal of Applied Polymer Science,* **64**(9), pp. 1797-1809.

LOVELL, P.A. and EL-AASSER, M.S., 1997. Emulsion polymerization and emulsion polymers. Chichester: J. Wiley.

MA, Y.D., SUNG, K.S., TSUJII, Y. and FUKUDA, T., 2001. Free-radical copolymerization of styrene and diethyl fumarate. Penultimate-unit effects on both propagation and termination processes. *Macromolecules,* **34**(14), pp. 4749-4756.

MORI, S., 1989. Compositional Analysis and Infrared-Spectra of Styrene Methyl-Methacrylate Random Copolymers. *Journal of Applied Polymer Science,* **38**(3), pp. 547-555.

MORTON, M., KAIZERMAN, S. and ALTIER, M.W., 1954. Swelling of Latex Particles. *Journal of colloid science,* **9**(4), pp. 300-312.

NAGATA, S., 1975. Mixing : principles and applications. Tokyo ; New York ; London etc.: Kodansha ;.

NOMURA, M., HARADA, M., EGUCHI, W. and NAGATA, S., 1976. Kinetics and Mechanism of Emulsion Polymerization of Vinyl-Acetate. *ACS Symposium Series,* (24), pp. 102-121.

NOMURA, M., NAGATA, S., EGUCHI, W. and HARADA, M., 1972. Effect of Stirring on Emulsion Polymerization of Styrene. *Journal of Applied Polymer Science,* **16**(4), pp. 835-&.

ODIAN, G., 2004. Principles of polymerization. 4th edn. New York ; Chichester: Wiley.

OZDEGER, E., SUDOL, E.D., EL-AASSER, M.S. and KLEIN, A., 1998. Role of mixing in copolymerizations of styrene and n-butyl acrylate. *Journal of Applied Polymer Science,* **69**(11), pp. 2277-2289.

PEREZ-CARRILLO, L.A., PUCA, M., RABELERO, M., MEZA, K.E., PUIG, J.E., MENDIZABAL, E., LOPEZ-SERRANO, F. and LOPEZ, R.G., 2007. Effect of particle size on the mechanical properties of polystyrene and poly(butyl acrylate) core/shell polymers. *Polymer,* **48**(5), pp. 1212-1218.

PIIRMA, I. and CHEN, S.R., 1980. Adsorption of Ionic Surfactants on Latex-Particles. *Journal of colloid and interface science,* **74**(1), pp. 90-102.

PLESSIS, C., ARZAMENDI, G., LEIZA, J.R., SCHOONBROOD, H.A.S., CHARMOT, D. and ASUA, J.M., 2001. Kinetics and polymer microstructure of the seeded semibatch emulsion copolymerization of n-butyl acrylate and styrene. *Macromolecules,* **34**(15), pp. 5147-5157.

RIVERA, M.R., RODRIGUEZ-HERNANDEZ, A.A., HERNANDEZ, N., CASTILLO, P., SALDIVAR, E. and RIOS, L., 2005. Controlled/living free radical copolymerization of styrene and butyl acrylate in bulk and emulsion with industrial monomers. Influence of monomer addition on polymer properties. *Industrial & Engineering Chemistry Research,* **44**(8), pp. 2792-2801.

ROMERO, I.G. and PASCH, H., 2005. High-throughput screening of the chemical composition distribution of random styrene-butyl acrylate copolymers. *E-Polymers,* , pp. 042.

SAJJADI, S. and BROOKS, B.W., 1999. Semibatch emulsion polymerization of butyl acrylate. I. Effect of monomer distribution. *Journal of Applied Polymer Science,* **74**(13), pp. 3094-3110.

SALDIVAR, E., ARAUJO, O., GIUDICI, R. and LOPEZ-BARRON, C., 2001. Modeling and experimental studies of emulsion copolymerization systems. II. Styrenics. *Journal of Applied Polymer Science,* **79**(13), pp. 2380-2397.

SANTOS, A.M. and COUTINHO, F.M.B., 1992. Study on Emulsion Copolymerization of Styrene and Normal-Butyl Acrylate. *Polymer Bulletin,* **29**(3-4), pp. 309-315.

SMITH, W.V. and EWART, R.H., 1948. Kinetics of Emulsion Polymerization. *Journal of Chemical Physics,* **16**(6), pp. 592-599.

STIGTER, D. and MYSELS, K.J., 1955. Tracer Electrophoresis .2. the Mobility of the Micelle of Sodium Lauryl Sulfate and its Interpretation in Terms of Zeta Potential and Charge. *Journal of Physical Chemistry,* **59**(1), pp. 45-51.

STUART, B., 2004. Infrared spectroscopy : fundamentals and applications. Chichester: Wiley.

SUN, X.Y., LUO, Y.W., WANG, R., LI, B.G., LIU, B. and ZHU, S.P., 2007. Programmed synthesis of copolymer with controlled chain composition distribution via semibatch RAFT copolymerization. *Macromolecules,* **40**(4), pp. 849-859.

THICKETT, S.C. and GILBERT, R.G., 2005. Midchain transfer to polymer in styrene-poly(butyl acrylate) systems: Direct evidence of retardative effects. *Macromolecules,* **38**(23), pp. 9894-9896.

URRETABIZKAIA, A. and ASUA, J.M., 1994. High Solids Content Emulsion Terpolymerization of Vinyl-Acetate, Methyl-Methacrylate, and Butyl Acrylate .1. Kinetics. *Journal of Polymer Science Part A-Polymer Chemistry,* **32**(9), pp. 1761-1778.

VULUGA, D.M., PANTIRU, M. and ABADIE, M.J.M., 1999. Photoinitiated cationic polymerization of 1,3-dioxepane. *European Polymer Journal,* **35**(12), pp. 2193-2195.

VULUGA, D.M., PANTIRU, M., HAMAIDE, T. and VASILESCU, D.S., 2004. Study of dioxolane-dioxepane copolymers through IR and DSC. *Polymer Bulletin,* **52**(5), pp. 349-354.

WALL, F.T., 1944. The Structure of Copolymers II. *Journal of the American Chemical Society,* **66**, pp. 2050-2057.

YANG, H.J. and YANG, C.H., 1998. Statistical experimental strategies approach to emulsion copolymerization of styrene and n-butyl acrylate. *Journal of Applied Polymer Science,* **69**(3), pp. 551-563.

ZUBITUR, M. and ASUA, J.M., 2001. Agitation effects in the semicontinuous emulsion polymerization of styrene and butyl acrylate. *Journal of Applied Polymer Science,* **80**(6), pp. 841-851.